MACHINING USING A DIAMOND-COATED CUTTING TOOL:

FINITE ELEMENT SIMULATIONS AND EXPERIMENTS

by

FENG QIN

Y. KEVIN CHOU, COMMITTEE CHAIR
VIOLA L. ACOFF
MARK E. BARKEY
DANIEL J. FONSECA
LEILA J. LADANI

A DISSERTATION

Submitted in partial fulfillment of the requirements
for the degree of Doctor of Philosophy in the
Department of Mechanical Engineering
in the Graduate School of
The University of Alabama

TUSCALOOSA, ALABAMA

2012

ABSTRACT

Chemical vapor deposition (CVD) diamond-coated tools have the advantage of a low cost and flexibility in fabrications when compared with sintered polycrystalline diamond (PCD) tools in machining lightweight high-strength materials. However, coating-substrate interface delaminations remain a major technical barrier. Further, the complex effects of the tool geometry and the deposition residual stress, as well the machining conditions on the tool performance, have hindered the industrial applications of CVD diamond-coated tools.

The objectives of this research are: (1) to develop finite element (FE) models of cutting simulations including deposition residual stresses for investigating tool edge radius effects on diamond-coated tool stress evolutions from depositions to machining; (2) to study diamond-coated tool performance in machining Al-Si alloys and Al-matrix composites with various cutting conditions; (3) to implement a cohesive zone interface in a diamond-coated tool for two-dimensional (2D) cutting simulations. The research methods include: (1) coupled thermo-mechanical finite element modeling of cutting simulations, including the deposition residual stress, for tool performance evaluations and tool stress evolutions; (2) machining of A390 alloy and A359/SiC-20p composite workpieces with a force sensor and tool wear evaluations at different conditions; and (3) incorporating a traction-separation law as the interface behavior in the FE cutting simulations for coating delamination analysis.

The major findings are summarized as follows: (1) In gentle cutting, deposition residual stresses remain dominant, but change noticeably at a large uncut chip thickness. (2) 2D FE results of the cutting simulation are compared with the machining experiments. The difference

between simulations and experiments is acceptable. (3) Increasing the edge radius will increase cutting forces; however, this increasing rate decreases at a higher feed. The combined effects of the tool geometry and cutting conditions result in complex wear behavior of diamond-coated tools. (4) The cutting simulations incorporating a cohesive-zone interface in a diamond-coated cutting tool demonstrate that the interface fracture energy is the major cause of coating delaminations. Furthermore, a larger uncut chip thickness tends to result in coating delaminations.

LIST OF SYMBOLS

C	Specific heat (J/kg-K)
C_T	The heat capacity
d	Depth of cut (mm)
E_{chip}	Friction energy into chip
E_{tool}	Friction energy into tool
f	Feed (mm/rev)
F_a	Axial cutting force in turning (N)
F_f	Frictional cutting force at rake face (N)
F_r	Radial cutting force in turning (N)
F_t	Tangential cutting force in turning (N)
k	Shear flow strength of the chip at the primary zone
K	Thermal conductivity of workpiece (W/m-K)
K_T	Thermal conductivity of cutting tool (N/m-K)
l_c	Tool-chip contact length (mm)
n	Spindle rotation speed (rev/min)
n	Correction factor
P_{fr}	Frictional energy dissipation rate per unit area
q	Heat flux (kJ/ m^2-s)
Q^{pl}	Heat flow rate per unit volume
r_e	Edge radius (μm)

t_u Uncut chip thickness in orthogonal cutting (mm)

t_c Chip thickness in orthogonal cutting (mm)

T_n Normal traction (MPa)

T_t Shear traction (MPa)

V Cutting velocity (m/s)

V_c Velocity of chip (m/s)

VB Width of flank wear (mm)

α Rake angle (rad)

α_c Thermal expansion coefficient of the coating

α_s Thermal expansion coefficient of the substrate

$\dot{\varepsilon}^{pl}$ Plastic strain rate

β_r Heat partition coefficient for rake face heat source

Δ_n Normal separation (μm)

Δ_n^c Critical normal separation

Δ_t Shear separation (μm)

Δ_t^c Critical tangential separation

ΔT Temperature difference

δ_n Non-dimensional normal displacement jump

δ_t Non-dimensional tangential displacement jump

δ Total displacement jump

δ_n Normal characteristic length (μm)

δ_t Shear characteristic length (μm)

δ Displacement jump (μm)

ϕ_n Normal work of separation (J/mm^2)

ϕ_t Shear work of separation (J/mm^2)

$\dot{\gamma}$ Slip rate at the chip tool interface

ρ Density (kg/m^3)

σ Normal stress (N/mm^2)

σ_1 First principal stress (N/mm^2)

σ_{eqv} Equivalent stress (N/mm^2)

σ_{max} Interfacial normal strength (N/mm^2)

σ_N Normal strength (N/mm^2)

σ_r Normal stress in the radial direction (N/mm^2)

σ_θ Normal stress in the tangential direction (N/mm^2)

θ_A Temperature of face A

θ_B Temperature of face B

τ Shear stress (N/mm^2)

τ_f Friction stress (N/mm^2)

τ_{max} Interfacial shear strength (N/mm^2)

$\tau_{r\theta}$ Shear stress along the interface (N/mm^2)

υ Poisson's ratio

w Correction factor

η Fraction coefficient of energy

ACKNOWLEDGMENTS

First, I am indebted to Dr. Y. Kevin Chou, my research advisor, for his guidance, encouragement, and support. This dissertation could never have been accomplished without him. His insights, patience, and educations always light my way during my research journey at The University of Alabama. I have learned a lot from him which benefits me now and will continue in my whole life.

Also, I would like to extend my deepest appreciation to my committee members, Dr. Viola L. Acoff, Dr. Mark E. Barkey, Dr. Daniel J. Fonseca, and Dr. Leila J. Ladani, for their invaluable suggestions on this work and for their support.

I give my thanks to the following people: Dr. Thompson, with Vista Engineering in Birmingham, supplied the nanocrystalline diamond-coated cutting tools and A390 bars for this research; Dr. Kwon and Mr. Park from Michigan State University selflessly gave me useful technical discussions; Dr. Yanfei Gao with the University of Tennessee provided me some insightful views of fracture mechanics; and Dr. Ivester and Mr. Whitenton from the National Institute of Standard and Technology provided detailed experimental validation for the 2D cutting simulations.

I also would like to give my thanks for the selfless help and support of my friends at the University of Alabama throughout this course of study. I am grateful to Dr. Jianwen Hu, Dr. Long Zhang, Peng Qu, Dr. Xiao Li, Bill, Sam, and James. Special thanks to the other members in our group, Dr. Jianwen Hu, Mr. Chao Miao, Mr. Ping Lu, Mr. Xibing Gong, and Mr. Ninggang Shen for their assistance in my research. Thanks are extended to The University of Alabama and

the Mechanical Engineering Department for providing me with such a wonderful opportunity to pursue my Ph.D. study here. Additionally, I definitely owe a “thank you” to my brothers and sisters in the Tuscaloosa Chinese Christian Church for their good will and endless encouragement.

The financial support for this research, from National Science Foundation (Grant No.: CMMI-0728228 & CMMI-0928627), is gratefully acknowledged.

Last but not least, I would like to thank my beloved parents, brother, wife, and little one for their continuing support and encouragement, and for always being there for me. I am indebted so much to them.

CONTENTS

LIST OF TABLES

LIST OF FIGURES

CHAPTER 1

INTRODUCTION

Background and Motivation

Man-made synthetic diamond, a special material produced through physical or chemical processes, has a unique combination of properties – high hardness, low friction coefficient, high elastic modulus, ultra-high thermal conductivity, optical transparency, and good chemical stability. These notable properties have led to many applications in the automotive and aerospace industries. Diamond has been extensively used for some special occasions such as machining metal-matrix composites, high silicon aluminum alloys, nonferrous metals, fiber-reinforced plastics, etc. These workpiece materials have been proven unsuitable for machining using traditional cemented carbide tools which experience rapid tool wear under these conditions.

In reality, two kinds of diamond tools have gained wide application: polycrystalline diamond (PCD) tools and chemical vapor deposited (CVD) tools. PCD is the most commonly used diamond tool material, made by distributing micrometer-sized diamond grains in a metal matrix (binder phase) and then hardening and sintering the matrix onto a tool tip. CVD diamond tools have been developed over the past fifteen years with the aid of chemical vapor deposition technology. As a protective coating, CVD diamond material has attracted interest from many researchers and has been used for various industrial situations, including electrical insulation, magnetic disk coating, biomedical equipment, cutting tools, etc.

Compared to PCD diamond tools, CVD diamond coatings have many advantages, such as the capacity to serve as coating for tools of complex geometry, coating growth over a large area,

and reduced fabrication costs. However, due to the poor adhesion of the diamond coating on the carbide substrate, the practical use of diamond-coated tools still has some limits. According to many sources, coating delamination is the major failure mode of CVD diamond coatings, even though CVD diamond coating is thought to exhibit high tribological behavior. Figure 1 shows the tool wear history of a diamond-coated tool in machining an A359/SiC composite. The machining conditions are as follows: cutting speed = 4 m/s, cutting feed = 0.10 mm/rev, and cut depth = 1 mm. After testing for about 3 minutes, a drastic increase of the tool flank wear is observed. Tool failure occurs suddenly during a single cut and is characterized by coating delamination and subsequent massive substrate material loss.

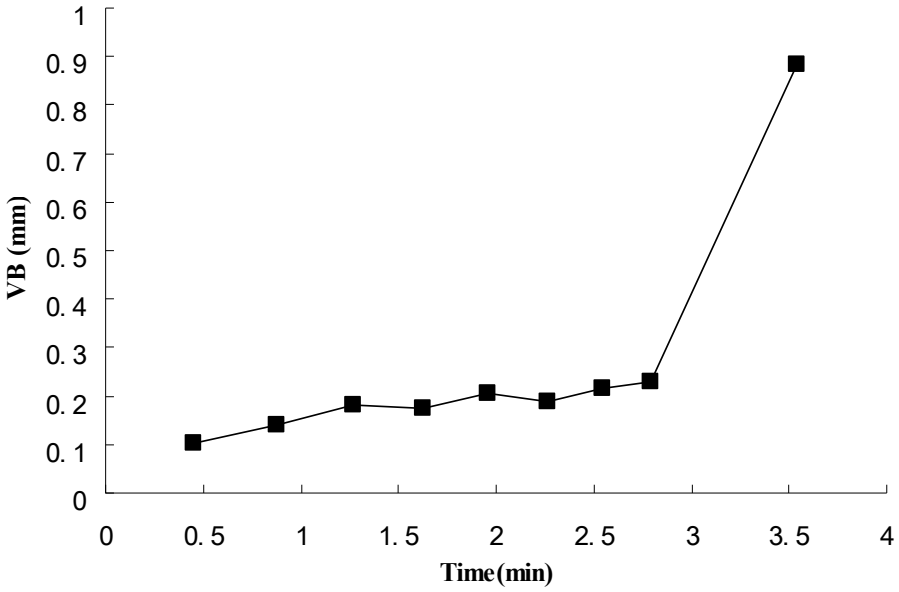

Figure 1. A diamond-coated tool history in machining an A359/SiC/20p composite bar.

Figure 2 demonstrates coating delamination and massive substrate material loss.

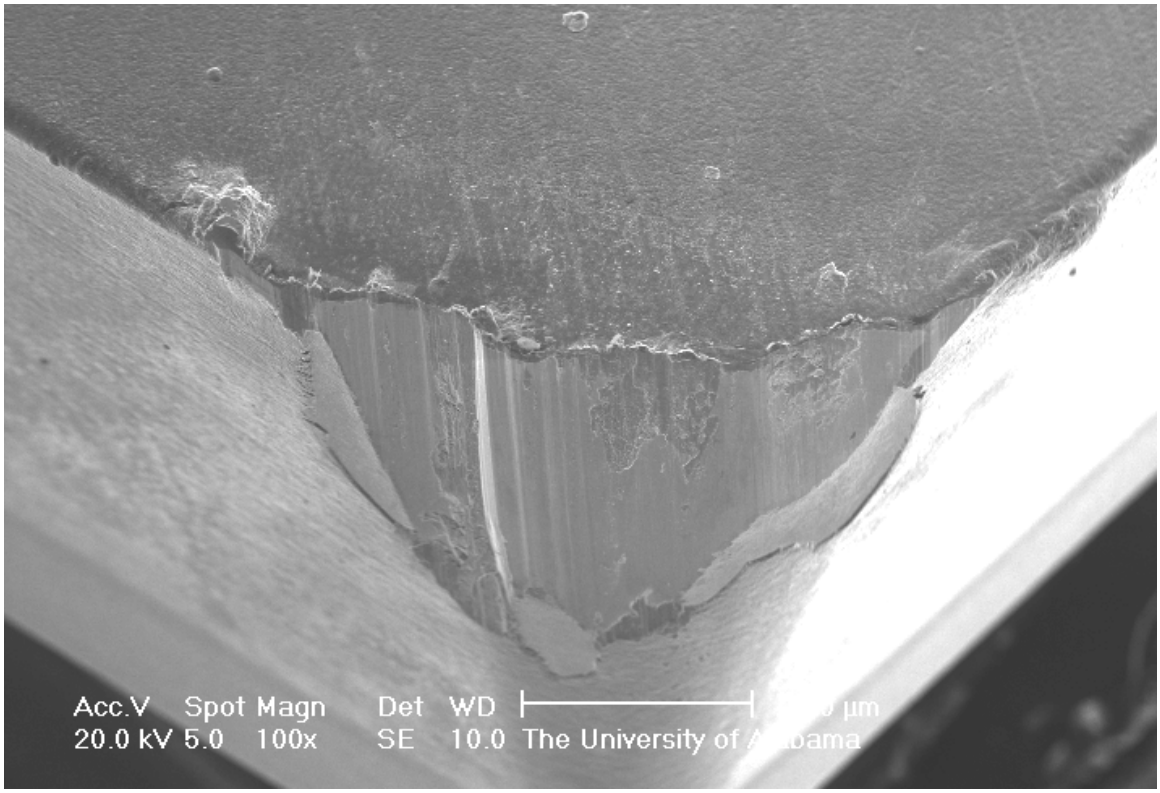

Figure 2. SEM micrograph of the tool tip after failure in machining a A359/SiC/20p composite with diamond-coated tools.

With the lightweight, high-strength requirement of products and parts, innovative materials such as Al-Si alloys and Al-matrix have been developed and applied increasingly in the automotive industry and aerospace industry. These relatively new materials have higher strength but lightweight, with stronger wear resistance and better stability of mechanical properties at elevated temperatures, in contrast to the conventional materials. Meanwhile, these characteristics are not advantageous to conventional carbide tools, which experience abrupt tool wear no matter whether they are plain or coated. However, diamond tools demonstrate the best performance among available tool materials and thus are considered the best choice. CVD diamond-coated tools, as the potential counterpart of the PCD tools, have been widely used in machining these highly abrasive materials.

Recent years have seen a significant number of studies performed on the machining of Al-Si alloys and Al-matrix composites by CVD diamond-coated tools and the tool geometry effect on deposition stress and machining performance, as well as the cutting conditions. Researchers have done many experiments investigating the effect of cutting conditions on tool performance. However, there is no coherent perspective on this effect.

Since deposition residual stress arising from the diamond coating process can affect adhesion strength, it has also attracted considerable interest from investigators, especially in how tool geometry affects the stress. A lot of researches have been devoted to investigating the tool geometry effect on deposition residual stress, but tool geometry is limited to some wider types, such as upsharp and round. The tool edge radius and coating thickness, as major features of CVD diamond-coated tools in fabrication, are not addressed.

How deposition stress influences tool performance is another issue which is infrequently addressed in the literature. Moreover, the existing model related to that effect is a simplified static sequential simulation, which does not take into account the simultaneous thermal loading and mechanical load, as occurs during the actual machining. This means that the model cannot represent the actual machining situation. Thus, a cutting simulation must be formulated to approximate the actual cutting.

Interface adhesion is also an important concern for coated tools, since it is essential to coating delamination. Much effort has been spent on this from theoretical and experimental angles. Many researchers have been trying two main methods, i.e., indentation and scratching tests, to investigate interface dehesion. Theoretically, many of them have been using the cohesive zone model to conduct finite element analysis on interface behavior. However, these two methods do not effectively address the cohesive zone model in coated tools in machining

performance. No literature exists regarding cohesive zone model application in cutting simulations.

Furthermore, the interwoven effects of tool geometry, deposition residual stress, the cohesive zone interface, and various cutting conditions in combined thermal and mechanical loads impact tool performance in a very complicated way. Difficulties in modeling make it an important research target in the study of metal cutting with coated tools. All of the above issues inspired us to conduct the research presented in this dissertation.

Research Objectives and Approaches

This research intended to investigate the performance of the newly developed nanocrystalline diamond-coated tools, made by microwave-plasma assisted CVD, when machining high-strength Al-Si alloys and Al-matrix composites. The primary objective is a better understanding of tool geometry effects combined with deposition residual stress and machining conditions on the performance and failure modes of CVD diamond-coated tools.

The specific objectives of this research include the following:

1. To investigate the performance of nanocystalline diamond-coated (NCD) tools in terms of cutting forces and tool life in machining Al-Si alloys and Al-matrix composites, to evaluate the effect of cutting parameters on the tool life.
2. To develop a numerical method to study the thermo-mechanical states of diamond-coated tools using orthogonal cutting simulation including deposition residual stresses, and to study the effect of tool edge radius on the stress evolutions of diamond-coated tools from deposition to machining, which may correlate the tool stresses to tool failure.

3. To implement a cohesive zone interface in a diamond-coated tool in 2D cutting simulations.

The approaches are described as follows,

1. Commercial WC-Co cutting inserts prepared with different edge radii are used to investigate the edge radius effects on cutting forces and tool wear. The diamond-coated inserts are examined for the geometry specifications. The coated tools with different substrate edge radii are further tested in the machining of composite bars. Two different cutting conditions: (4m/s and 0.05 mm/rev) and (1.3 m/s and 0.15 mm/rev) are tested. The machining forces are monitored by Kistler force sensor and analyzed against the edge radius, and tool flank-wear is measured and evaluated. SEM is employed to examine wear features.
2. 2D cutting simulations with a diamond-coated tool are developed in Abaqus explicit. The tool is modeled as elastic behavior and the workpiece is modeled with plastic behavior characterized by Johnson-Cook model. The deposition residual stresses in the coated tool are first simulated, and the model results are carried over into the cutting simulations. The simulations are used to evaluate the edge radius effects on cutting tool stress contours and temperature distributions, as well as interface stresses.
3. A cohesive zone model is embedded for the interface of tool coating and substrate. The cohesive element is constructed in the code to avoid node numbering issue for curved cohesive elements. Substrate is modeled with plastic behavior. The cohesive interface is modeled with different facture energy, and then a suitable parameter is chosen for 2D cutting simulation. Uncut chip thickness effect is investigated.

Outline of Dissertation

Chapter 2 presents a literature review on cutting mechanics in orthogonal cutting and cutting simulation. Tool wear, diamond-coated tool failure mode, and the machining of high-strength Al-Si alloys and Al-matrix composites are also discussed. The cohesive zone model for characterizing interfacial failure is also introduced. Chapter 3 introduces the finite element modeling of orthogonal cutting.

Chapter 4 presents the experimental results on machining an A359/SiC composite with different edge radii nanocrystalline diamond-coated tools under certain cutting conditions. The machining performance of these diamond tools is compared in terms of cutting force, tool wear, surface roughness of the machined part, and tool life. The effect of the cutting condition on the performance of NCD tools is also investigated.

Chapter 5 presents a 2D orthogonal cutting simulation with a diamond-coated tool, including deposition residual stress. Two different edge radii tools are simulated under two combinations of cutting conditions. The stress evolutions, cutting forces, and cutting temperature are investigated. The preliminary results are evaluated.

Chapter 6 develops a 2D orthogonal cutting simulation with a cohesive zone model embedded in a diamond-coated tool, including deposition residual stress. Different cohesive fracture energy values are tested for the cutting simulations. The edge radius effect is also investigated when modeling tool geometry with the cohesive zone model.

The last chapter summarizes the primary results and contributions from this study; recommendations for the future directions of this research are also presented.

CHAPTER 2

LITERATURE REVIEW

Fundamentals of Metal Cutting

Metal cutting refers to the manufacturing process designed to remove unnecessary material from the workpiece so as to produce the mechanical part with desired dimensions and proper surface quality. The three most widely used metal cutting operations are turning, milling, and drilling. This research focuses on turning as the basis for other metal cutting operations, due to the current available facility.

Figure 3 is a typical three-dimensional schematic diagram of the turning operation, where the tool moves an axial distance of *f* (feed) relative to the workpiece to reduce the workpiece radius by an amount of *d* (depth of cut) while the workpiece revolves one cycle.

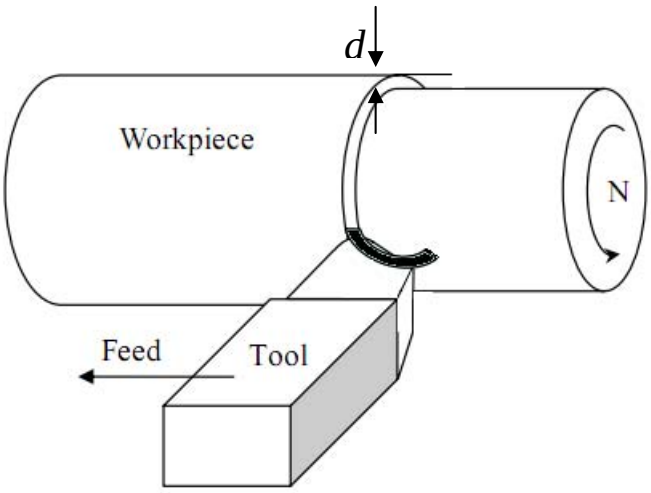

Figure 3. A schematic drawing of the turning process.

Understanding the metal cutting process is important for the following reasons. First of all, even minor improvements in cutting techniques are of major importance for productivity in

high-volume production. With the rapid development of modern industry, productivity is crucial to manufacturing, and the improvement of cutting techniques can bring higher production efficiency and reduce manufacturing costs. A better understanding of the metal cutting process is also beneficial for products of greater precision and longer useful life. For customers who want to achieve the desired quality of the machined part in an efficient fashion, better knowledge of the cutting process can help them to utilize a more effective machine workpiece with certain material and geometric specifications. As for the machine tool makers who wish to optimize the tooling design and evaluate the effect of cutting process parameters on the quality of machined parts, a better understanding of the cutting process can help them develop advanced cutting tools to broaden their machining scope and optimize fabrication of current tools.

The research related to metal cutting has a long history and can date back to the 18^{th} century. People have tried different methods of studying the metal cutting process from various perspectives. In the beginning, research primarily focuses on the chip formation mechanism. For example, Merchant (1945) proposes the concept of shear plane and formulated a mathematic model of the shear angle by using the minimum energy principle. Lee and Shaffer (1951) present an approach to analyzing plastic deformation, the slip-line field model of the metal cutting process. This slip line theory applies to plane strain conditions only, and the material properties are also simplified to rigid perfectly plastic such that the method is limited to steady state, orthogonal cutting conditions.

Thereafter, researchers developed more and more complex and sophisticated models involving various aspects of cutting mechanisms, such as work-hardening, cutting temperature, strain rate, and friction. Hahn (1951) formulates cutting temperature analysis by using an oblique shear plane heat source moving in the cutting direction with the cutting velocity in an infinite

medium. Trigger and Chao (1951) extend Hahn's cutting temperature model by considering a semi-infinite medium. Bowden and Tabor (1950) investigated the relationship between friction and the lubrication of solids. Naerheim and Trent (1977) investigate tool wear mechanisms when turning steels using carbide tools. Henriksen (1951) investigates the effect of various rake angles on residual stress. Later, Liu and Barash (1976) carry out their study related to residual stress on the mechanical state of the machined layer affected by tool wear. Usui, Hirota, and Masuko (1978) present an analytical prediction of the three-dimensional cutting process. Shirakashi and Usui (1976) and Childs and Maekawa (1990) carry out finite element machining simulation. Maekawa and Itoh (1995) present a molecular dynamics approach to studying friction and tool wear in nano-scale machining. Kim and Moon (1996) apply a molecular dynamics approach in micro-cutting to study the configuration of tools. Waldorf, Kapoor, and DeVor (1998) proposes a ploughing force model based on slip-line field. Chou and Evans (1999) investigate white layer and thermal modeling of hard turned surfaces. Smithey, Kapoor, and DeVor (2001) proposes a new mechanistic model for predicting worn tool cutting forces. In addition, the investigators also focus on evulating the cutting mechanism effect on workpieces with different materials, such as steel, aluminum, copper, various kinds of alloys, metal matrix composites, etc.

Orthogonal Cutting

Metal cutting processes can be categorized into two kinds: orthogonal and oblique metal cutting. Owing to its simplicity, orthogonal cutting, proposed by Ernst and Merchant (1941), has been applied widely in metal cutting research. The typical orthogonal cutting model can be illustrated in Figure 3, where tool cutting edge is perpendicular to the relative cutting velocity and normal to the feed direction. The wedge-shaped tool consists of two intersected surfaces,

termed rake face and flank face, shown forming the cutting edge in Figure 3. The relative motion of tool to workpiece shapes the machined surface by removing unwanted material. Orthogonal cutting eliminate many of the independent variables, since the chip is produced in plane stain, enabling us to simplify metal cutting in a two-dimensional rather than a three-dimensional model. Therefore, the majority of analytical and numerical works on chip formation and cutting force modeling are formulated with this simplified model. Orthogonal cutting usually can be implemented experimentally by turning either thin-wall tubing or rings.

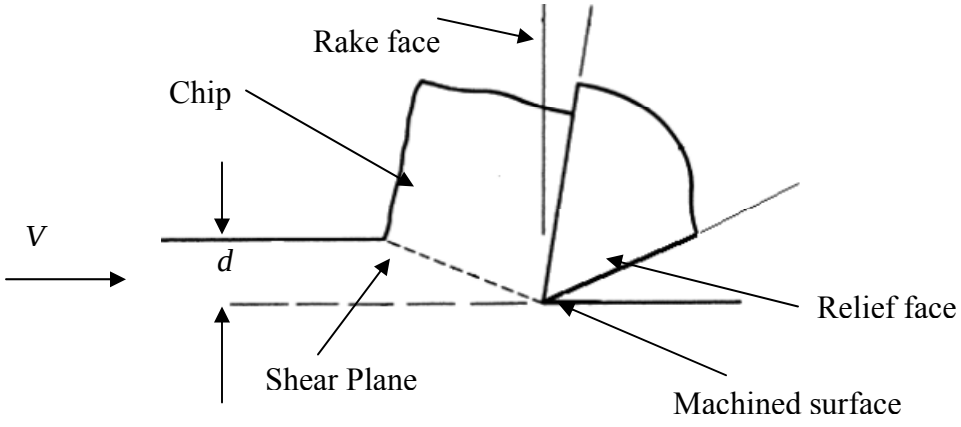

Figure 4. A schematic drawing of orthogonal cutting.

Numerical Simulation in Metal Cutting

Although metal cutting is a widely used process, the modeling and simulation of this phenomenon is not trivial. Metal cutting actually has been proven to be particularly complicated, since this physical phenomenon involves large elastic-plastic deformation, complicated contact/friction conditions, thermo-mechanical coupling, and chip formation mechanisms. Over 100 years, the study of metal cutting has been a challenging task. Early theoretical models were developed to describe the problem qualitatively, but the drawback of existing models for chip formation is oversimplification of the problem with disregard for the interaction of different

parameters. This issue has been solved with numerical simulation by the finite element method, made possible by the rapid development of high-speed computers and some related algorithms dealing with large strain/displacement problems and adaptive meshing methods. These newly developed techniques make numerical simulation of metal forming involving material removal possible. Pioneering studies by Usui and Shirakashi (1974, 1982) and Klamecki (1973) contributed to the finite element method. In the following sections, a literature review concerning a wide range of aspects in numerical simulation of machining is presented.

Solution Methods

The solution methods in metal cutting can be grouped into three categories, called updated Lagrangian, Eulerian, and Arbitrary Lagrangian Eulerian formulations. The difference between these methods is how the relationship between mesh and material is handled. The Lagrangian method assumes that mesh is attached to and moves with the material, which is helpful for simulating the transient process and discontinuous chip. The shortcoming of the method is inevitable element distortion during simulation. Shih and Yang (1993), Lin and Lo (2001), and Mabrouki and Rigal (2006) utilize pre-distorted mesh, and some researchers (Baker, 2006; Monaghan & McGinley,1999; Ozel & Altan,2000; Yen, Jain, & Altan, 2004) attempt a remeshing method to minimize this problem. The Eulerian method fixes the mesh in space and material can flow through the element surfaces, thereby allowing the simulation of a steady state. No chip separation is required in the modeling. The disadvantage is the need for predefined chip geometry and the tool/chip contact length. The Arbitrary Lagrangian Eulerian method (ALE) combines both benefits of the above formulations. Detailed descriptions of the ALE method can be found in Adibi-Sedeh and Madhavan (2003); Movahhedy, Gadala, and Altintas (2000); and Rakotomalala, Joyot, and Touratier (1993).

Workpiece and Tool

Generally workpiece is assumed as elastic-plastic material. Some authors also used rigid-plastic and rigid-viscoplastic materials to simplify the analysis. This choice would not give rise to thermal strains and residual stresses. As for tool modeling, most authors assumed tool as rigid so as to simplify the analysis. However, some authors target to evaluate tool choose elastic behavior. For example, in Carrol III and Strenkowski's work (1988), and MacGinley and Monaghan's work (2001), elastic model was utilized to represent their tools.

Couple Thermo-mechanical Process

Heat generation and dissipation from plastic work and frictional work will be distributed to the workpiece, chip, and tool and lost to the surrounding environment by means of convection and radiation. Most finite element models approximate temperature through the weak form of the governing equation, which can be stated as:

$$C_T\dot{T} + K_T T = Q(t), \tag{2.1}$$

where C_T is the heat capacity, K_T is the heat conduction, T is the nodal temperature at time t, and Q is the heat flux and heat generation from the plastic deformation.

In some researchers' models (Guo & Dornfeld, 1998, 2000; Guo & Liu, 2002), the adiabatic processes are frequently assumed, so heat conduction is not required. However, this choice is limited to application in low diffusivity materials or in high speed processes. Considering the residual stress of the workpiece, thermal-mechanical coupling analysis should be adopted instead of adiabatic method.

Chip Formation

Chip formation has been an interest for investigators of metal cutting. Actually, there are several kinds of chip, such as continuous chip, discontinous chip, saw-type chip, etc. However,

simulating chip types besides the continuous chip has been an issue, because of insufficient computer capacity, convergence problems, or lack of a suitable chip separation mechanism. Hashemi, Tseng, and Chou (1994) and Marusich and Ortiz (1995) make breakthroughs by using explicit algorithms but without predefined chip separation or breakage paths to simulate discontinuous chip formation. Recent years have seen a vast body of simulations using chip breakage strategies (Barge et al. 2005; Hua & Shivpuri, 2004). Three-dimensional chip formation has developed with the advance of computer capacity and new modeling strategies. Lin and Lin (1999, 2001) simulate a 3D machining operation by using a structure mesh and a predefined parting line. Guo and Dornfeld (2000) and Guo and Liu (2002) simulate incipient drilling and hard turning. Pantale et al. (2004) use the ALE method to simulate 2D and 3D oblique cutting and milling. Ceretti et al. (2000) and Fang and Zeng (2005) combine a remeshing technique and unstructured mesh to simulate oblique cutting.

An ideal numerical model of machining should be able to simulate different types of chip morphology, not just one form. However, due to the complexities of the physical phenomena involved in large plastic deformation, heat generation, contact and friction, damage evolution, etc., chip separation could not be generated in one strategy. Currently, there are three main methodologies to address the issue: to use a predefined parting plane to realize continuous chip separation, to define criterion for chip separation and breakage, and to use no chip separation. Actually, researchers use different chip separation and breakage criteria, such as nodal distance (Zhang & Bagchi, 1994), equivalent plastic strain (Guo & Dornfeld, 2000), energy density (Lin & Lin, 1999), tensile plastic work (Hua & Shivpuri, 2004), maximum principal stress (Hashemi, Tseng, & Chou, 1994), and toughness (Barge et al., 2005; Johnson & Cook, 1983; Marusich & Ortiz, 1995).

Tool Geometry Effect on Tool Performance

Tool geometry has a significant influence on machining performance. It has attracted increasing interest from researchers studying metal cutting, whether with diamond-coated tools or plain tools. Sheikh-Ahmad, Stewart, and Feld (2003) conduct research on the failure characteristics of diamond-coated carbide in machining wood-based composites using uncoated and CVD diamond-coated cemented carbide tools. The work indicates that a honed cutting edge may greatly reduce fracture and delamination of the diamond coating and generally improve tool performance. Yen, Jain, and Altan (2004) establish a finite element orthogonal machining model to investigate the effect of different tool edge geometries on cutting 0.2% carbon steel. Hone tools and chamfer tools with different edge radii were investigated. They compare the predicted cutting forces and chip geometries for tools with different edge preparations. Tool temperatures and tool stresses on the tool rake face were also calculated. M'Saoubi and Chandrasekaran (2004) apply a dedicated charge-couple device (CCD) sensor based on near infrared (0.85-1.1μm) imaging technique to investigate the effects of tool micro-geometry and coating on tool temperature during orthogonal turning of quenched and tempered steel. Uncoated cemented carbide tools with geometries such as sharp, round, and prehoned flank land, and PVD-coated TiN tools are tested in their experiments. The results show that an increase in edge radius resulted in a certain increase in temperature. Almeida et al. (2005) investigate the effect of tool using CVD diamond direct coated ceramic tools to machine hard metal on tool edge geometry. Their results show that the cutting forces increase with the bluntness of the cutting edge. The film delaminated and edge fractured for the honed edge tools at all tested conditions.

Tool Geometry Effect on Deposition Stress of Diamond-coated Tools

The diamond coating process can produce considerable deposition stress, which is different from intrinsic stress, and can affect adhesion strength, which may directly impact their in-service performance. The formation of the thermal residual stress is attributed to the large mismatch of the thermal expansion coefficients between diamond and substrate. Diamond coating, with a smaller thermal expansion coefficient, is subject to a compressive residual stress while the carbide substrate in tension. The analytical treatment of the thermal residual stress in the coating for the nominal biaxial stress condition is given by Strawbridge and Evans (1995):

$$\sigma_c = \frac{E}{1-\upsilon_c}(\alpha_c - \alpha_s)\Delta T \tag{2.2}$$

where υ_c is Poisson's ratio of the coating, α_c and α_s are thermal expansion coefficients for the coating and substrate, respectively, and ΔT is the temperature difference between room and deposition temperature. Using data from the literature (2.5 and 5.5 μm/(m·K) as thermal expansion coefficients for CVD diamond and WC, and 1200 GPa and 0.07 for elasticity and Poisson's ratio of diamond, respectively), a deposition temperature of 800°C can generate a nominal stress in the coating as high as 3.0 GPa in compression. Such high residual stresses will have a compound impact on the coating performance. Deuerler, Woehrl, and Buck (2006) point out that in some cases, diamond coating even peels off from the substrate right after being cooled down to room temperature, due to the high residual stress.

In addition to material properties, deposition residual stress can also be influenced by tool geometry. Gunnars and Alahelisten (1996) investigate the tool geometry effect on thermal residual stresses in diamond coatings. They report that residual stresses around the substrate edge increase significantly compared to the uniform coating area, and small edge radii will drastically

increase stress concentrations. They further propose that adjusting residual stress can be realized by changing the ratio of edge radius over coating thickness.

The Confound Effect of Combined Tool Geometry, Deposition Stress and Cutting Conditions on Tool Performance

The complicated effects of combined tool geometry, deposition stress, and cutting conditions are not well represented in the literature. Hu, Chou, and Thompson (2007b) present a study on stress analysis of diamond-coated cutting tools to evaluate tool performance. A finite element method was applied to investigate stress distributions focused on the edge radius effect in diamond-coated tools, considering depositions and machining. Their conclusions are, firstly, that the stress concentrations can be alleviated by a large edge radius, and secondly, that imposed machining loading will reverse stresses. A large edge radius at a low feed will reduce the maximum tangential normal stress and exhibits minimal effect at a high feed. Hu, Chou, & Thompson (2008b) later use a simplified 2D finite element (FE) thermo-mechanical model to investigate the stress distributions in diamond-coated tools. Their results show that diamond-coated tools can have high residual stresses from the deposition and concentrate around the cutting edge. Furthermore, mechanical loading tends to lead to stress reversal, which may correlate with tool wear severity.

Machining High-Strength Al-based Materials with Diamond-coated Tools

The high-strength Al-based materials, i.e., the Al-matrix composites and Al-Si alloys, have been widely used in the aerospace and automotive industry for almost three decades, which can be attributed to their enhanced physical properties: wear resistance, fatigue strength, thermal stability, etc. However, due to these superior characteristics, they have proven to be extremely difficult to cut with the conventional tools.

In this research, two Al-based high-strength materials, i.e. an A359/SiC/20p composite and an A390 alloy, are studied. The reinforcement phases in these materials cause rapid, abrasive wear on conventional tools, e.g., cemented carbides, and diamond is considered to be by far the best for machining them. Two types of diamond tools, brazed polycrystalline diamond (PCD) tools and chemical vapor deposition (CVD) diamond-coated tools, are commonly used in the manufacturing industry. A vast body of work has been devoted to investigating the performance of diamond tools in machining high-strength Al-based materials.

Hung, Loh, and Xu (1996) compare carbide tools with CBN and PCD tools and conclude that the carbide tools produce maximum subsurface damage of the machined part and an unacceptable short tool life. More recently, researchers (Durante, Rutelli, & Rabezzanna, 1997; El-Gallab & Sklad, 1998) have reported that only PCD tools and CVD diamond-coated tools can achieve a satisfactory tool life that meets industrial requirement, even though frequent detachment of the coating remains a problem.

Due to some advantages, such as the capability of coating tools with complex geometry and a large surface area and low production costs compared to PCD tools, CVD diamond-coated tools have attracted researchers in metal cutting, though they often demonstrate a shorter tool life than PCD tools. Some researchers have developed new technology to address this issue. Saito et al. (1993) strengthen the adhesion strength of the coating-substrate interface by experiments. They form a thin, solid solution layer which contains a large amount of a metal, excluding cobalt, on the surface of a heat-treated, cemented carbide insert containing a metal belonging to group 4a or 5a in front of the deposition process diamond film. Their machining tests with the Al-18%Si alloy show that the evolution of the flank wear of the CVD diamond tools was comparable to the PCD tools. Oles, Inspektor, and Bauer (1996) employ different pre-deposition

treatments to increase the diamond coating adhesion strength. The authors then conduct machining testing on hypereutectic Si-Al alloys and Al-matrix composites and conclude that CVD diamond tools can meet or exceed the tool life of PCD tools in certain applications but with worse surface finishes. Davim (2002) conducts machining tests on A6061/SiC/20p, and the tests demonstrate that flank wear was the most important type of diamond cutting tool wear. Additionally, he finds that feed performs opposite to the cutting speed in the tool life curves obtained, which demonstrates the importance of selecting moderate cutting conditions, including cutting speed, feed, and depth of cut. Polini et al. (2003) test different types of PCD and CVD diamond-coated tools on dry turning Al-10% Al_2O_3 MMC, and find that the performance of diamond-coated tools depends on the appropriate combination of substrate microstructure, surface pretreatment, CVD process parameters, and coating thickness. Shen (1996) conducts machining tests on an A390 Al alloy for CVD diamond tools from various sources. These diamond tools varied differently in some characteristics, such as substrates, grain sizes, film thickness, roughness, and thereby adhesion strengths. He reports that only two or three coating sources had good film-to-substrate adhesion and similar machining performance to that of PVD tools.

The wear mechanism of diamond-coated tools is also investigated by many researchers. Karner et al. (1996) attribute the major failure mechanisms of the CVD diamond-coated tools to the flaking of the coating and its sensitivity to the stability of machining conditions. Later on, Yoshikawa and Nishiyama (1999) investigate the wear mechanisms of CVD diamond-coated tools in machining high Si-Al alloys. The results show that the tool life of thin coating was very short due to the easy peeling of the diamond layer. Two stages were observed for the tool wear of a coated insert. In the first stage, tool wear occurs continuously, with diamond grains chipping

and falling off the tool flank face. In the second stage, deep cracks formed in the substrate surface while the remaining coating kept wearing until it eventually peeled off the substrate unexpectedly. Andrewes et al. (2000) examines the tool performances of both CVD diamond-coated tools and PCD tools in an A380 aluminum alloy with 20 vol.% SiC particles turning. He remarks that the initial flank wear on both types of diamond tools and further tool wear in the worn areas were a result of the combination of abrasive wear and adhesive wear mechanisms, which is thought to explain of the faster rate of flank wear observed on the CVD diamond tool. Chou and Liu (2005) conduct machining tests on an MMC A359/SiC/20p bar by using CVD diamond-coated tools with various combinations of cutting conditions. Catastrophic coating failure was the dominant wear mechanism observed and may indicate that the bonding of the coating and the substrate is critical to tool performance. The results also demonstrate that cutting parameters, e.g., cutting speed and feed rate, have a significant influence on the sensitivity of tool wear. Later on, Hu, Chou, and Thompson (2007a) test newly developed nanocrystalline diamond (NCD) coating tools in dry turning a high-strength Al alloy, and compare them with microcrystalline diamond-coated (MCD) tools and PCD tools. The results show that the performance of NCD tools substantially surpasses that of MCD tools and is comparable to that of PCD tools. They confirm that coating delamination is the major tool wear mode for both the NCD and MCD tools.

In addition to experimental studies on machining high-strength Al-based materials with diamond tools, some researchers also focus on theoretical studies, i.e., empirical, analytical, and numerical methods. Pramanik, Zhang, and Arsecularatne (2006) establish an analytical mechanics model for predicting the forces of Al-based SiC/Al_2O_3 particle reinforced MMC turning with PCD tools. In their model, they state that the force generation mechanism was

attributed to three factors: the chip formation force, the ploughing force, and the particle fracture force, which can be obtained by Merchant's model, slip line field theory, and Griffith fracture theory, respectively. The comparison of the predicted forces and experiment results show that the established model could capture the major material removal/deformation mechanisms in MMC cutting. Ramesh et al. (2001) formulate a transient finite element model of turning an Al6061/SiC metal matrix composite. By applying a novel chip separation criterion, the simulated cutting force results, with small variations, were evaluated and found to be consistent with the experiment findings. Chan et al. (2001) investigate the factors affecting surface generation in the ultra-precision machining of Al6061/SiC MMC by using the finite element method and spectrum analysis. They find that surface roughness and surface integrity could be significantly improved by using high speed and a fine feed rate. The effect of depth-of-cut on surface roughness was negligible, except for the low cutting speed condition. Their non-linear multiple regression model of surface roughness is found to be in agreement with experimental results. In addition, their FEM model proves that it is possible to conjecture stain patterns. Hu, Chou, and Thompson (2007b) apply a finite element analysis to study stress distributions of diamond-coated cutting tools after deposition and machining. After deposition, high residual stress concentrates around the tool edge, compressive for radial components and tensile for tangential components. This stress can be alleviated by increasing edge radius. They also find that at a low feed, increasing the hone radius will reduce the maximum tangential normal stress, while at a high feed the edge radius has minor effects. Hu et al. (2008b) investigate the cohesive zone effects on coating failure evaluations of diamond-coated tools. Their indentation simulation results show that increasing coating thickness will generally increase the critical load for surface cracking but will have a reversal effect when the thickness exceeds a certain value. In addition, thicker coating

tends to reduce interface delamination. Renaud et al. (2008) present a numerical simulation of 3D diamond-coated cutting tools to investigate deposition residual stresses. Via the design of experiments approach and the finite element analysis method, they systematically investigate tool geometry effects on deposition residual stresses and conclude that the cutting edge radius is the most significant factor.

Cohesive Zone Model

Cohesive zone model is used to simulate crack initiation and crack growth in fracture mechanics. The original work can be traced back to the works of Dugdale (1960) and Barenblatt (1962). The traction-separation law, described in cohesive zone model, is to depict the phenomena, where the traction across the interface first increases as the separation increases until the traction reaches a maximum value, then falls down and finally vanishes with the separation reaches the designated value. Detailed information is described in Chapter 6.

Summary

In this Chapter, the fundamentals of metal cutting were summarized, and numerical studies of metal cutting and the machining of high-strength Al-based materials with diamond-coated tools were reviewed. The literature review mainly focused on two aspects, i.e., numerical research of metal cutting and high-strength Al-based materials machining by diamond-coated tools, especially CVD tools.

Due to their superior properties, such as high wear resistance, good fatigue strength, low density, and stable strength at elevated temperatures, hypereutectic Si-Al alloys and particulate-reinforced Al-matrix composites have been used extensively in the automotive and aerospace industries. However, the hard particles, i.e., Si and SiC, embedded in the materials also result in severe abrasive wear and thus decrease tool life significantly during machining. Through

multiple machining tests, brazed polycrystalline diamond tools and CVD diamond-coated tools have been proven to be by far the best choice to machine hard-to-cut materials.

Compared to PCD tools, the CVD diamond-coated tools are regarded as potential replacements because of their much lower production cost and flexibility for making complex geometry tools and coating large areas, even though the majority of studies reported the tool life of CVD diamond-coated tools to be inferior to that of PCD tools. The wear mechanism of CVD diamond-coated tools is primarily coating delamination through continuous abrasive wear on the flank face. It has been found that the CVD diamond tool's performance might be improved significantly through varying the deposition conditions, properly pretreating the substrate, increasing the coating thickness, and optimizing selection of cutting conditions. It is well known that the diamond coating endures compressive residual stress in the order of several GPa after the deposition because of the much smaller thermal expansion of the diamond compared to the substrate. Some researchers (Stjernberg, 1980; Suzuki & Hayashi, 1981) have proven that tensile residual stress will reduce the transverse rupture strength (TRS) and chipping resistance of the CVD-coated tools at interrupted cutting. However, few studies investigated the effect of diamond-coated tools geometry on deposition stress or the influence on machining.

In the following chapters, the effect of tool geometry on deposition residual stress via finite element analysis will be detailed, and finite element modeling of an orthogonal cutting simulation, including the deposition stress, will be introduced, as well as some investigations using machining tests with various cutting conditions.

CHAPTER 3

FINITE ELEMENT MODELING OF ORTHOGONAL CUTTING

Introduction

The finite element method has been widely used in formulating orthogonal machining processes. Compared to the analytical method, it is better able to solve complicated calculations in metal cutting by incorporating detailed physical parameters, such as material properties involving strain, temperature, friction, etc.

Formulations used in the finite element method of metal cutting are crucial to the simulation results due, to their different internal characteristics. Researchers in metal cutting have applied three kinds of formulations, called the Lagrangian method, the Eulerian method, and the Arbitrary Lagrangian Eulerian (ALE) method. These are detailed in the following section.

In addition, the proper friction model, located between interfaces such as tool-chip and tool-workpiece, is also difficult to formulate. Investigators have developed various models to simulate friction behavior. However, accurate description of this complicated mechanical behavior remains elusive. From the earliest simple friction model, only applied with a coulomb friction coefficient, to the complicated friction models incorporating shear limit and temperature dependence, more researchers are trying to optimize these models. However, available literature shows that all models fail to replicate the obtained results.

Last but not least, the heat transfer involved in metal cutting is one of the most important concerns for researchers. The cutting temperature affects tool wear and tool life such that modeling the thermal behavior effect with precision is essential for simulating metal cutting.

Finite Element Formulations

The Lagrangian formulation method has been employed frequently in the simulation of metal cutting. In the Lagrangian formulation, the mesh will deform following the material. The mesh deforms in time increments, and thus, the mesh domain can be updated based on material coordinates after each time increment. Hence, the finite element simulation can take the history of the material into account by using the updated material point as the initial condition. Apparently, the updated method is costly, since possible element distortion must be minimized so that the calculation can be continued.

The Eulerian formulation is also used often in cutting simulations. Compared to the Lagrangian formulation, the Eulerian formulation constrains the mesh in space and the work material flows through the mesh. The Eulerian method erases the element distortion occurring often in the Lagrangian method, because the mesh is fixed for the whole simulation. The disadvantage of the Eulerian method is that the mesh does not conform to the material, and hence, it is hard to obtain accurate data from free surfaces. However, due to the minimal elements requirement and calculation costs, this method has been applied widely by many researchers in the available literature (Strenkowski & Moon, 1990; Tay, Stevenson, & de Vahl, 1974). The Eulerian formulation does not require failure criterion for chip formation, so element distortion rarely happens. Childs and Maekawa (1990) investigate the tool wear of cemented carbide tools in high speed machining using the Eulerian method, and their results were in agreement with experimental data, except for small errors in cutting forces.

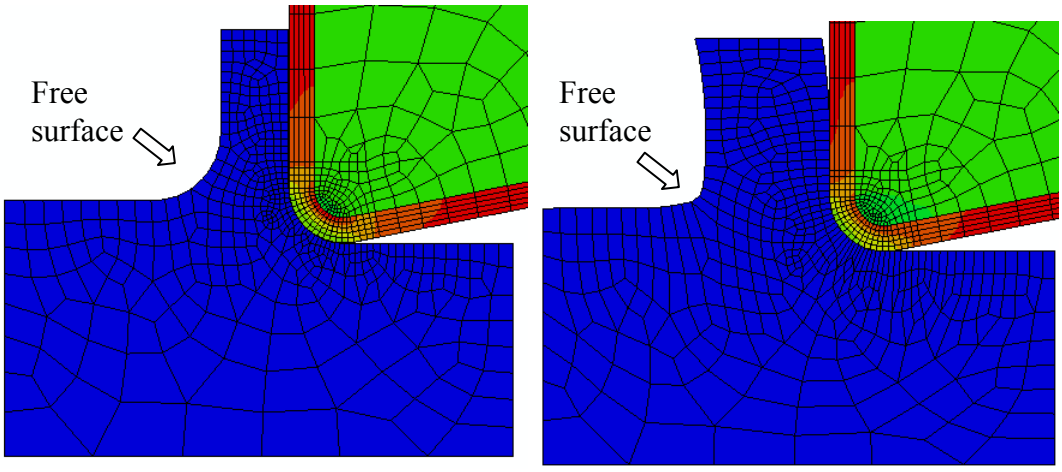

(a) Undeformed Shape (b) Deformed Shape

Figure 5. An example of the Arbitrary Lagrangian Eulerian simulation result.

More recently developed, the ALE formulation combines the dual advantages of the Lagrangian method and the Eulerian method. It was first introduced into the finite element method by Belytschko and Kenndy (1978), who apply it to solve some finite strain deformation problems encountered in solid mechanics, where large deformation often happens. Later, Movahhedy, Gadala, and Altintas (2000, 2002) utilize ALE analysis in cutting simulations with a chamfered tool and present a decent chip removal process. Arrazola et al. (2003, 2008) model finite element simulation of the sensitivity of chip formation to the tool/chip friction coefficient using the ALE method. Figure 5 is a typical result of the ALE formulation.

Adaptive Mesh

In machining simulations, there are often element distortions due to large deformation and/or poor mesh. Adaptive mesh is used to decrease the calculation difficulty due to poor mesh by replacing poor mesh with new mesh. This method is comparable to the re-meshing in the ABAQUS standard but with less calculation cost in that the re-meshing and the fine interested area mesh is updated, while adaptive mesh does not change the element numbers in the meshed domain. During adaptive mesh, the nodal and element information will be transferred from the

mesh in the previous step to the new step. Thus, adaptivity is essential to a high quality solution. In reality, adaptive mesh is typically applied at the areas where high strain gradients occur, thereby possibly resulting in extreme element distortion. Proper application of adaptive mesh can minimize calculation difficulty and obtain an accurate solution.

To define an ALE adaptive mesh, Eulerian domains should be defined on the areas where the material can flow in and flow out, and Lagrangian domains ought to be distributed where the mesh follows the material inside. The adaptive mesh method can be defined to the mesh domains so that the mesh can move independently of the material meanwhile keeping the mesh topology. In ABAQUS, users can take advantage of related functions such as mesh frequency and sweep, and the adaptive mesh constrains to optimize mesh quality. The mesh frequency defines how often the re-mesh shall take, and the mesh sweep makes the mesh smoother so the nodes in the domain can be relocated based on the current positions of neighboring nodes and elements to decrease element distortion. Adaptive mesh constraints are used to control the nodes explicitly, to free them from boundary conditions, and thus Eulerian regions can be constructed properly, with fixed nodes.

Contact Algorithms

Two kinds of contact algorithms are defined in ABAQUS Explicit to describe the contact between two surfaces: Kinematic contact and Penalty contact. Kinematic contact is the default setting in ABAQUS, and Penalty contact is used to define more general contact situations.

Kinematic contact is defined using the forces in a pure master-slave contact situation. During simulation, the Kinematic contact algorithm decides which nodes on the slave surface will penetrate into the master surface so that the suitable resistance force can be applied. In this work, the Kinematic contact is applied.

Penalty contact is a common alternative to the Kinematic contact algorithm in ABAQUS. Penalty contact uses one extra element in the model, where no stiffness is considered when a gap occurs between two surfaces. The stiffness will get a high value if contact happens. The Penalty algorithm defines one surface as the master surface and the other as a slave surface, and it can determine which slave nodes might penetrate into the master surface so that it can use corresponding forces on the slave nodes to prevent the possible penetration. In addition, there are three kinds of sliding formulations available in the contact, which are termed finite sliding, small sliding, and infinitesimal sliding. For cutting simulations, finite sliding is the optimum option, since small sliding makes the slave nodes interact in a small local region in the master nodes, while infinitesimal sliding cannot be applied to nonlinear geometry.

Friction Models

Friction force is the tangential reaction force between two surfaces in contact under a normal force. Friction force depends on different aspects, such as contact geometry, the material properties of the contact surfaces, and the relative motion of the contact bodies. Since friction can influence chip formation and heat generation, modeling friction properly is important and has been attracting interest from many researchers in the study of metal cutting. However, there is still no unified friction model which can represent the physics of the metal removal process accurately. The friction existing in metal cutting is complicated because the chip/tool interface depends on variable factors, for instance, cutting speed, feed rate, and tool geometry, such that few investigators can give reliable predictive friction models. Usui and Takeyama (1960) perform cutting experiments to investigate the shear stress and normal stress at the tool rake face so as to formulate a friction model. Figure 6 shows their findings. The shear stress keeps constant

over half of the tool chip contact length close to the tool cutting edge (see AD), termed the sticking region, and then falls to zero over the sliding region (from D to C).

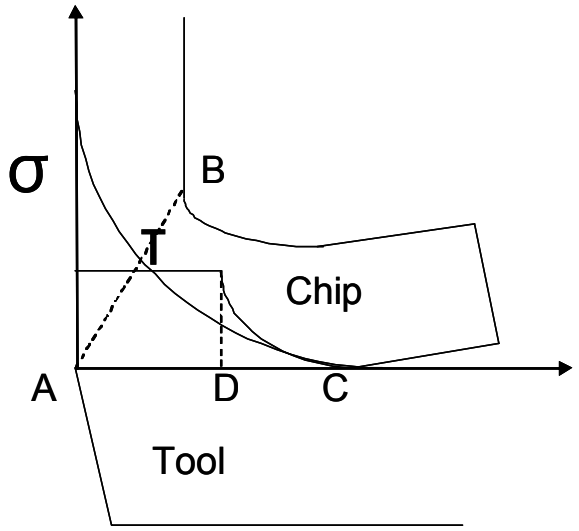

Figure 6. Stresses distribution at the tool/chip interface (Usui and Takeyama, 1960).

The values of the shear stress in the sliding and sticking regions can be calculated by the following equations:

$$\tau = \mu\sigma \text{ if } \mu\sigma < \tau_{max} \text{ (sliding)} \quad (3.1)$$

$$\tau = \tau_{max} \text{ if } \mu\sigma \geq \tau_{max} \text{ (sticking)} \quad (3.2)$$

Thereafter, various friction models at the tool/chip interface were established by some investigators. Ng et al. (2002) and Adibi-Sedeh and Madhavan (2003) present the basic Coulomb friction law. Liu and Guo (2000) investigate the tool chip friction effect on residual stress in the machined layer by employing the limiting shear stress Coulomb friction law. Arrazola, Meslin, and Marya (2003) and Sextro (2002) present devised friction models based on experiments. The Coulomb friction theory describes friction behaviour as a result of two contact surfaces adhering or interlocking with each other; thus, a tangential force is required to allow the two surfaces to slide over one another. Figure 7 shows the basic Coulomb friction law, including the relationship between shear stress and normal stress at the tool chip interface. It can be observed that the

critical shear stress distinguishes the sticking zone and the sliding zone at the tool chip interface. If the contact shear stress is under the critical shear stress, the friction will stay in the sliding region. Otherwise, the rest part of the tool chip contact region is grouped into the sticking zone. As for the limit of the shear stress, a lot of researchers choose $\sigma_y / \sqrt{3}$ as the reference value. σ_y is the yield stress of the work material adjacent to the tool chip interface. For example, Liu and Guo (2000) and Kishawy, Rogers, and Balihodzic (2002) choose this to describe the limiting shear stress. The same reference value is used in this work.

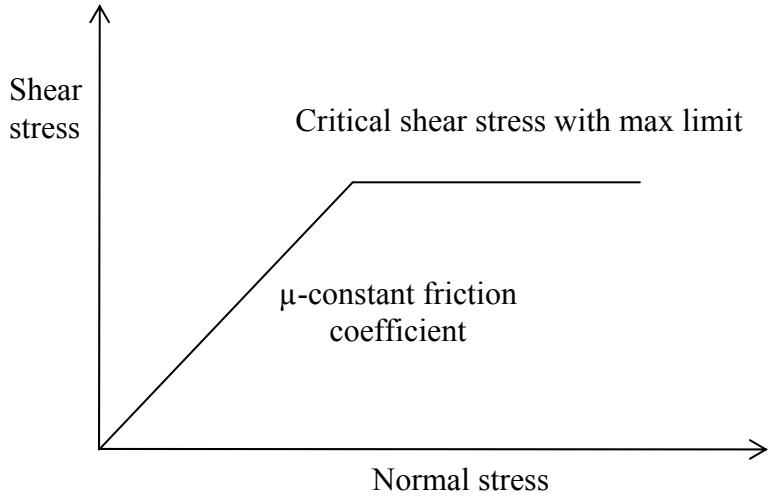

Figure 7. A simple schematic of the basic Coulomb friction law.

In addition to the above model, some researchers (Guo & Liu, 2002; Potdar & Zehnder, 2003) suggest that the friction coefficient should be related to the temperature, since the yield strength affects the critical shear stress differently depending on temperature.

Obtaining the Coulomb friction coefficient has attracted some research. Albrecht (1960) presents his attempt to estimate the friction coefficient along the tool chip interface by eliminating cutting edge effect. Arrazola et al. (2003, 2008) later obtain various friction coefficients with the application of Albrecht's method. They use variable feed rates to create the plot of the cutting feed force versus the cutting force. They find that higher coefficients exist

adjacent to the tool tip, while lower ones occur at the contact ending position for the tool chip interface.

Many researchers have attempted to formulate other firction models. Usui and Shirakashi (1982) formulate the friction force as a function of the normal force, which depends on the material combination of workpiece and tool:

$$\tau_f = k[1 - \exp(-\frac{\mu\sigma_N}{k})] \tag{3.3}$$

where τ_f is the friction stress, k is the shear flow strength of the chip at the primary zone, μ is the friction coefficient obtained from experiments related to different workpiece tool material combinations, and σ_N is the normal stress. Ozel (2006) later extends the above model with the following modification:

$$\tau_f = wk[1 - \exp(-\frac{\mu\sigma_N}{wk})^n]^{\frac{1}{n}} \tag{3.4}$$

where w and n are correction factors used to make the friction stress less than the material shear flow stress.

Heat Generation and Heat Transfer

The heat produced during machining is a critical effect on tool wear, as well as chip formation. Heat generation comes from two sources during machining, i.e., the high plastic deformation occurring in the shearing zone and the friction heat at the tool chip contact interface.

According to the majority of available literature (Mamalis et al., 2001; Shih, 1995), most plastic deformation energy, approximately 90%, is converted to heat. The heat from plastic strain can be expressed as:

$$Q^{pl} = \eta\sigma_{eqv} \bullet \dot{\varepsilon}^{pl} \tag{3.5}$$

where Q^{pl} is the heat flow rate per unit volume, η is a fraction coefficient of energy converted to heat, σ_{eqv} is the equivalent stress, and $\dot{\varepsilon}^{pl}$ is the plastic strain rate (ABAQUS manual v6.9).

Friction heat from the friction at the tool chip interface can be formulated as:

$$P_{fr} = \tau\dot{\gamma} \tag{3.6}$$

where P_{fr} refers to the frictional energy dissipation rate per unit area, τ is the frictional stress, and $\dot{\gamma}$ is the slip rate at the chip tool interface.

Heat dissipation between chip and tool along the contact interface decides how much heat goes to chip and tool. It can be represented by:

$$q_{chip} = f_w \eta P_{fr}, \quad q_{tool} = (1 - f_w)\eta P_{fr}, \tag{3.7}$$

where q_{chip} is the heat flux into the chip surface, f_w is the weighting factor between the interacting surfaces, and q_{tool} is the heat flux into the tool surface. f_w is determined by:

$$f_w = \frac{E_{chip}}{E_{chip} + E_{tool}} \tag{3.8}$$

$$E_{chip,tool} = \sqrt{K_{chip,tool}\,\rho_{chip,tool}\,C_{\rho chip,tool}} \tag{3.9}$$

where K_{chip}, ρ_{chip}, and $C_{\rho chip}$ are the thermal conductivity, density, and specific heat of the chip, respectively, and K_{tool}, ρ_{tool}, and $C_{\rho tool}$ are the thermal conductivity, density, and specific heat of the tool, respectively (Ng et al., 2002).

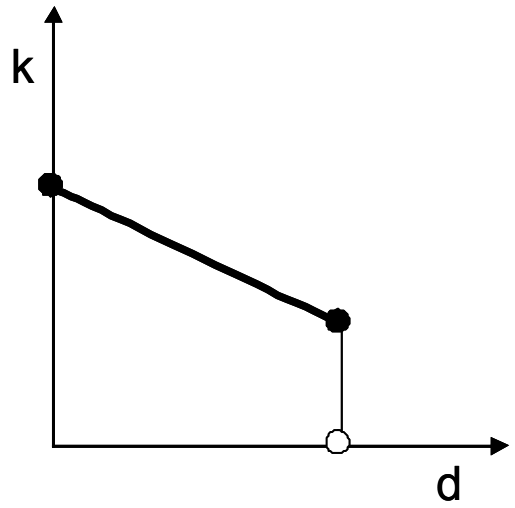

Figure 8. Gap heat conductance model.

Heat conduction between chip surface and tool surface is a function of gap conductance, k, and the temperatures of the surfaces, θ_A and θ_B. The heat flow rate per unit area can be formulated as:

$$q = k(\theta_A - \theta_B) \tag{3.10}$$

The gap conductance is dependent on the average temperature on the surfaces, gap clearance, d, surface pressure, p, and the average of any predefined field variable (ABAQUS manual 6.8). In this research, the gap conductance is a function of the gap clearance, d, shown in Figure 8.

Summary

In this chapter, finite element modeling of orthogonal cutting is introduced. The main portions of finite element modeling for orthogonal cutting, such as adaptive mesh for decreasing element distortion, contact algorithms in dynamic simulation, common friction models for metal cutting, and heat generation and heat transfer during cutting, are described. These lay the fundamentals for later finite element modeling of cutting simulation with a diamond-coated tool.

CHAPTER 4

2D CUTTING SIMULATIONS WITH A DIAMOND-COATED TOOL INCLUDING DEPOSITION RESIDUAL STRESSES

Introduction

Advanced surface engineering technologies such as chemical vapor deposition (CVD) have been widely applied for wear resistant functions. CVD-grown diamond films have also been explored for various tooling applications. Coating delamination has been identified as the major failure mode of CVD diamond-coated tools (Chou & Liu, 2005). High thermal and mechanical loading during machining and insufficient coating adhesion result in coating failure and catastrophic wear. Moreover, the thermal mismatch between the diamond coating and the carbide substrate generates high residual stresses, on the order of GPa, in the tool. Besides, the cutting edge results in severe stress concentrations around the tool tip, which will strongly affect the tool performance (Renaud et al., 2008).

While the cutting edge geometry affects the deposition stresses around the tool tip, it also complicates the thermal and mechanical loads imposed during machining. The radius edge can significantly affect the chip formations and stress/temperature fields, especially when the uncut chip thickness is close to or smaller than the edge radius, known as the "size effect" (Schimmel, Endres, & Stevenson, 2002; Fang & Xiong, 2008).

The literature on cutting edge effects on diamond-coated tool performance is limited. Almeida et al. (2005) investigate edge preparations of diamond-coated tools in machining hard metals. Three types of edge conditions, up-sharp, chamfer, and hone, were tested. The edge

conditions are found to be significant in machining forces, wear pattern, and tool life. The authors report that coating delamination occurred first at the honed tool. Hu et al. (2007) investigate stress evolutions in a diamond-coated tool using 2D analysis, from deposition to machining, with simplified machining load conditions. It is reported that at a low feed, increasing the edge radius will reduce the maximum circumferential normal stress. However, the edge radius seems to have minor effects at a high feed. It has been demonstrated that the edge radius plays a critical role in machining by diamond-coated tools (Qin et al., 2009). In particular, at the 1.3 m/s and 0.15 mm/rev condition, a 65 μm hone extends the tool life 5 times over the 5 μm sharp tools, though tools of either radii have a similar tool wear results at the 4 m/s and 0.05 mm/rev condition.

It is not clear how the cutting edge affects the machining performance of diamond-coated tools. To effectively use diamond-coated tools, it is essential to understand the combined effects of the edge radius, due to the film deposition during subsequent machining. Compared to experimental approaches, numerical simulations for studying machining processes are more affordable. Finite element (FE) modeling has been applied frequently in machining simulations. Mackerle (1999) compiles a bibliography of literature about most machining simulations. The studies can be grouped into the following topics: (i) material removal and cutting processes in general, (ii) computational models for specific machining processes, (iii) the effects of geometric and process parameters, (iv) thermal aspects in machining, (v) residual stresses in machining, (iv) dynamic analysis and control of machine tools, (vii) tool wear and failure, and (viii) the chip formation mechanism. In general, there are two types of models for numerical analysis in modeling deformation processes: Eulerian and Lagrangian. The Lagrangian method requires the computational grid to deform with the material, while the Eulerian requires the grid to be fixed in

space. The Lagrangian formulation also requires chip separation criteria. In recent years, more researchers are using the Arbitrary Lagrangian Eulerian (ALE) technique to combine the features of pure Lagrangian analysis and Eulerian analysis. Ozel and Zeren (2007) investigate the influence of edge roundness on the stress and temperature fields induced by high-speed machining. Kishawy, Deiab, and Haglund (2008) use ALE analysis to investigate cutting with a honed tool. As for diamond tools, Liu and Melkote (2007) investigate the influence of tool edge radius on the size effect in orthogonal micro-cutting processes using FE. For coated tools, MacGinley and Monaghan (2001) model an orthogonal machining process using coated cemented carbide cutting tools with FEA package FORGE2. Grzesik, Bartoszuk, and Nieslony (2005) investigate temperature distribution on coated carbide tool in orthogonal cutting of steels. Yen et al. (2004) investigate cutting temperature in orthogonal cutting with a multilayer-coated (TiN-Al2O3-TiC) carbide tool. Al-Zkeri et al. (2009) study optimization of the cutting edge geometry of physical vapor deposition (PVD) coated carbide tools in the dry turning of steels using a finite element analysis with Deform-2D software. Olortegui-Yume, Park, and Kwon (2008) used ALE to investigate the tool wear of coated carbides in machining 1045 steel.

Literature focused on machining simulations with CVD diamond-coated tools is rather rare. Furthermore, cutting simulations have not considered deposition residual stresses. In this Chapter, orthogonal cutting simulations with a diamond-coated tungsten carbide (WC) tool are developed to include residual stresses in the tool from depositions. The objective is to numerically investigate the combined deposition and machining effects on the thermal and mechanical states of diamond-coated tools in 2D cutting. In particular, the role of the edge radius and its impact on resultant interface stresses at different cutting conditions are emphasized. First, FE modeling is used to evaluate the deposition stresses in tools with different edge radii. Second,

the tool with deposition stresses is imported into FE software to continue cutting simulations under different cutting conditions. The coating-substrate interface stresses were further analyzed.

Deposition Stress Analysis

Model and Simulations

Diamond-coated cutting tools were modeled in ABAQUS/CAE version 6.8, according to a simplified geometry: 2D inserts that are 2 mm wide and 1 mm thick with a 79° wedge angle and different edge radii, 5 or 50 μm. The diamond coating on the substrate has a uniform thickness at the rake, 15 μm, and at the flank surface, the coating extends to the substrate bottom. The CAD models of the tool (substrate and coating) are then imported into ABAQUS/Explicit for thermal stress simulations. Four-node bilinear displacement and temperature quadrilateral elements (CPE4RT) are used for structural analysis.

Convergence Test for a Typical 2D Insert

The tested 2D insert has an edge radius of 50 μm and a coating thickness of 15 μm (re50t15). The wedge angle and the other geometry parameters are the same as specified in the prior section. In this convergence test, two simulation schemes, couple thermal displacement in standard mode and dynamic couple thermal displacement in explicit mode, and three specifications of mesh density, 3 layers, 5 layers, and 15 layers, on coating, are investigated. Deposition condition is the same condition as shown above. In this convergence test, stress contours along the Y direction are compared. Interface stresses located at the coating side are examined. The interface stress extracted method can be referenced in Renaud et al. (2008).

Figure 9 demonstrates the σ_y component result of the static mode and explicit mode for two different coating layers, 3 and 15. From the contours, it can be observed that the stress are very close even though the explicit mode is not as smooth as the standard mode.

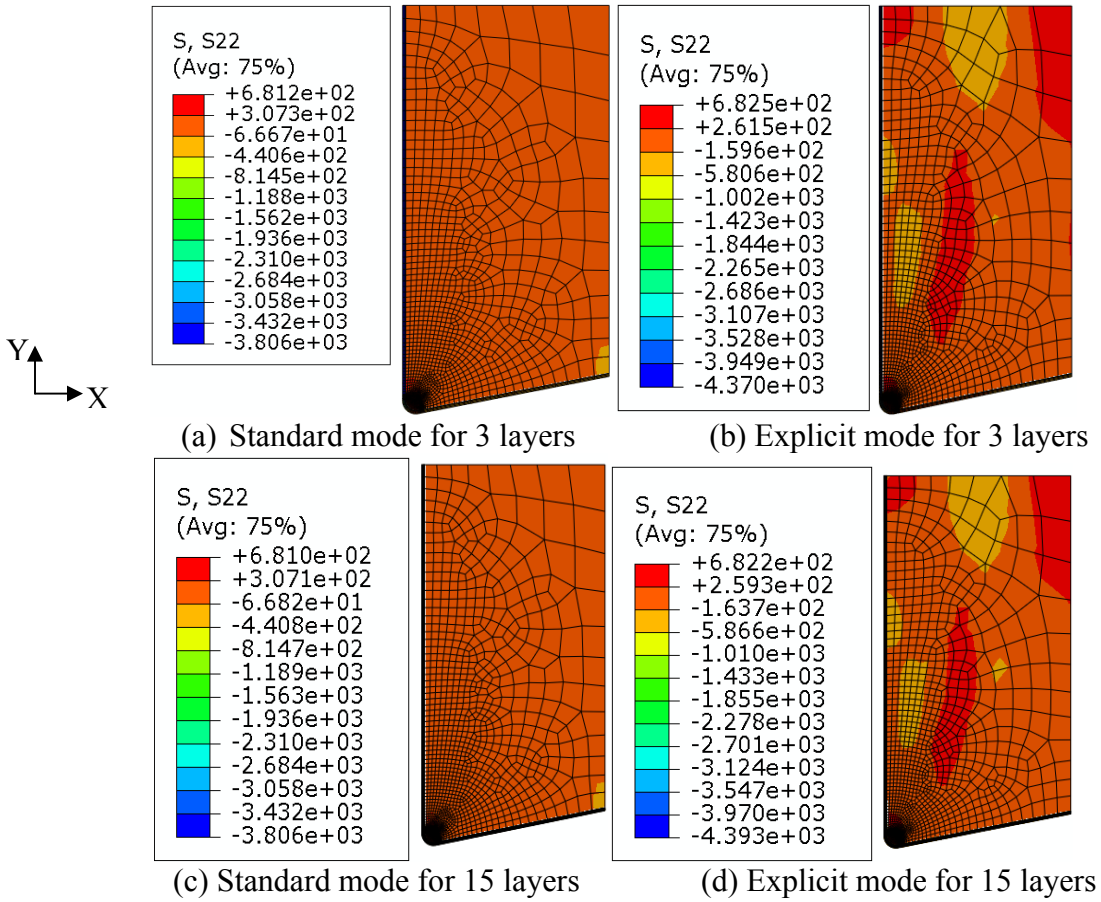

Figure 9. σ_y component result of standard mode and explicit mode for different coating mesh density (unit: MPa).

A quantitative comparison is made according to the interface stress-normal stress normal to the interface termed σ_r. Interface stress is converted from the Descartes coordinate system to the polar coordinate system. The positive direction points from the intersection of the radius and the rake face with the flank face. Figure 10 schematically illustrates the interface stress components to be extracted from simulations results, including three components: radial normal stress (σ_r), circumferential normal stress (σ_θ), and shear stress ($\tau_{r\theta}$).

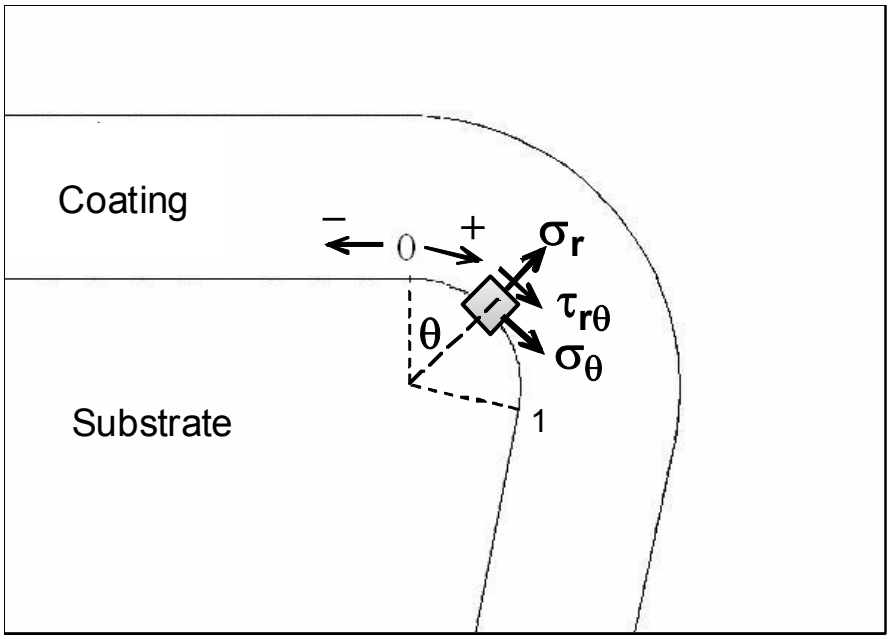

Figure 10. A schematic drawing showing the interface stress components around the edge area.

Figure 11 plots the interface stress results at different modes. It is observed that the larger the number of mesh layers on the coating the higher interface stress σ_r. Furthermore, simulation modes do not significantly affect the interface results.

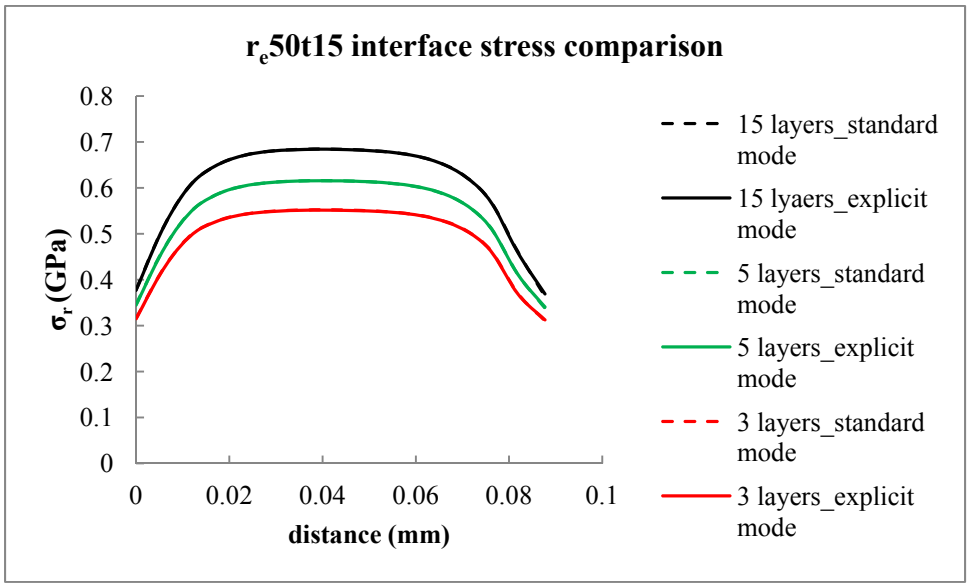

Figure 11. Interface stress comparison for re50t15 under different simulation modes and three various mesh densities.

Figure 12 (unit: GPa) is the column contour of the maximum interface stress σ_r for the three mesh densities under the two simulation modes.

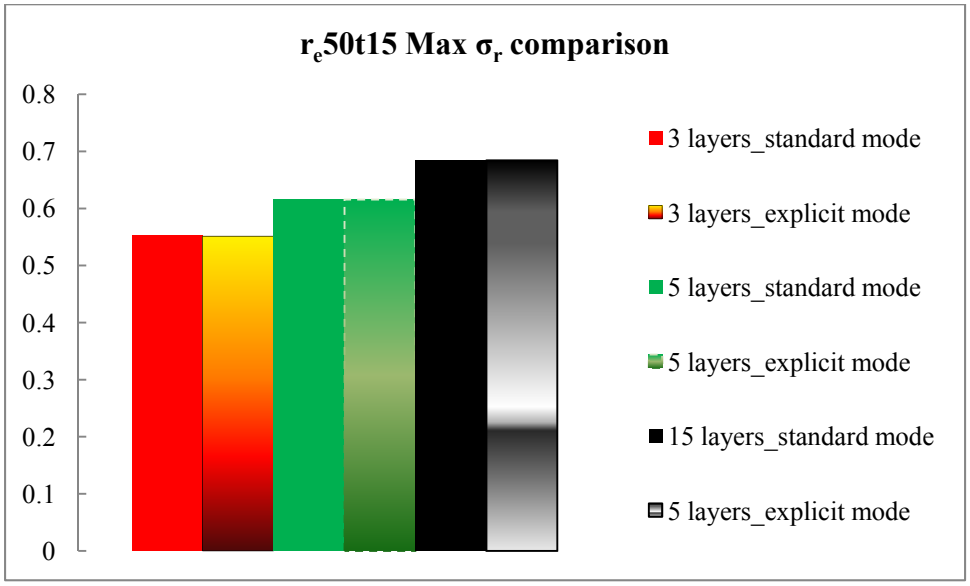

Figure 12. Maximum σ_r comparison for different conditions.

Figure 13 plots the ratio of the three explicit mode results with the reference value, which is valued from 15 layers of mesh density under the explicit mode. Three and five layers of mesh result in 19% and 10% distance from the reference value, respectively.

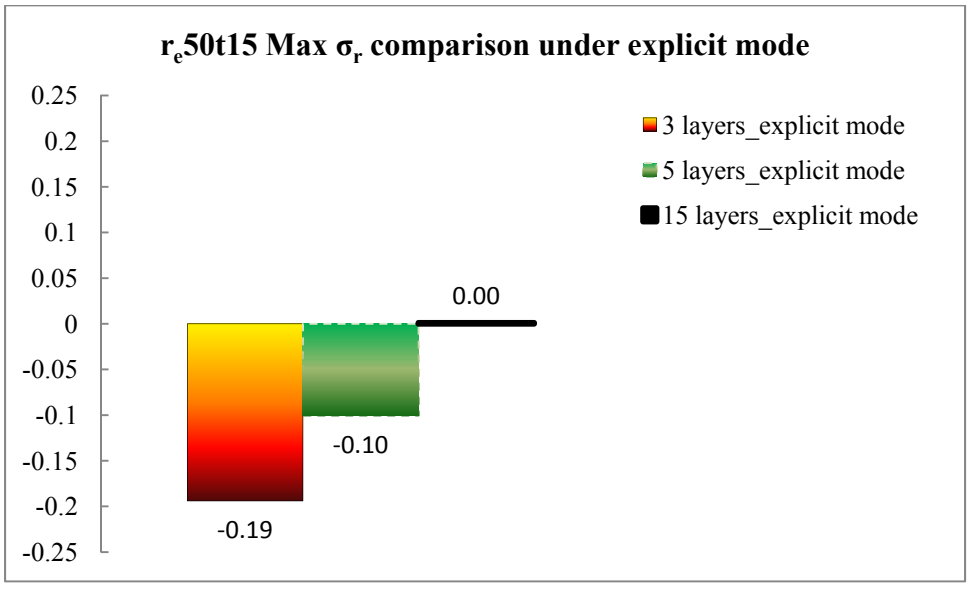

Figure 13. Comparison with the reference value of 15 layers mesh density.

However, due to limitation of the computation facility, three layers of mesh is chosen as the consistent consideration. The following section continues the residual deposition stress simulation for the explicit mode and its result.

Explicit dynamic analysis considering thermal strains is conducted. A uniform deposition temperature of 800°C was set as the initial condition, and a room temperature of 25°C was set as the final temperature. Linear-elastic material models independent of temperatures are used for both diamond and WC tools. The elasticity, Poisson's ratio, and the thermal expansion coefficient of diamond (Heath, 1986) and WC (Amirhagni et al., 2001) are 1200 GPa, 0.07, 2.5 μm/(m·K), and 620 GPa, 0.24, 5.5 μm/(m·K), respectively. After the model setup, the analysis is executed to obtain displacement, strain, and stress data.

Figure 14 shows the stress contours (σ_y component, parallel to the rake, unit: MPa) in a diamond-coated tool with a 50 μm edge radius. It can be noted that the stress in the coating, away from the edge is about 3.5 GPa in compression, which is consistent with the previous analysis (Hu, Chou, & Thompson, 2007b). Moreover, the stress distribution around the tool edge shows considerable stress concentration.

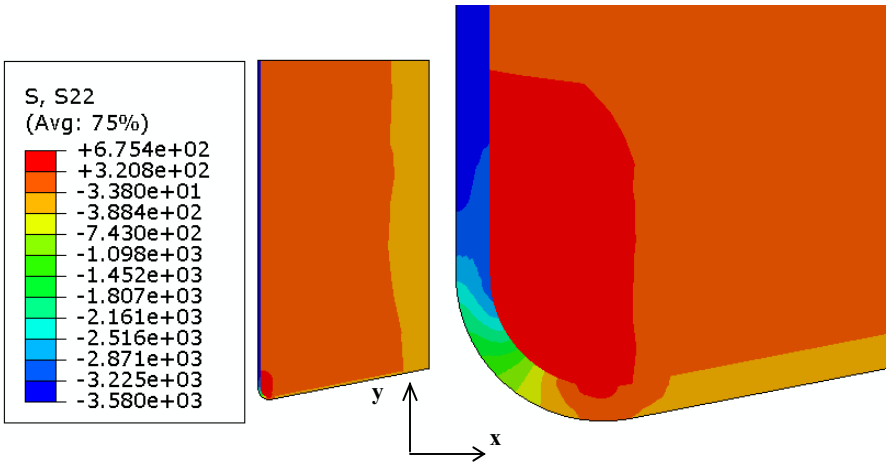

Figure 14. Deposition stress contour, normal stress parallel to rake face (50 μm edge radius).

Further, the stress data along the interface can be extracted and then transformed into the local polar coordinate to evaluate the interface stresses along the cutting edge, including three components: the radial normal stress (σ_r), the circumferential normal stress (σ_θ), and the shear stress ($\tau_{r\theta}$), which are functions of the location. The procedures were detailed in Renaud et al., (2008). The deposition stress profiles at the interfaces will be shown in the following cutting simulation section.

Cutting Simulations

Modeling Details

The modeled diamond-coated tool is then imported into the cutting simulation, carrying the deposition stress states. The ALE formulation is adapted for orthogonal cutting simulation, also using the ABAQUS/Explicit. The same element type (CPE4RT) is used for the workpiece. The cutting tool is assumed as a deformable body. The Coulomb friction model between the workpiece and the diamond coating is implemented with a frictional coefficient of 0.6. The variable friction modeling is composed of the sticking region and the sliding region with parameters μ and K_{chip} (K_{chip} = 143MPa, μ=0.6), which can be referenced in the work of Ozel & Zeren (2007). The heat flowing into the chip is obtained using the following analysis (Ng et al., 2002):

$$f = \frac{E_c}{E_c + E_t}, \tag{4.1}$$

$$E_{t,c} = \sqrt{K_{t,c}\rho_{t,c}C_{pt,c}}, \tag{4.2}$$

where $K_{c,t}$ is the thermal conductivity of the chip or tool, $\rho_{t,c}$ is the density of the chip or tool, $C_{pt,c}$ is the specific heat of the chip or tool, and the fraction of the heat energy conducted into the chip is calculated as f = 0.75.

The Johnson-Cook (J-C) material constitutive model is implemented for its simplicity and the availability of material parameters (Johnson & Cook, 1983). The J-C constitutive model, applied for metal deformation simulations with large strains, high strain rates, and high temperatures, is used for AA356-T6 as the workpiece material. It can be expressed as:

$$\sigma = (A + B\varepsilon^{n})(1 + C\ln\tilde{\varepsilon}^{*})(1 - T^{*m}), \quad (4.3)$$

where σ is the stress, ε is the equivalent strain, $\tilde{\varepsilon}^{*} = \tilde{\varepsilon}/\tilde{\varepsilon}_{0}$ is the dimensionless strain rate, and A, B, C, n, and m are the material constants from Sartkulvanich, Sahlan, and Altan (2007), listed in Table 1 below. T^{*m} is equal to $(T\text{-}T_r)/(T_m\text{-}T_r)$ where T_r is a reference temperature (20 ℃) and T_m is the melting temperature of the workpiece. Other general material properties for the substrate, the coating and the workpiece, are listed in Table 2.

Table 1

Surface Workpiece Material Constitutive Constants

Material Constants for J-C model (AA356.0-T6)					
A(MPa)	B(MPa)	C	N	m	Tm
0	477	0.0067	0.144	1.62	585

Table 2

Material Properties

Items	(AA356.0-T6)	WC-Co	Diamond
Young's modulus, E(GPa)	72.4	620	1200
Poisson's ratio	0.33	0.24	0.07
Thermal conductivity, (W/m-°C)	151	84.02	900
Specific heat (J/g-°C)	0.963	2	0.509
Density(g/mm^3)		15.8	3.5
Thermal expansion (m/m-K)		5.5E-6	2.5E-6

The tool is modeled as an orphan mesh deformed part and imported from the previous deposition stress analysis result. Here, the assembly is different from general ALE cutting simulations with a coated tool. Because the tool deforms in the deposition stress simulations, it is challenging to make the workpiece match the tool perfectly. In the case of mesh penetration, the initial contact does not match perfectly with the outer profiles of the workpiece and the tool. A small distance was added between the tool rake face and to the right side of the initial chip to minimize assembly difficulty. This method is practical and only needs some additional cutting time to reach steady state. The assembly of the workpiece and the tool is shown in Figure 15.

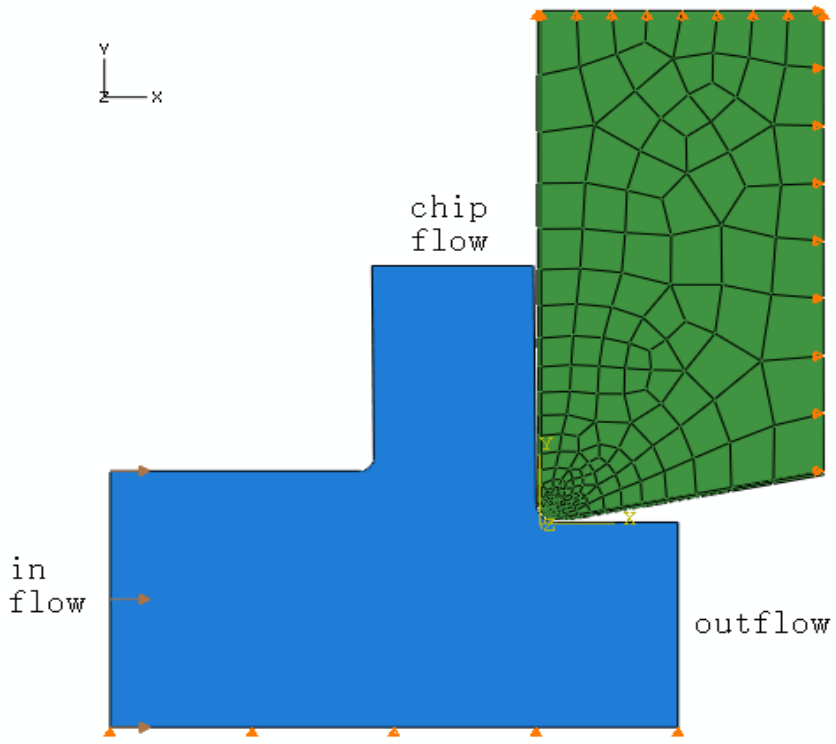

Figure 15. Assembly of workpiece and tool.

In the cutting simulation, the ALE method is employed. The material flows in from the left side of the workpiece and exits at the right side of the workpiece and the top side of the chip. Thus, the right side and left side of the workpiece and the top of the chip are defined as the

Eulerian boundaries. Other boundaries on the workpiece are defined as Lagrangian boundaries. Adaptive mesh constraints are used to constrain the inflow boundary in the x and y directions, to constrain the outflow boundary in the x direction, and to constrain the chip flow boundary in the y direction. Constraints are also imposed at the top surface of the tool material in the y direction and at the right side of the substrate in the x direction. The workpiece material is constrained in the y direction. The material flows in at the cutting speed. The initial temperature of the workpiece is 20 ˚C. The workpiece deformation zone region is defined as the adaptive mesh domain. The established ALE method was first validated against known results from the literature (Kishawy, Deiab, & Haglund, 2008) using a cemented carbide tool and AISI 4140 steel workpiece. The cutting parameters are 0.2 mm uncut chip thickness (h) and 200 m/min cutting speed (V). The differences between the current results and the literatures in the maximum von Mises stresses and tool temperatures are less than 4 %.

Once validated, cutting simulations with a diamond-coated tool inherited with deposition stresses are conducted. The initial stress state of the tool comes from the residual deposition stress analysis. Two levels of edge radii (r_e), 5 μm and 50 μm, and two different cutting conditions were tested: (1) 3.0 m/s (V) and 0.05 mm (h), representing the thermal-load dominant case, and (2) 1.0 m/s (V) and 0.15 mm (h), for the mechanical-load dominant case. The rake and relief angles were 0° and 11°, respectively. The set simulated cutting time is 0.3 ms. A total of 529 CPE4RT elements are distributed in the workpiece. Mesh needs to be denser close to the edge radius. The elements and properties of the tool are the same as in the residual deposition stress analysis. For a larger uncut chip thickness, more elements should be used in the primary shear zone.

Results and Discussion

Figure 16 illustrates an example of typical stress contours (von Mises stress) from the simulation. The parameters in this specific case were 3 m/s (V) and 0.05 mm (h) and a 5 µm edge radius. It can be seen that high deposition stresses are still dominant, only marginally altered by the cutting load in this gentle cutting condition. As shown in Figure 16b, the stress level in the chip is substantially lower than the tool stresses.

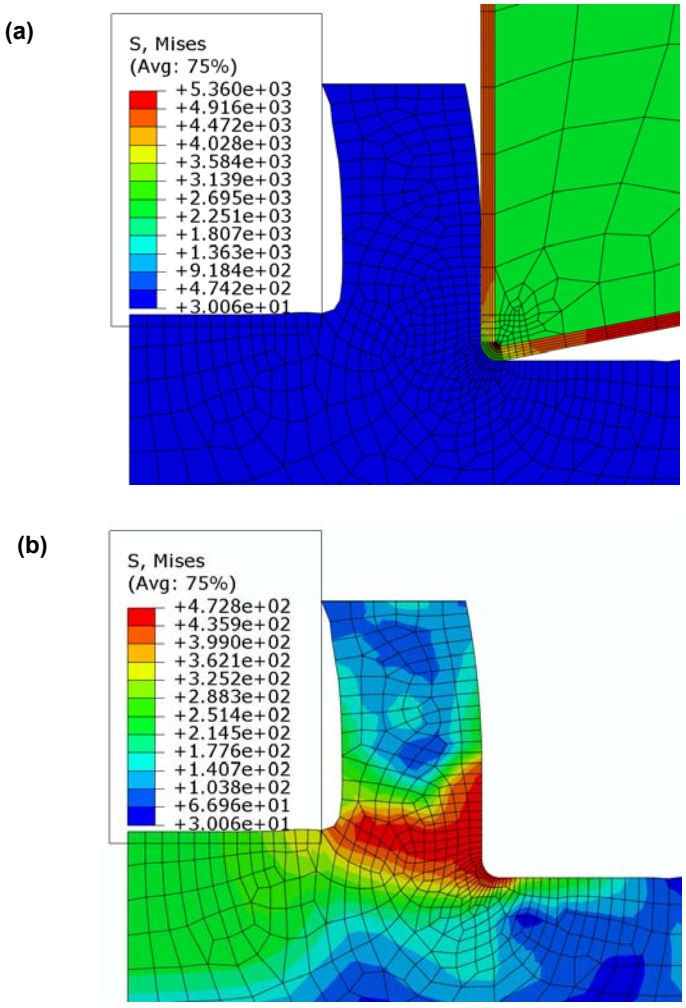

Figure 16. An example of simulated stress contours (v=3.0 m/s, h=0.05 mm, r_e=5 µm): (a) overall and (b) chip and workpiece.

A case (3 m/s, 0.05 mm) without deposition stresses in the tool was also tested for comparison purposes. The tool still has the diamond coating and the WC substrate with the same

properties. Figure 17 demonstrates the importance of the deposition residual stresses (unit: MPa), showing much greater first principal stresses for the case with deposition stresses included. Moreover, unreasonably high stress concentrations occur around the edge area for the case without deposition stresses considered.

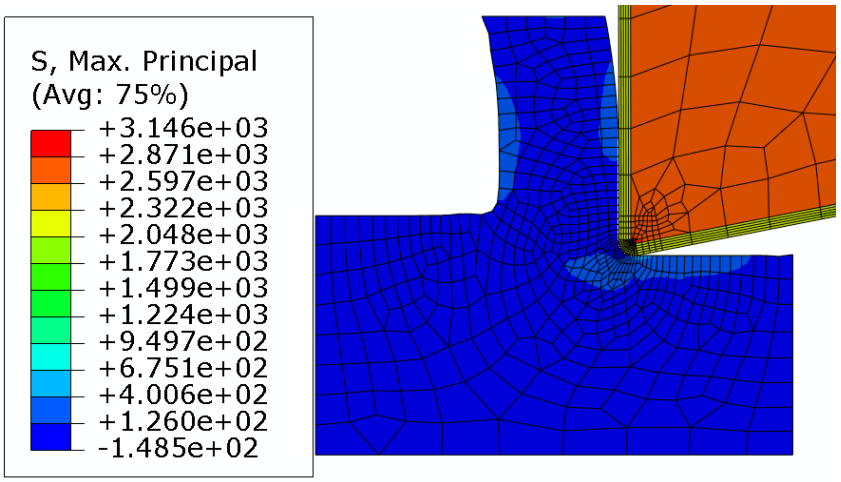

(a) with deposition stresses

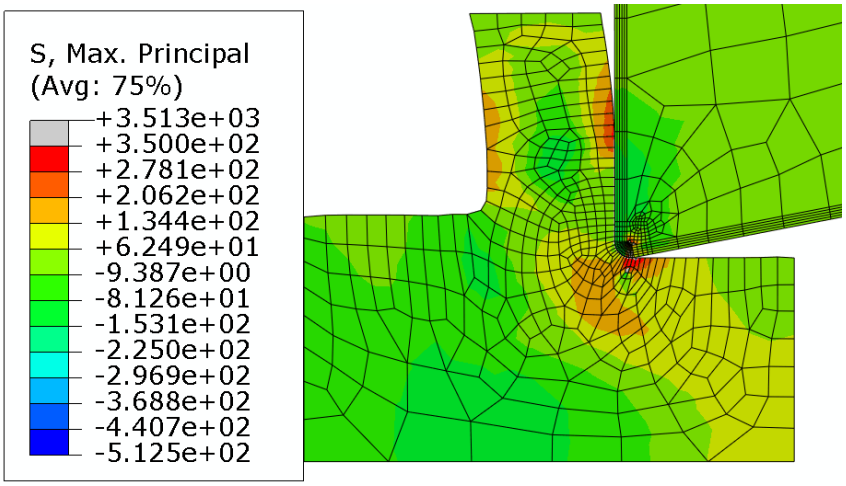

(b) without deposition stresses

Figure 17. Stress contour comparisons (v=3.0 m/s, h=0.05 mm, r_e=5 μm): (a) with deposition stresses; (b) without deposition stresses.

Figure 18 compares the first principal stress (unit: MPa) contours at different edge radii and different cutting conditions. It shows higher stress concentrations at the coating interface. A

similar phenomenon was also reported in previous research (MacGinley & Monaghan, 2001). This tends to increase the possibility of cracking in the coating. It is also noted that a smaller edge radius may result in a higher level of stress, especially at larger uncut chip thickness.

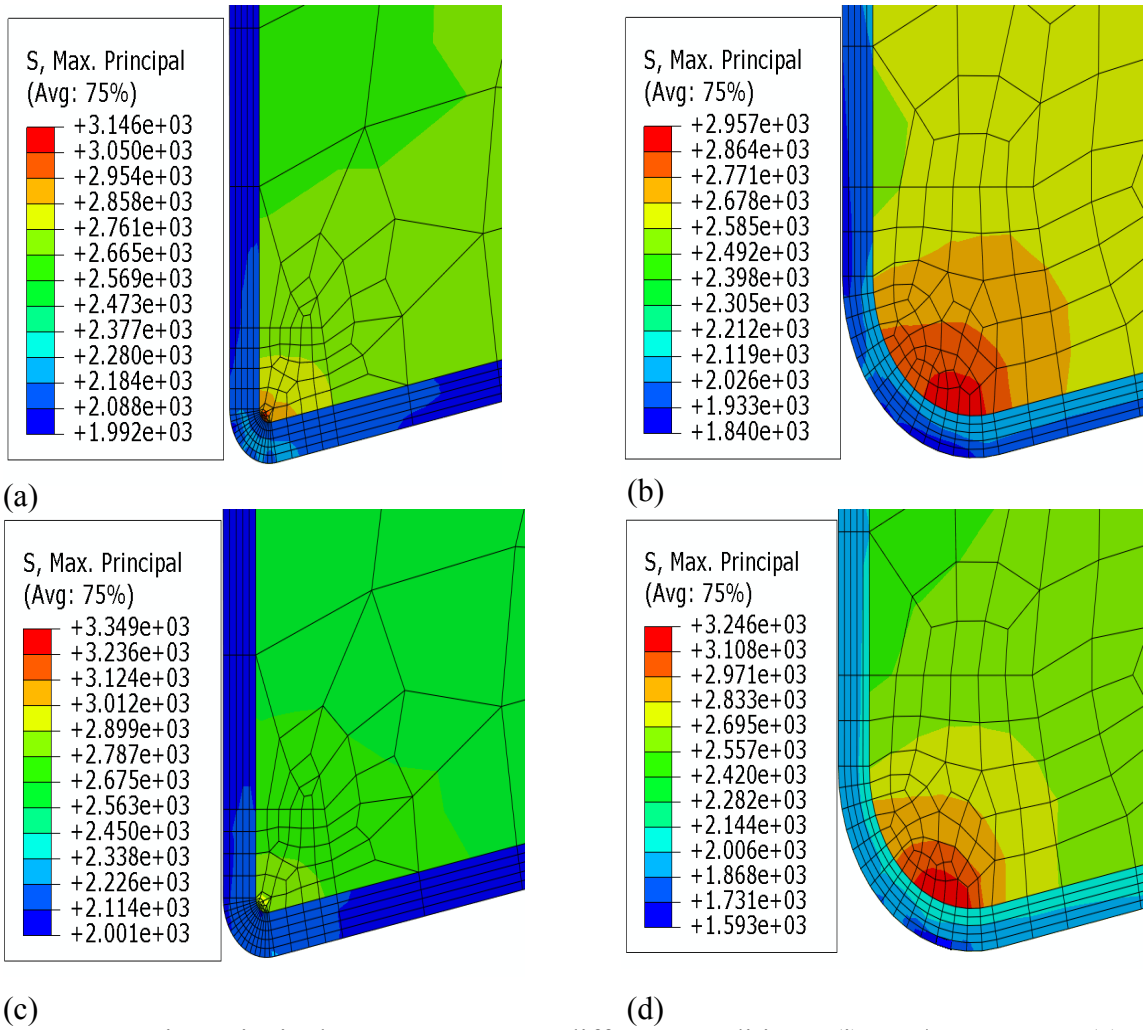

Figure 18. First principal stress contours at different conditions: (i) 3 m/s, 0.05 mm: (a) r_e=5 µm, (b) r_e=50 µm; and (ii) 1 m/s, 0.15 mm: (c) r_e=5 µm, (d) r_e=50 µm.

Figure 19 compares tool temperature distributions from different simulation cases. Under the current simulated cutting conditions, tool temperatures seem to be typically low. Increasing the uncut chip thickness will elevate the cutting tool temperatures. In addition, increasing the edge radius will also increase the tool temperature and the maximum temperature at the edge rounding area. Due to the size effect, for smaller uncut chip thicknesses, the high temperature

concentrates around the cutting edge because of the chip-tool contact length. The high temperature shifts from the rake face toward the round edge when the edge radius is greater than the uncut chip thickness. Possibly, it is due to the workpiece material flowing downward along the tool edge profile, and which is then compressed into the bulk material beneath the tool (Yan, Zhao, & Kuriyagawa, 2009).

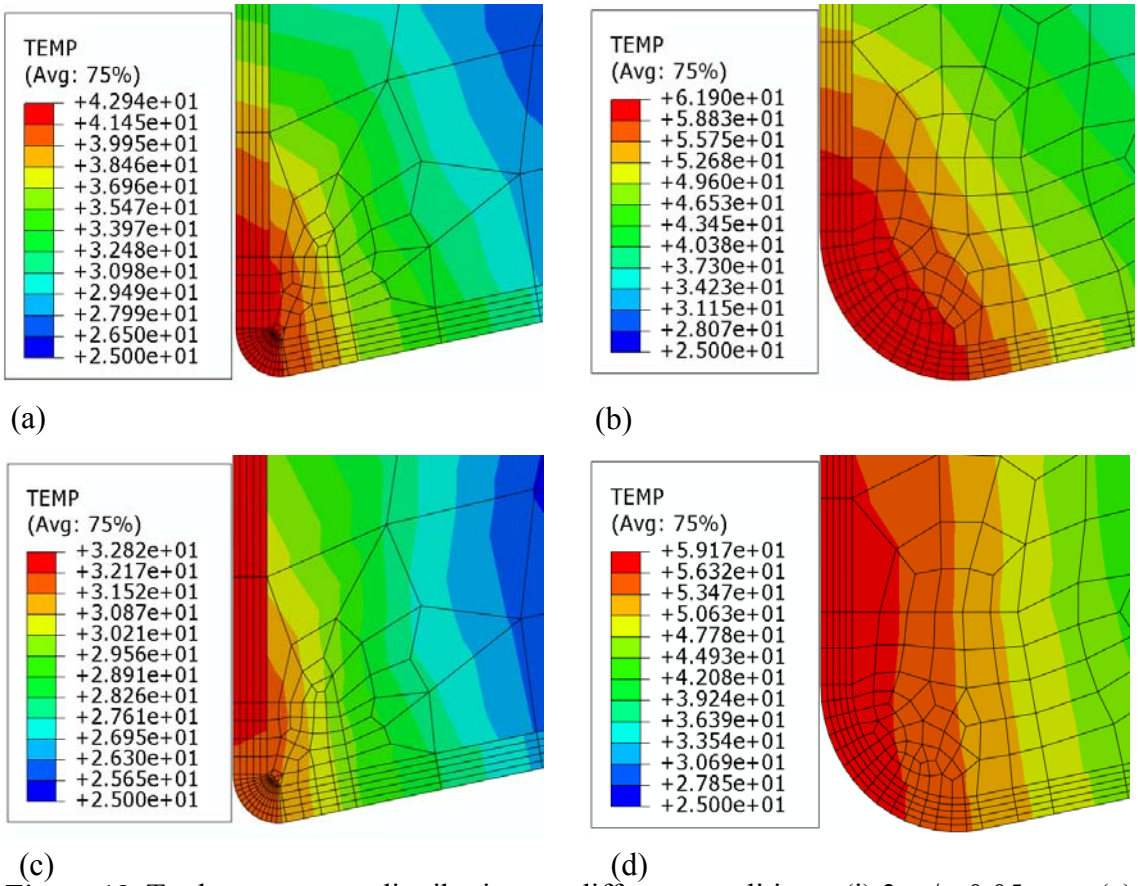

Figure 19. Tool temperature distributions at different conditions: (i) 3 m/s, 0.05 mm: (a) r_e=5 µm, (b) r_e=50 µm; and (ii) 1 m/s, 0.15 mm: (c) r_e=5 µm, (d) r_e=50 µm.

The interface stresses are crucial to coating delamination. Thus, the interface stresses around the cutting edge are further analyzed.

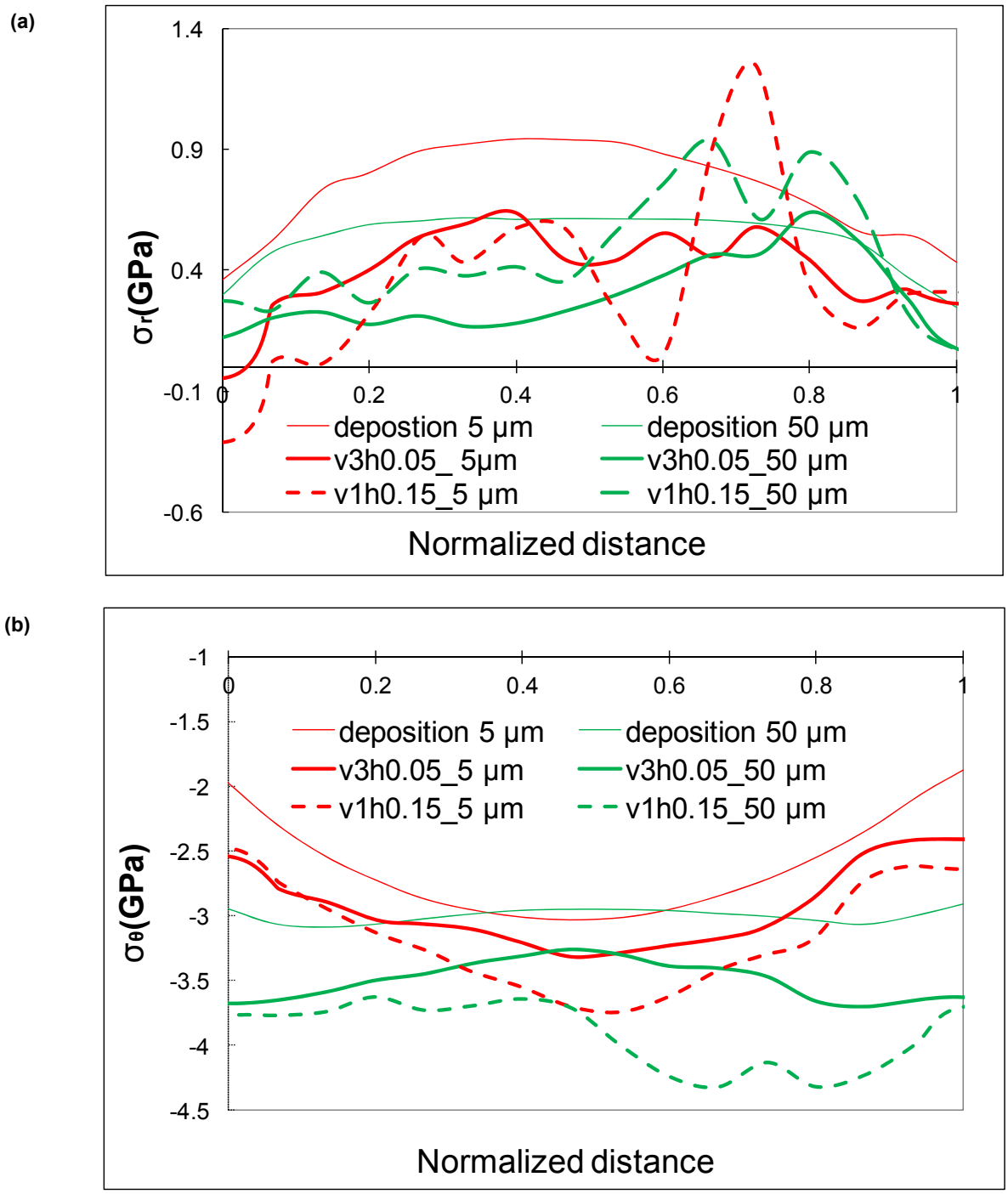

Figure 20. Interface stress profiles at different conditions: (a) radial and (b) circumferential normal components.

Figure 20a plots the interface radial normal stresses around the tool edge at 4 different conditions, plus the stresses due only to deposition. First, the edge radius effects on the radial

normal stresses are evident, as reported before. Moreover, at a smaller uncut chip thickness, the stress level is marginally reduced by contact stress from the chip. The maximum σ_r is in a close range between different edge radii. However, at a larger uncut chip thickness, the radial normal stresses change noticeably due to machining, especially high tensile stresses close to the end of the edge rounding (transition to flank surface). It is noted that the maximum σ_r is greater for the 5 μm edge: 1.2 GPa vs. 0.9 GPa for 50 μm.

The circumferential normal stress profiles around the edge are shown in Figure 29b for different conditions, also including plain deposition stresses, ~ 3 GPa in compression. Again, a smaller uncut thickness has little effect on stress, and the edge radius effect is minor. However, a larger uncut thickness will induce more compressive stresses, and the larger edge radius shows a greater compressive stress at the edge end close to the flank side.

A previous experimental study (Qin, 2009) shows that at a small feed, the edge radius has little effect on diamond-coated tool wear. However, at a larger feed, a larger edge radius can extend tool life drastically. Results from the previous and current studies indicate that the edge radius effects on the interface stresses may play a crucial role to delamination wear of diamond-coated tools.

The following section comes from the work of Ivester et al. (2012), which provides a detailed experimental validation for the 2D cutting simulation.

Experimental Validation

Cutting Tool Preparations

The substrates used for the diamond coating experiments are grooving type inserts (A4G-U-B-6) from Kennametal Inc. The insert material selected was fine-grain WC with 6 wt.% cobalt (K68 from Kennametal). The edge radius of cutting inserts, measured by a white-light

interferometer, NT1100 from Veeco Metrology, was about 25 μm. To facilitate temperature measurements (by infrared thermography), the side relief surface near the cutting edge is precision-ground to flat.

For the coating process, diamond films are deposited using a high-power microwave plasma-assisted CVD process. A gas mixture of methane in hydrogen is used as the feedstock gas. Nitrogen, maintained at a certain ratio to methane, is inserted to the gas mixture to obtain nanostructures by preventing cellular growth. The pressure is about 90 Torr, and the substrate temperature is about 800°C. The coated inserts are further inspected by the interferometer to measure the edge radius and to estimate the coating thickness. The coating thickness was estimated between 20 and 25 μm. Surface roughness, R_a, is about 0.5 μm for coated tools.

Workpieces

The workpieces are thin disks (127 mm diameter, 3 mm thick), with a hub (25.4 mm diameter), precision machined from a bar stock made of an A356 aluminum alloy that was cast and heat treated (supplied by General Motors). This particular alloy is chosen because of the material properties reported in studies using it in FE cutting simulations (Sartkulvanich, Sahlan, & Altan, 2007).

The 2D cutting test-bed is modified from an Edgetek grinding machine, with multiple sensors added. Figure 21a shows the machine, and Figure 21b shows the cutting tool and workpiece arrangement in the machine.

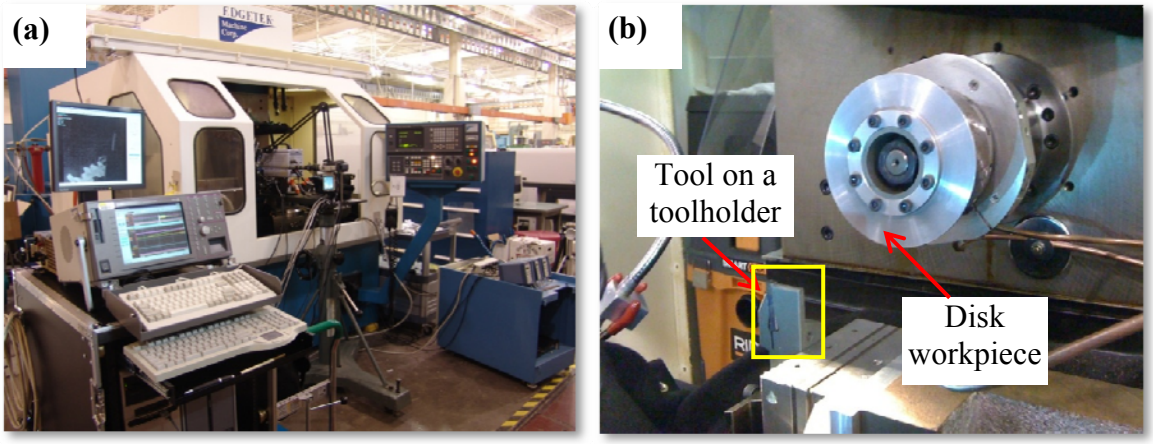

Figure 21. Experiment setup: (a) 2D orthogonal cutting test-bed, and (b) Workpiece and tool arrangement in the machine.

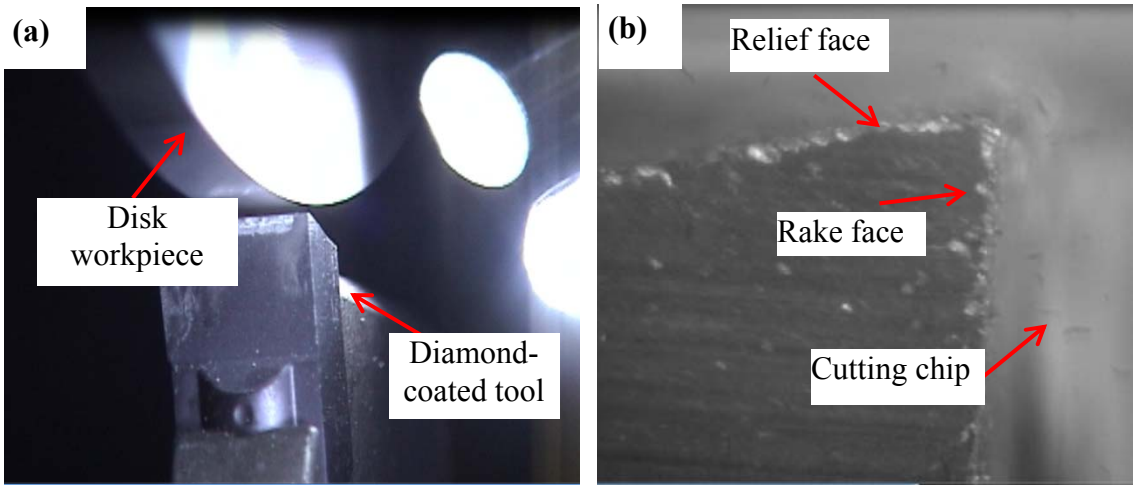

Figure 22. Setup for workpiece and tool: (a) Closed-up view of tool and workpiece setup, and (b) Side view of a diamond-coated tool tip.

Figure 22 depicts (a) the setup of a diamond-coated tool and the disk-shaped workpiece, and (b) the side view of a diamond-coated tool tip. A digital oscilloscope records the dynamometer signals at a sampling rate of 2 MHz before down sampling to 500 Hz for analysis. A high speed visible light camera (shutter speed of 30 000 frames per second (fps), integration time of 33 μs) and a medium speed infrared camera (600 fps shutter speed, 10 μs to 25 μs integration time, 3 μm to 5 μm wavelength) simultaneously record the cutting process. The disk-shaped workpiece rotates on the horizontal spindle and moves on a vertical axis (feed direction).

Synchronizing the dynamometer, the visible light camera, and the infrared camera signals by reading each signal with an oscilloscope at 2 MHz sampling rate provides confidence the signals represent nearly identical instances in time. Further details are described by Heigel, Ivester, and Whitenton (2008).

Testing Parameters

The toolholder used is an A4SML 160624, 25.4 mm steel shank holder. The resulting cutting geometry is 7° of rake angle and 4° of relief angle. The uncut chip thickness (h) value is 0.15 mm. The cutting speed (V) tested is 5 m/s. The linear cutting length is over 5 revolutions, to be sure of full uncut thickness. The machining is conducted at room temperature without coolant. In each cutting test, cutting forces and tool temperatures are acquired and further analyzed using MATLAB scripts developed at NIST (Ivester, 2011). For infrared temperature measurements, the emissivity of diamond-coated tools is determined by heating up the tools to a range of temperatures and measuring them with a thermocouple and an infrared camera. The emissivity is between 0.72 and 0.79 for a temperature range of about 150°C to 200°C. Linear extrapolation is used for the temperature range outside of the emissivity testing range.

Experimental Results and Discussion

The post-processed data from the experiment is plotted and compared. The section below presents the cutting variable plots/contours for different cutting conditions. Figure 23 shows the cutting force history from a typical cutting test with steady state forces of about 400 N and 200 N for the cutting and thrust components, respectively. The side force is close to 0, as expected. Figure 24 shows the temperature, at a specific tool location, along the cutting time. Tool temperature distributions at different times are also shown as thermal images. The temperature

contours during the steady state cutting period are averaged to obtain the mean temperature distribution at the tool tip area (insert below the curve in Figure 24).

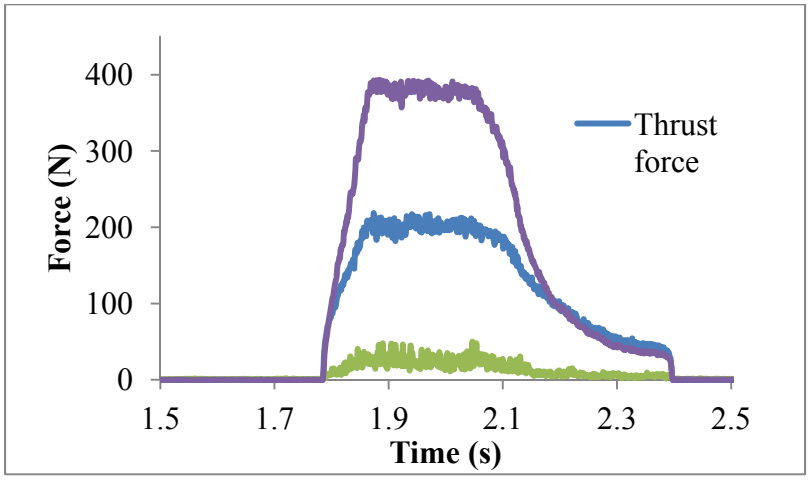

Figure 23. Cutting force history from one set of testing.

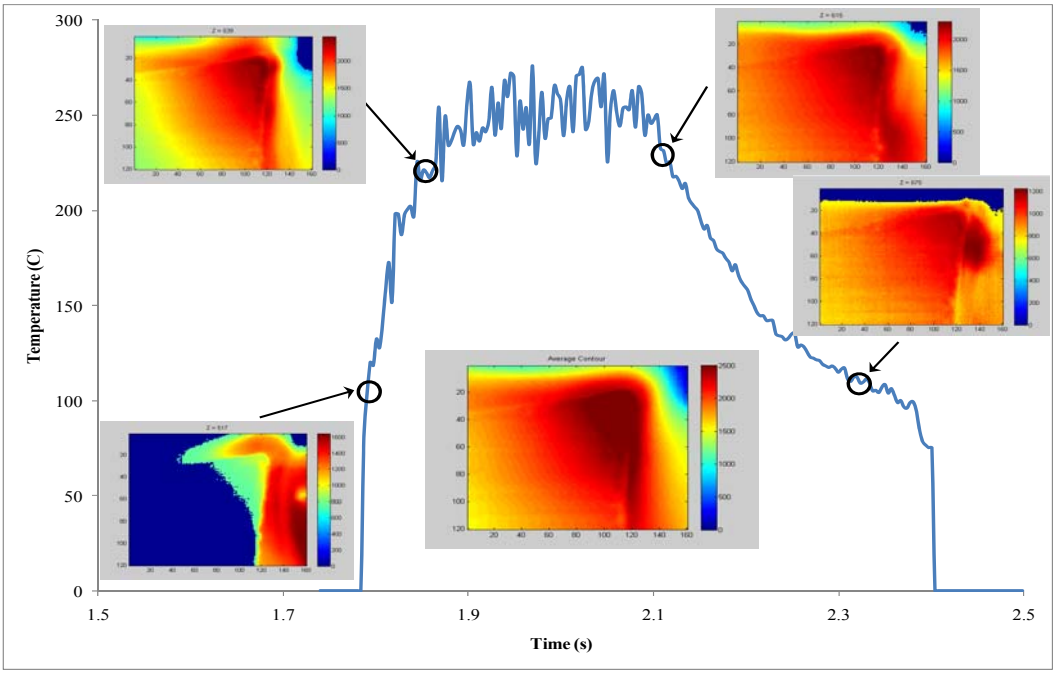

Figure 24. Temperature history at a specific tool location; inserts are thermal images at different times.

Figure 25 displays the temperature distribution at the tool tip (an approximately 1.2 mm by 1.6 mm area). The tool edge profiles are recognizable from the contours. The infrared spectrum camera obtains 120 pixel by 160 pixel video frames at approximately 300 frames per

second with 49 μs integration time (Ivester, 2011). The maximum temperature is around 300°C. Note that all temperature fields are converted to true temperatures using the linear emissivity of the tools (diamond-coated tools). Therefore, the chip temperature information may not be correctly represented.

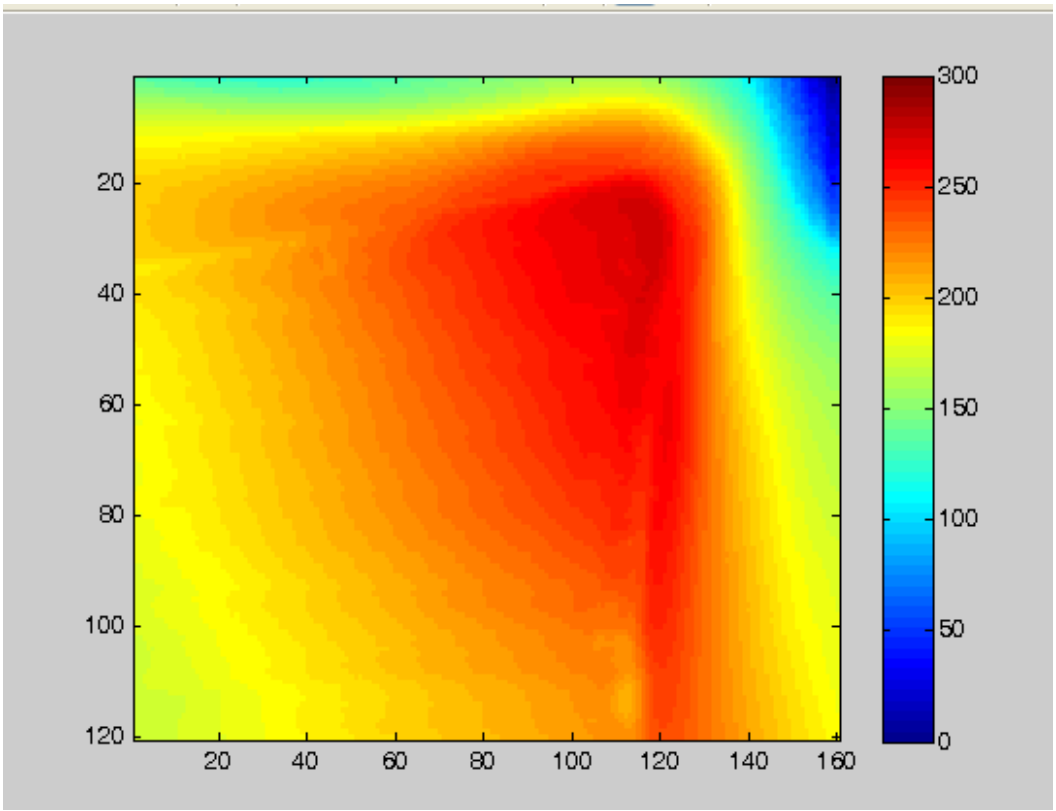

Figure 25. Cutting tool temperature contours at different uncut thicknesses.

Simulation Comparison

For comparison with the experiment, FE simulations of 2D cutting with a diamond-coated tool are realized using ABAQUS software. The simulation parameters are 25 μm edge radius, 20 μm coating thickness, 5 m/s cutting speed, and 0.15 mm uncut chip thickness. Simulation results are shown in the following context. Figure 26 plots the von Mises stress contours during cutting, (a) in the workpiece and chip, and (b) in the diamond-coated tool. It is noted that the stress level in the primary shear zone is on the order of 300 to 400 MPa; however,

the tool has a very high localized stress, over 7 GPa, in the edge-flank transition area. Note that the residual stress from the diamond deposition can be as high as 4 GPa, observed from the previous analysis. Cutting forces calculated from the simulation are 162 N and 72 N of the cutting and thrust components for 1 mm uncut width, respectively, which is comparable to the experimental results (128 N and 73 N per mm width of cut).

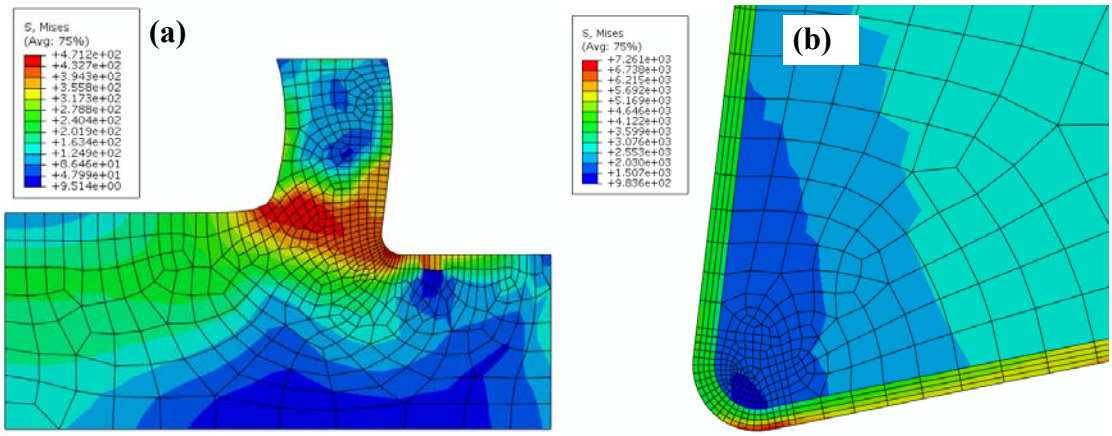

Figure 26. Stress contour from cutting simulations: (a) Workpiece and chip, and (b) Tool alone (unit: MPa).

Figure 27 plots the temperature contours, (a) for the tool-chip-workpiece, and (b) for only the tool. The maximum tool temperature is around 330°C, compared to 275°C from the experiment. Note that the cutting simulation was 2D, and thus, did not consider heat transfer along the in-plane direction, which deviates from the actual cutting and its inevitable heat loss parallel to the cutting edge direction. Hence, the higher simulated cutting tool temperature may be due to such a departure.

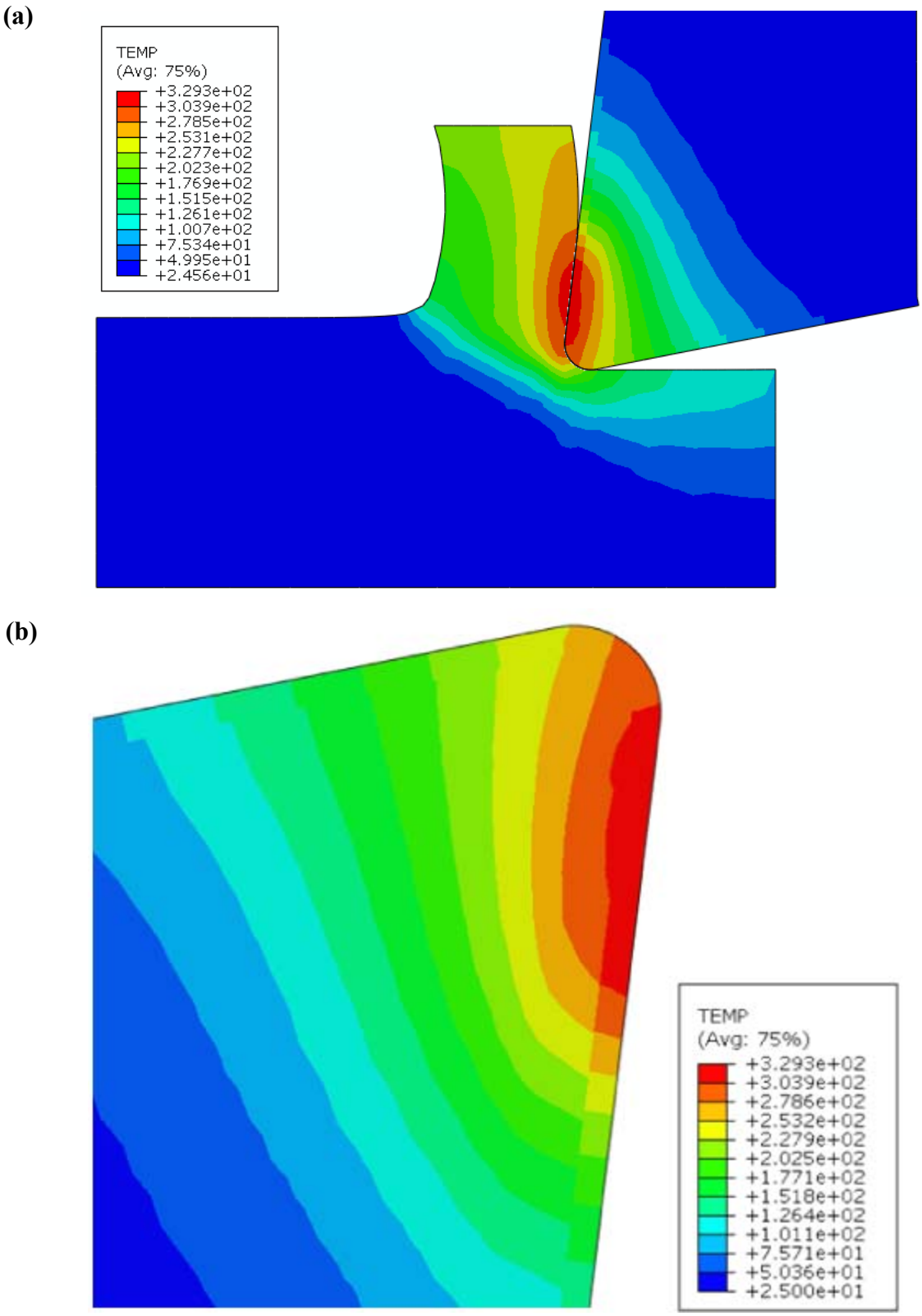

Figure 27. Cutting tool tip temperature contours: (a) Overall, and (b) Tool alone (Unit: °C).

Summary

It is well known that edge radius has a complex effect on diamond-coated tool performance. The edge radius affects both deposition residual stresses and machining loads, and the combined effects result in the sophisticated thermo-mechanical behaviors of diamond-coated tools in machining. In this study, 2D cutting simulations with a diamond-coated tool are developed. The deposition residual stresses in the coated tool are first simulated, and the model results are carried over into the cutting simulations. The simulations are used to evaluate the edge radius effects on cutting tool stress contours and temperature distributions, as well as interface stresses.

The major findings can be summarized as follows: (1) The deposition residual stresses can remain dominant in gentle cutting, e.g., small uncut chip thicknesses. At a small uncut chip thickness, the stress level is marginally reduced by the contact stress from the chip. The maximum σ_r is in a close range between different edge radii. (2) However, at a large uncut chip thickness, the radial normal stresses change noticeably due to machining, especially high tensile stresses close to the end of edge rounding (transition to flank surface). It is noted that the maximum σ_r is greater at the 5 μm edge, 1.2 GPa as compared to 0.9 GPa at the 50 μm edge. (3) A large uncut chip thickness induces more compressive stresses to the circumferential normal stress, and such phenomenon is more evident for a large edge radius. Future work will include a wider cutting speed range, as the associated higher temperatures will greatly influence thermal stresses in diamond-coated tools. In addition, cutting experiments will be designed to validate the simulation model. (4) Experiments conducted by NIST researchers present comparable results when studying cutting forces. As for cutting temperature, the maximum tool temperature is around 330°C, as compared to 275°C in the experiment. Note that the cutting simulation was 2D

and did not consider heat transfer along the in-plane direction; this deviates from the actual cutting, with inevitable heat loss parallel to the cutting edge direction. Hence, the higher simulated cutting tool temperature may be due to such a departure.

CHAPTER 5

CUTTING TOOL GEOMETRY EFFECT ON DIAMOND-COATED CUTTING TOOL PERFORMANCE

Introduction

Diamond coatings using technologies such as chemical vapor deposition (CVD) are replacing costly polycrystalline diamond cutting tools in machining abrasive lightweight materials. It has been shown that coating delamination, often occurring prematurely, is the major failure mode of CVD diamond-coated tools (Chou & Liu, 2005). High thermal and mechanical loading during machining and insufficient coating adhesion results in coating failure, and then the exposed substrate encounters massive deformation and catastrophic wear. Moreover, in CVD processes, the thermal mismatch between the coating and substrate materials generates high residual stresses in the tool. Diamond coatings, with a smaller thermal expansion coefficient, receive compressive residual stress on the order of GPa; however, the substrates, generally cobalt (Co)-cemented tungsten carbide (WC), receive a tensile stress. Such a high level of deposition residual stresses may impact coating functions (Kitamura, Hirakata, & Itsuji, 2003). Moreover if any geometry features changes, such as edges, the local stress fields may be severely altered (Gunnars & Alahelisten, 1996).

The edge radius has a significant effect on the chip formations and cutting processes. A significant number of studies related to the effects of edge radius on chip formations, friction conditions, and part surface integrity, etc., have been widely studied (Fang & Xiong, 2008; Nasr, Ng, & Elbestawi, 2007; Thiele et al., 2000; Tian & Shin, 2004). Most studies indicate that the

normal force increases with the edge radius and it is much more sensitive to the edge radius size compared to the cutting component.

Literature on cutting edge effects on coating tool performance is limited. Bouzakis et al. (2003) study the wear behavior of physical vapor deposition (PVD) coatings on cemented carbide inserts with various cutting edge radii in milling. The authors claim that increasing the cutting edge radius can lead to a longer tool life. Rech et al. (2004) investigate the effects of the edge radius of PVD coated tools upon chip formation and tool stresses in the orthogonal cutting of steel. The authors report that an optimum cutting edge radius exists that minimizes tool stresses, especially within the coating layer, and prolongs tool life. Almeida et al. (2005) investigate the effects of edge radius preparations on diamond-coated tools in machining hard metals. Their experiments utilized three types of edge conditions: up-sharp, chamfer, and hone. The results show that the edge conditions have a significant influence on machining forces, wear pattern, and tool life, etc. The honed tool yields to coating delamination first among all three edge types. Hu, Chou, and Thompson (2007b) use a 2D finite element analysis to investigate stress evolutions of a diamond-coated tool from deposition to machining with simplified machining load conditions. They find that at a low feed, the edge radius increase will reduce the maximum circumferential normal stress while producing minor effects at a high feed.

How the cutting edge affects the machining performance of diamond-coated tools is still difficult to determine. The fabrication of coated tools uses off-the-shelf substrates, and the tool edge geometry has not been integrated into the coating tool design. To effectively use diamond-coated tools, it is necessary to understand the effect of edge radius on machining. In this study, WC-Co cutting inserts with different edge radii are investigated. The inserts are commercial WC-Co cutting inserts with different edge radii which are diamond-coated and further tested in

composite machining. Cutting force is analyzed and tool wear is evaluated. The goal is to analyze how the cutting edge geometry affects the coating tool wear due to machining loads at different conditions.

Machining Investigation

Experimental Details

The substrates used in the diamond coating experiments are also square-shaped inserts (SPG422), as in the deposition stress analysis. The insert material selected is fine-grain WC with 6 wt% cobalt (K68 from Kennametal). Four levels of edge radii are evaluated: nominally, 5µm, 15µm, 30µm, and 65µm. The edge radius of cutting inserts prior to coating is measured by a white-light interferometer, NT1100 from Veeco Metrology. Measurement results indicate that the edge radii average at: 3.79µm, 13.7µm, 29.8µm, and 66.4µm. Figure 28 shows examples of cutting edge images from the interferometer. Surface textures of the inserts are also assessed by the interferometer, with surface roughness analyzed. It is shown that the surface roughness of the inserts is in a similar range, 0.29µm to 0.32µm of Ra.

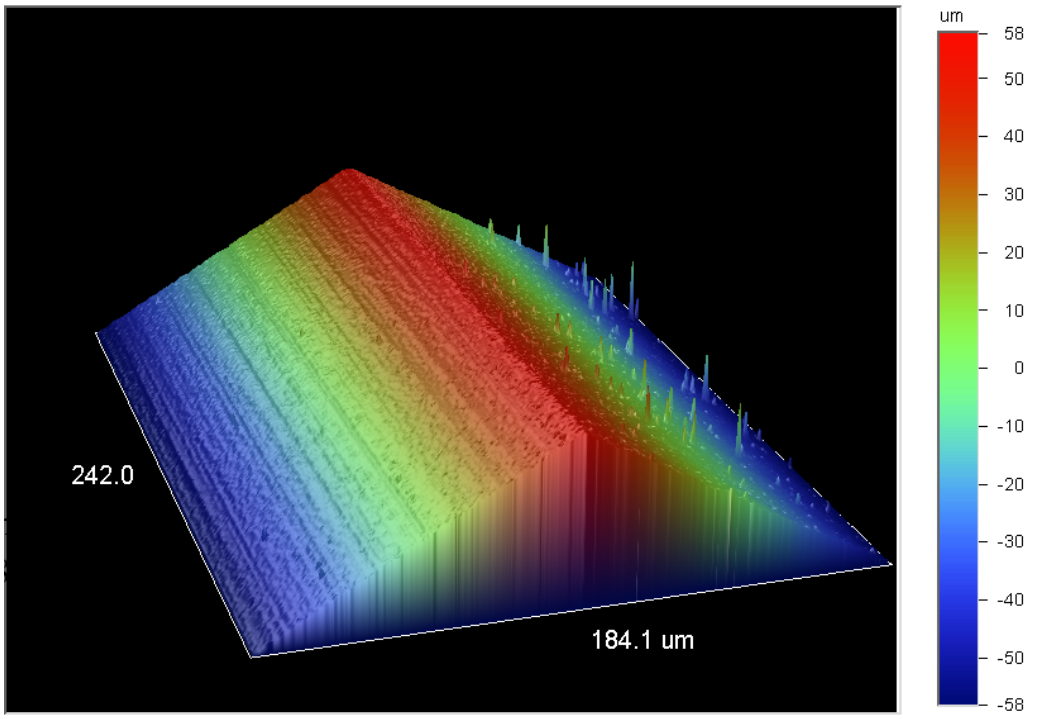

(a) 5 µm edge radius

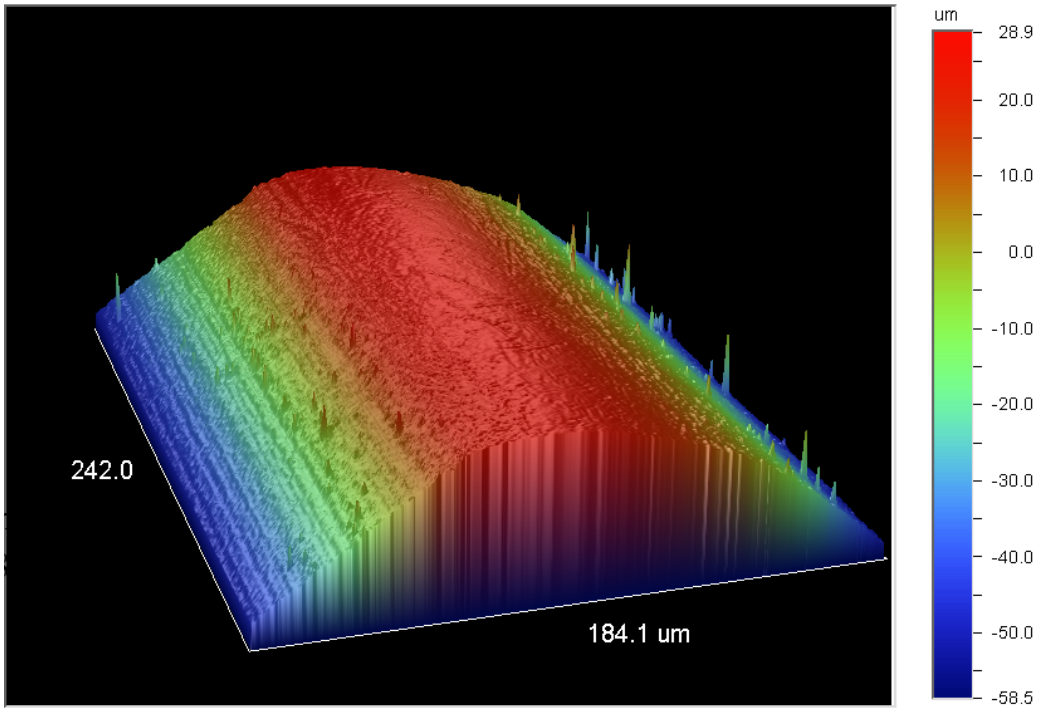

(b) 65 µm edge radius

Figure 28. Cutting edge images under white interferometer.

For the coating process, diamond films are deposited using a high-power microwave plasma-assisted CVD process. A gas mixture of methane in hydrogen is used as the feedstock gas. Nitrogen, maintained at a certain ratio to methane, is inserted into the gas mixture to obtain the appropriate nanostructure by preventing cellular growth. The pressure is about 90 Torr, and the substrate temperature is about 800 °C. The coated inserts are further inspected by the interferometer to measure the edge radius and to estimate the coating thickness. Figure 29 shows examples of cutting edge images of coated tools. The coating thickness is estimated between 5 and 8μm. Surface roughness, Ra, is about 0.5 μm for coated tools. A computer numerical control lathe, Hardinge Cobra 42, is used to perform machining experiments, outer diameter turning, to evaluate the tool wear of diamond-coated tools. With the tool holder used (CSRNL-164D), the diamond-coated cutting inserts form a 0° rake angle, a 11° relief angle, and a 75° lead angle. The workpieces are round bars made of an A359/SiC-20p composite. The set-up of the experiment is shown in Figure 30. Two machining conditions are used: one is 4 m/s and 0.05 mm/rev, and the other is 1.3 m/s and 0.15 mm/rev. The depth of cut is set at 1 mm. Machining is conducted at room temperature without coolant. For each machining condition, two tests are repeated. During machining testing, the cutting inserts are periodically inspected by optical microscopy to measure flank wear-land. Worn tools after testing are also examined by scanning electron microscopy (SEM). In addition, cutting forces are monitored during machining using a Kistler dynamometer.

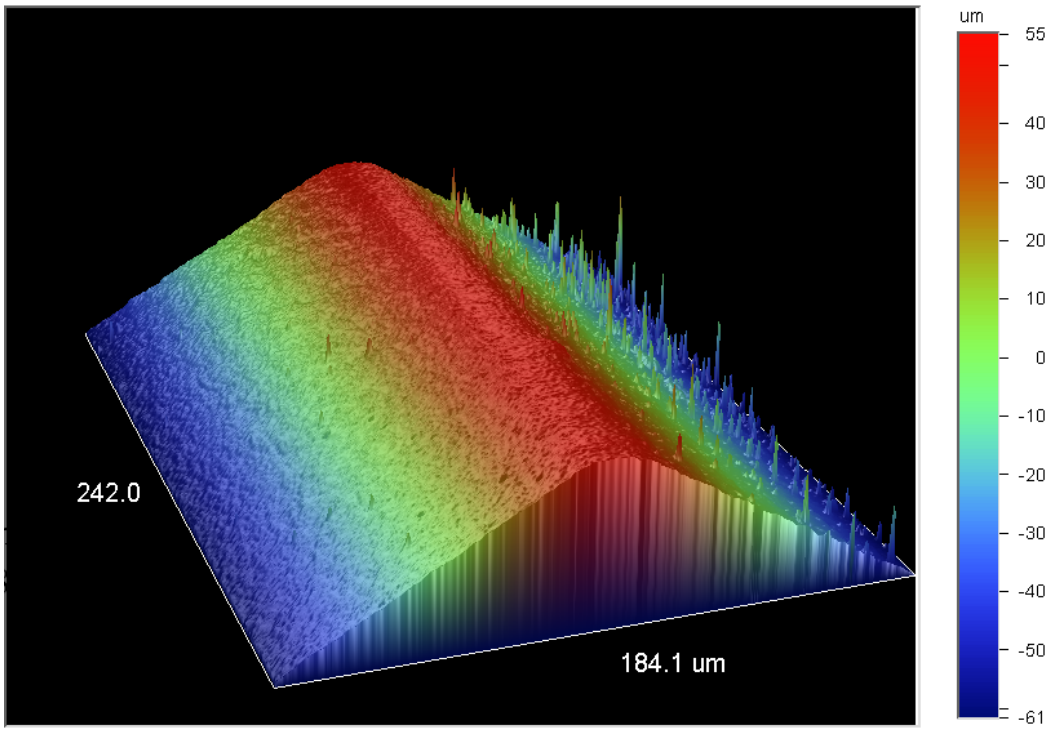

(a) 5 µm edge radius

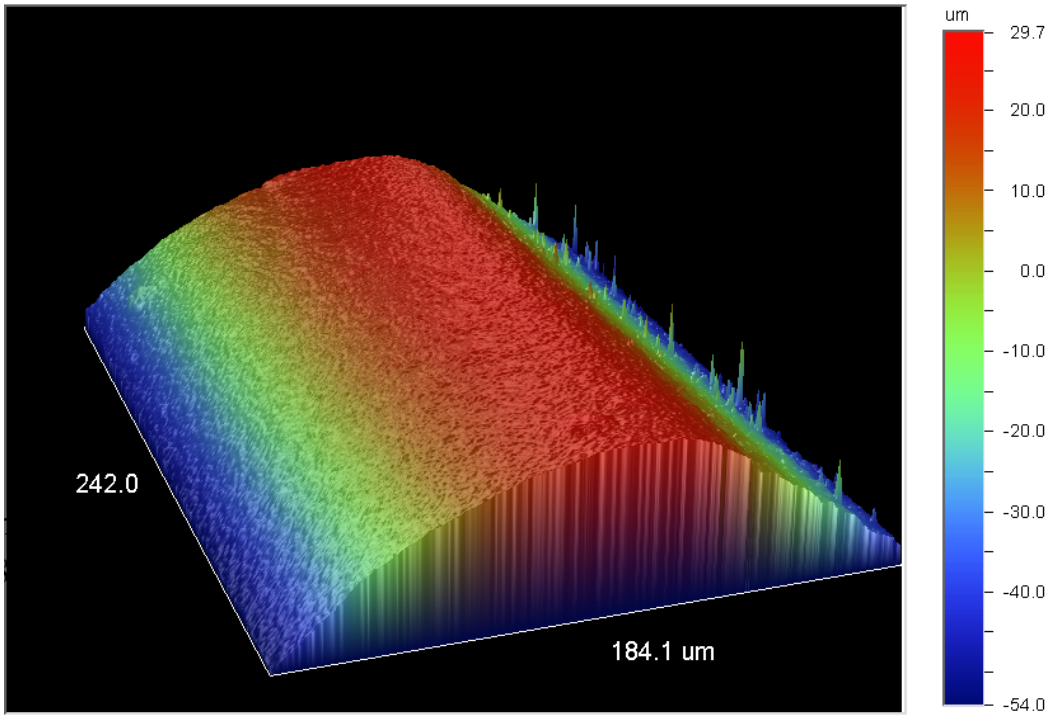

(b) 65 µm edge radius

Figure 29. Cutting edge images of coated tools under white interferometer.

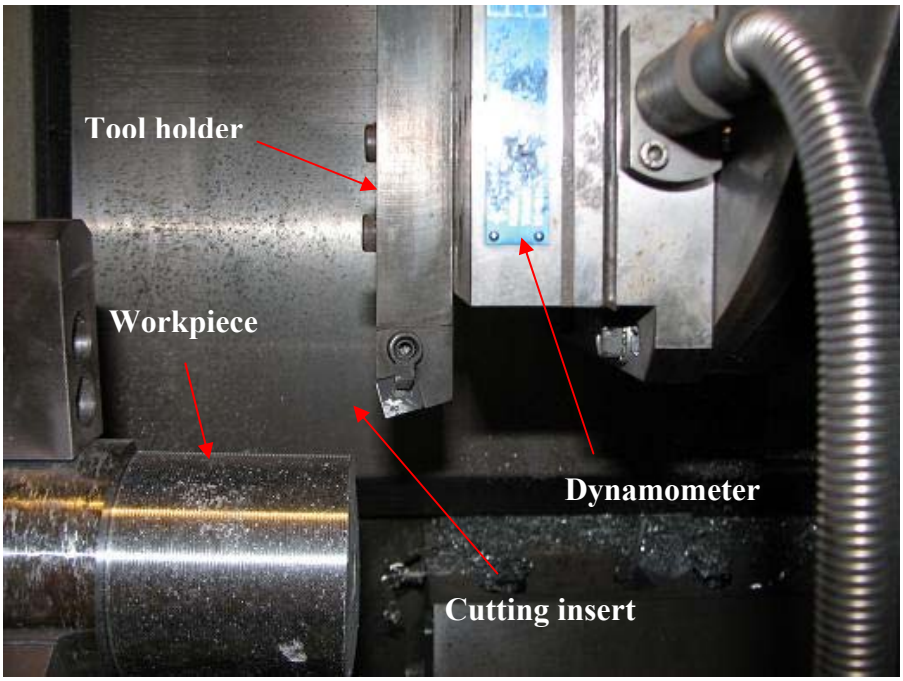

Figure 30. Experiment setup in CNC machine.

Cutting Forces

Figure 31 shows cutting forces during initial cutting (first pass) at 4 m/s and 0.05 mm/rev for 2 different edge radii. The force values of all 3 components, tangential (Ft), radial (Fr), and axial (Fa), are reasonably steady during the entire pass. Even the signal seems to be a little noisy, the further FFT with the force signal is analyzed but no specific frequency content to the data is found.

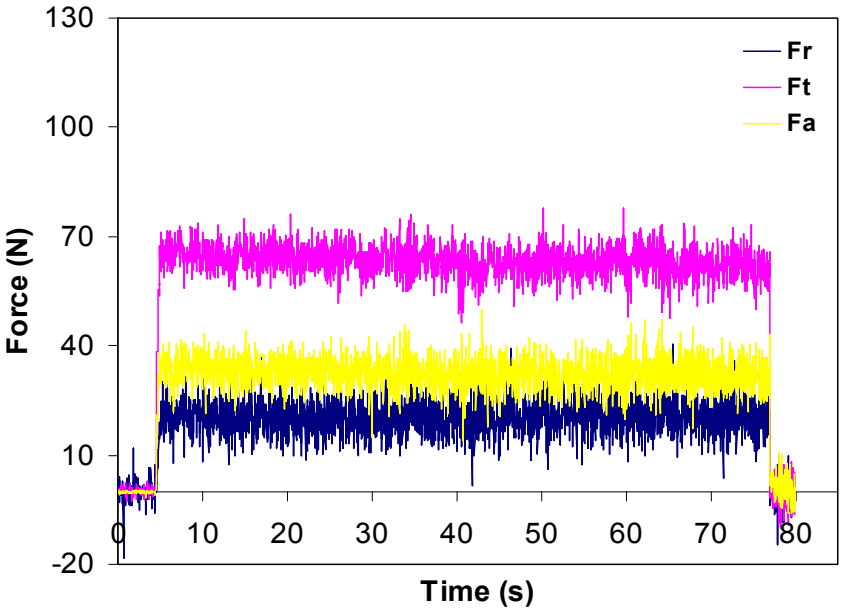

(a) 5 µm edge radius

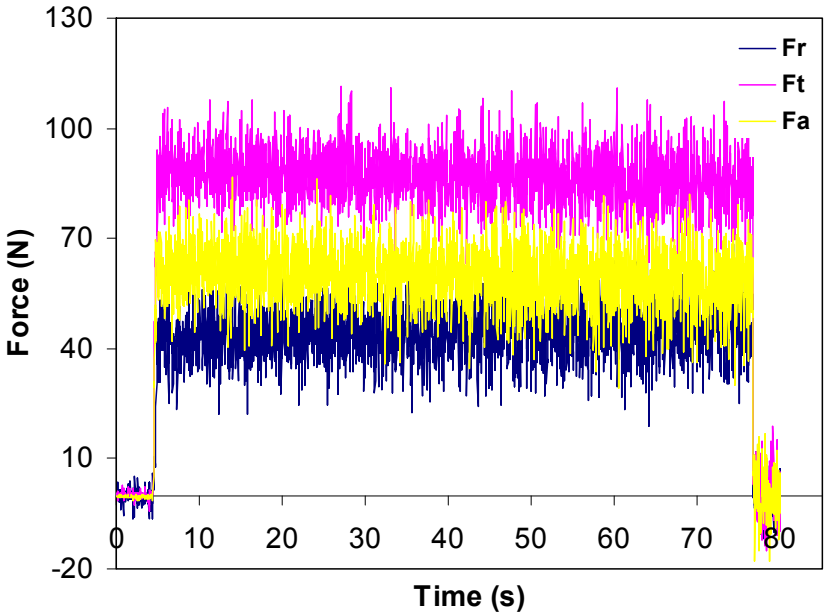

(b) 65 µm edge radius

Figure 31. Cutting forces at 4 m/s and 0.05 mm/rev for two types of edge radii.

For the 65 µm radius tool, cutting forces were higher than those from the sharp tool, in particular, the radial component.

Figure 32 shows cutting forces at 1.3m/s and 0.15 mm/rev for different edge radii. The force increasing due to the edge hone is less than that in the 4 m/s and 0.05 mm/rev condition. It

is noted that for the sharp tools, cutting forces show a step increase during cutting. This may be caused by the high deposition stresses combined with the high mechanical load.

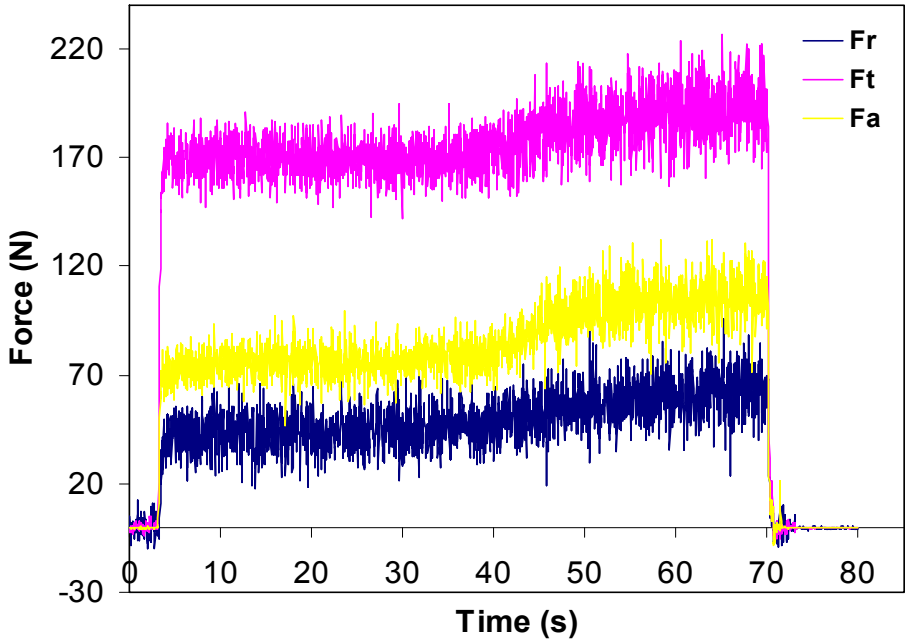

(a) 5 µm edge radius

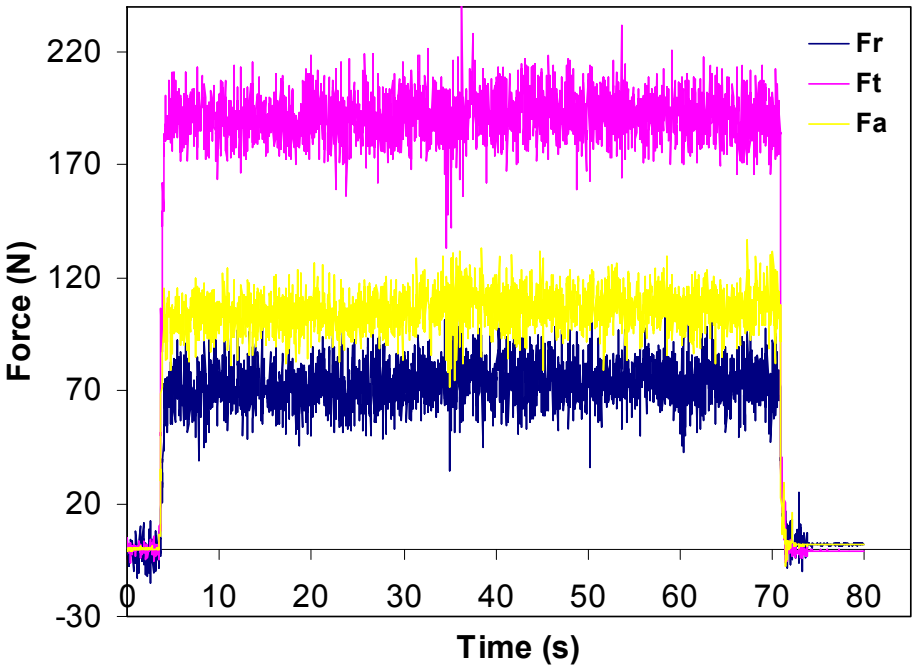

(b) 65 µm edge radius

Figure 32. Cutting forces at 1.3 m/s and 0.15 mm/rev for two types of edge radii.

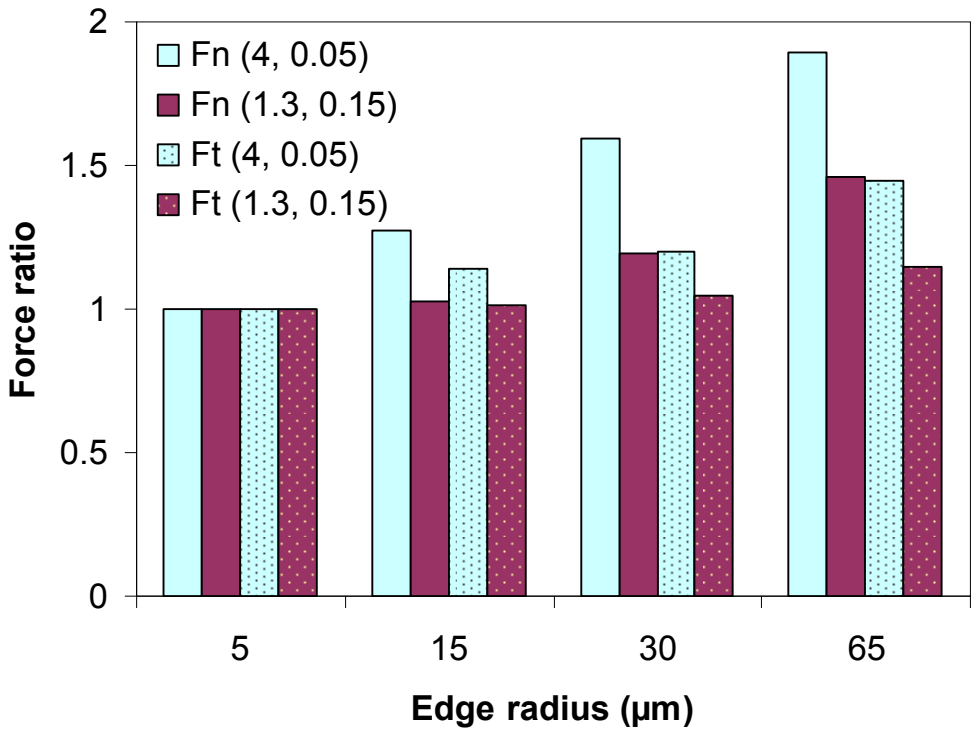

Figure 33. Cutting force ratio comparisons (normalized by force at 5 μm); parameter pair denotes cutting speed (m/s) and feed (mm/rev).

Figure 33 compares cutting force increases with the edge radius at two different machining conditions. The force ratios are obtained by normalizing with the forces from the 5 μm radius tools. It is noted that (1) the normal force, Fn (resultant of Fr and Fa), shows a higher rate compared to the cutting force (Ft), and (2) the increasing rate is much greater at a small feed.

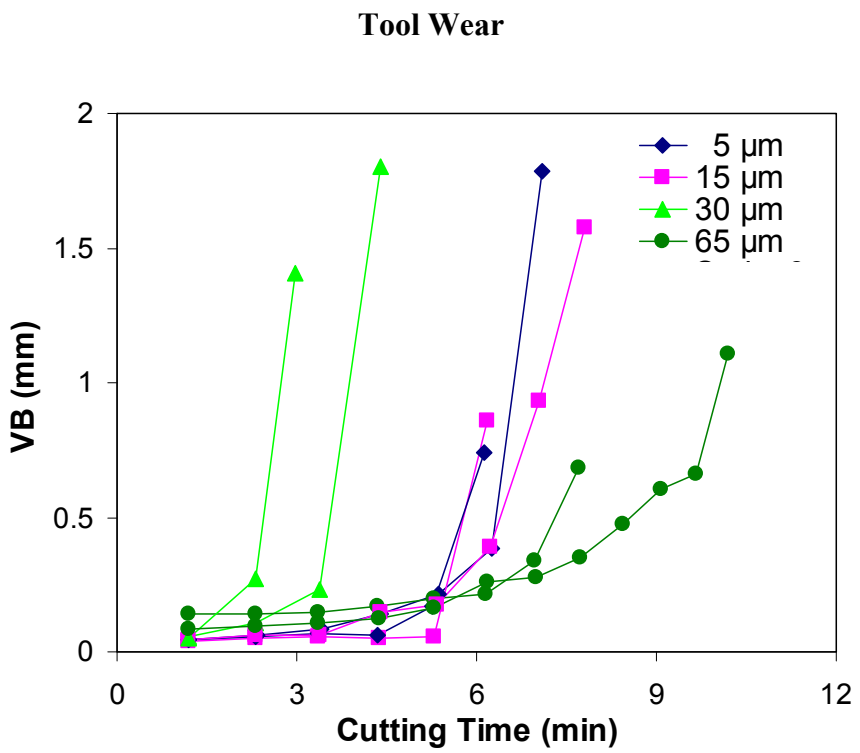

Figure 34. Tool wear development at 4 m/s and 0.05 mm/rev.

Figure 34 shows tool wear, specifically flank wear-land width (VB), along cutting time at the 4 m/s and 0.05 mm/rev condition for different edge radii. Results of two replicates are shown. In general, the tools show a gradual increase of tool wear followed by an abrupt increase of wear-land in one or two passes. It is believed that, during that specific passes, coating delamination occurred and resulted in rapid wear of the exposed substrate material. Tool wear and the onset of coating delamination (abrupt wear increase) are dependent on the edge radius. The tools with 5 µm and 15 µm substrate edge radii have similar wear growth curves. Sixty five µm radius tools show slightly greater wear resistance and delay of delamination-induced catastrophic wear. Surprisingly, the 30 µm radius tools result in the poorest tool life. Figure 35 shows flank wear-land width (VB) versus cutting time at the 1.3 m/s and 0.15 mm/rev condition for different edge radii. The tools with 5 µm and 15 µm substrate edge radii have a rather rapid linear wear growth and the shortest tool life. The 5 µm tool also shows a high initial wear which

might be caused by the high deposition stress and result in a significant increase in force (Figure 32). The 30 µm tools show a somewhat better tool life, but most strikingly, 65 µm radius tools demonstrate significantly delay of abrupt wear. A general trend can be noted: the larger the edge radius, the better the wear resistance among the edge radii tested. Using 0.5 mm VB as the life criterion, 65 µm radius tools have an average of ~20 min of tool life vs. ~3 min for 5 µm radius tools.

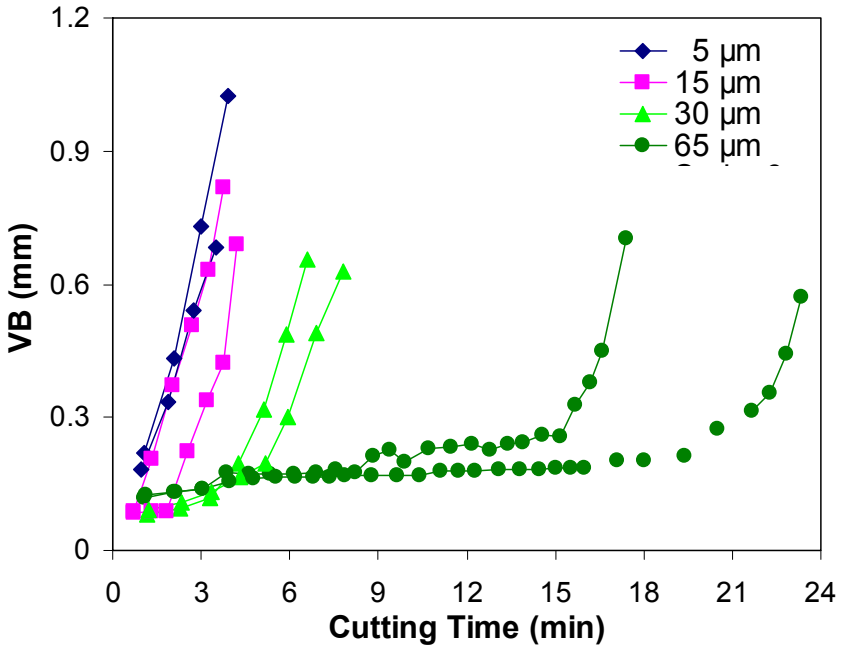

Figure35. Tool wear development at 1.3 m/s and 0.15 mm/rev.

It is also noted that for the sharp tools (5 µm and 15 µm), the tool life at 1.3 m/s and 0.15 mm/rev is shorter than at 4 m/s and 0.05 mm/rev, which is consistent with observations from previous studies, because the mechanical effect seems to be more dominant to delamination onset. However, for the large hone tools (30 µm and 65 µm), the tool life at 1.3 m/s and 0.15 mm/rev is longer than that at 4 m/s and 0.05 mm/rev, contradictory to the sharp tool cases, implying that the alleviation of deposition stresses by the rounded edge may outweigh the added machining loads due to the enlarged edge radius.

(a)

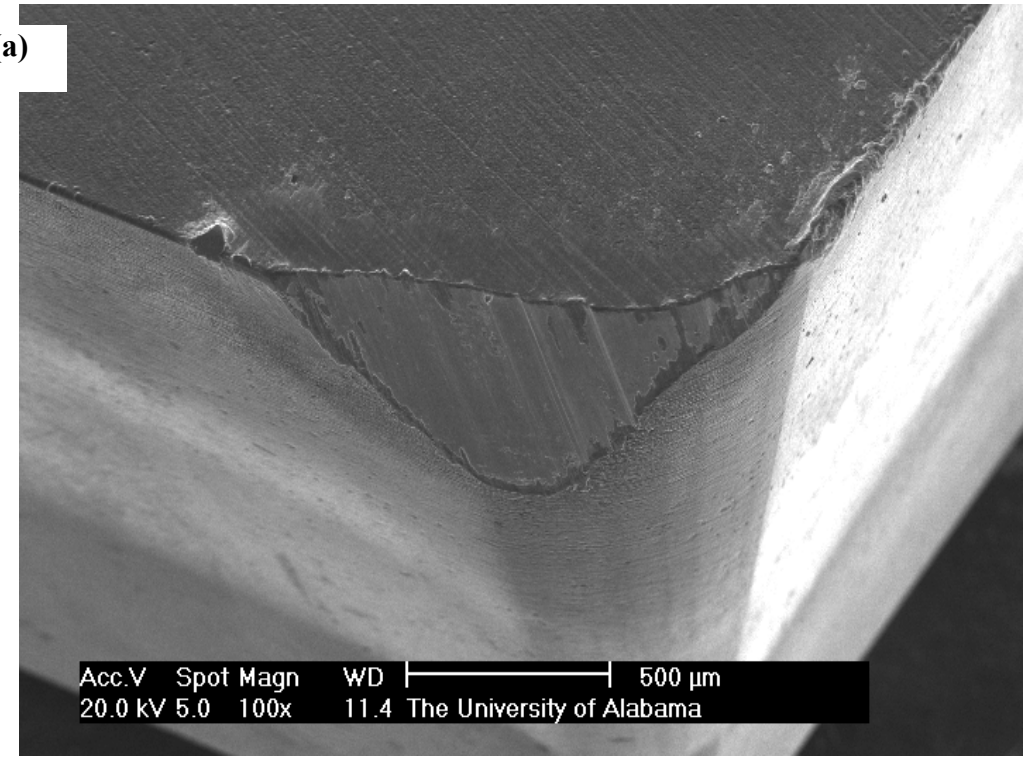
Acc.V Spot Magn WD 500 µm
20.0 kV 5.0 100x 11.4 The University of Alabama

(b)

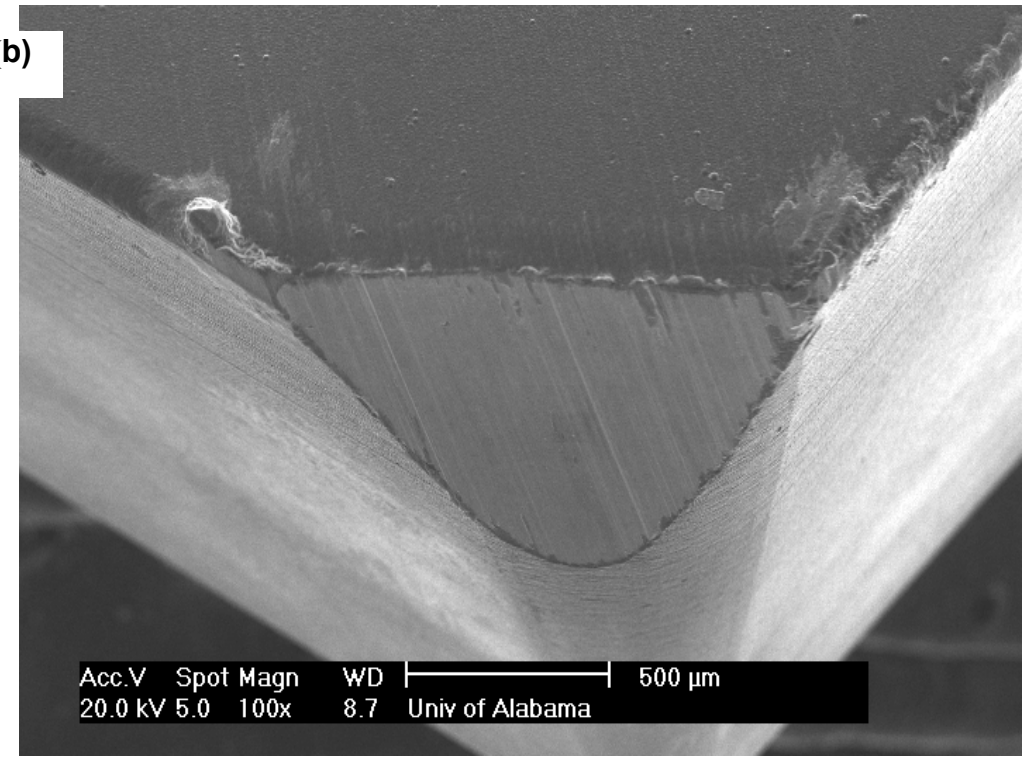
Acc.V Spot Magn WD 500 µm
20.0 kV 5.0 100x 8.7 Univ of Alabama

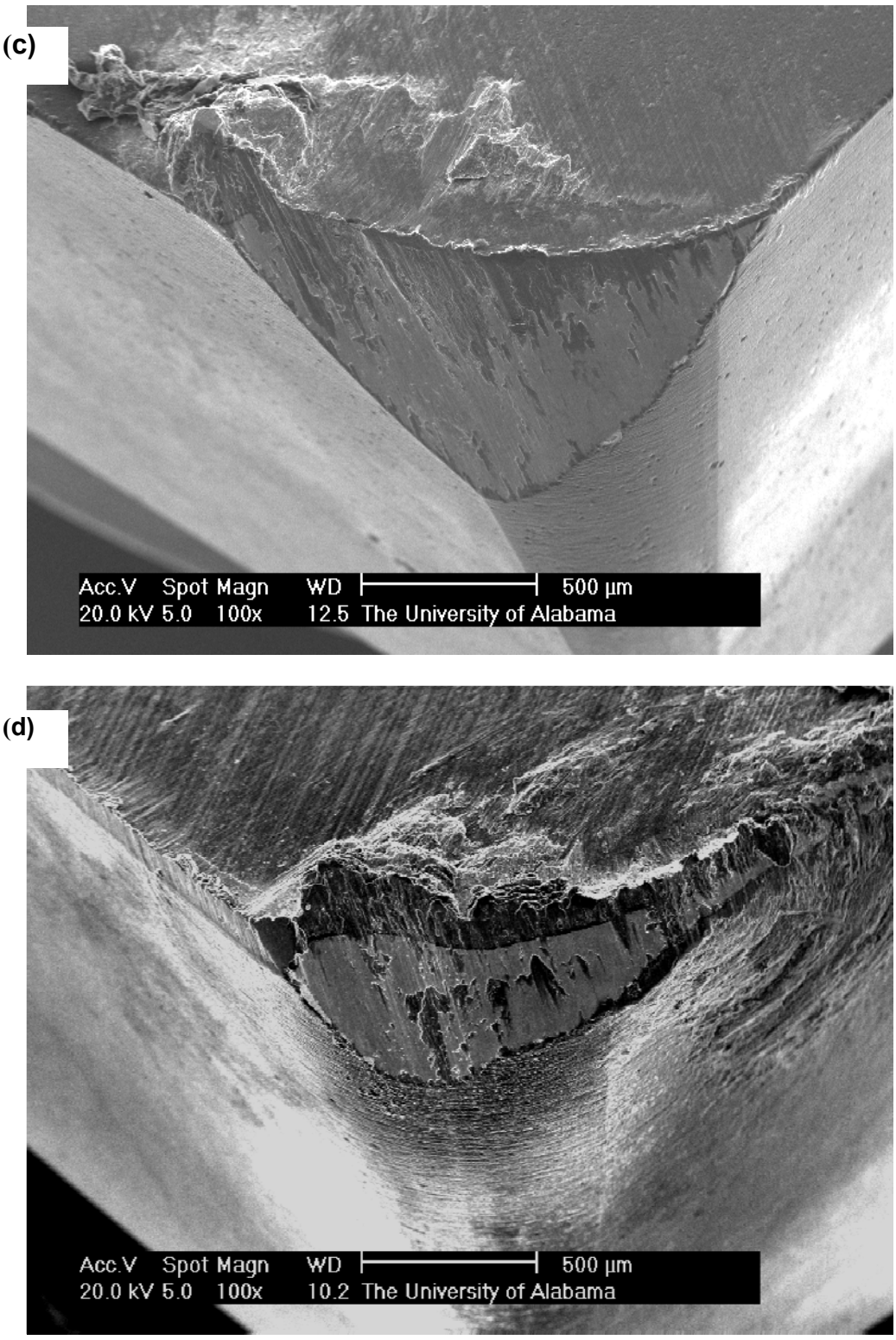

Figure 36. Worn tool SEM images at 4 m/s and 0.05 mm/rev: (a) 5 µm and (b) 65 µm Edge radius, and at 1.3 m/s and 0.15 mm/rev: (c) 5 µm and (d) 65 µm Edge radius.

Figure 36 shows examples of worn tool images (from SEM) of two different edge radii after machining testing. Flank wear-land is the major wear pattern. Moreover, inserts with both large and small edge radii show similar wear features, a large wear-land coating being delaminated with substantial metal deposits for the high feed condition.

The part surface finish produced by different edge-radius tools, at the first cutting pass, is also measured by a stylus profilometer. The results show a similar surface roughness range between different edge radii averaging: 0.85μm and 0.99 μm of Ra for 5 μm and 65 μm tools at 4 mm/rev. Ra is 1.39 μm vs. 1.16 μm, on average, for the 5 μm and 65 μm tools, respectively.

Summary

In this chapter, WC-Co cutting inserts are used to investigate the edge radius effects on cutting forces and tool wear. Commercial WC-Co inserts are prepared with different edge radii. The inserts are diamond-coated, under identical conditions, with a thickness of 5 to 8 μm. The coated tools with different substrate edge radii are further tested in the machining of composite bars. Two different cutting conditions: (4m/s and 0.05 mm/rev) and (1.3 m/s and 0.15 mm/rev) are tested. The machining forces are monitored and analyzed against the edge radius, and tool flank-wear is measured and evaluated. Wear features are examined by SEM.

The findings can be summarized as follows. (1) Increasing the edge radius will increase cutting forces, mainly the radial and axial components; moreover, the increasing rate decreases at a higher feed. (2) The combined effects above result in the complex wear behavior of diamond-coated tools with different edge radii. In particular, at the 1.3 m/s and 0.15 mm/rev condition, a 65 μm hone results in a tool life over 5 times longer than 5 μm sharp tools, though tools of either radii have similar tool wear results at the 4 m/s and 0.05 mm/rev condition. The effects of more geometry characteristics, combined with various cutting conditions, on the machining

performance of CVD diamond-coated tools need to be investigated so that a better understanding of tool geometry effects, and machining condition influences can be achieved for suitable tool specification and corresponding cutting parameters in industry application.

CHAPTER 6

IMPLEMENTING A COHESIVE ZONE INTERFACE IN 2D CUTTING SIMULATIONS

Introduction

Chemical vapor deposition (CVD) diamond-coated tools have been used as a result of reduced fabrication costs, in spite of its shorter tool life. In the literature, experiments regarding CVD diamond-coated tool performance have confirmed that coating delamination is the major failure mode of CVD diamond-coated tools (Chou & Liu, 2005). In machining, residual stress from the deposition process due to thermal expansion (Renaud et al., 2008) in the coupled materials and mechanical and thermal loads from service have a significant effect on tool life.

Interface adhesion is an essential issue in coating delamination, as has been demonstrated from theoretical and experimental angles. Griffith's (1920, 1924) theory of brittle fracture provides the fundamentals of fracture mechanics. His ideas are not limited to brittle fracture, and Irwin (1957, 1964) succeeds his work and applies it to ductile materials. Fracture toughness is critical to understand energy dissipation mechanisms in the process zone, which characterizes the onset of fracture during the fracture process. Generally, two types of mechanisms are developed (Brocks, 2005). One is the emission and motion of dislocations from the crack tip (Rice, 1992; Rice & Thomson, 1974; Rice & Tracy, 1969; Thomason, 1985; Tvergaard, 1982), a mechanism involving the formation, growth, and coalescence of voids. To address the interface fracture, the crack problem, a cohesive zone model is introduced ahead of the crack tip to simulate material degradation and separation. Barenblatt (1962) and Dugdale (1960) first formulate and apply the concept of cohesive zone models (CZM) with the traction-separation law (Figure 37) to interpret

interface decohesion involving crack initiation, growth, and coalescence. In their model, the interface traction first increases with separation until it reaches a maximum value; then it falls due to interface weakening and eventually decreases to zero. Xu and Needleman (1994) present a cohesive zone model for simulating dynamic crack growth. Their results agree with a wide range of experiments on fast crack growth in brittle solids. Later, Nakamura and Wang (2001) apply a cohesive zone model to simulate crack propagation in porous materials. The observed numerical errors from the cohesive elements increasing with model compliance need to be minimized by carefully choosing the parameters for the cohesive model. Gao and Bower (2004) make some improvement in avoiding convergence problem in finite element simulations of crack nucleation and growth on cohesive interfaces. They solve the convergence problem in quasi-static finite element computations by introducing a small viscosity in the constitutive equations for the cohesive interfaces. Repetto, Radovitzky, and Ortiz (2000) apply a tension-shear cohesive law model to simulate dynamic fracture and fragmentation of glass rods. They demonstrate that cohesive law, unlike damage theories, introduces well-defined fracture energy with spurious mesh-dependencies, such that the cohesive models endow materials with a characteristic length. Xia et al. (2007) apply the cohesive zone model, including the factor stability found by Gao and Bower, to simulate coating delamination under contact loading. They establish delamination mechanism maps for a strong elastic coating on an elastic-plastic substrate subjected to contact loading.

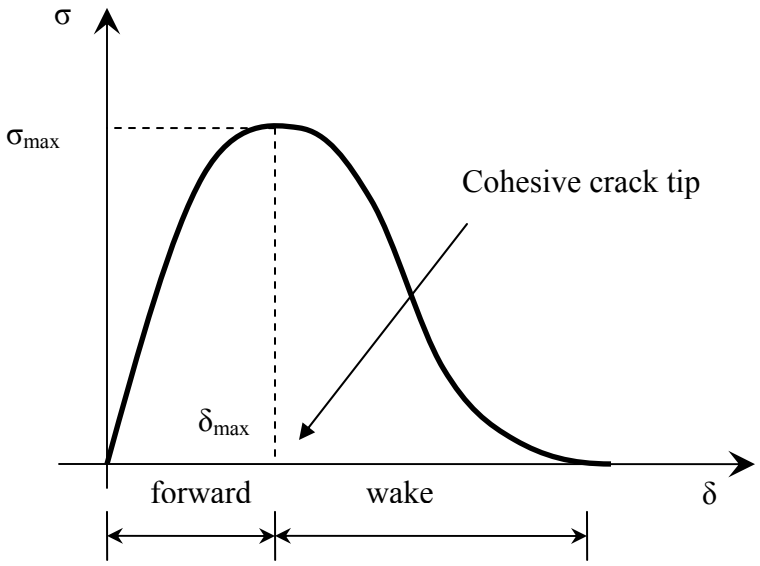

Figure 37. Typical traction-separation response (Hu et al., 2008).

Coating failure, as well as interface fracture, exhibits complicated behavior and is difficult to measure accurately. Interface adhesion strength can be affected by many coupled and uncoupled factors, such as material properties, deposition condition, surface roughness, etc. Mallika and Komanduri (1999) test diamond coatings on cemented tungsten carbide tools by low-pressure microwave CVD with various surface pretreatment techniques (removal of surface cobalt with aqua regia, the Murakami treatment, and the Murakami followed by ultrasonic microscratching with fine diamond suspension). Their results show significant improvement in the adhesion of diamond coatings on various cobalt content WC tools obtained by appropriate surface treatment and processing conditions. Almeida et al. (2011) also investigate pretreatment to improve adhesion performance and reduce interface effect. The interface toughness was improved from 1.4 kgf/μm to 1.6kgf/μm after decreasing the Co content of the substrate surface with the etching method for the highest Co content grade (5.75 wt. % Co). Measuring interface toughness is not entirely quantatively accurate, due to the complexity of the measurement process. Indentation and scratch tests are two widely used methods of investigating interface

adhesion strength. However, a wide range of factors may deteriorate the approximation of measured strength with the real condition. Coating failure mode such as spalling, buckling, and cracking complicates the measurement. Bull and Rickerby (1988, 1990) conclude that the coating failure mechanisms investigated by indentation and scratch testing are similar over a broad range. The indentation-induced interfacial shear stresses favor delamination and may contribute to coating failure in scratch testing. Later, they suggest using interface toughness value rather than critical load to characterize the adhesion of a particular coating, since there is no reliable relationship between the critical load and the physical measure of coating adhesion; and interface toughness enables factors such as the variation in the critical load with internal stress to be eliminated. Volinsky, Moody, and Gerberich (2002) summarize some measurement methods for interfacial adhesion of thin films on substrate and also briefly address some theoretical models specific to the resistance side (the items of resistance to crack propagation) of the delamination equation. In the physical process, the thin film and/or the substrate usually have plastic deformation such that it is difficult to separate the true adhesive energy from the total energy measured. With the development of depth sensing indentation and scratch systems with a high resolution of relevant measuring factors, the possibility of making more accurate measurements of interfacial fracture energy for thin coatings is increasing. However, it demands more investigation for any new indentation and scratch system since a large amount of development and validation work is required considering a lot of factors such as the development of good constitutive equations for coating and substrate, the incorporation of a suitable fracture model and a mechanism to handle interfacial and surface roughness, the incorporation of residual stresses into the model, etc. (Bull & Berasetegui, 2006).

Due to difficulty in measuring interfacial fracture energy, the finite element method may be an alternative means to investigating coating detachment or interfacial failure. In this paper, a 2D cutting simulation with a cohesive zone model is developed, with residual deposition stress included, to investigate the possible effect from tool edge radius and uncut chip thickness. Besides, interface fracture energy effect and deposition temperature effect on cohesive failure after deposition process are also investigated. The cohesive zone model is defined as follows. For $\delta_n>0$:

$$T_n = \begin{cases} \frac{\sigma_{max}}{\delta_{max}}\delta_n & (\delta \le \delta_{max}) \\ \frac{\sigma_{max}}{\delta}\frac{1-\delta}{1-\delta_{max}}\delta_n & (\delta \ge \delta_{max}) \end{cases} \quad (1)$$

$$T_t = \begin{cases} \frac{\sigma_{max}}{\delta_{max}}\frac{\Delta_n^c}{\Delta_t^c}\delta_t & (\delta \le \delta_{max}) \\ \frac{\sigma_{max}}{\delta}\frac{1-\delta}{1-\delta_{max}}\frac{\Delta_n^c}{\Delta_t^c}\delta_n & (\delta > \delta_{max}) \end{cases} \quad (2)$$

For $\delta_n=0$:

$$T_t = \begin{cases} \frac{\sigma_{max}}{\delta_{max}}\frac{\Delta_n^c}{\Delta_t^c}\delta_t & (\delta \le \delta_{max}) \\ \frac{\sigma_{max}}{\delta}\frac{1-\delta}{1-\delta_{max}}\frac{\Delta_n^c}{\Delta_t^c}\delta_n & (\delta > \delta_{max}) \end{cases} \quad (3)$$

where σ_{max} equals interface normal strength, τ_{max} equals interface tangential strength, and δ_{max} is interface characteristic length parameter. Δ_n^c and Δ_t^c are the critical normal and tangential separations at which complete separation is assumed; and δ_n, δ_t and δ represent the non-dimensional normal, tangential and total displacement jumps respectively, defined by the following equations.

$$\delta_t = \frac{\Delta_t}{\Delta_t^c},\ \delta_n = \frac{\Delta_n}{\Delta_n^c},\ \delta = \sqrt{\delta_t^2 + \delta_n^2} \quad (4)$$

Pure opening is corresponding to Δ_t=0 and pure shear separation is represented by Δ_n=0. The normal (ϕ_n) and tangential (ϕ_t) works of separation per unit area of interface are defined by (Chandra et al, 2002)

$$\emptyset_n = \frac{\sigma_{max}\Delta_n^c}{2}, \emptyset_n = \frac{\tau_{max}\Delta_t^c}{2} \quad (5)$$

This bilinear cohesive constitutive model can be plotted in Figure 38.

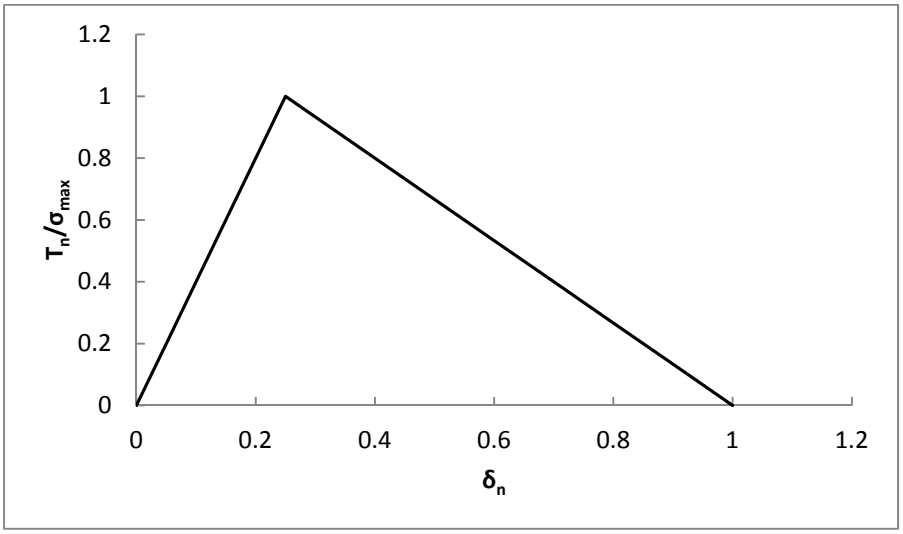

(a) Normal traction T_n as a function of the normal separation Δ_n for Δ_t=0

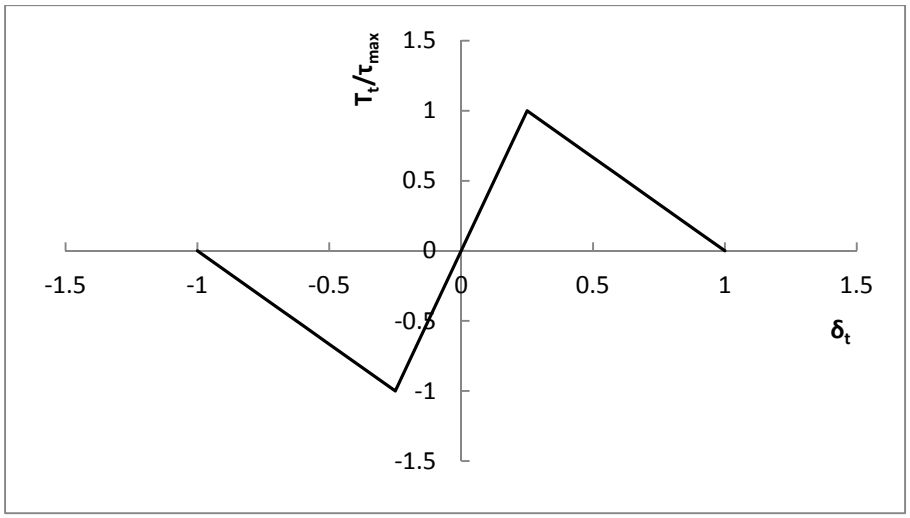

(b) Shear traction T_t as a function of the shear separation Δ_t for Δ_n=0

Figure 38. The cohesive zone model for normal traction and shear traction for two separate modes (Geubelle & Baylor, 1998).

The general procedure for creating a cutting simulation is similar to that described in the previous model. First, deposition stress is simulated with a cohesive zone included. Then, the residual deposition stress and strain are conveyed through the cutting simulation. However, it is noted that the cohesive zone cannot be constructed in a CAE model due to rounding issues in some large curvature areas. An alternative method is chosen to implement the same function and is detailed in the next section. Once the simulation is established, the extracted stress and strain data on the cohesive interface are collected to investigate the possible effects from tool edge radius and uncut chip thickness on cohesive failure. Typical stress-strain relations, represented by the traction-separation curve, are also plotted to gain insight into the cohesive zone's and edge radius's effect on cohesive failure. The following flowchart summarizes the above sequence of the simulations with cohesive zone and deposition residual stress included in a diamond-coated tool.

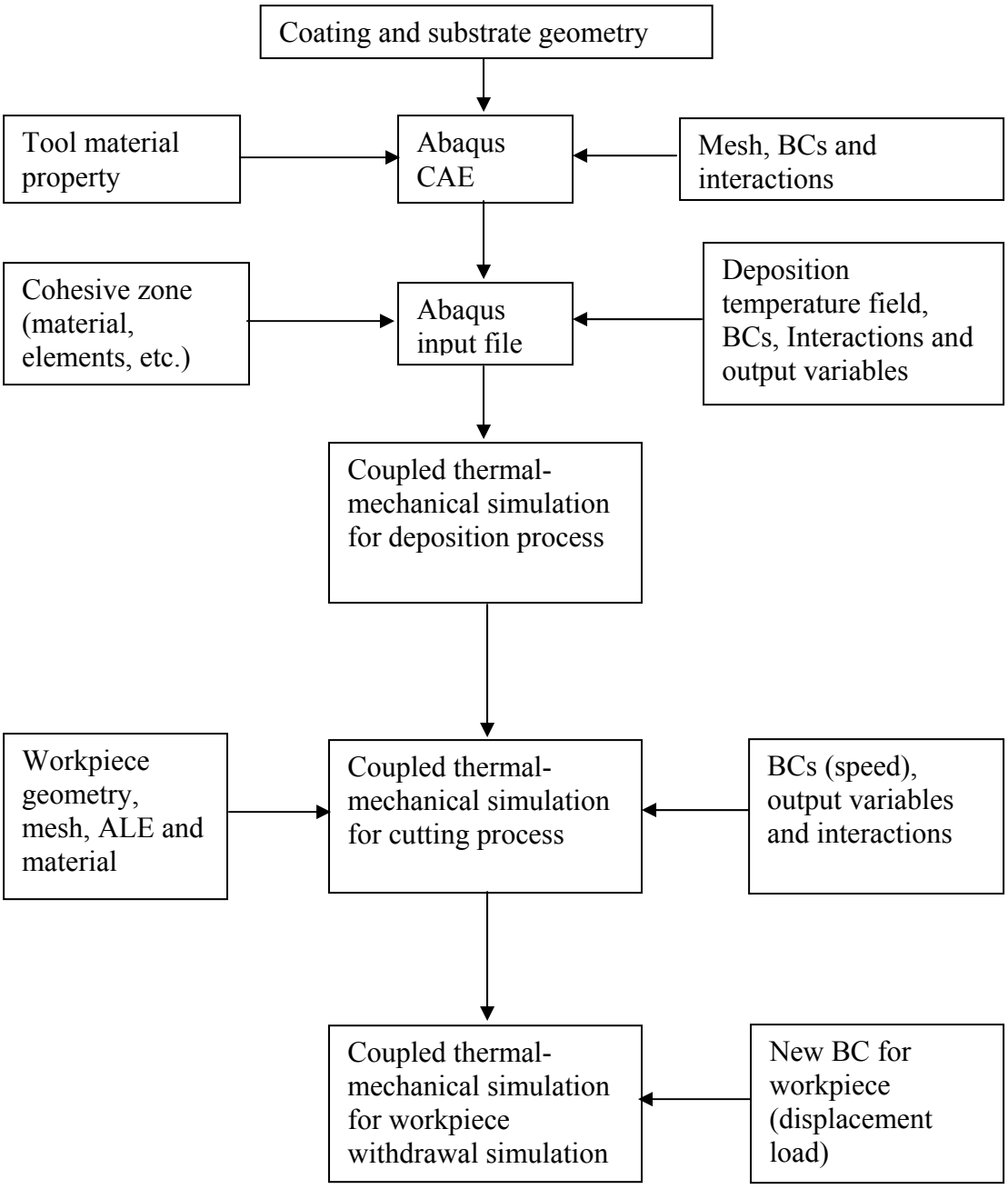

Figure 39. Flowchart of the simulations with cohesive zone residual stress included in a diamond-coated tool.

Deposition Stress Analysis

Model and Simulation

Diamond-coated cutting tools are modeled in ABAQUS/CAE version 6.10, according to same method used in the previous simulation. Two edge radii, 15 or 50 μm, are employed here.

Due to the complex geometry involved, the CAE method and code method are employed together to realize the cohesive elements included in this two-stage simulation. To start, the CAD model of the tool (substrate and coating) is constructed and translated into an Abaqus input file.

Instead of merging cohesive element nodes in the Abaqus CAE, cohesive elements are written into the Abaqus code. This is to prevent node numbering problems due to the issue described above. Tie constraints are applied to all components of the tool for thermal stress simulations. The elements used for the structural analysis are four-node bilinear displacement and temperature quadrilateral elements (CPE4RT). The cohesive element type is a linear quadrilateral COH2D4. A total of 120 elements are assigned to cohesive zone. Fine mesh (1 μm element size) is assigned to the cohesive elements and solid elements on the coating and substrate at the rounding area. In total, there are 1046 elements on the tool.

The cohesive zone property parameters employed in this investigation are listed in the following table.

Table 3

The Cohesive Zone Parameters for the Diamond-Coated WC Tool

Material #	E/GPa	G1/GPa	σ_{max}/MPa	τ_{max}/MPa	Fracture energy (J/m^2)	Deposition temperature /°C
1	5.0	5.0	500	100000	100	800
2	4.0	4.0	400	100000	80	800
3	5.0	5.0	500	100000	100	600

In the above list, the material parameter interfacial tangential strength is selected with a large value in order to ignore the shear failure (Gao, personal communication, Sept, 2011). Material parameters #3 is different from the above with the purpose of investigation of deposition temperature effect on cohesive failure after the deposition process. The stress-strain relation can be expressed by the traction-separation curve shown in Figure 38(a). The stress-

strain relation under the shear failure mode can be expressed with a similar curve plotted in Figure 38(b) (Geubelle & Baylor, 1998).

All deposition stress simulations are further conducted removing tie constraints between the coating and substrate to examine whether the cohesive zones undergo element failure after the deposition process.

During the deposition stress simulation, an explicit dynamic analysis, with consideration of thermal strains, is constructed. The initial deposition temperature is uniformly 800°C, and the final temperature of 20°C is selected here. The linear-elastic material model is used for the diamond coating, independent of temperatures, while an elastic-plastic material property is assigned to the WC substrate. The elastic property parameters can be found in the work of Qin and Chou (2010). The isotropic material property of WC's constitutive relation is listed in the following table (Dias et al., 2006), where σ_0 is strength coefficient, n is strain hardening exponent, and σ_y is the yield strength.

Table 4

Material Properties of the WC-Co Substrate

E (GPa)	ν	σ_0 (MPa)	n	σ_y (GPa)
620	0.24	18036	0.244	5.76

Figure 40 shows the stress contours (σ_y component, parallel to the rake) in a diamond-coated tool with a 15 μm edge radius and cohesive fracture energy of 80 J/m^2. It can be observed that compressive stress is distributed on the coating and tensile stress on the substrate. Around the tool tip, the stress concentration shows a large gradient, which is consistent with previous simulations.

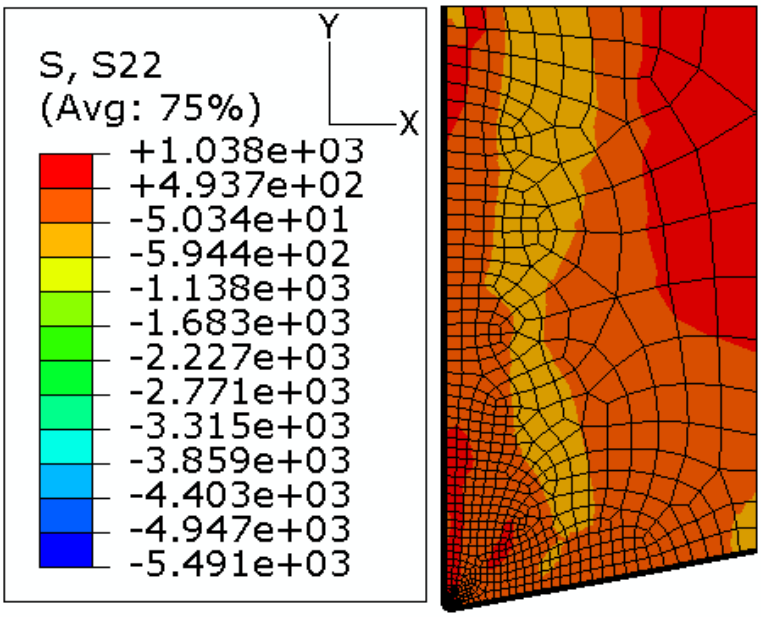

(a) Whole tool

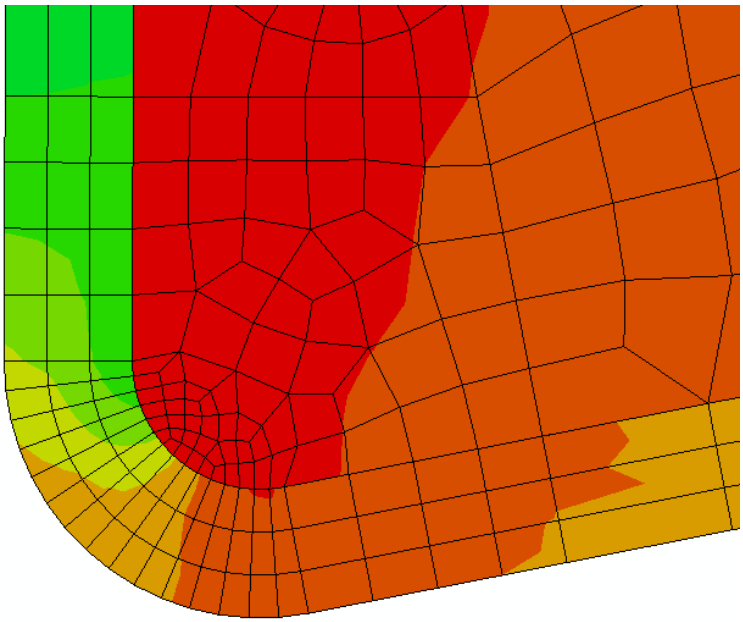

(b) zoom-in for the tip area

Figure 40. Deposition stress contour, normal stress parallel to rake face (15 μm edge radius).

Figure 41 demonstrates the typical normal stress in a cohesive zone after deposition stress analysis. Deposition stresses in the coating and substrate cause cohesive zone failure, where two elements fail at the rounded area of the interface.

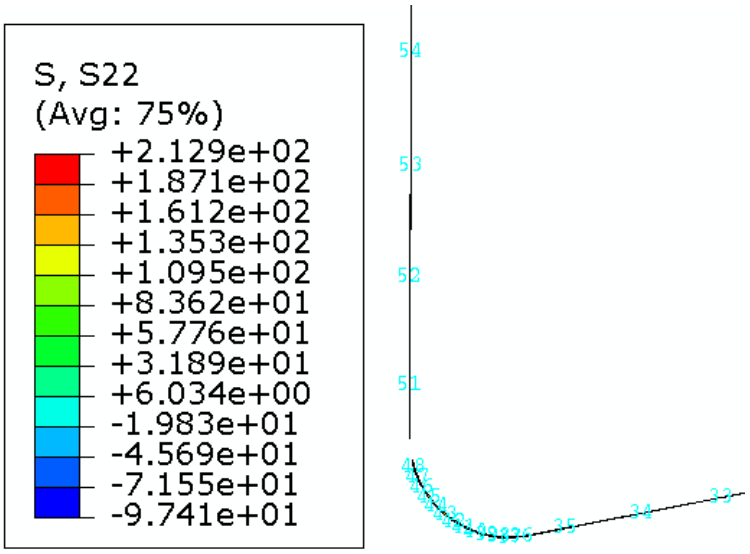

Figure 41. Normal stress (σ_n) in cohesive zone after deposition.

Cutting Simulation

Modeling Details

After finishing the deposition process, the results are imported into the cutting simulation. A workpiece for AA356-T6 is assembled with the diamond-coated cutting tool from the deposition residual stress simulation. The material properties of the workpiece are listed in a previous work by Qin and Chou (2010). The element type for the workpiece is CPE4RT, which considers the thermal and mechanical behavior of stress and strain, independent of temperature.

To conduct the cutting simulation, the ALE method is employed to simulate a steady-state cutting process. The details of the implementation, including the adaptive mesh region, constraints, and the Eulerian and Lagrangian surfaces can be found in Qin and Chou (2010). Here, the tie constraints are only applied to coating-cohesive elements and the cohesive elements-substrate. To implement this method, the CAE model of the cutting simulation is translated into an Abaqus input file (See Appendix for details); then relevant surfaces, element sets, node sets, and constraints for the interactions are created. The friction model and contact interactions can also be found in Qin and Chou's (2010) work. Since the cohesive element model

in Abaqus cannot consider heat transfer, a gap conductance model for heat transfer across the cohesive zone is constructed. A large gap conductance model is employed here to make the heat transfer across the gap. For the boundary conditions, the tool top, including coating nodes, cohesive nodes, and substrate nodes on the top edge, is constrained along the Y direction, and the right edge of the tool, composed of coating nodes, cohesive nodes, and substrate nodes, is constrained along the X direction. The boundary conditions of workpiece are set as before. The initial temperature of the workpiece is 20˚C. A predefined initial state of stress and strain from the deposition process is required for the coating, cohesive elements, and substrate of the diamond-coated tool. Once the above considerations are implemented, the cutting process, including cohesive elements, is simulated. One typical illustration of the workpiece and diamond-coated tool assembly, including cohesive elements, is shown in Figure 42.

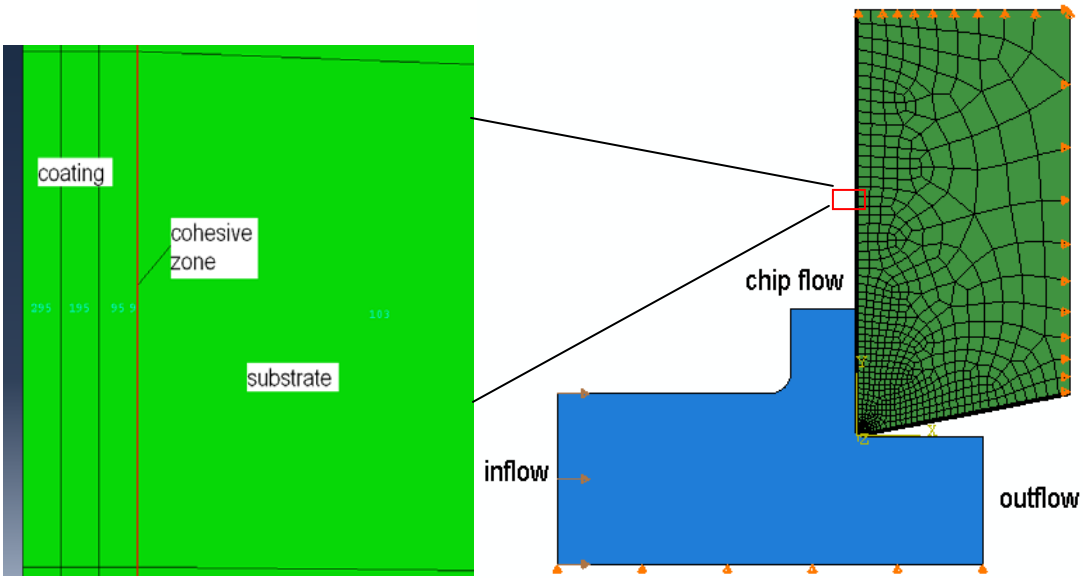

Figure 42. Workpiece and diamond-coated tool assembly, including cohesive elements.

During this research, the tool has a 50 µm edge radius (r_e) and a 15 µm coating thickness, and cutting condition are tested at 5.0 m/s (v) and two uncut chip thickness, 0.05 and 0.45 mm (h), with a cohesive fracture energy of 100 J/m^2. The interfacial tensile strength, σ_{max}, of 500

MPa, is chosen to conduct a low-temperature (600˚C) deposition process. Further cutting simulations and workpiece withdrawal simulations demonstrate that cohesive delamination can happen during cutting and further workpiece withdrawal at certain large uncut chip thickness condition. The elements number and properties of the tool are the same as in the deposition residual stress analysis.

Results and Discussion

Deposition Stress Simulation

The tool specification edge radius = 15 μm, coating thickness = 15 μm (re15t15) is chosen to conduct the deposition stress simulations incorporating a cohesive zone model. The following sections illustrate the cohesive zone results from three angles.

Fracture Energy Effect

Figure 43 demonstrates the results of an interface normal strength of 500 MPa at two different fracture energies for the cohesive zone, 100 J and 80 J. It is observed that the lower cohesive fracture energy case of 80 J presents cohesive element failure after deposition, while the 100 J case maintains the cohesive element without any failure at the same interface normal strength.

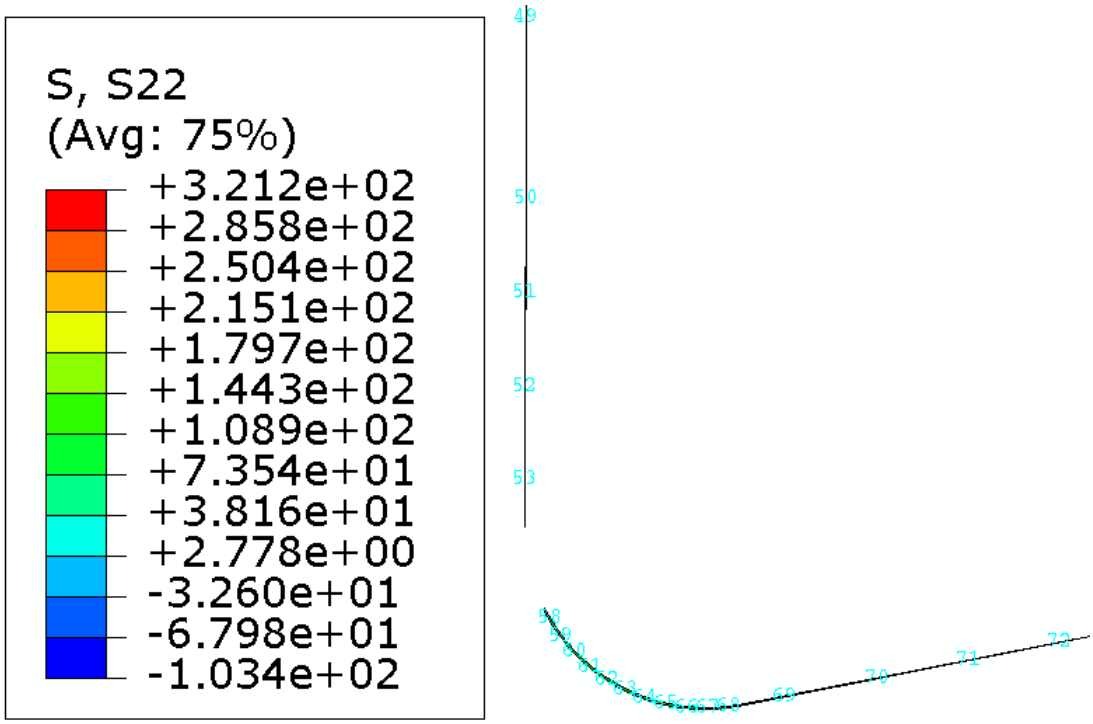

(a) Fracture energy 80 J

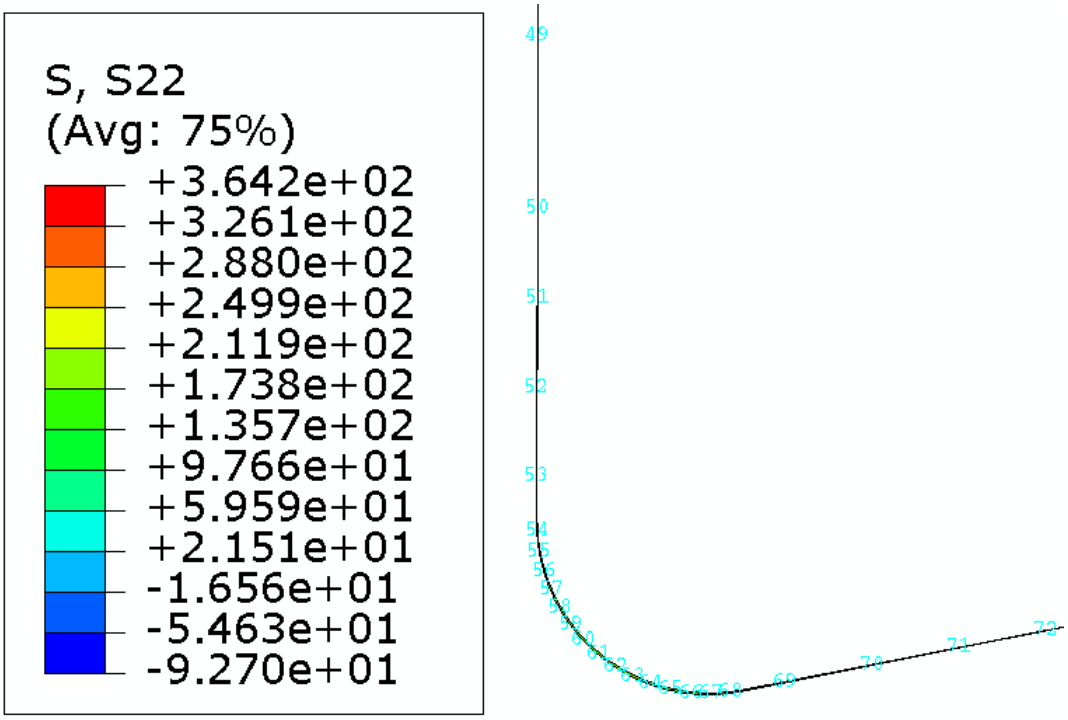

(b) Fracture energy 100 J

Figure 43. σ_n results of cohesive zone at two different fracture energy values after deposition at the interface strength of 500 MPa.

Interface Normal Strength Comparison

100 J is chosen for the comparison of different interface normal strengths. Here, the cohesive zone parameters are selected as follows: two interface normal strength values, 500 MPa and 400 MPa, are employed. The interface shear strength is the same, 100 GPa, which is chosen to eliminate the shear strength influence.

The results are shown in Figure 44. Cohesive element failure occurs with the lower interface normal strength. This demonstrates that the cohesive zone with a lower interface normal strength tends to be susceptible to interface delamination.

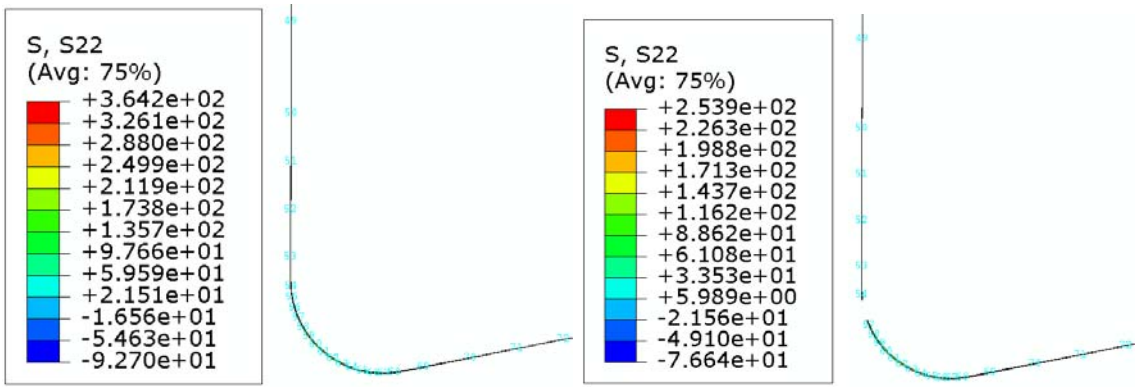

(a) σ_{max} = 500MPa (b) σ_{max} = 400MPa

Figure 44. σ_n responses for different interface normal strength, 500MPa and 400 MPa at the same fracture energy 100 J/m^2 and interface shear strength 100 GPa.

Deposition Temperature Effect

Deposition Simulation Results

A low deposition temperature tends to reduce deposition residual stress in diamond-coated tools. This effect will decrease the possibility of cohesive failure after deposition. To observe an aggressive uncut chip thickness effect, a tool model that maintains a good cohesive zone after the deposition process must be realized. In the investigation, the cohesive zone property implemented is corresponding to #3 shown in Table 3. Deposition temperature is 600

˚C. The tested diamond-coated tool is with 50 μm edge radius (r_e) and coating thickness 15 μm (t).

Figure 45 demonstrates no cohesive failure after deposition.

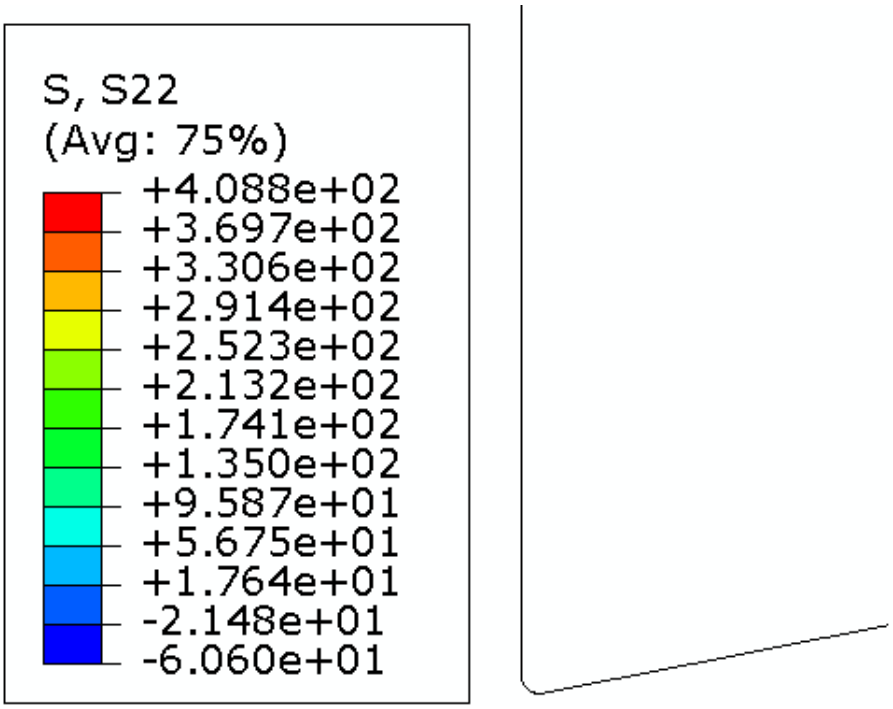

Figure 45. Cohesive zone without failure after deposition.

Cutting Simulation

To conduct the uncut chip thickness effect on cohesive interface failure the deposition residual stress of the tool is inherited in the following cutting simulation with two uncut chip thickness values, 0.45 mm and 0.05 mm, were tested and the same cutting speed was5 m/s. Large uncut chip thickness, 0.45 mm, is chosen to conduct the cutting simulation and workpiece withdrawal to investigate whether cohesive delamination happens. The following series of figures display the progressive cohesive condition during the cutting simulation process.

Figure 46 presents the initial state of the cutting simulation. There is no cohesive failure evident at the beginning of the cutting simulation.

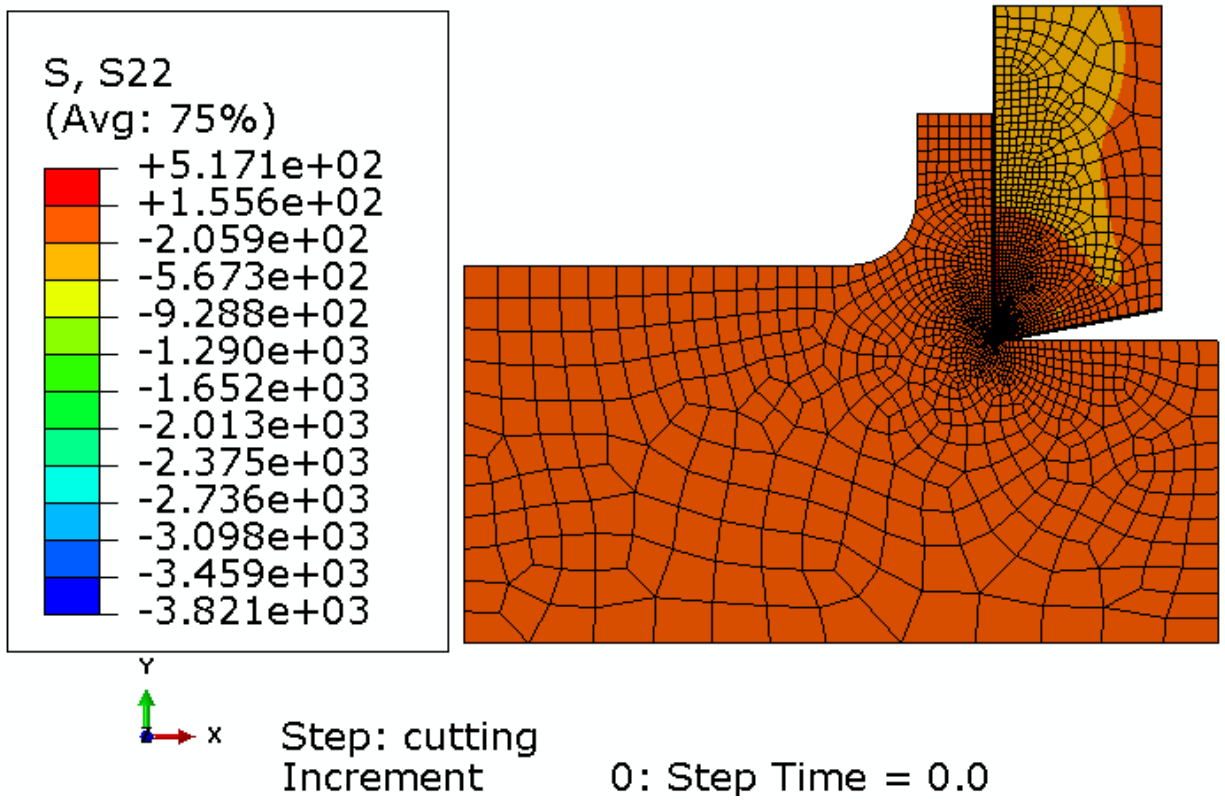

Figure 46. Initial state of the workpiece, tool, and cohesive zone.

Figure 47 illustrates the status at the last time increment before cohesive delamination during cutting.

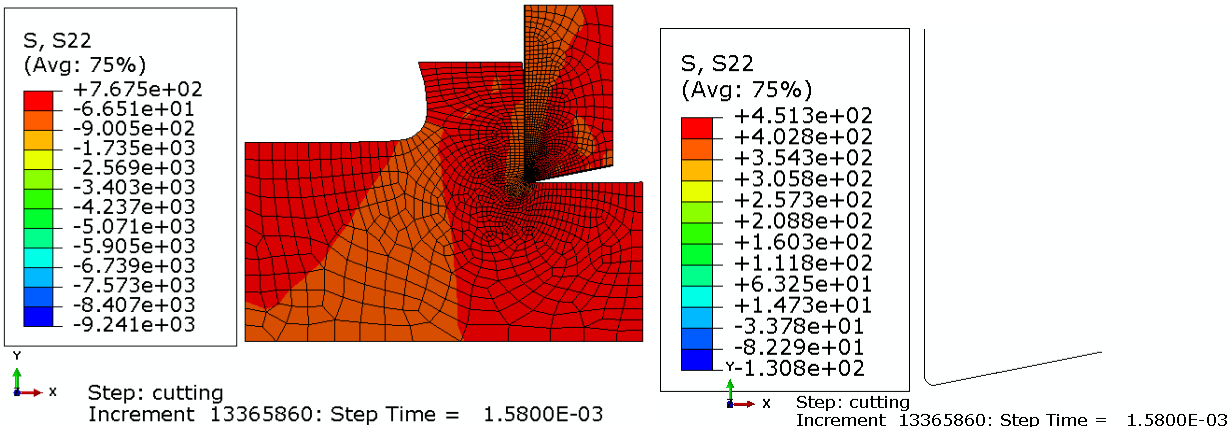

Figure 47. No cohesive failure at cutting step time 0.00158 seconds.

Figure 48 demonstrates that cohesive failure initiation happens at the simulation step time 1.60 microseconds. At this time, cohesive element failures happen at elements number 83 to 85,

located at the flank face of the tool near the round edge. The failure length is approximately 16 μm.

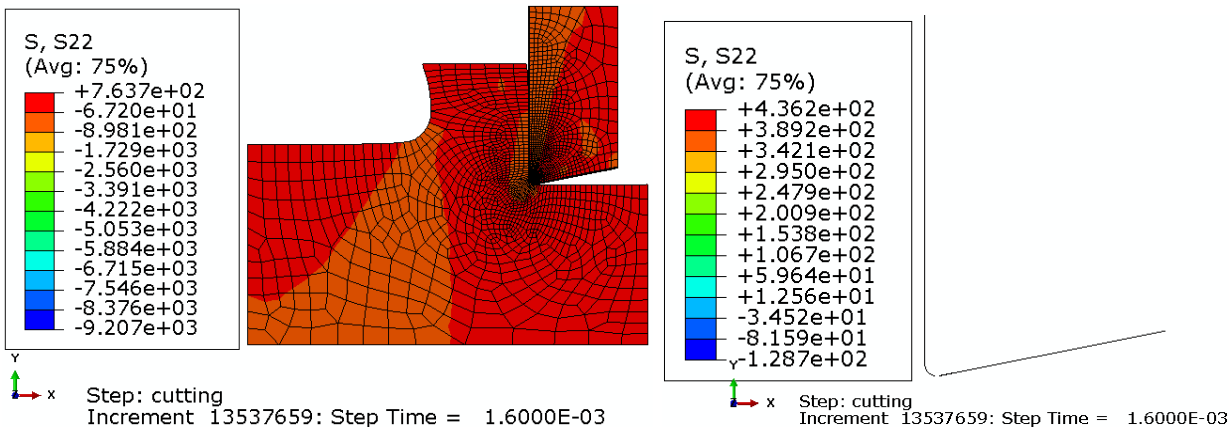

(a) workpiece and tool (b) initial cohesive failure

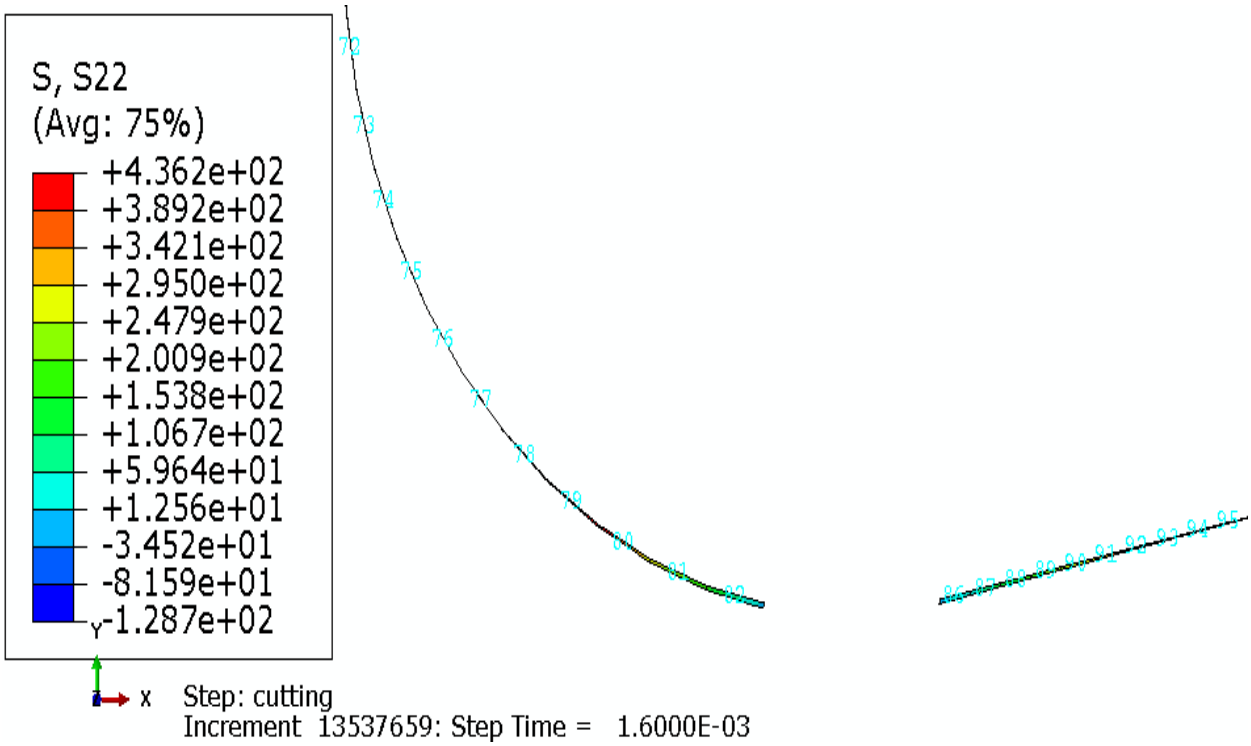

(c) Zoom-in image of the cohesive failure

Figure 48. Cutting and initial cohesive failure at step time 0.00160 seconds.

Figure 49 shows traction-separation curves for two cohesive nodes, which belong to failed and unfailed cohesive elements respectively. Node 224 is located at unfailed cohesive element at the

flank face while node 145 belongs to the failed cohesive element number 84, between unfailed element 82 and 86, shown in Figure 48.

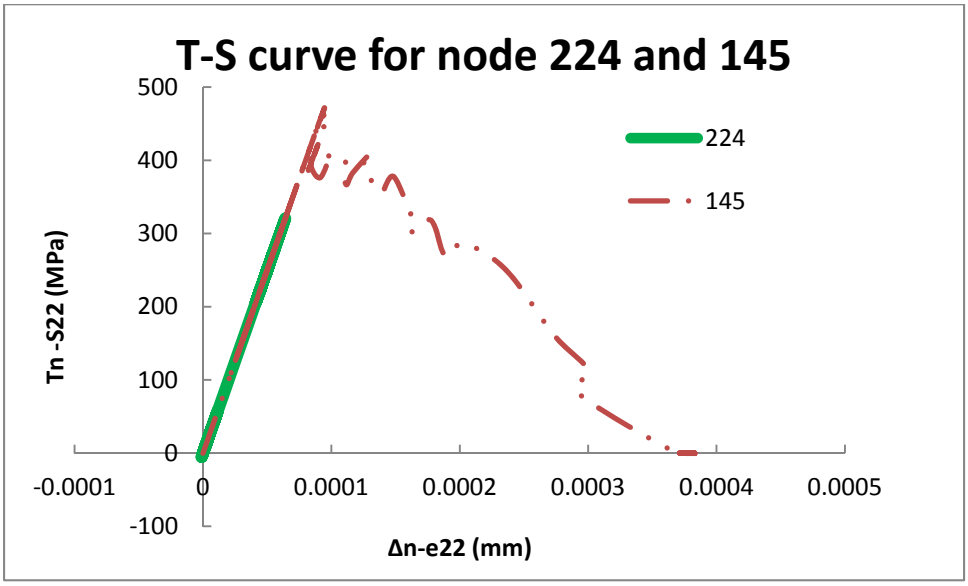

Figure 49. Traction-separation curve for nodes 224 and 145 located at unfailed and failed cohesive elements respectively.

Figure 50 is the final state of cohesive failure in the cutting simulation. A total of four elements fail after the cutting simulation.

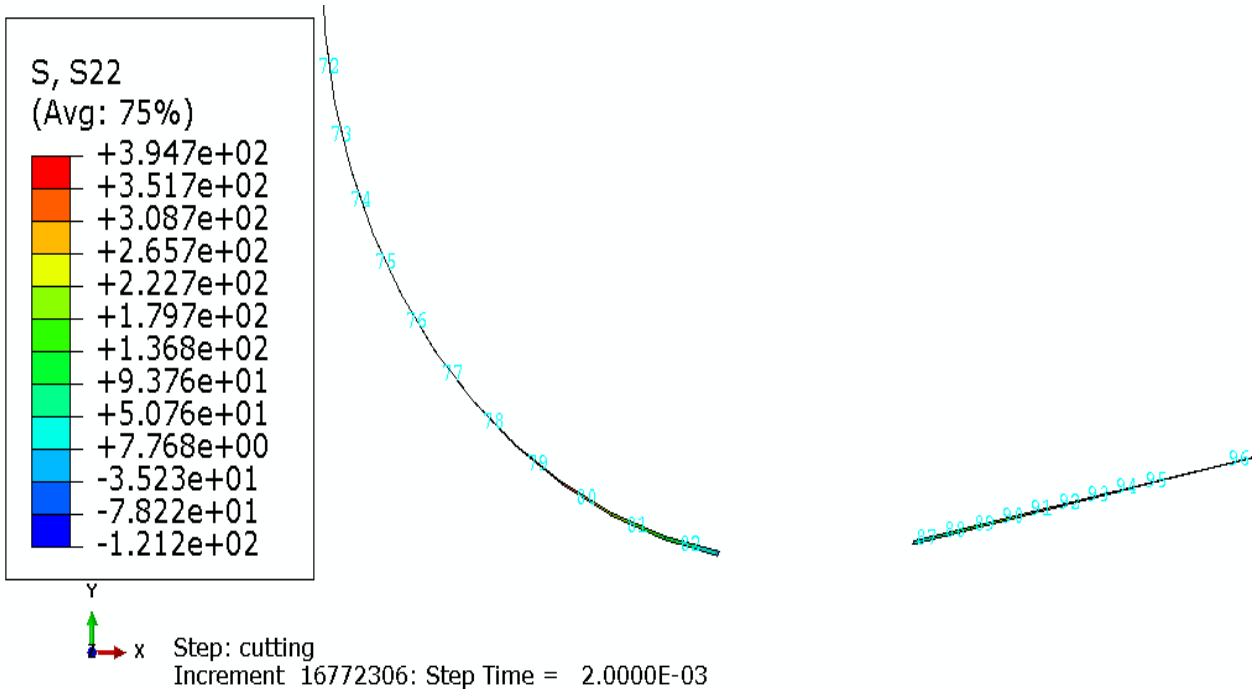

Figure 50. Cohesive failure final state in the cutting simulation.

Figure 51 is the final state of chip formation in the cutting simulation reaching its steady state. Figure 52 is the final state of the top-right chip zoom-in image, which shows the steady state when the curly chip forms and the chip-tool contact length stays roughly constant.

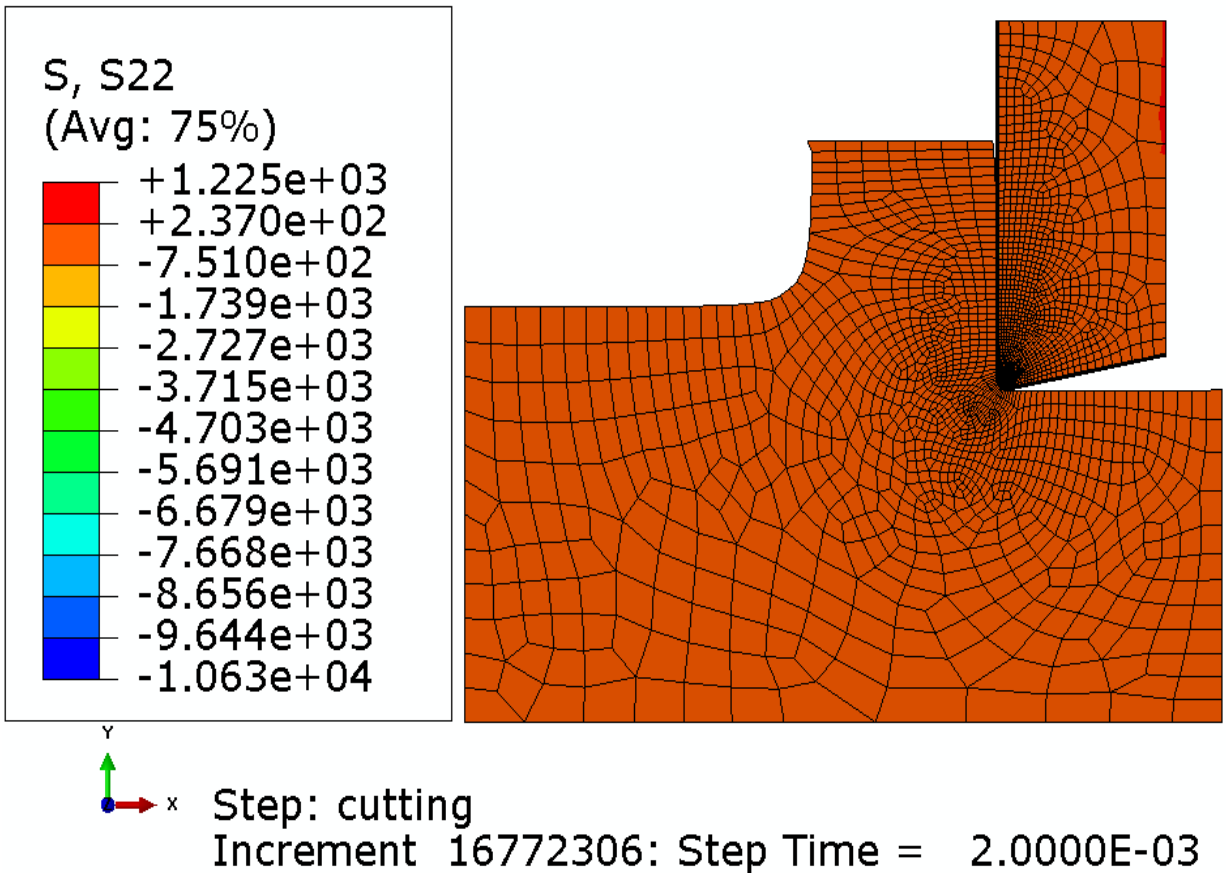

Figure 51. Final state of chip formation in the cutting simulation.

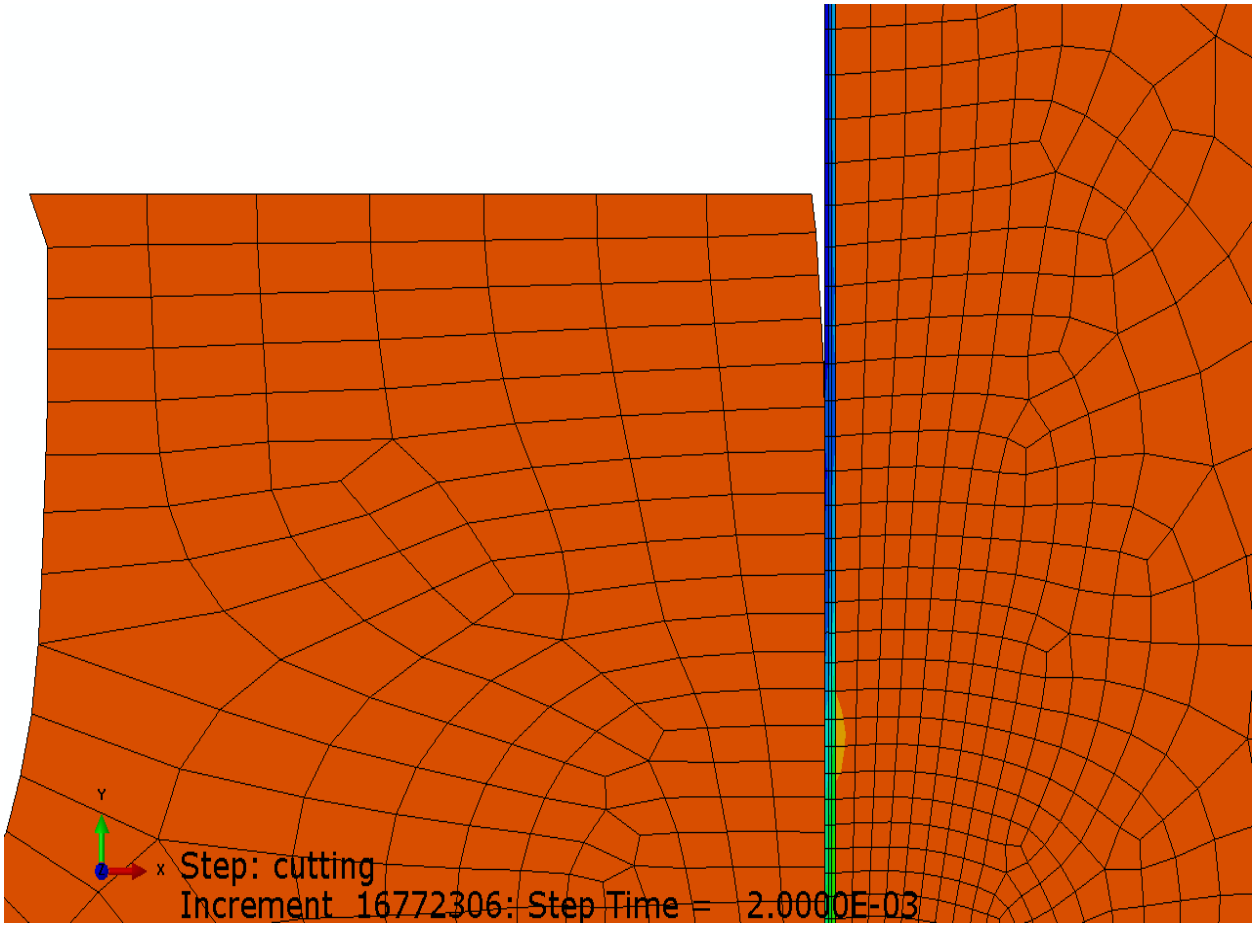

Figure 52. Final state (zoom-in of top-right chip) of chip formation in the cutting simulation.

Workpiece withdrawal shows further cohesive delamination, since the contact between the tool and the chip is removed progressively. Figure 53 demonstrates further cohesive element failures after workpiece withdrawal. At this simulated time, a total of 18 elements fail. The cohesive failure extends further to the flank face and the rounded area.

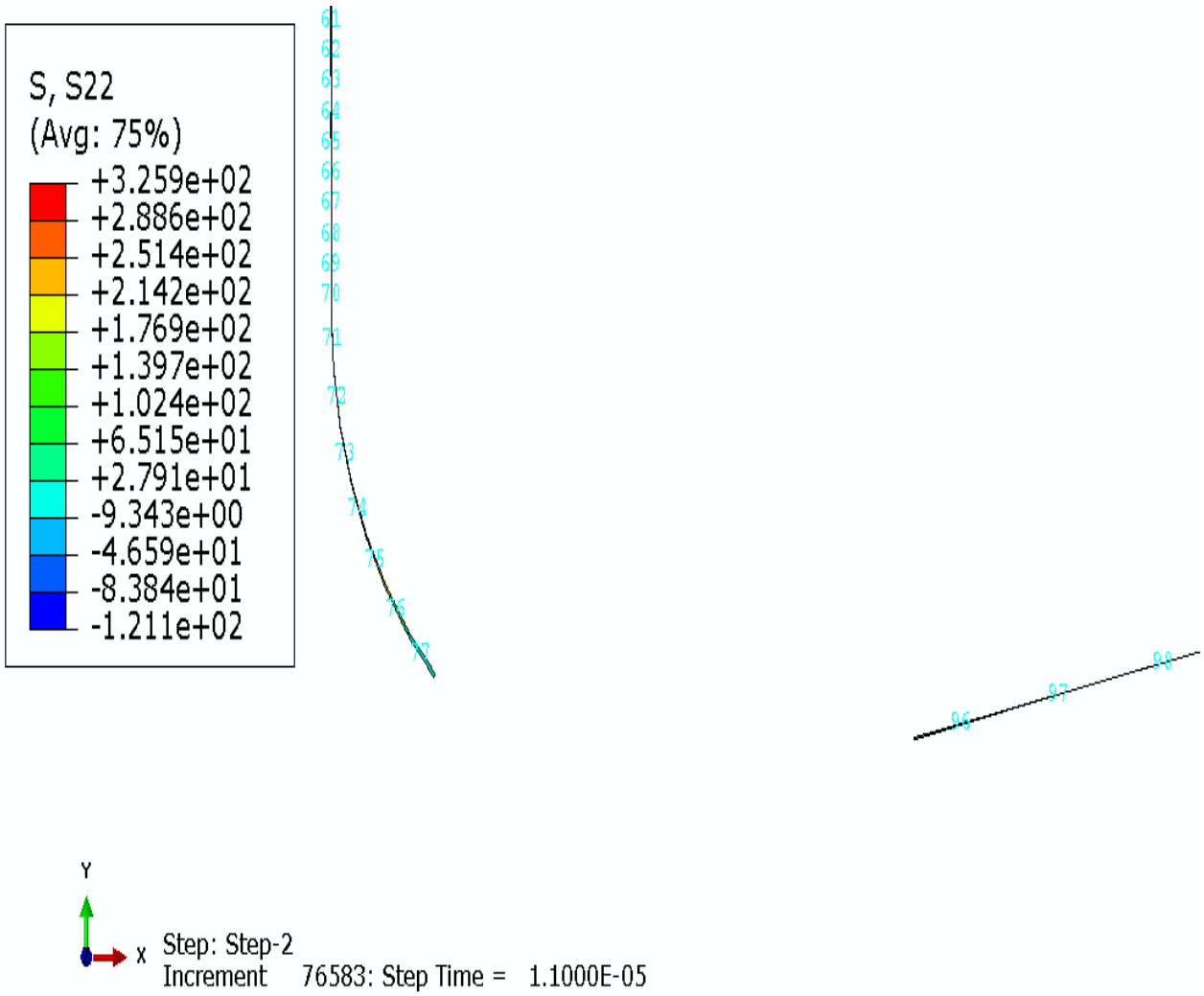

Figure 53. Cohesive failure at workpiece withdrawal simulation step time 0.000011 seconds.

Figure 54 shows the final state of the cohesive zone after the workpiece withdrawal process. A total of 18 elements without further failure exist in the workpiece withdrawal simulation.

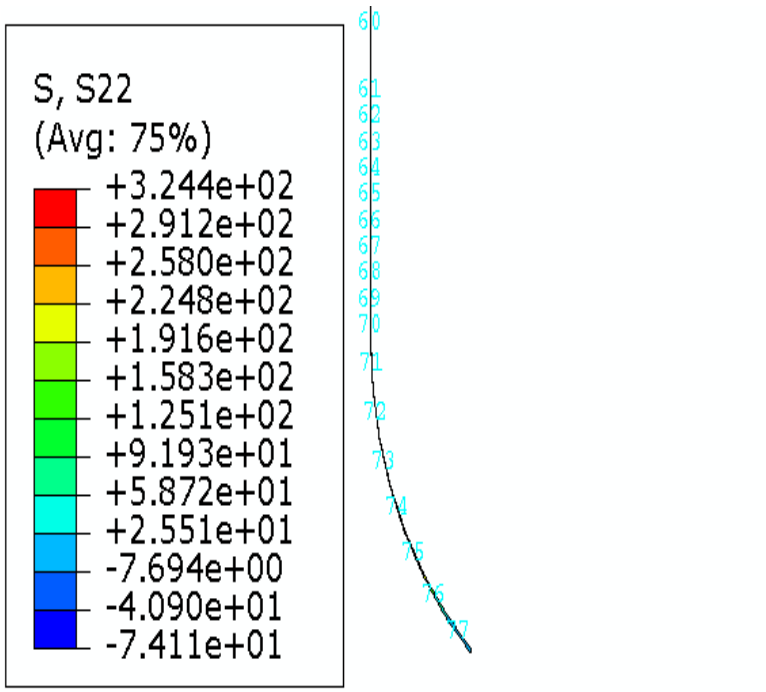

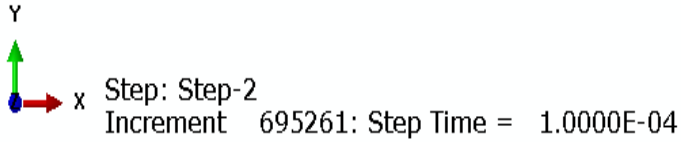

Figure 54. Final state of the cohesive zone after the workpiece withdrawal.

Figure 55 displays the final state of the workpiece and the tool in the workpiece withdrawal simulation. The workpiece is completely separated from the tool. It is evidently observed that no chip change happens in the workpiece retreatment.

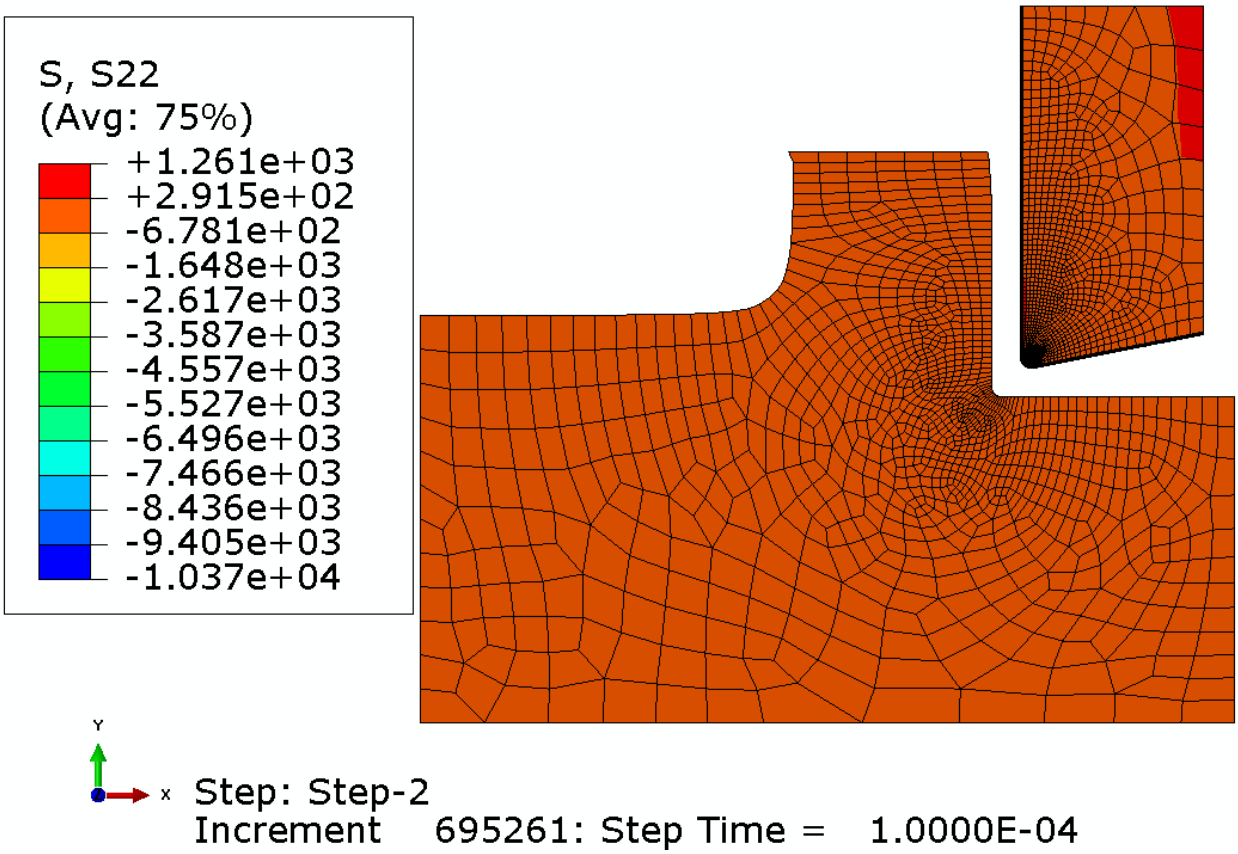

Figure 55. Final state of workpiece and tool in workpiece withdrawal simulation.

The following case is one example without cohesive zone failure during cutting simulation and after workpiece withdrawal process. In this case, the cutting speed is the same while the uncut chip thickness is different, which is 0.05 mm, a gentle condition, compared to the previous one.

Figure 45 (page 93) demonstrates no cohesive failure after the deposition process. Figure 56 shows the initial state of the workpiece, tool, and cohesive zone. No cohesive failure is observed at the beginning of the cutting simulation.

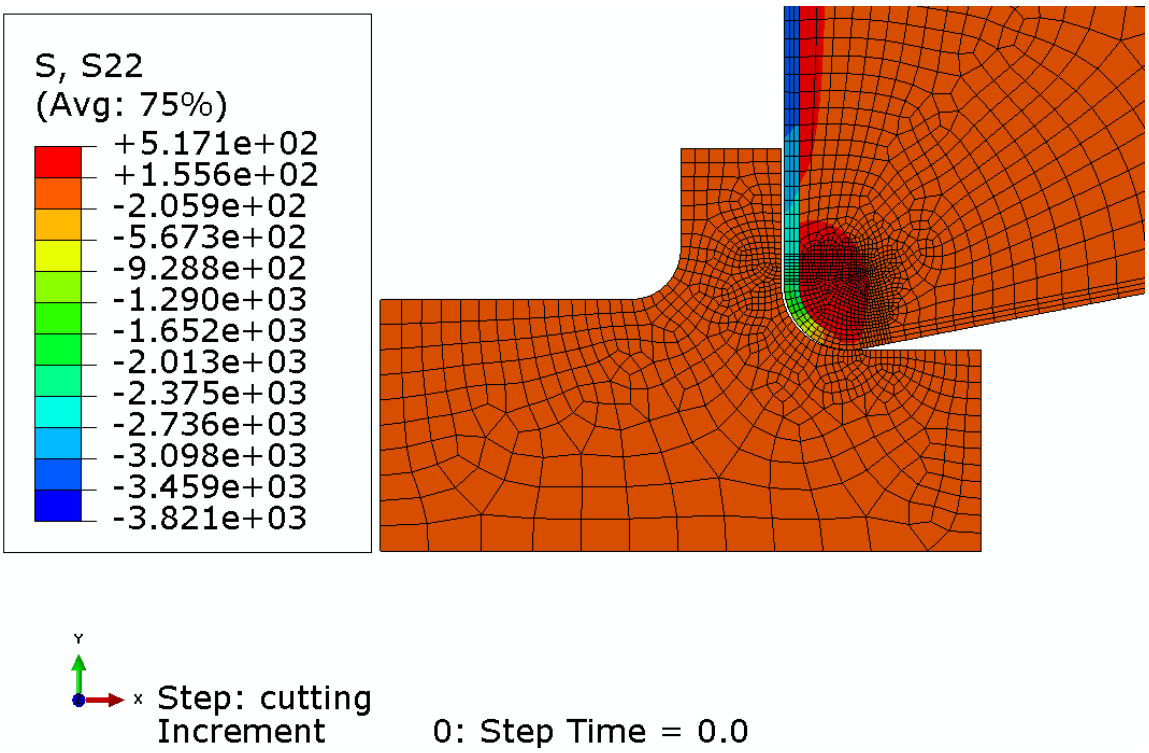

Figure 56. Initial state of the workpiece, tool, and cohesive zone in cutting parameter v5h0.05.

Figure 57 shows no cohesive failure at the end of the cutting simulation. The cutting process has reached steady state shown in Figure 56 (c) according to the chip shape.

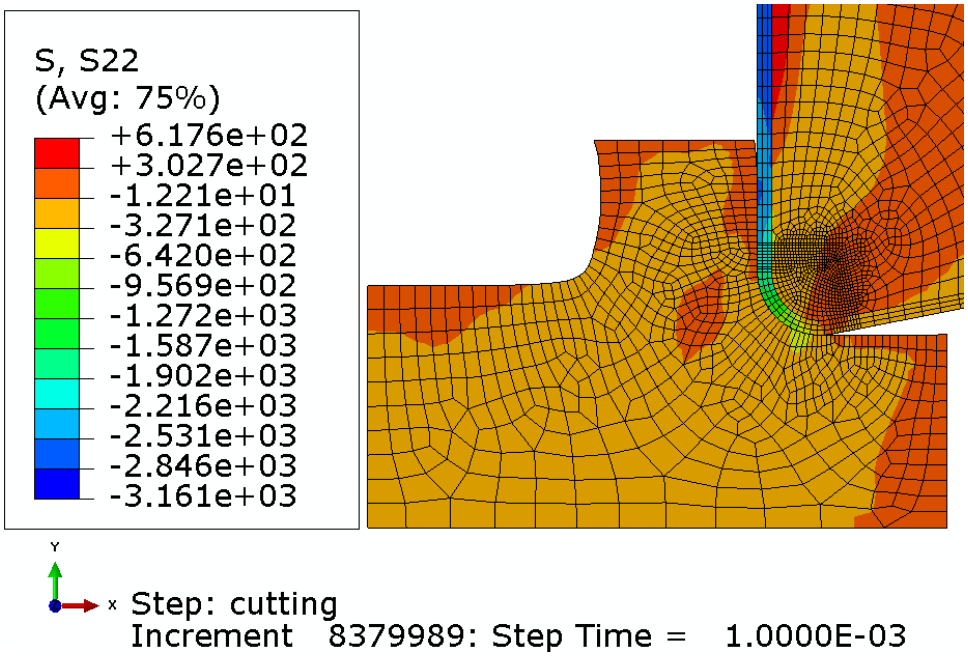

(a) workpiece and tool

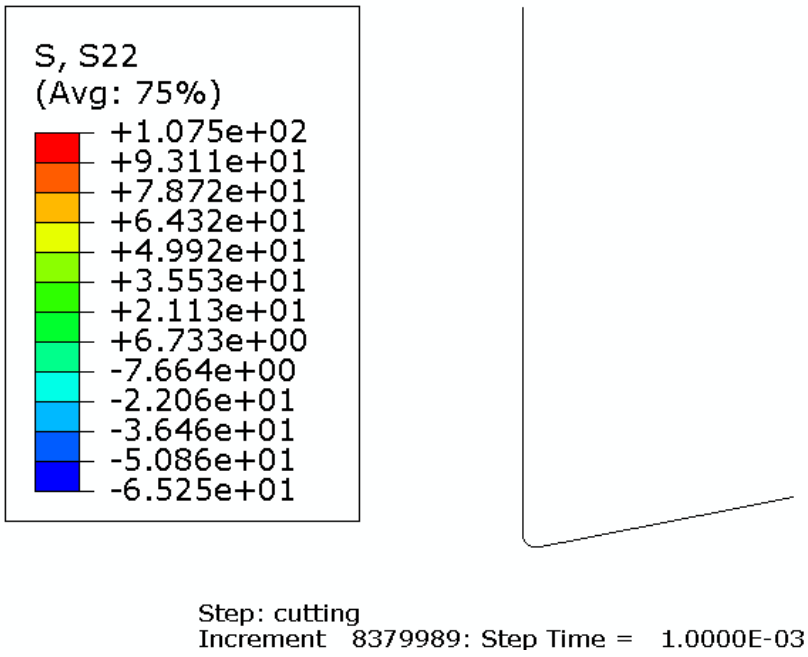

(b) cohesive zone

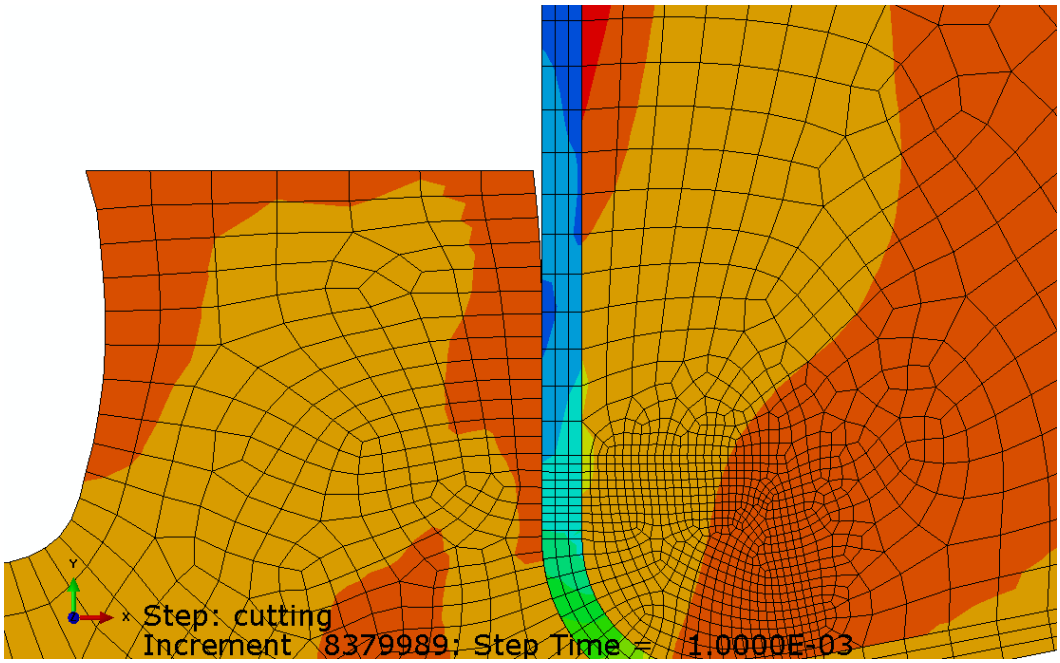

(c) Final state (zoom-in) of chip formation in the cutting simulation

Figure 57. Final state of workpiece, tool, and cohesive zone in the cutting simulation.

Figure 58 displays the final state of the workpiece, tool, and cohesive zone in the workpiece withdrawal simulation.

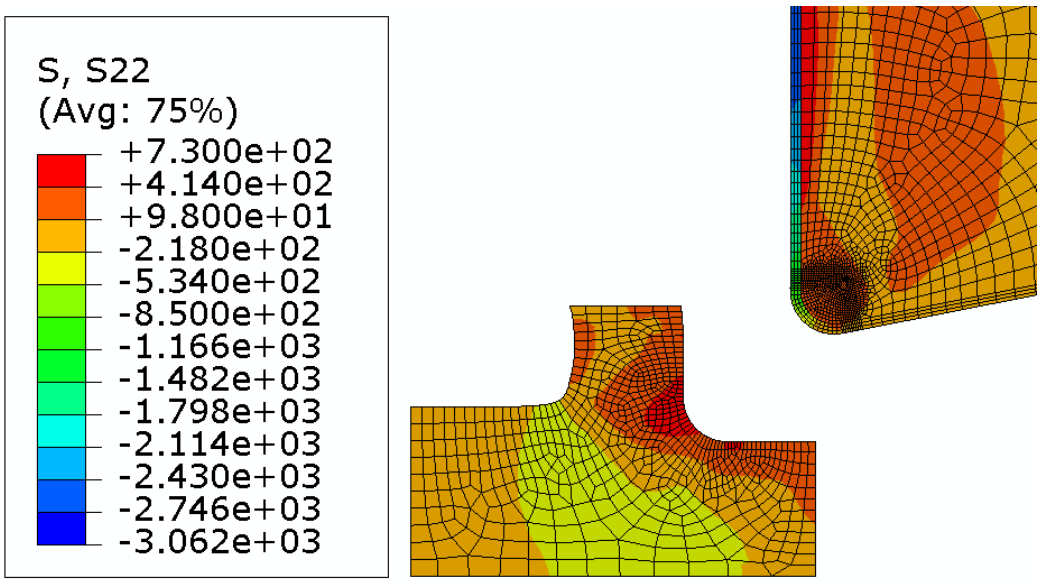

(a) workpiece and tool

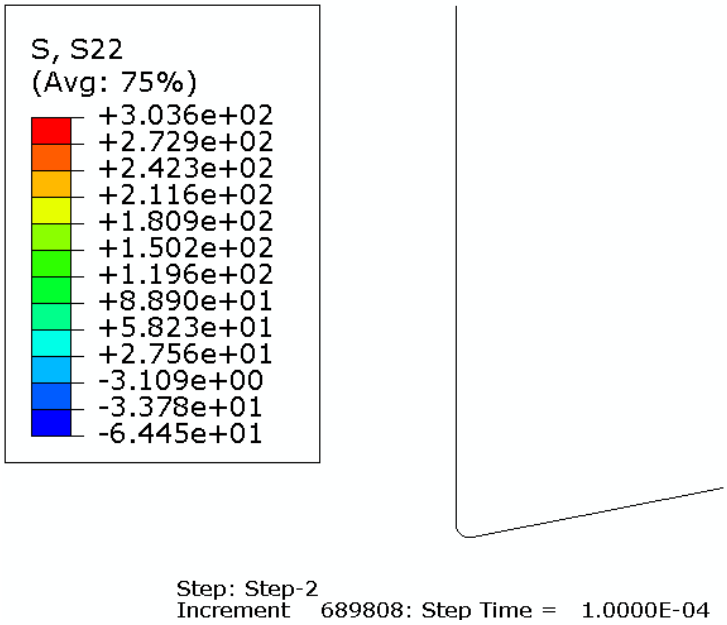

(b) cohesive zone

Figure 58. Final state of workpiece, tool, and cohesive zone in the workpiece withdrawal simulation.

The above deposition stress simulation, cutting simulation, and workpiece withdrawal simulation demonstrate that no cohesive delamination happens in all of the three stages for the diamond-coated tool with deposition at 600˚C, a cohesive parameter (σ_{max}) of 500 MPa, and cutting conditions of a speed of 5.0 m/s, and an uncut chip thickness of 0.05 mm.

Summary

Coated tool failure is complicated due to different failure mechanisms existing(e.g. coating fracture & delamination) and possibly interacting with each other and complexed by the tool geometry effect, and residual deposition stress, etc. In this study, a cohesive zone model is first included in 2D cutting simulations using the finite element method. The different cohesive fracture energy values are employed in the cutting simulations to investigate the energy effect on cohesive zone failure. Two different interface normal strengths are also tested. Last but not least, an example of progressive cohesive failure test in cutting and workpiece withdrawal simulations is realized with conditions of low deposition residual stress and large uncut chip thickness.

The major findings can be summarized as follows: (1) Residual deposition stress has a significant effect on cohesive failure. With deposition residual stress, the cohesive zone is more susceptible to element failure. (2) Large cohesive fracture energy tends to noticeably reduce the chances of cohesive failure. (3) The feasibility of cohesive interface failure for diamond-coated tools including deposition residual stress in cutting simulation has been demonstrated. (4) The developed model has been utilized to investigate cutting parameter uncut chip thickness effect in cutting simulation. The results show that large uncut chip thickness tends to cause cohesive interface failure.

CHAPTER 7

CONCLUSIONS AND RECOMMENDATIONS FOR FUTURE RESEARCH

Conclusions

Increasing use of high-strength Al alloys and composites in the automotive and aerospace industries for functional parts has created machining difficulties for the tooling industry. Conventional cutting tools made of plain or coated cemented carbides cannot withstand the rapid abrasive wear produced by the hard reinforcements embedded in those materials. Diamond is considered by far the best tooling material for machining these high-strength materials. Sintered polycrystalline diamond (PCD) and CVD diamond coatings are two competitive options, and CVD diamond-coated tools have attracted more interest due to their low cost and flexibility in fabrication. However, coating-substrate interface delaminations remain a major technical barrier, and the complex effects of tool geometry and deposition residual stress, as well the effect of machining conditions on tool performance, have been hindering industrial application of CVD diamond-coated tools. The goal of this research is to improve the understanding of the effects of tool geometry and deposition residual stress as well the machining conditions on CVD diamond-coated tool performance in machining high-strength Al-based materials. Experimental and numerical approaches are utilized to achieve this objective. The major findings are summarized as follows.

1. Certain diamond-coated tools with different substrate edge radii have been tested in machining composite bars under two different cutting conditions: (4m/s and 0.05 mm/rev; 1.3 m/s and 0.15 mm/rev). Machining forces were monitored and analyzed against the different edge

radii. Tool flank-wear was measured and evaluated, and wear features were examined by SEM. The results show that increasing the edge radius will increase cutting forces, mainly the radial and axial components; moreover, the increasing rate decreases at a higher feed. The combined effects above result in complex wear behavior of diamond-coated tools with different edge radii. In particular, at the 1.3 m/s and 0.15 mm/rev condition, a 65 μm hone presents a tool life over 5 times longer than 5 μm sharp tools, though tools of either radii have similar tool wear results at the 4 m/s and 0.05 mm/rev condition.

2. A 2D couple thermo-mechanical finite element model of orthogonal cutting has been established. The stress and temperature fields of the diamond-coated tool, with and without deposition residual stress, are compared. The result shows the deposition residual stress remains largely inside the tool. The developed finite element orthogonal cutting model has been applied to investigate the tool stress evolution from deposition to machining, with two different edge radii, under two sets of cutting conditions. The simulations indicate that deposition residual stresses can remain dominant in gentle cutting, e.g., smaller uncut chip thicknesses. At a smaller uncut chip thickness, the stress level is marginally reduced by the contact stress from the chip. The maximum σ_r is in a close range between the different edge radii. However, at a larger uncut chip thickness, the radial normal stresses change noticeably due to machining, especially high tensile stresses close to the end of edge rounding (transition to flank surface). It is noted that the maximum σ_r is greater at the 5 μm edge, at 1.2 GPa versus 0.9 GPa at the 50 μm edge.

3. Cutting experiments have been conducted to validate the simulation model. Experiments conducted by researchers in NIST measure the cutting force and thrust force for the following condition: 25 μm edge radius, 20 μm coating thickness, 5 m/s cutting speed, and 0.15 mm uncut chip thickness at 128 N and 73 N per mm width of cut. This is comparable to the

simulation results of 162 N and 72 N of the cutting and thrust components for 1 mm uncut width. Cutting temperature is also compared. The maximum tool temperature is 330˚C, versus 275˚C from the experiment. Since the cutting simulation was 2D, it did not take heat transfer along the in-plane direction into consideration, which deviates from the actual cutting, with heat loss parallel to the cutting edge direction. Hence, the higher simulated cutting tool temperature may be due to such a departure.

4. A cohesive zone model has been incorporated at the interface of the diamond coating and the substrate. Finite element models of residual deposition stress simulations and cutting simulations have been developed to investigate the interface behavior during cutting simulations under various machining conditions.

Contributions of the Study

The contributions of this study are summarized below.

1. This study correlates deposition residual stresses, cutting conditions, and tool geometry parameters with diamond-coated tool performance.

2. A 2D finite element model of diamond-coated tool cutting simulation, including residual deposition stress, was established for evaluating tool performance for different tool geometry parameters, deposition residual stress conditions, and machining parameters.

3. A cohesive zone model has been incorporated into 2D cutting simulations. Using this method, the effects of interface properties, and machining and tool parameters on coating delaminations can be evaluated during cutting, where thermal load and mechanical load can be combined together.

Recommendations for Future Research

This study provides a better understanding of the effect of diamond-coated tool geometry as well cutting conditions on tool performance in machining Al-Si alloys and Al-matrix composites. Furthermore, the finite element model of cutting simulation, incorporating the cohesive zone model, provides better understanding of the wear and failure mechanisms of CVD diamond-coated cutting tools in machining. Future research can be pursued in the following directions:

1. The developed finite element model of cutting simulation is based on a 2D model, which may limit understanding of the actual machining operation. Therefore, developing a 3D finite element model of cutting simulation may bring research results much closer to the real conditions.

2. The advantage of CVD diamond-coated tools over PCD tools is fabrication flexibility, especially in tools with complex geometry. The above research should be extended to more general 3D conditions and more complex geometries, such as drills, milling cutters, etc.

3. The 2D cutting simulation employs a constitutive model for one workpiece material. To investigate tool performance in cutting simulation with other workpiece materials, more experimental and analytical tests may be required to acquire more related constitutive parameters.

4. In the cutting simulation model, the diamond coating is assumed to be elastic and of no plastic behavior. No abrasive or material loss in the coating is accounted for in the simulation, which is not in agreement with regular machining operations and conditions. Therefore, an advanced constitutive model of diamond-coated tools with coating wear rate or a coating fracture

model might be introduced so as to investigate the effects of the cutting conditions, tool geometry effect, and interface bonding conditions on diamond-coated tool performance.

REFERENCES

Adibi-Sedeh, A. H., Madhavan, V. (2003). Understanding of finite element analysis results under the framework of Oxley's machining model. In: *Proceedings of the sixth CIRP international workshop on modeling of machining operations*, Hamilton, Canada, 2003.

Albrecht, P. (1960). New developments in the theory of the metal-cutting process, Part I. The ploughing process in metal cutting. *Journal of Engineering for Industry*, November, 348-358.

Almeida, F. A., Oliveira, F. J., Sousa, M., Fernandes, A.J.S., Sacramento, J., & Silva, R.F. (2005). Machining hardmetal with CVD diamond direct coated ceramic tools: effect of tool edge geometry. *Diamond and Related Materials*, *14*, 651-656.

Almeida, F. A., Soares, E., Fernandes, A. J. S., Sacramento, J., Silva, R. F., & Oliveira, F. J. (2011). Diamond film adhesion onto sub-micrometric WC-Co substrates. *Vacuum*, *Vol. 85*, 1135-1139.

Al-Zkeri, I., Rech, J., Altan, T., Hamdi, H., & Valiorgue, F. (2009). Optimization of the cutting edge geometry of PVD coated carbide tools in dry turning of steels using a finite element analysis. *Machining Science and Technology*, *13*, 36-51.

Amirhagni, S., Reehal, H. S., Wood, R. J. K., & Wheeler, D. W. (2001). Diamond coatings on tungsten carbide and their erosive wear properties. *Surface and Coatings Technology*, *135*, 126-138.

Andrewes, C. J. E., Feng, H. –Y., & Lau, W. M. (2000). Machining of an aluminium/SiC composite using diamond inserts. *Journal of Materials Processing Technology*, *102*, 25-29.

Arrazola, P. J., Meslin, F., & Marya, S. (2003). A technique for the identification of friction at tool/chip interface during machining. *Proceedings 6th CIRP International Workshop on Modeling of Machining Operations*, Hamilton, ON, Canada.

Arrazola, P. J., Ugarte, D., & Dominguez, X. (2008). A new approach for the friction identification during machining through the use of finite element modeling. *International Journal of Machine Tools and Manufacture*, *48*, 173-183.

Baker, M. (2006). Finite element simulation of high speed cutting forces. *Journal of Materials Processing Technology*, *Vol. 176*, 117-126.

Barenblatt, G. I. (1962). Mathematical theory of equilibrium cracks in brittle fracture. *Advances in Applied Mechanics*, Academic Press, New York, 55-129.

Barge, M., Hamdi, H., Rech, J., & Bergheau, J.-M. (2005). Numerical modeling of orthogonal cutting: influence of numerical parameters. *Journal of Materials Processing Technology*, *164-165*, 1148-1153.

Belytschko, T., & Kennedy, J. M. (1978). Computer models for subassembly simulation. *Nuclear Engineering and Design*, *49*, 17-38.

Bouzakis, K. -D., Michailidis, N., Skordaris, G., Kombogiannis, S., Hadjiyiannis, S., Efstathiou, K., Erkens, G., Rambadt, S., & Wirth, I. (2003). Optimization of the cutting edge roundness and its manufacturing procedures of cemented carbide inserts, to improve their milling performance after a PVD coating deposition. *Surface and Coating Technology*, *163-164*, 625-630.

Bowden, F. P., & Tabor, D. (1950). *Friction and lubrication of solids*. Oxford University Press.

Brocks, W. (2005). Cohesive strength and separation energy as characteristic parameters of fracture toughness and their relation to micromechanics. *Structural Integrity & Durability*, *1*, 233-243.

Bull, S. J., & Berasetegui, E. G. (2006). An overview of the potential of quantitative coating adhesion measurement by scratch testing. *Tribology International*, *39*, 99-114.

Bull, S. J., & Rickerby, D. S. (1988). The use of scratch adhesion testing for the determination of interfacial adhesion: The importance of frictional drag. *Surface and Coatings technology*, *36*, 503-517.

Bull, S. J., & Rickerby, D. S. (1990). New developments in the modeling of the hardness and scratch adhesion of thin films. *Surface and Coatings technology*, *42*, 149-164.

Carroll III, J. T., & Strenkowski, J. S. (1988). Finite element models of orthogonal cutting with application to single point diamond turning. *International Journal of Mechanical Science*, *30*, 899-920.

Ceretti, E., Lazzaroni, C., Menegardo, L., & Altan, T. (2000). Turning simulations using a three-dimensional FEM code. *Journal of Materials Processing Technology*, *98*, 99-103.

Chan, K. C., Cheung, C. F., Ramesh, M. V., Lee, W. B., & To, S. (2001). A theoretical and experimental investigation of surface generation in diamond turning of an Al6061 SiCp metal matrix composite. *International Journal of Mechanical Sciences*, *43*, 2047-2068.

Chandra, N., Li, H., Shet, C. & Ghonem, H. (2002). Some issues in the application of cohesive zone models for metal-ceramic interfaces. *International Journal of Solids and Structures, 39*, 2827-2855.

Childs, T. H. C., & Maekawa, K. (1990). Computer aided simulation and experimental studies of chip flow and tool wear in the turning of low alloy steels by cemented carbide tools. *Wear*, *139*, 235-250.

Chou, Y. K., & C. J. Evans, (1999). White layers and thermal modeling of hard turned surfaces. *International journal of machine tools and manufacture*, *39*, No.12, 1863-1881.

Chou, Y. K., & Liu, J. (2005). CVD Diamond Tool Performance in Composite Machining. *Surface and Coatings Technology*, *200*, 1872-1878.

Davim, J. P. (2002). Diamond tool performance in machining metal-matrix composites. *Journal of Materials Processing Technology*, *128*, 100-105.

Deuerler, F., Woehrl, N., & Buck, V. (2006). Characterisation of nanostructured diamond coatings on various hardmetal surfaces. *International Journal of Refractory Metals and Hard Materials*, *24*, 392-398.

Dias, A. M. S., Modenesi, P. J., & de Godoy, G. C. (2006). Computer simulation of stress distribution during Vickers hardness of WC-6Co. *Materials Research*, *Vol. 9*, 73-76.

Dugdale, D. S. (1960). Yielding of steel sheets containing slits. *Journal of Mechanics and Physics of Solids*, *Vol. 8*, 100-104.

Durante, S., Rutelli, G., & Rabezzana, F. (1997). Aluminum-based MMC machining with diamond-coated cutting tools. *Surface and Coatings Technology*. *94-95*, 632-640.

El-Gallab, M, & Sklad, M. (1998). Machining of Al/SiC particulate metal-matrix composites: part I: tool performance. *Journal of Materials Processing Technology*, *83*, 277-285.

Ernst, H. J. & Merchant, M. C. (1941). Chip formation, friction, and finish. *Trans. Am. Soc. Metals*. *29*, 299

Fang, G., & Zeng, P. (2005). Three-dimensional thermo-elastic-plastic coupled FEM simulations for metal oblique cutting processes. *Journal of Materials Processing Technology*, *168*, 42-48.

Fang, N., & Xiong, L. S. (2008). Determination of friction and material-flow boundary condition on the tool round cutting edge. *Transactions of the North American Manufacturing Research Institute of SME*, *36*, 413-420.

Gao, Y. F., & Bower, A. F. (2004). A simple technique for avoiding convergence problems in finite element simulations of crack nucleation and growth on cohesive interfaces. *Modelling and Simulation in Materials Science and Engineering*, *12*, 453-463.

Gao, Y. F. (Sep. 2011). Private communication contribute.

Geubelle, P. H., & Baylor, J. S. (1998). Impact-induced delamination of composites: a 2D simulation. *Composites Part B: Engineering*, *29 (5)*, 589-602.

Griffith, A. A. (1920). The phenomena of rupture and flow in solids. *Philosophical Transactions of the Royal Society of London*, *Vol. A211*, 163-198.

Griffith, A. A. (1924). Theory of rupture. Proceedings of the First International Congress for Applied Mechanics, 55-63.

Grzesik, W., Bartoszuk, M., & Nieslony P. (2005). Finite difference method-based simulation of temperature fields for application to orthogonal cutting with coated tools. *Machining Science and Technology*, *9(4)*, 529-546.

Gunnars, J., & Alahelisten, A. (1996). Thermal stresses in diamond coatings and their influence on coating wear and failure. *Surface and Coatings Technology*, *80*, 303-312.

Guo, Y. B., & Dornfeld, D. A. (1998). Finite element modeling of burr formation process in drilling 304 stainless steel. *Transactions of NAMRI/SME*, *XXVI*, 207-212.

Guo, Y. B., & Dornfeld, D. A. (2000). Finite element modeling of burr formation process in drilling 304 stainless steel. *Journal of Manufacturing Science and Engineering, Trans. ASME*, *122*, 612-619.

Guo, Y. B., & Liu, C. R. (2002). 3D FEA modeling of hard turning. *Journal of Manufacturing Science and Engineering Trans. ASME*, *124*, 189-199.

Hahn, R. S. (1951). On the temperature developed at the shear plane in the metal cutting process. *Proceedings of First U.S. National Congress of Applied Mechanics*, 661-666.

Hashemi, J., Tseng, A., & Chou, P. C. (1994). Finite element modeling of segmental chip formation in high-speed machining. *J. Mater Eng Perform*, *3*, 712-721.

Heigel, J. C., Ivester, R. W., & Whitenton, E. P. (2008). Temperature measurements of segmented chips using dual-spectrum high-speed microvideography. *Transactions of NAMRI/SME*, *36*, 73-80.

Henriksen, E. K., (1951). Residual stress in machined surfaces. *Trans. ASME*, ***73***, 69-76

Heath, P. J. (1986). Properties and Uses of Amborite. *Industrial Diamond Review*, *46*, 120-127.

Hu, J., Chou, Y. K., & Thompson, R. G. (2007a). Characterization of nanocrystalline diamond coating cutting tools. *International Conference on Metallurgical Coatings and Thin Films*, San Diego, CA, April 23 – 27, 2007, accepted for publication.

Hu, J., Chou, Y. K., & Thompson, R. G. (2007b). On stress analysis of diamond coating cutting tools. *Transactions of NAMRI/SME*, *37*, 177-184

Hu, J., Chou, Y. K., & Thompson, R. G. (2008a). Nanocrystalline diamond coating tools for machining high-strength Al alloys. *International Journal of Refractory Metals and Hard Materials*, *26*, 135-144.

Hu, J., Chou, Y. K., & Thompson, R. G. (2008b). Cohesive zone effects on coating failure evaluations of diamond-coated tools. *Surface and Coating Technology*, *203*, 730-735

Hua, J., & Shivpuri, R. (2004). Prediction of chip morphology and segmentation during the machining of titanium alloys. *Journal of Materials Processing Technology*, *150*, 124-133.

Hung, N. P., Loh, N. L., & Xu, Z. M. (1996). Cumulative tool wear in machining metal matrix composites Part II: Machinability. *Journal of Materials Processing Technology*, *58*, 114-120.

Irwin, G. R. (1957). Analysis of stresses and strains near the end of a crack traversing a plate. *Journal of Applied Mechanics*, *24*, 361-364.

Irwin, G. R. (1964). Structural aspects of brittle fracture. *Applied Materials Research*, 3, 65-81.

Ivester, R. W. (2011). Tool temperatures in orthogonal cutting of alloyed Titanium. *Proceedings of NAMRI/SME*, *39*, 2011.

Ivester, R., Whitenton, E., Hershman, J., Chou, K., & Wu, Q. (2012). 2D orthogonal cutting experiments using diamond-coated tools with force and temperature measurements. *Proceedings of 40th Annual SME North American Manufacturing Research Conference (NAMRC 40)*, Notre Dame, IN, June 4-8, 2012, submitted, Nov., 2011.

Johnson, G. R., & Cook, W. H. (1983). A constitutive model and data for metals subjected to large strains, high strain rates and high temperatures. *Proceedings of the 7th International Symposium on Ballistics*, Hague, The Netherlands, April 1983, 541-547.

Klamecki, B. E. (1973). *Incipient chip formation in metal cutting-a three-dimensional finite element analysis*. Ph.D. thesis, University of Illinois at Urbana-Champaign, Urbana

Karner, J., Pedrazzini, M., Reineck, I., Sjöstrand, M. E., & Berrmann, E. (1996). CVD diamond-coated cemented carbide cutting tools. *Materials Science and Engineering A*, *209*, 405–413.

Kim, J. D., & Moon, C. H. (1996). A study on microcutting for the configuration of tools using molecular dynamics. *Journal of Materials Processing Technology*, *59*, 309-314.

Kishawy, H. A., Rogers, R. J., & Balihodzic, N. (2002). A numerical investigation of the chip tool interface in orthogonal machining. *International Journal of Machining Science and Technology*, *5*, No. 3, 397-414.

Kishawy, H. A., Deiab, I. M., & Haglund, A. J. (2008). Arbitrary Lagrangian Eulerian analysis on cutting with a honed tool. *Proc. IMechE (2008), Part B: J. Engineering Manufacture*, *222*, 155-162.

Kitamura, T., Hirakata, H., & Itsuji, T. (2003). Effect of residual stress on delamination from interface edge between nano-films. *Engineering Fracture Mechanics*, *70*, 2089-2101.

Lee, E. H., & Shaffer, B. W. (1951). The theory of plasticity applied to a problem of machining. *Journal of Applied Mechanics*, *18*, 405-413.

Lin, Z. -C., & Lin, Y. -Y. (1999). Fundamental modeling for oblique cutting by thermo-elastic-plastic FEM. *International Journal of Mechanical Sciences*, *41*, 941-965.

Lin, Z. –C, & Lin, Y. Y. (2001). A study of oblique cutting for different low cutting speeds. *Journal of Materials Processing Technology*, *115*, 313-325.

Lin, Z. -C., & Lo, S. –P. (2001). 2-D discontinuous chip cutting model by using strain energy density theory and elastic-plastic finite element method. *International Journal of Mechanical Sciences*, *Vol. 43*, 383-398.

Liu, C. R., & Barash, M. M. (1976). The mechanical state of the sublayer of a surface generated by chip-removal process, *Part 2: Cutting With a Tool With Flank Wear. Trans. ASME*, *98*, No. 4, 1202-1208.

Liu, C. R., & Guo, Y. B. (2000). Finite element analysis of the effect of sequential cuts and tool chip friction on residual stresses in a machined layer. *International Journal of Mechanical Sciences*, *42*, 1069-1086.

Liu, K., & Melkote, S. N. (2007). Finite element analysis of the influence of tool edge radius on size effect in orthogonal micro-cutting process. *International Journal of Mechanical Sciences*, *49*, 650-660.

Mabrouki, T., & Rigal J. -F, (2006). A contribution to a qualitative understanding of thermo-mechanical effects during chip formation in hard turning. *Journal of Materials Processing Technology*, 176, 214-221.

MacGinley, T., & Monaghan J. (2001). Modeling the orthogonal machining process using coated cemented carbide cutting tools. *Journal of Materials Processing Technology*, *118*, 293-300

Mackerle, J. (1999). Finite-element analysis and simulation of machining: a bibliography (1976-1996). *Journal of Materials Processing Technology*, *86*, 17-44.

Maekawa, K., & Itoh, A. (1995). Friction and tool wear in nano-scale machining - a molecular dynamics approach. *Wear*, *188*, 115-122.

Mallika, K., & Komanduri, R. (1999). Diamond coatings on cemented tungsten carbide tools by low-pressure microwave CVD. *Wear*, *Vol. 224*, 245, 266.

Mamalis, A. G., Horvath, M., Branis, A. S., & Manolakos, D. E. (2001). Finite element simulation of chip formation in orthogonal metal cutting. *Journal of Materials Processing Technology*, *110*, 19-27.

Marusich, T. D., & Ortiz, M. (1995). Modeling and simulation of high-speed machining. *International Journal of Numerical Methods Engineering*, *38*, 3675-3694.

Merchant, M. E. (1945). Basic mechanics of the metal cutting process. *Journal of Applied Mechanics*, *11*, 168-175.

Monaghan, J., & MacGinley, T. (1999). Modelling the orthogonal machining process using coated carbide cutting tools. *Computational Materials Science*, *16*, 275-284.

Movahhedy, M., Gadala, M. S., & Altintas, Y. (2000). Simulation of the orthogonal metal cutting process using an Arbitrary Lagrangian Eulerian finite element method. *Journal of Material Processing Technology*, *103*, 267-275

Movahhedy, M., Altintas, Y., & Gadala, M. S. (2002). Numerical analysis of metal cutting with chamfered and blunt tools. *Journal of Manufacturing Science and Engineering*, *124*, No. 2, 178-188

M'Saoubi, R., & Chandrasekaran, H. (2004). Investigation of the effects of tool micro-geometry and coating on tool temperature during orthogonal turning of quenched and tempered steel. *International Journal of Machine Tools and Manufacture*, *44*, 213-224.

Naerheim, Y., & Trent, E. M. (1977). Diffusion wear of cemented carbide tools when cutting steel at high speeds. *Metals Technology*, *4*, 548-556.

Nakamura, T., & Wang, Z. (2001). Simulations of crack propagation in porous materials. *Journal of Applied Mechanics*, *Vol. 68*, 242-251.

Nasr, M. N. A., Ng, E. -G., & Elbestawi, M. A. (2007). Modeling the effects of tool-edge radius on residual stresses when orthogonal cutting AISI 316L. *International Journal of Machine Tools and Manufacture*, *47(2)*, 401-411.

Ng, E., Tahany, I., Wardany, E. I., Dumitrescu, M., & Elbestawi, M. A. (2002). 3D finite element analysis for the high speed machining of hardened steel. *ASME International Mechanical Engineering Congress & Exposition*, New Orleans, Lousiana, 2002

Oles, E. J., Inspektor, A., & Bauer, C. E. (1996). The new diamond-coated carbide cutting tools. *Diamond and Related Materials*, *5*, 617-624.

Olortegui-Yume, J. A., Park, K. -H., & Kwon, P. (2008). Understanding tool wear of multilayer coated carbides in machining 1045 steel. *Transactions of NAMRI/SME*, *36*, 525-532.

Ozel, T., & Altan T. (2000). Process simulation using finite element method-prediction of cutting forces, tool stresses and temperatures in high speed flat end milling. *International Journal of Machine Tools and Manufacturing*, *40*, 713-738.

Ozel, T. (2006). The influence of friction models on finite element simulations of machining. *International Journal of Machine Tools & Manufacture*, *46*, 518-530.

Ozel, T., & Zeren, E. (2007). Finite element modeling the influence of edge roundness on the stress and temperature fields induced by high-speed machining. *International Journal of Advanced Manufacturing Technology*, *35*, 255-267.

Pantale, O., Bacaria, J. –L., Dalverny, O., Rakotomalala, R., & Caperaa, S. (2004). 2D and 3D numerical models of metal cutting with damage effects. *Computers Methods in Applied Mechanics and Engineering*, *193*, 4383-4399.

Polini, R., Casadei, F., D'Antonio, P., & Traversa, E. (2003). Dry turning of alumina/aluminum composites with CVD diamond-coated Co-cemented tungsten carbide tools. *Surface and Coatings Technology*, *166*, 127-134.

Potdar, K, & Zehnder, T. (2003). Measurements and simulations of temperature and deformation fields in transient metal cutting. *Journal of Manufacturing Science and Engineering*, *125*, 645-655.

Pramanik, A., Zhang, L. C., & Arsecularatne, J. A. (2006). Prediction of cutting forces in machining of metal matrix composites. *International Journal of Machine Tools and Manufacture*, *46*, 1795-1803.

Qin, F., Chou, Y. K., Noland, D., Thompson, R., & Ni, W. Y. (2009). Cutting edge radius effects on diamond-coated tools. *Transactions of the North American Manufacturing Research Institution of SME*, *37*, 653-660.

Qin, F., & Chou, Y. K. (2010). Case studies of diamond-coated tool cutting simulations: coating thickness and cutting speed effects. *Proceedings of the 2010 International Manufacturing Science and Engineering Conference*, October 12-15, 2010, Erie, Pennsylvania, MSEC2010-34306.

Rakotomalala, R., Joyot, P., & Touratier, M. (1993). Arbitrary Lagrangian-Eulerian thermomechanical finite-element model of material cutting. *Communications in Numerical Methods in Engineering*, *9*, 975-987.

Ramesh, M. V., Chan, K. C., Lee, W.B., & Cheung, C. F. (2001). Finite-element analysis of diamond turning of aluminum matrix composites. *Composites Science and Technology*, *61*, 1449-1456.

Rech, J., Yen, Y.-C., Hamdi, H., Altan, T., & Bouzakis, K. D. (2004). Influence of cutting edge radius of coated tool in orthogonal cutting of alloy steel. *Aip Conference Proceedings*, 1402-1407.

Renaud, A., Hu, J., Qin, F., & Chou, Y. K. (2008). Numerical simulations of 3D Tool geometry effects on deposition residual stresses in diamond-coated cutting tools. *Proceedings of the 2008 International Manufacturing Science and Engineering Conference*, October 7-10, 2008, Evanston, Illinois, 2008, MSEC2008-72204.

Renaud, A., Hu, J., Qin, F., & Chou, Y. K. (2009). Numerical simulations of 3D tool geometry effects on deposition residual stresses in diamond-coated cutting tools. *International Journal of Mechatronics and Manufacturing Systems*, *2*, 490-502.

Repetto, R., Radovitzky, R., & Ortiz, M. (2000). Finite element simulation of dynamic fracture and fragmentation of glass rods. *Computer Methods in Applied Mechanics and Engineering*, *183*, 3-14.

Rice, J. R. (1992). Dislocation nucleation from a crack tip: an analysis based on Peierls concept. *Journal of the Mechanics and Physics of Solids*, *vol. 40*, *issue 2*, 239-271

Rice, J. R., & Thomson, R. (1974). Ductile versus brittle behavior of crystals. *Philosophical Magazine*, *29*, 73-97.

Rice, J. R., & Tracey, D. M. (1969). On the ductile enlargement of voids in triaxial stress fields. *Journal of the Mechanics and Physics of Solids*, *17*, 201-217

Saito, Y., Isozaki, T., Masuda, A., Fukumoto, K., Chosa, M., & Ito, T. (1993). Adhesion strength of diamond film on cemented carbide insert. *Diamond and Related Materials*, *2*, 1391-1395.

Sartkulvanich, P., Sahlan, H., & Altan, T. (2007). A finite element analysis of burr formation in face milling of a cast aluminum alloy. *Machining Science and Technology*, *11*, 157-181.

Schimmel, R. J., Endres, W. J., & Stevenson, R. (2002). Application of an internally consistent material model to determine the effect of tool edge geometry in orthogonal machining. *Transactions of the ASME, Journal of Manufacturing Science and Engineering*, *124*, 536-543.

Sextro, W. (2002). *Dynamical contact problems with friction*, Springer-Verlag Berlin Heidelberg. 1st ed.

Sheikh-Ahmad, J. Y., Stewart, J. S., & Feld, H. (2003). Failure characteristics of diamond-coated carbides in machining wood-based composites. *Wear*, *255*, 1433-1437.

Shen, C. H. (1996). The importance of diamond-coated tools for agile manufacturing and dry machining. *Surface and Coatings Technology*, *86-87*, 672-677.

Shih, A. J., & Yang H. T. (1993). Experimental and finite element predictions of residual stresses due to orthogonal cutting. *International Journal for Numerical Methods in Engineering*, *Vol. 36*, 1487-1507.

Shih, A. J. (1995). Finite element simulation of orthogonal metal cutting. *ASME Journal of Engineering for Industry*, *117*, 84-93.

Shirakashi, T., & Usui, E. (1976). Simulation analysis of orthogonal metal cutting process. *Journal of the Japan Society for Precision Engineering*,*42:5*, 340-345.

Shirakashi, T., & Usui E. (1974). Simulation analysis of orthogonal metal cutting mechanisam. *Proceedings of the first international conference on production engineering*, *part I*, 535-540.

Smithey, D. W., Kapoor, S. G., & DeVor, R. E. (2001). A new mechanistic model for predicting worn tool cutting forces. *Machining Science and Technology*, *5*, 23-42.

Stjernberg, K. G. (1980). Fracture Toughness of Tic-Coated Cemented Carbides. *Metal Science*. *14*, 189-192.

Strawbridge, A., & Evans, H. E. (1995). Mechanical failure of thin brittle coatings. *Engineering Failure Analysis*, *2*, 85-103.

Strenkowski, J. S., & Moon, K. J. (1990). Finite element prediction of chip geometry and tool/workpiece temperature distributions in orthogonal metal cutting. *ASME Journal of Engineering for Industry*, *112*, 313-318.

Suzuki, H., & Hayashi, K. (1981). The Strength Decrease in WC-Co Cemented Carbides Having Coated-Layer by CVD. *Journal of the Japan Society of Powder and Powder Metallurgy*. *28*, 257-259.

Tay, A. O., Stevenson, M. G., & de Vahl, G. D. (1974). Using the finite element method to determine temperature distributions in orthogonal machining. *Proceedings of Institution of Mechanical Engineers*, 1988, 627-638.

Thiele, J. D., Melkote, S. N., Peascoe, R. A., & Watkins, T. R. (2000). Effect of cutting-edge geometry and workpiece hardness on surface residual stresses in finish hard turning of AISI 52100 steel. *Transactions of the ASME, Journal of Manufacturing Science and Engineering*, *122*, 642-649.

Thomason, P. F. (1985). A three-dimensional model for ductile fracture by the growth and coalescence of microvoids. Acta Metallurgica, 33 (6), 1087-1095.

Tian, Y., & Shin, Y. C. (2004). Finite element modeling of machining of 1020 steel including the effect of round cutting edge. *Transactions of the North American Manufacturing Research Institute of SME*, *32*, 111-118.

Trigger, K. J., & Chao, B. T. (1951). An analytical evaluation of metal cutting temperature. *Transactions of ASME*, *73*, 57-68.

Tvergaard, V. (1982). On localization in ductile materials containing spherical voids. *International Journal of Fracture*, *Vol. 18*, *Issue 4*, 237-252.

Usui, E., & Takeyama, H. (1960). A photoelastic analysis of machining stresses. *ASME Journal of Engineering for Industry*, *82A*, 303-308.

Usui, E., Hirota, A., & Masuko, M. (1978). Analytical prediction of three dimensional cutting process, part III cutting temperature and crater wear of carbide tool. *ASME Journal of Engineering for Industry*, *100*, 236-243.

Usui, E., & Shirakashi, T. (1982). Mechanics of machining –from descriptive to predictive theory. The Art of Cutting Metals-75 years later. *ASME Publication PED*, *Vol. 7*, pp. 13-35.

Volinsky, A. A., Moody, N. R., & Gerberich, W. W. (2002). Interfacial toughness measurements for thin films on substrates. *Acta Materialia*, *50*, 441-466.

Waldorf, D. J., Kapoor, S. G., & DeVor, R. E. (1998). A slip-line field for ploughing during orthogonal cutting. *ASME Journal of Manufacturing Science and Engineering*, *120*, No. 4, 693-699.

Xia, S. M., Gao, Y. F., Bower, A. F., Lev, L. C., & Cheng, Y. -T. (2007). Delamination mechanism maps for a strong elastic coating on an elastic-plastic substrate subjected to contact loading. *International Journal of Solids and Structures*, *44*, 3685-3699.

Xu, X. P., & Needleman, A. (1994). Numerical simulations of fast crack growth in brittle solids. *Journal of Mechanics and Solids*, *42*, 1397-1434.

Yan, J. W., Zhao, H. W., & Kuriyagawa, T. (2009). Effects of tool edge radius on ductile machining of silicon: an investigation by FEM. *Semiconductor Science and Technology*, *24*, 1-11.

Yen, Y. -C, Jain A, & Altan, T. (2004). A finite element analysis of orthogonal machining using different tool edge geometries. *Journal of Materials Processing Technology*, *146*, 72-81.

Yen, Y. -C., Jain, A., Chigurupati, P., Wu, W. -T., & Altan, T. (2004). Computer simulation of orthogonal cutting using a tool with multiple coatings. *Machining Science and Technology*, *8(2)*, 305-326.

Yoshikawa, H., & Nishiyama, A. (1999). CVD diamond-coated insert for machining high silicon aluminum alloys. *Diamond and Related Materials*, *8*, 1527-1530.

Zhang, B., & Bagchi, A. (1994). Finite element simulation of chip formation and comparison with machining experiments. *ASME Journal of Engineering for Industry*, *116*, 289-297.

APPENDIX A

PROCEDURE OF IMPLEMENTING CZM AT DIAMOND-COATED INSERT INTERFACE

Part I: Deposition process simulation

1. Construct geometry models of coating and substrate in CAE

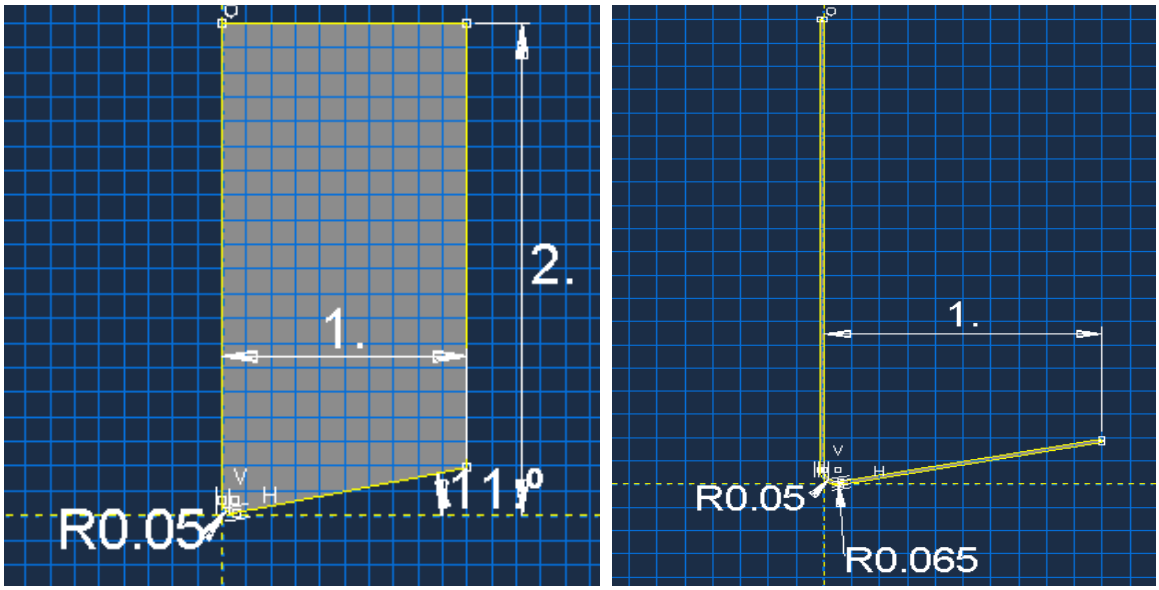

Figure A1. Substrate model (left) and coating model (right).

2. Create materials properties for coating and substrate
3. Create sections and assign them to coating and substrate
4. Assembly coating and substrate (here I choose option-mesh on part)
5. Partition coating and substrate for mesh preparation

   Figure A2 shows the operation example for coating, which also applies to substrate.

Figure A3 displays the final state of tool after partition operation.

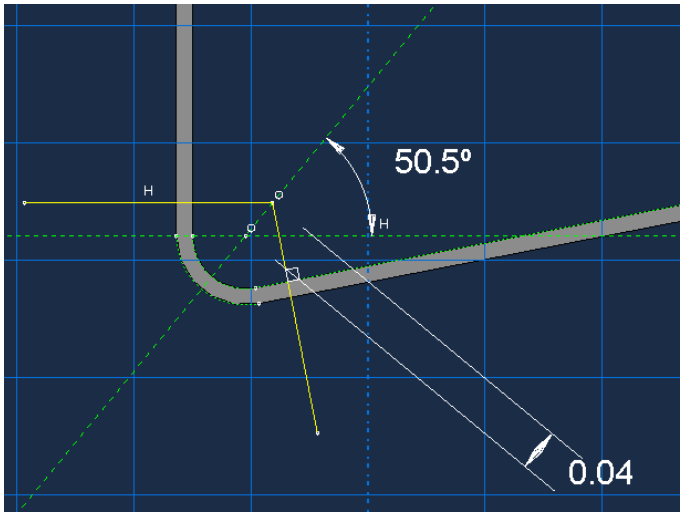

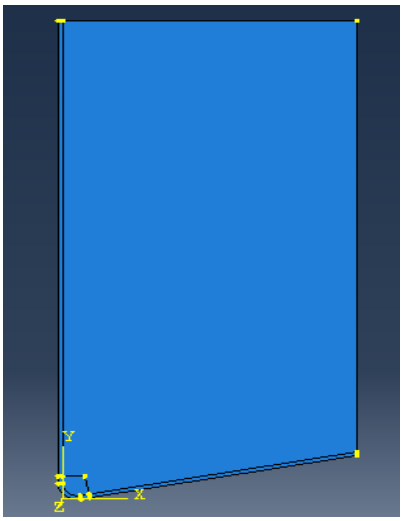

Figure A2. The partition operation for coating.

Figure A3. Tool after partition.

6. Create element sets for internal surface of coating (Figure A4) and outer surface of substrate (Figure A5)

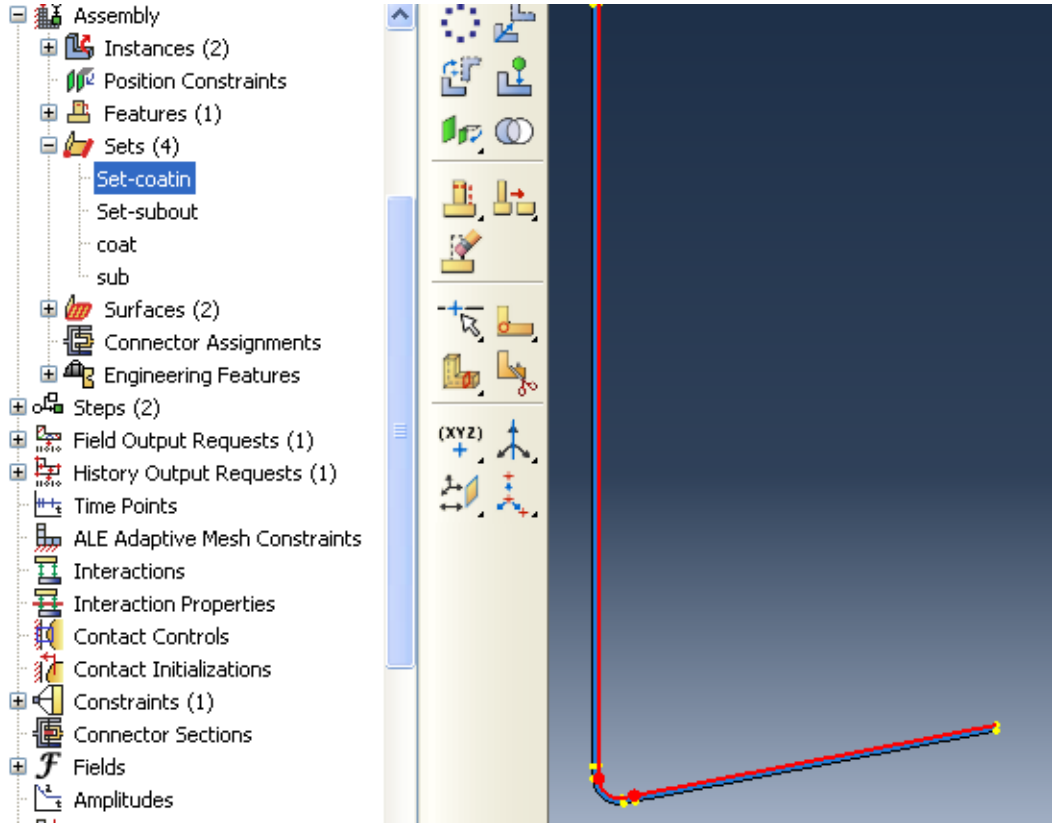

Figure A4. Create element set for coating internal surface.

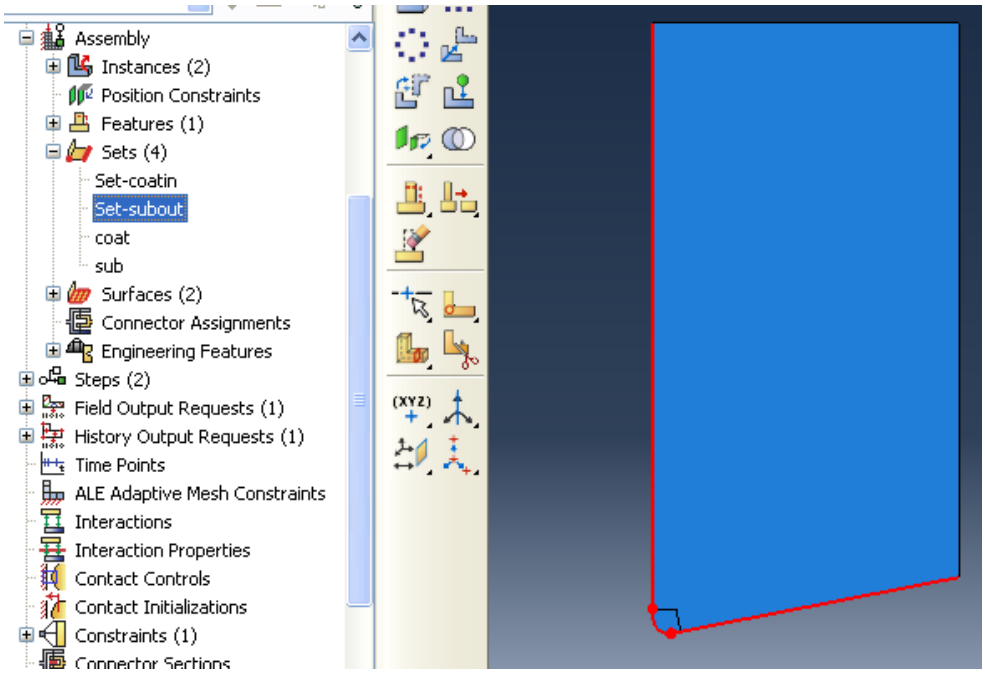

Figure A5. Create element set for substrate outer surface.

7. Create surfaces for coating (Figure A6) and substrate (Figure A7) for the purpose of later interaction definitions

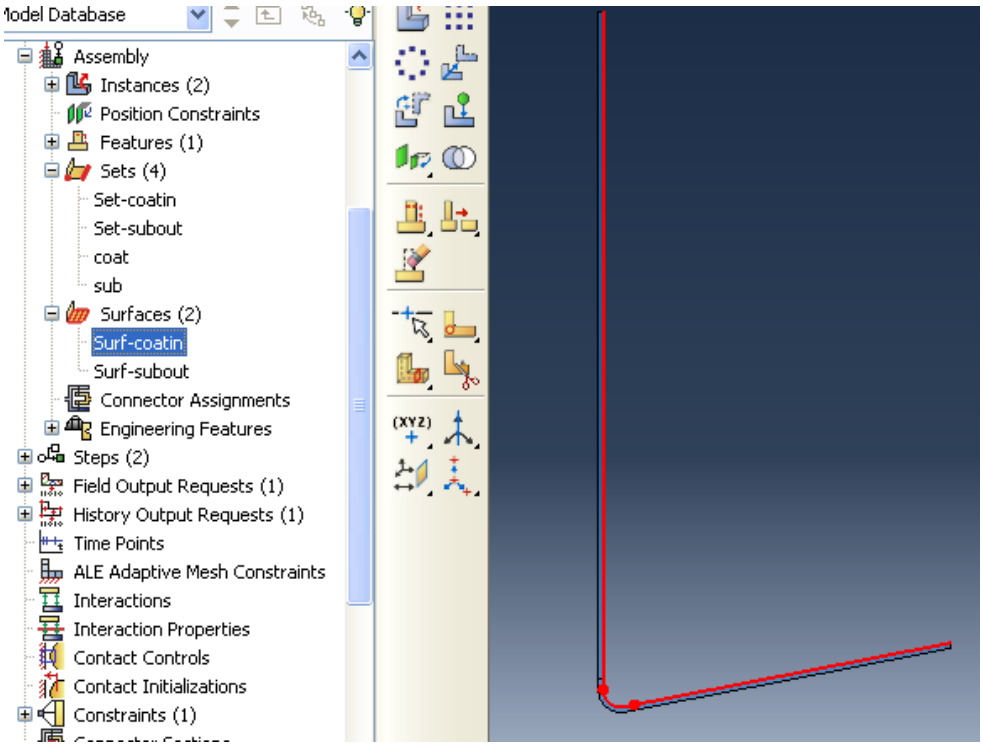

Figure A6. Create element-based surface for coating (choose geometry option).

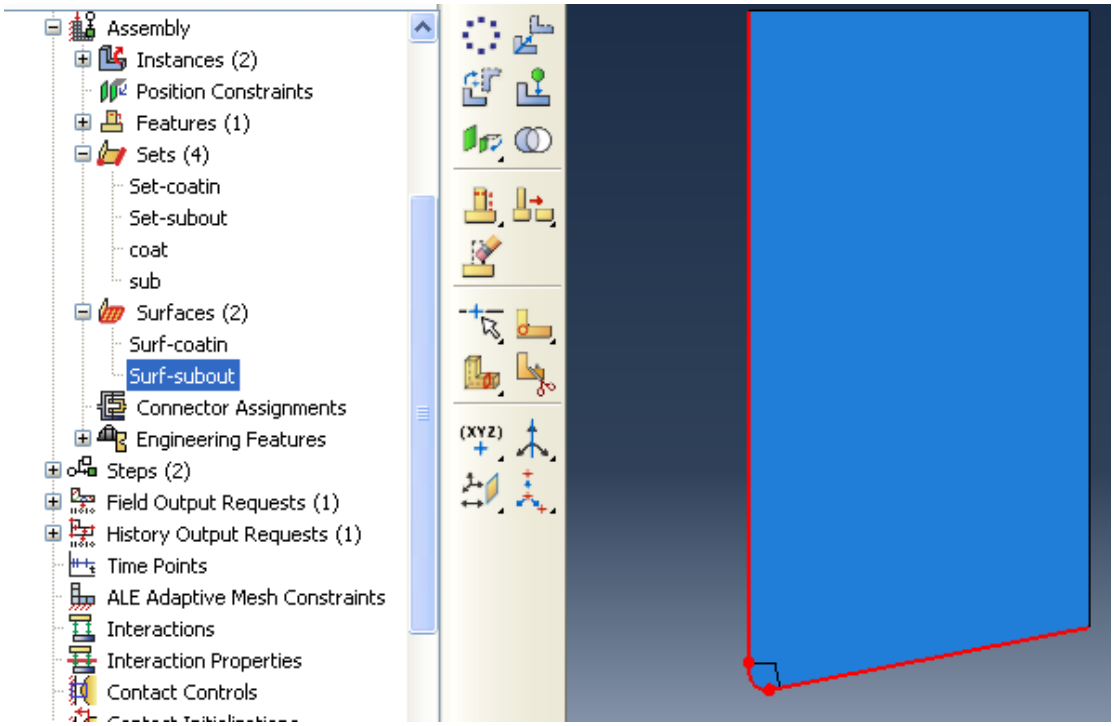

Figure A7. Create element-based surface for substrate (choose geometry option).

8. Create deposition step time=0.001s (dynamic explicit mode), and turn nlgeom on.

9. Define field output variables as follows:

   CSTRESS,DAMAGEC,DAMAGEFC,DAMAGEFT,DAMAGEMT,DAMAGESHR,DAMAGET,DMICRT,E,HFL,LE,MISESMAX,NT,PE,PEEQ,RF,RT,S,SDEG,STATUS,TEMP,U,

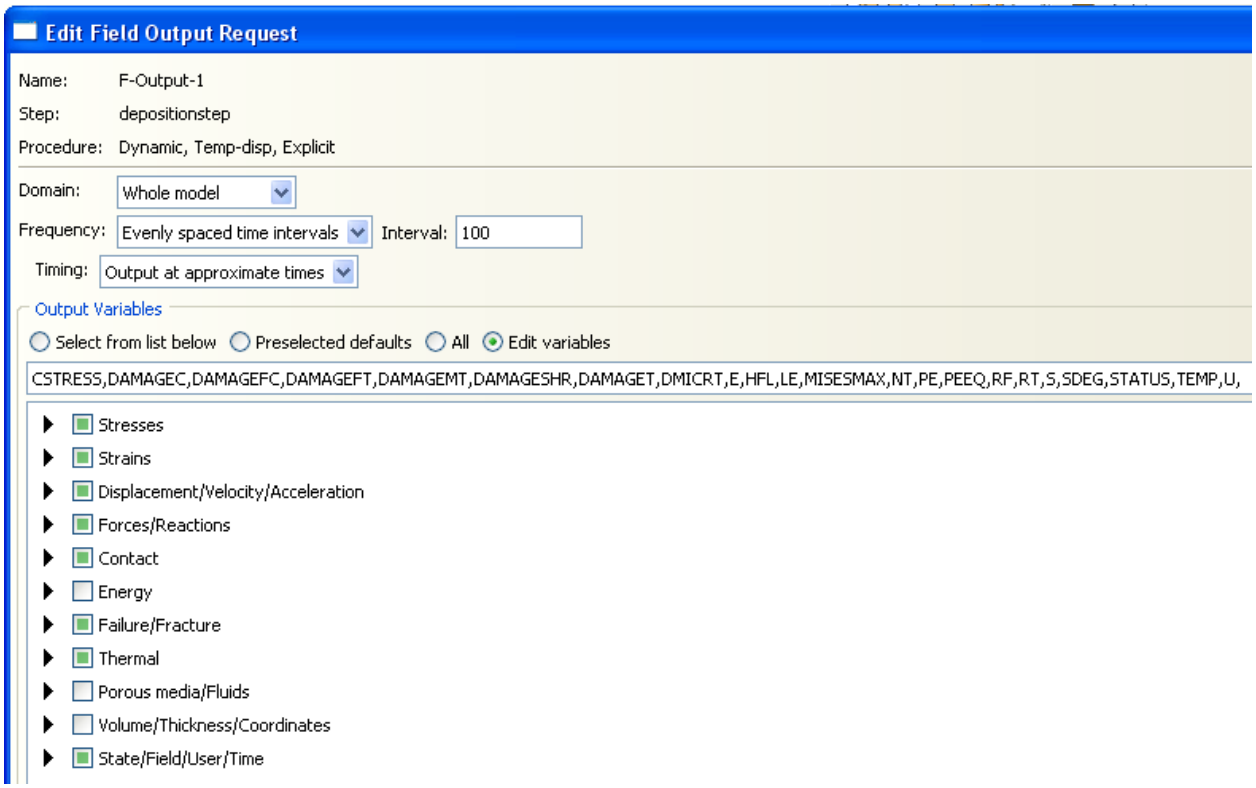

Figure A8. Define field output variables.

10. Define penalty interaction for coating surface and substrate surface, which have been defined in the preceding: coating surface as the master surface and substrate surface as the slave surface
11. Define tie constraint for coating and substrate: coating surface as Master surface and substrate surface as Slave surface
12. Define deposition temperature field for tool: initial temperature field is 600 ˚C
13. Define boundary conditions: constrain tool right edge in x direction and tool top edge in y direction (shown in Figure A9 and A10), and define final tool temperature 20 ˚C (shown in Figure A11)

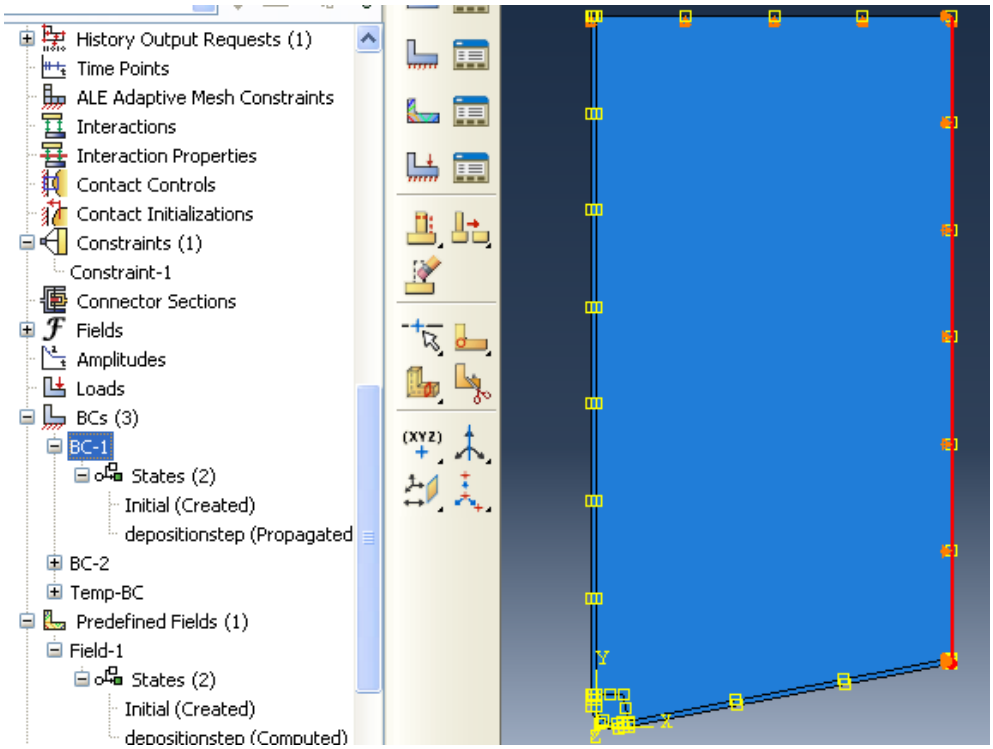

Figure A9. X-contraint boundary condition definition.

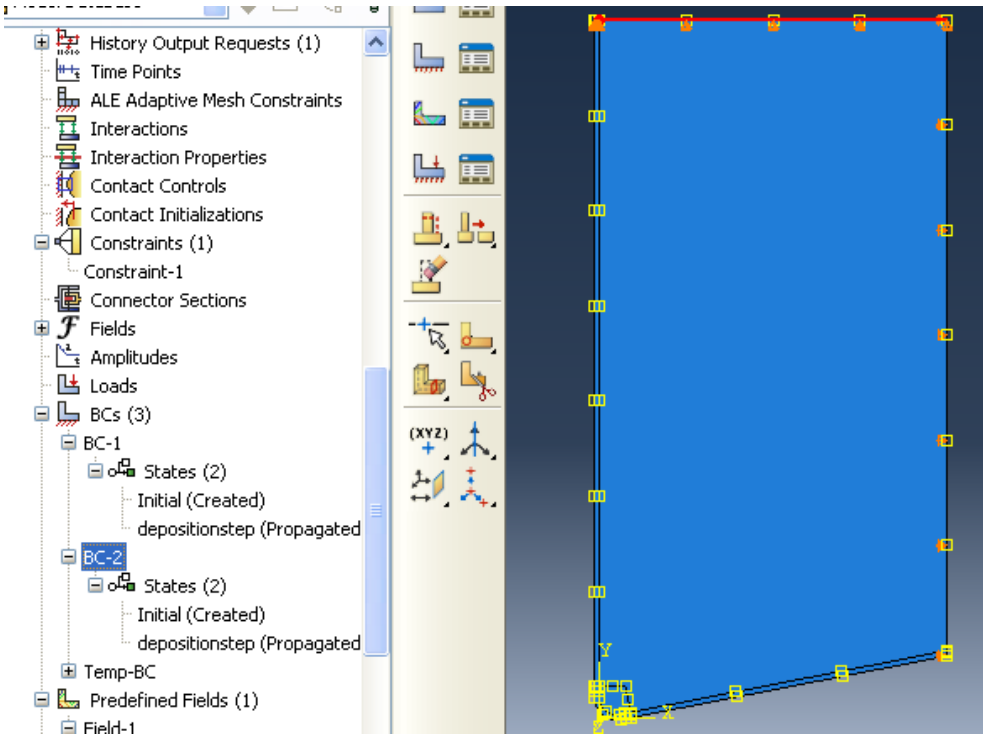

Figure A10. Y-contraint boundary condition definition.

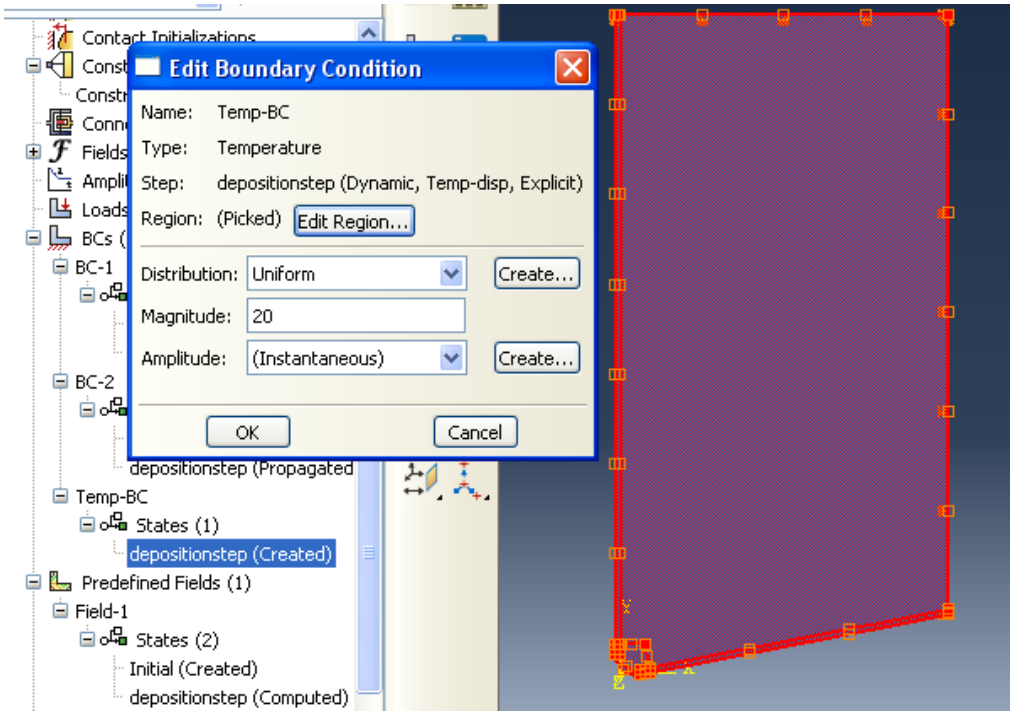

Figure A11. Tool final temperature definition.

14. Meshing. Apply Element type-CPE4RT on both coating and substrate. Free mesh for substrate and sweep mesh for coating so as to point to the stack direction to coating thickness outward.

    Substrate edge seeds are assigned as following: top edge-8elements with bias ratio of 3; right edge-12 elements with bias ratio of 3; flank edge (long segment) - 25 elements with bias ratio of 5; flank edge (short segment connected to arc) - 10 elements; arc- 15 elements; rake edge (short segment connected to arc) - 10 elements; rake edge (long segment) - 60 elements with bias ratio of 5.

    Coating edge seeds are similar to substrate except the thickness direction, where 3 elements are assigned.

15. Define restart simulation requirement for later cutting simulation.

16. Save the nodes and elements information for later use in cohesive zone editing process. The interface of coating side is chosen for ease later cohesive zone editing, where cohesive nodes share the same node coordinates with the connecting nodes on coating. For example, partial coating interface node and element numbers are shown in Figure 12. Element 205 is composed of node 157, 7, 393, and 392. In constructing cohesive element, the same direction should rule there.

17. Generate abaqus input file for later use in next step.

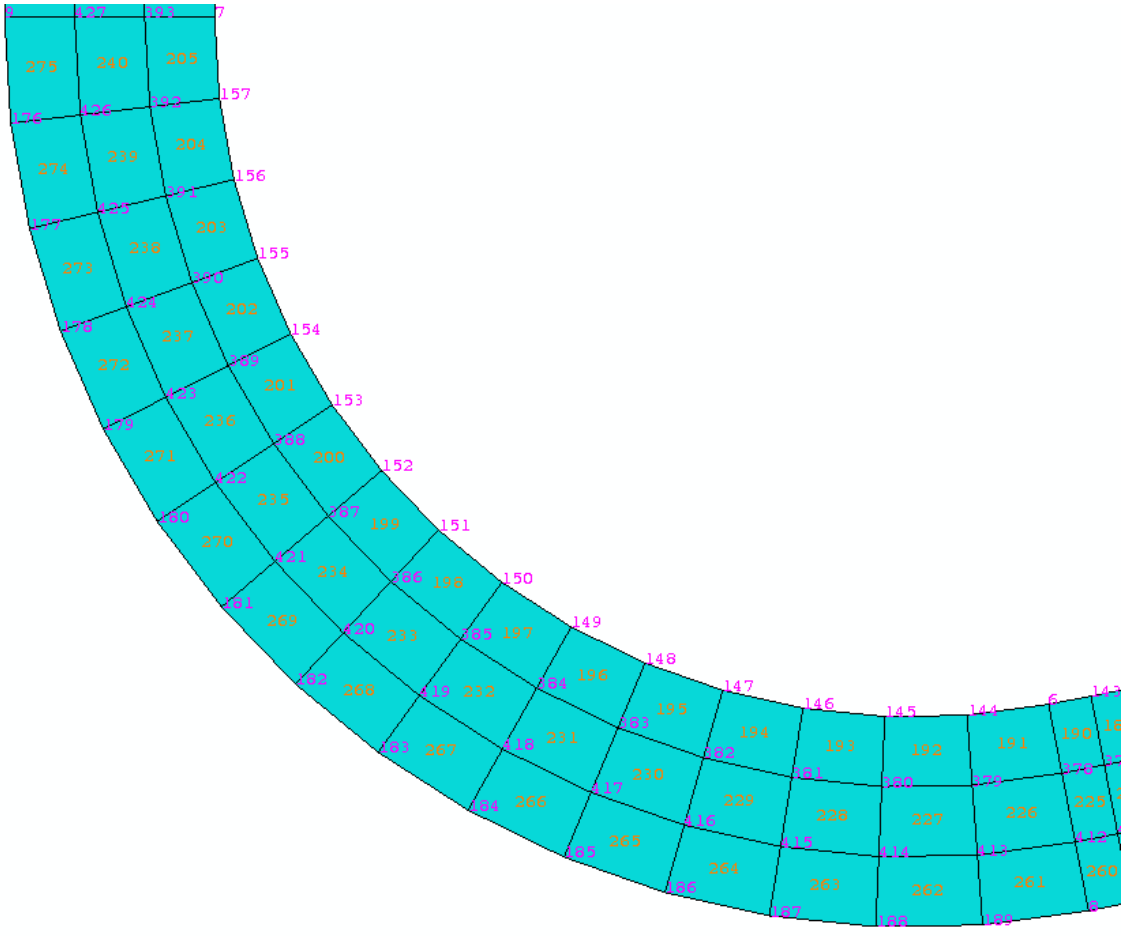

Figure A12. Coating interface node and element numbering.

18. Add cohesive nodes, elements and sections in abaqus.

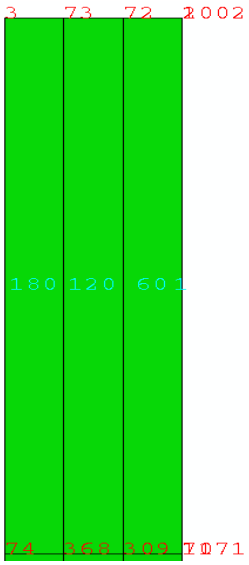

Figure A13. An example of cohesive nodes and coating nodes.

Cohesive nodes share the same coordinates with the nodes on coating interface. For convenience, here, one group of cohesive node numbers is same as those on coating interface. Then the node number information was copied and pasted beneath and with node numbering augment 1000 so as to construct all required cohesive nodes. Figure 13 gives an example of cohesive nodes (element) and coating nodes (element) configuration. Cohesive element 1 is composed of cohesive node 2, 2002, 71, and 1071. Cohesive nodes 2 and 1002 share same coordinate with coating interface node 2. Cohesive nodes 71 and 1071 share same coordinate with coating interface node 71.

The following code shows an example of how to implement cohesive nodes, elements, and sections in an input file.

```
** PARTS
**
*Part, name=COAT
*Node
      1,           0., 0.0915198326
```

```
     ...
     13,           0.,  0.104273289
     14,           0.,  0.117379434
    ...
    134, -0.00499999989, 0.0915198326
    ...
    251, -0.00499999989,  0.104273289
    252, -0.00499999989,  0.117379434
    ...
*Element, type=CPE4RT
  1,   1,  13, 251, 134
  2,  13,  14, 252, 251
...
360, 484, 199,  10, 225
*Nset, nset=_PICKEDSET22, internal, generate
   1,  484,    1
*Elset, elset=_PICKEDSET22, internal, generate
   1,  360,    1
** Section: Section-1-_PICKEDSET22
*Solid Section, elset=_PICKEDSET22, material=COAT
,
*End Part
**Create cohesive zone part with the name of INTERLAY-1
**Share the same node coordinates corresponding to nodes on coating interface
**
*Part, name=INTERLAY-1
*Node
      1,           0., 0.0915198326
      2,           0.,           2.
```

```
      5, 0.0898383558, 0.0174628068
      6, 0.0595404506, 0.0115734907
      7,           0., 0.0606548488
     11,           1.,  0.194380313
     13,           0.,  0.104273289
     14,           0.,  0.117379434
     ...
     70,           0.,   1.87418139
     71,           0.,   1.93623269
    ...
    224,  0.104361326, 0.0202857871
   1001,           0., 0.0915198326
   1002,           0.,           2.
   ...
   1201,  0.927385151,  0.180265412
   ...
   1224,  0.104361326, 0.0202857871
** Create cohesive elements
*Element, type=COH2D4
  1,   71,    2, 1002, 1071
  2,   70,   71, 1071, 1070
...
120,   11,  201, 1201, 1011
** Define cohesive node sets
*Nset, nset=_PICKEDSET2, internal
    1,    2,    5,    6,    7,   11,   13,   14,   15,   16,   17,   18,
19,   20,   21,   22
   23,   24,   25,   26,   27,   28,   29,   30,   31,   32,   33,   34,
35,   36,   37,   38
```

```
   39,   40,   41,   42,   43,   44,   45,   46,   47,   48,   49,   50,
51,   52,   53,   54
   55,   56,   57,   58,   59,   60,   61,   62,   63,   64,   65,   66,
67,   68,   69,   70
   71,  135,  136,  137,  138,  139,  140,  141,  142,  143,  144,  145,
146,  147,  148,  149
  150,  151,  152,  153,  154,  155,  156,  157,  158,  159,  160,  161,
162,  163,  164,  165
  166,  201,  202,  203,  204,  205,  206,  207,  208,  209,  210,  211,
212,  213,  214,  215
  216,  217,  218,  219,  220,  221,  222,  223,  224, 1001, 1002, 1005,
1006, 1007, 1011, 1013
 1014, 1015, 1016, 1017, 1018, 1019, 1020, 1021, 1022, 1023, 1024, 1025,
1026, 1027, 1028, 1029
 1030, 1031, 1032, 1033, 1034, 1035, 1036, 1037, 1038, 1039, 1040, 1041,
1042, 1043, 1044, 1045
 1046, 1047, 1048, 1049, 1050, 1051, 1052, 1053, 1054, 1055, 1056, 1057,
1058, 1059, 1060, 1061
 1062, 1063, 1064, 1065, 1066, 1067, 1068, 1069, 1070, 1071, 1135, 1136,
1137, 1138, 1139, 1140
 1141, 1142, 1143, 1144, 1145, 1146, 1147, 1148, 1149, 1150, 1151, 1152,
1153, 1154, 1155, 1156
 1157, 1158, 1159, 1160, 1161, 1162, 1163, 1164, 1165, 1166, 1201, 1202,
1203, 1204, 1205, 1206
 1207, 1208, 1209, 1210, 1211, 1212, 1213, 1214, 1215, 1216, 1217, 1218,
1219, 1220, 1221, 1222
 1223, 1224
** Define cohesive element sets for cohesive section definition
*Elset, elset=_PICKEDSET2, internal, generate
```

```
   1,  120,    1
** Section: Section-2-_PICKEDSET2
*Cohesive Section, elset=_PICKEDSET2, material=COHESIVE, response=TRACTION
SEPARATION
,
...
```

19. Add cohesive instance in assembly portion

```
** ASSEMBLY
**
*Assembly, name=Assembly
**
*Instance, name=COAT-1, part=COAT
*End Instance
**
*Instance, name=INTERLAY-1, part=INTERLAY-1
*End Instance
**
*Instance, name=SUB-1, part=SUB
*End Instance
**
```

20. Create cohesive surface for later interaction and constraints definitions

```
*Elset, elset=_SURFMIDIN_S1, internal, instance=INTERLAY-1, generate
   1,  120,    1
*Elset, elset=_SURFMIDOUT_S3, internal, instance=INTERLAY-1, generate
   1,  120,    1
*Elset, elset=cohesive, internal, instance=INTERLAY-1, generate
   1,  120, 1
```

```
*Surface, type=element, name=cohesivein
cohesive, S1
*Surface, type=element, name=cohesiveout
cohesive, S3
```

21. Define tie constraints for all three contact pairs between coating surface, substrate surface, and cohesive zone surface

```
** Constraint: TIE1
*Tie, name=TIE1, adjust=yes
cohesiveout, SURF-COATIN
** Constraint: TIE2
*Tie, name=TIE2, adjust=yes
SURF-SUBOUT, cohesivein
** Constraint: TIE3
*Tie, name=TIE3, adjust=yes
SURF-COATIN, SURF-SUBOUT
```

22. Create cohesive zone material

```
**
*Material, name=COHESIVE
*Damage Initiation, criterion=MAXS
500.,100000.,     0.
*Damage Evolution, type=ENERGY
 0.1,
*Density
 7.9e-09,
*Elastic, type=TRACTION
 5e+06, 5e+06,       0.
```

23. Check boundary conditions for all three parts (coating, substrate, and cohesive zone) and submit job. In simulations, the job is submitted via command:

C:\Abaqus\abq6101 Job=… int

The above steps are made for deposition process simulation.

Part I: Cutting simulation and workpiece withdrawal simulation

After deposition simulation, the following simulation is cutting process. The major procedure is shown below.

1. Create workpiece part in CAE.

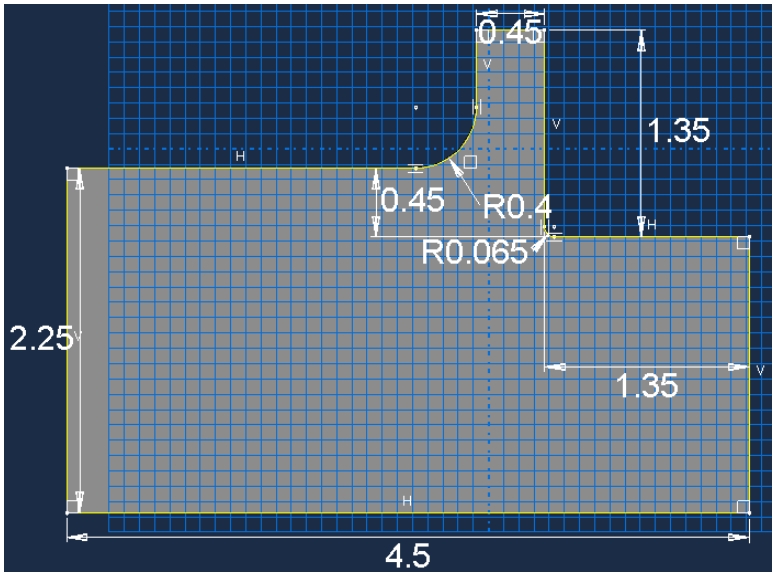

Figure A14. Workpiece geometry for simulation of speed condition 5 m/s and uncut chip thickness 0.45 mm.

2. Create workpiece material and section.
3. Import tool model. Three deformed parts of diamond-coated tool need to be imported one by one. The imported part name needs to delete "-1" from the default name so as to make

the later assembled part name same as in previous deposition result. Besides, the parts need to cite their final state in the previous deposition job.

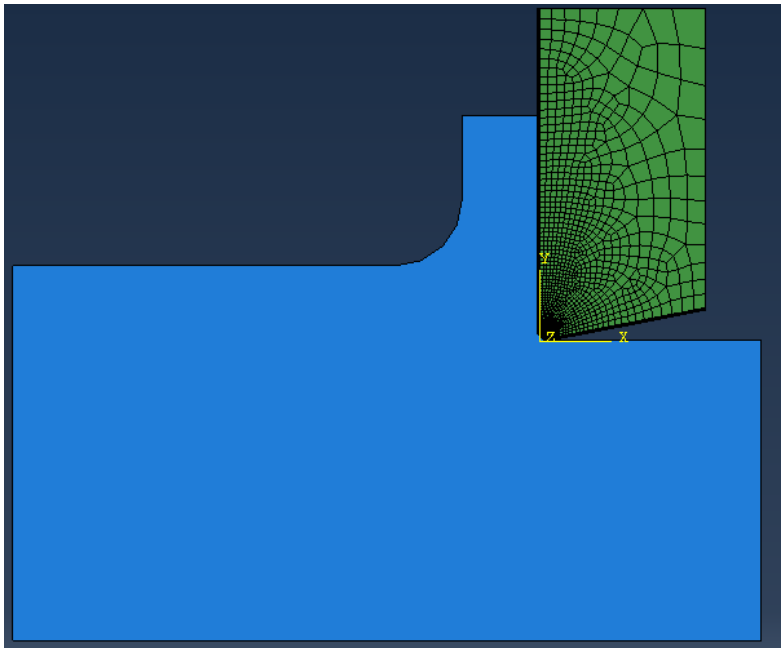

Figure A15. Assembly of workpiece and tool.

4. Set up the workpiece and the tool together. Here, workpiece instance mesh is dependent on geometry. During the assembly process, it is not allowed to move the tool since this will affect the imported stress state of the tool. The adjustment of Workpiece location is chosen instead to make the tool and workpiece be as close as possible. Figure 15 shows image of the assembly.

5. Create cohesive element set in assembly by select the imported cohesive zone (shown in Figure 16). The purpose is for the preparation of adding cohesive surfaces later in generated input file because the element set defined in the previous deposition simulation cannot be inherited automatically in job transfer operation.

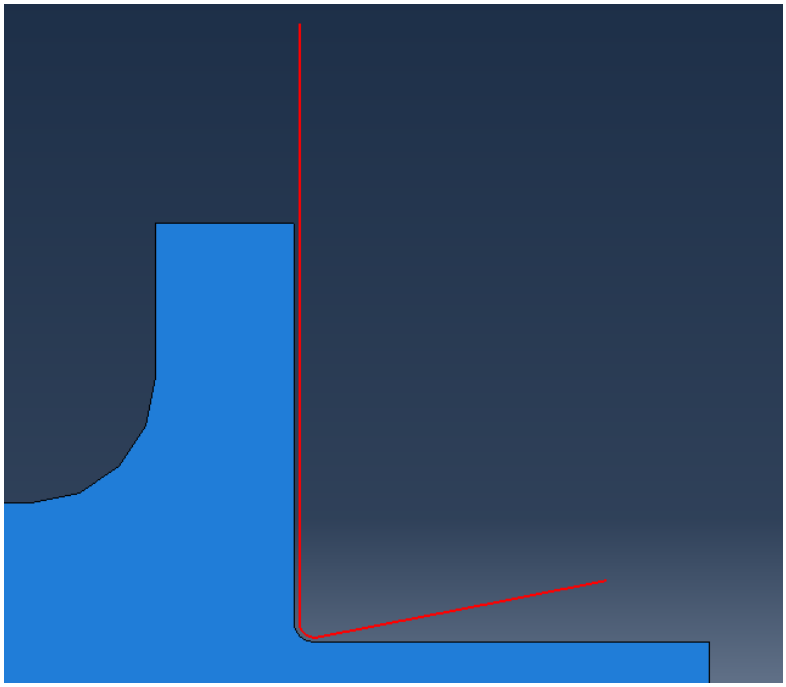

Figure A16. Create cohesive element set.

6. Define tool surface, coat internal surface, substrate outer surface, workpiece bottom surface, and possible tool-chip contact surface of workpiece during cutting.

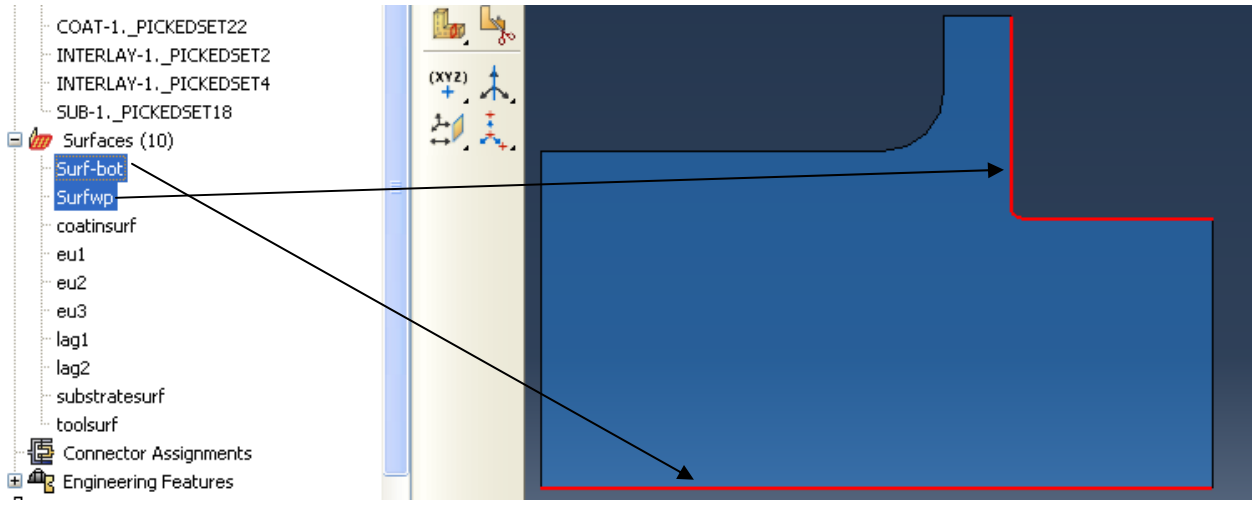

Figure A17. Definition of workpiece bottom surface, and possible tool-chip contact surface of workpiece as highlighted.

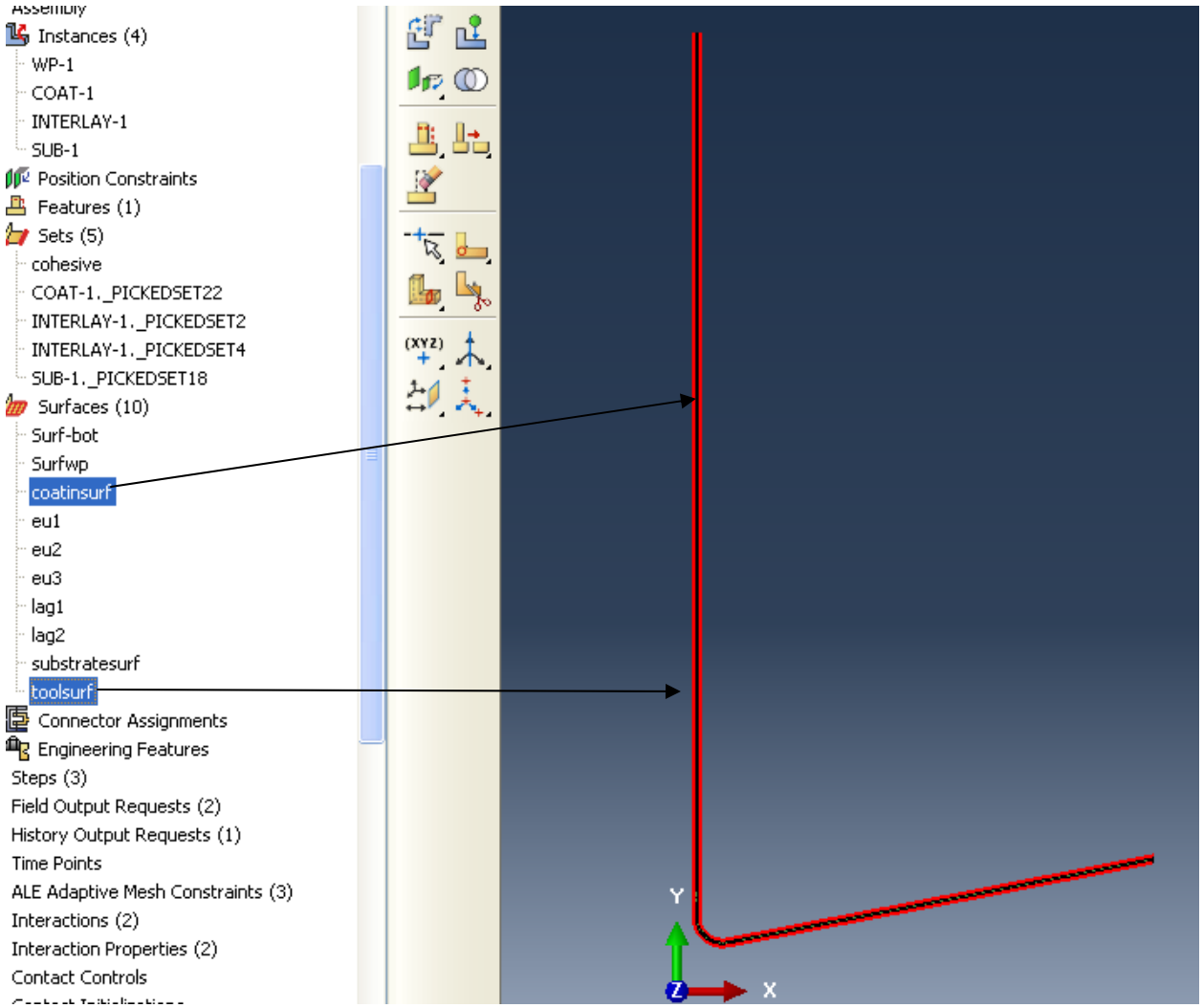

Figure A18. Definition of coat internal surface and tool surface as highlighted.

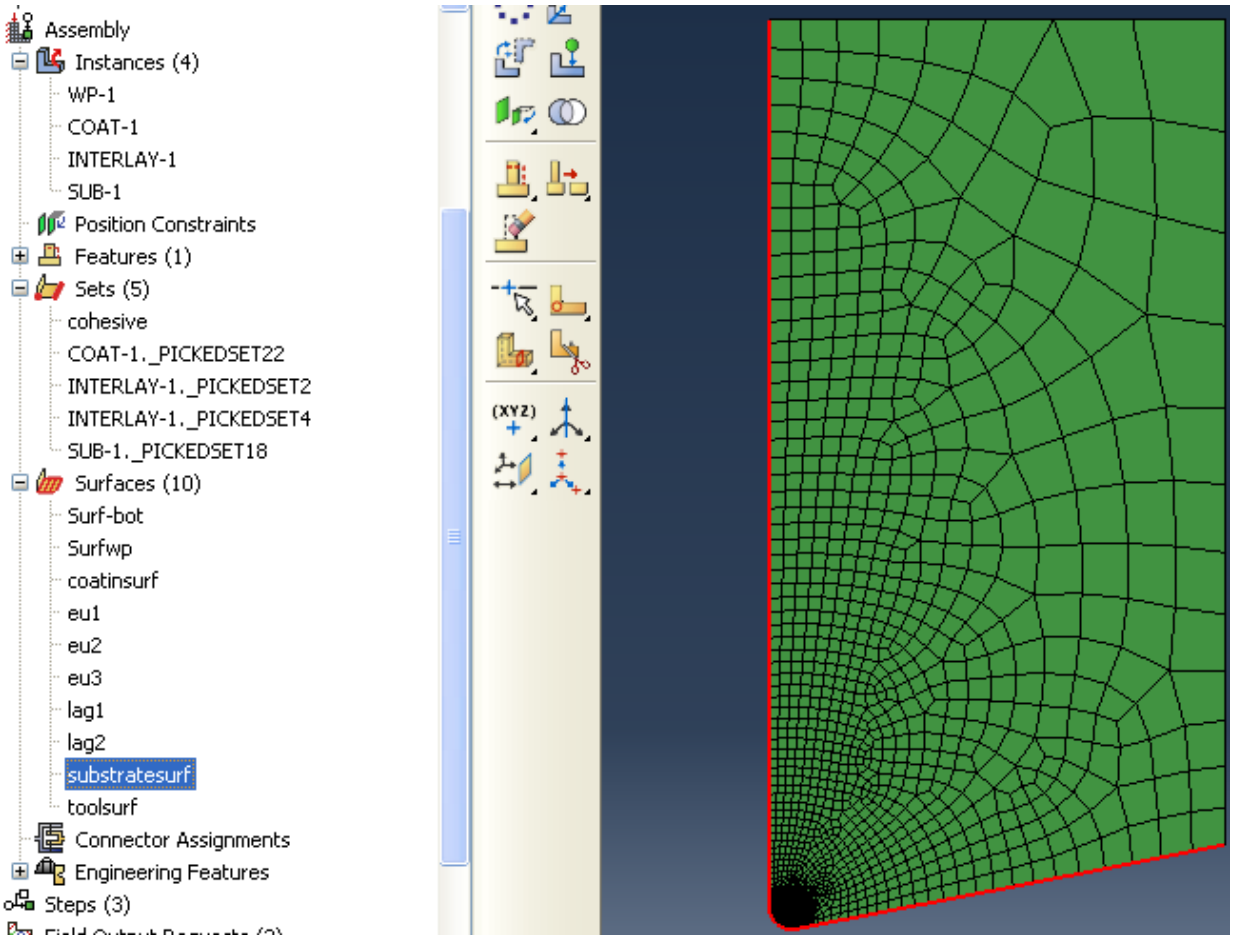

Figure A19. Definition of substrate outer surface as highlighted.

7. Define Eulerian and Lagrangian surfaces for workpiece. First create surfaces with geometry option, and then modify the keywords of those surfaces. Figure A20 shows the created surfaces, where eu1, eu2, and eu3 are defined as Eulerian surfaces, and lag1 and lag2 are defined as Lagrangian surfaces.

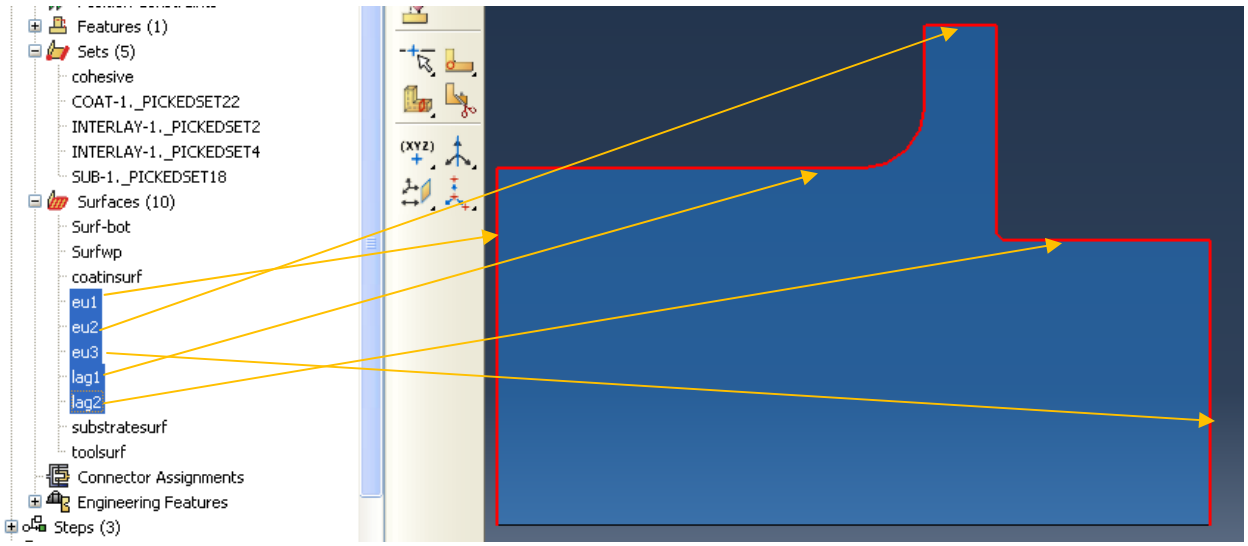

Figure A20. Create Eulerian and Lagrangian surfaces in assembly as pointed by the arrows.

Figure A21 shows the modification of the related keywords.

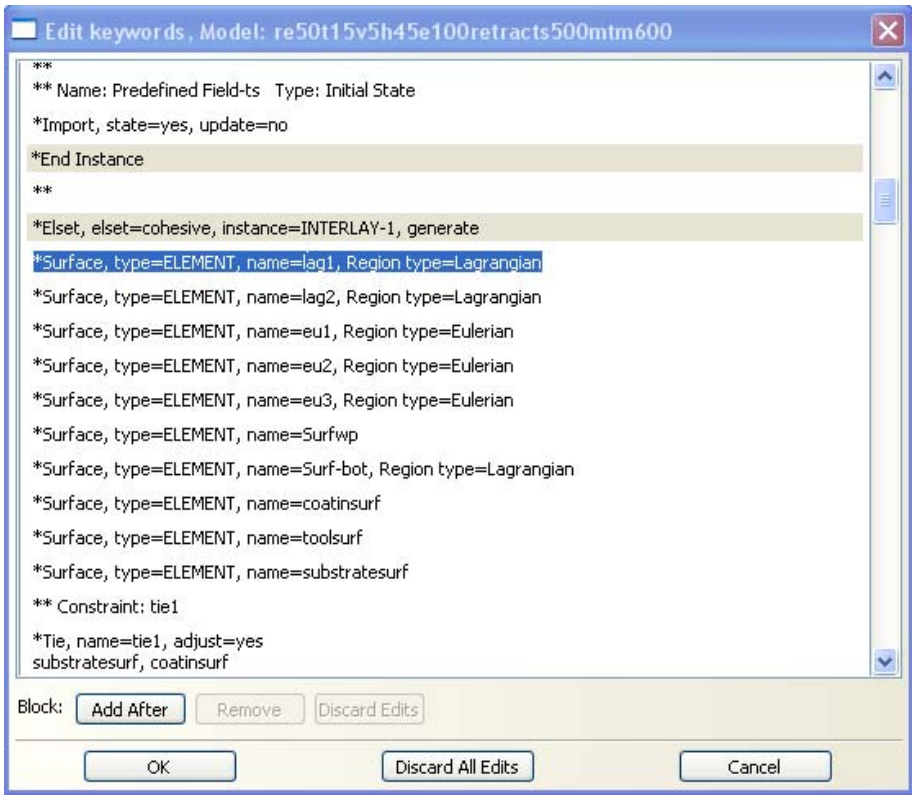

Figure A21. Keywords modifications of Eulerian and Lagrangian surfaces.

8. Create cutting analysis and workpiece withdrawal analysis steps. Both are dynamic, temp-displacement, explicit option. For cutting, the step time is 0.002 seconds, which depends on the cutting conditions. Turn on the nonlinear analysis option. For workpiece withdrawal process, the step time is 0.0001 seconds.
9. Create ALE adaptive mesh constraints. Choose cutting step and create adaptive mesh for workpiece left boundary, right boundary, and the chip top respectively. Figure A22-A24 show the detail of those definitions.

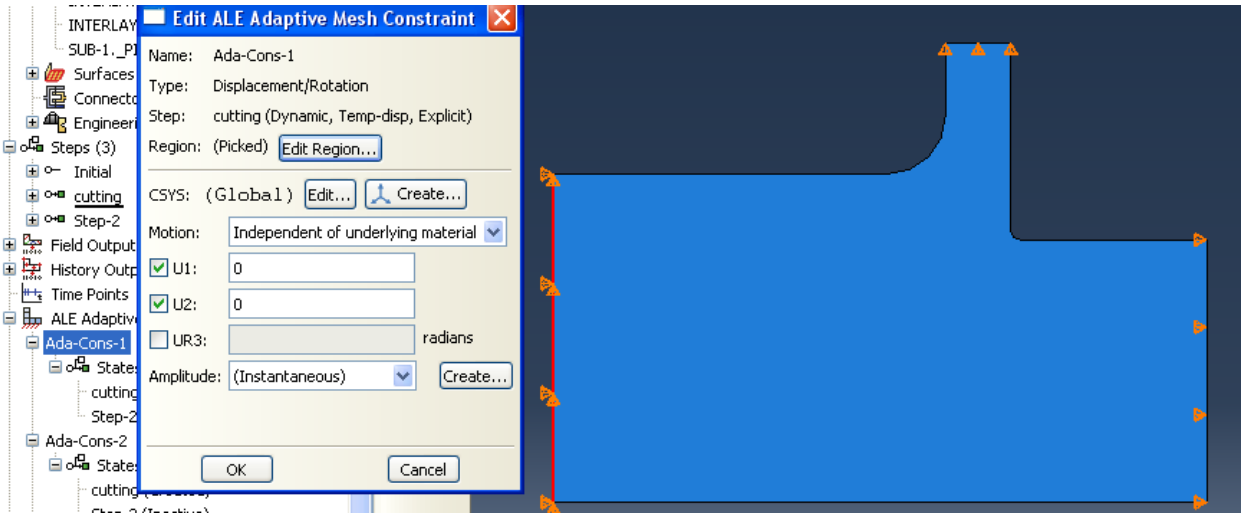

Figure A22. Definition of adaptive mesh constraint for workpiece left boundary as highlighted

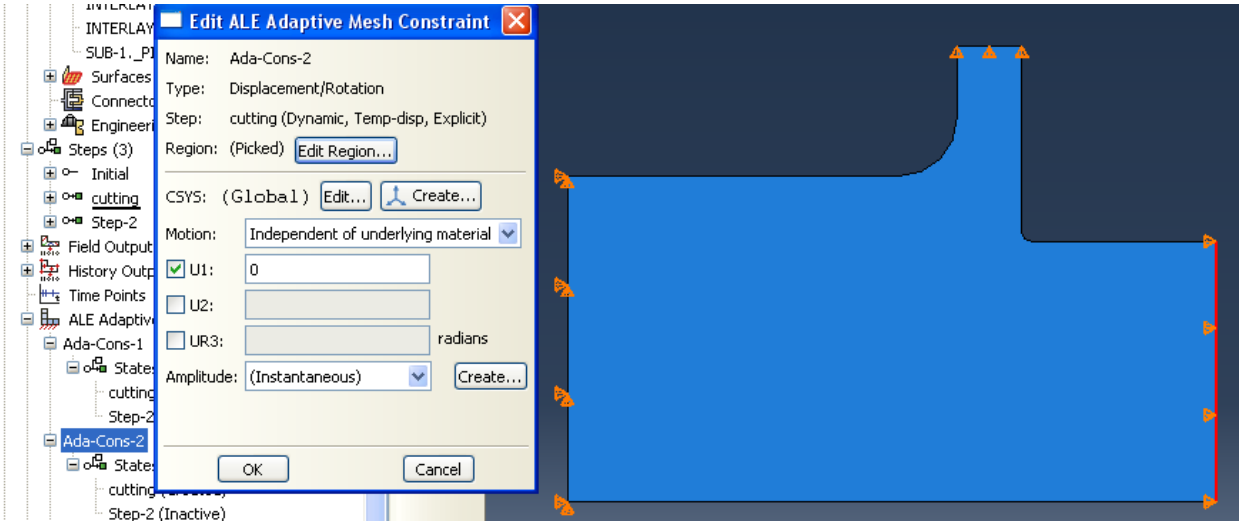

Figure A23. Definition of adaptive mesh constraint for workpiece right boundary as highlighted

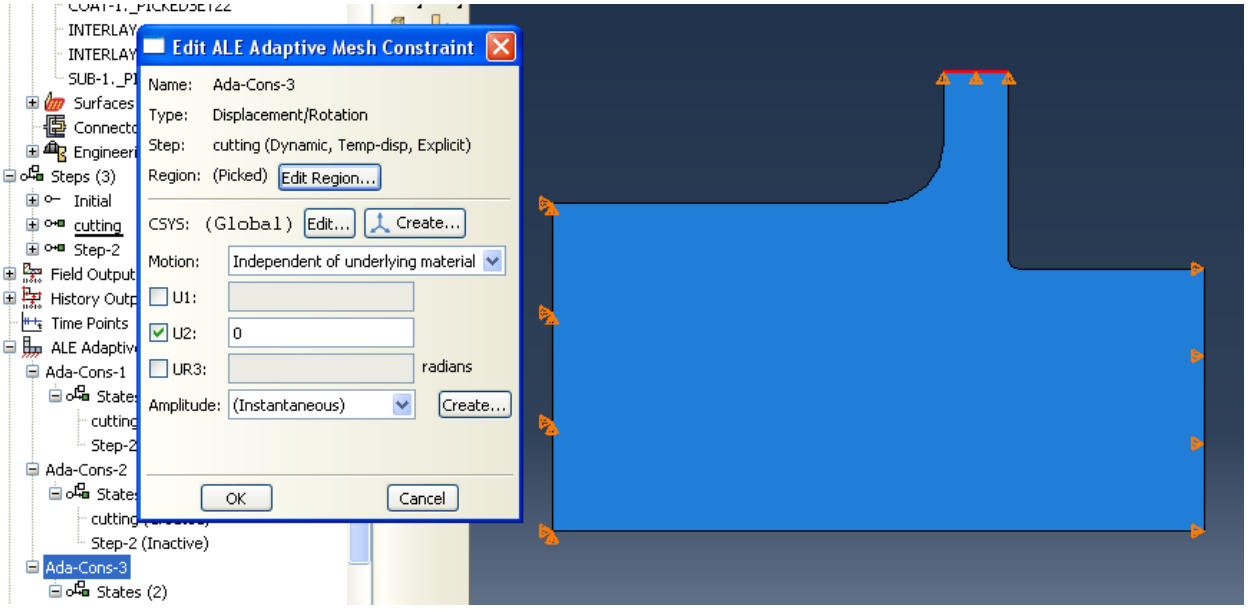

Figure A24. Definition of adaptive mesh constraint for the chip top boundary as highlighted

10. Create two interaction properties for interactions to be used. Figure A25 shows the definition of interaction-1.

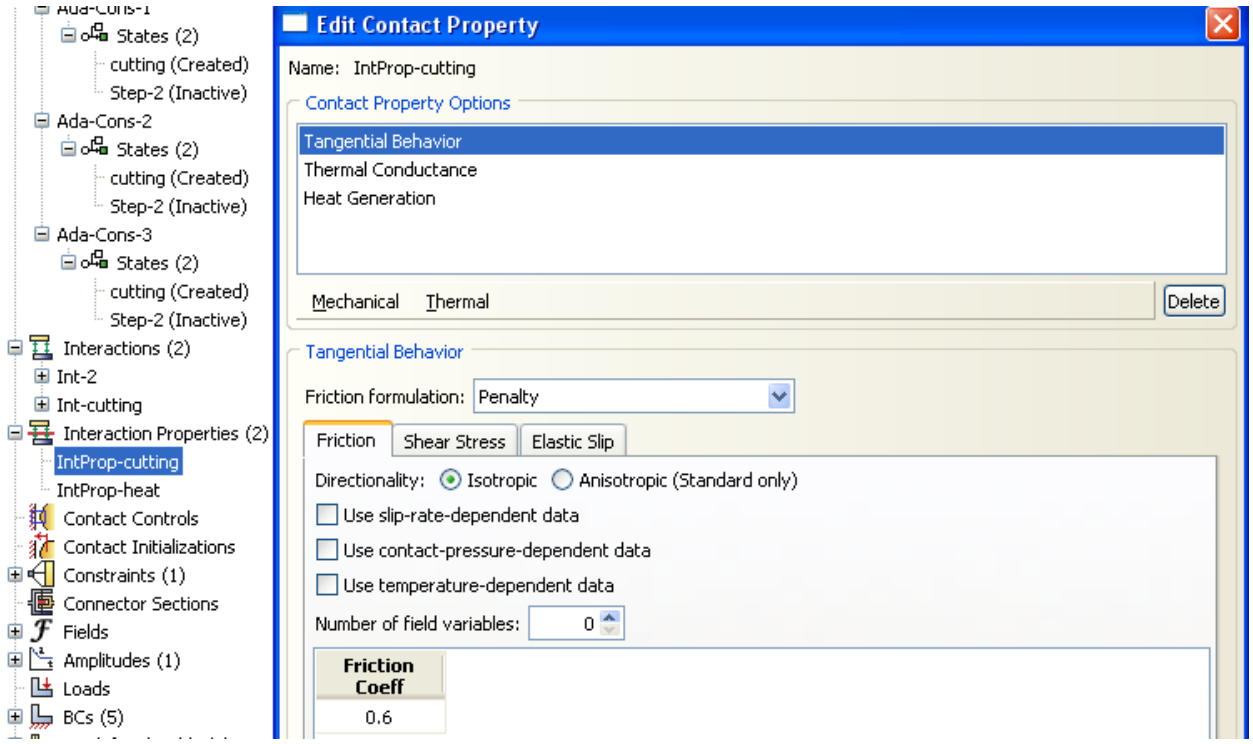

(a) Tangential behavior

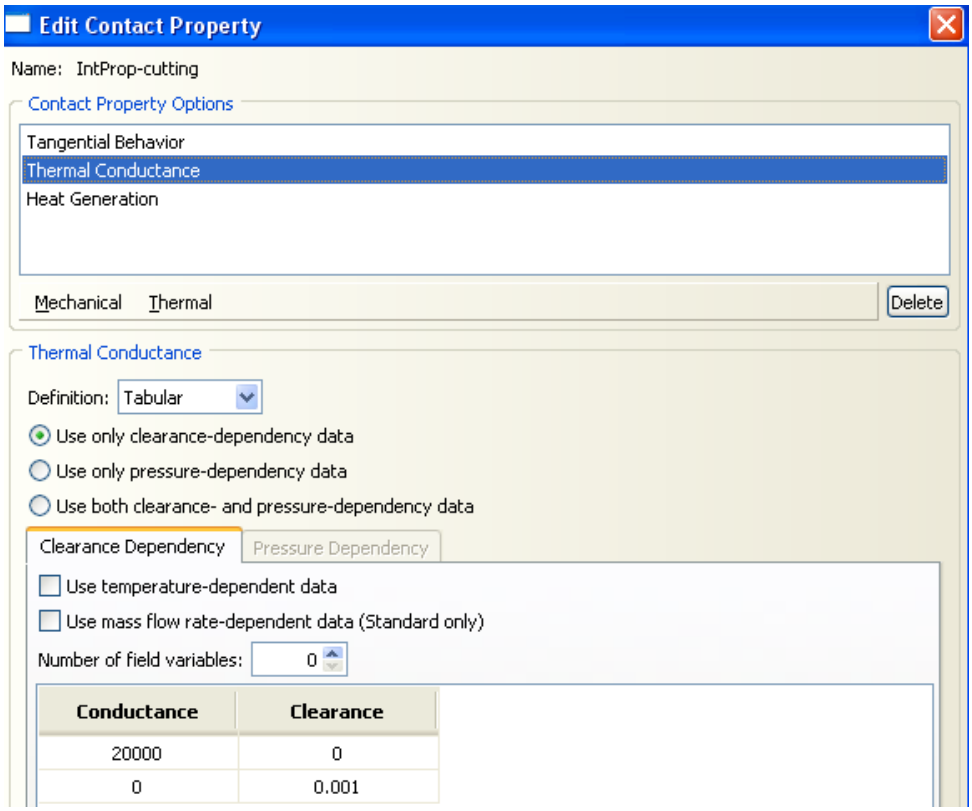

(b) Thermal conductance

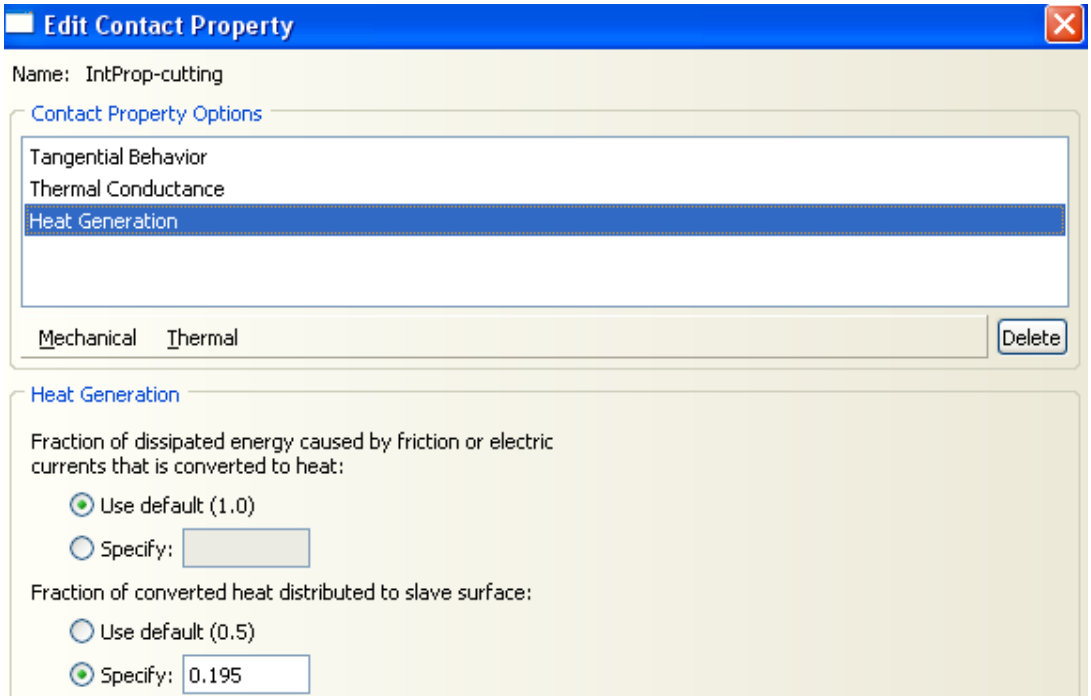

(c) Heat generation

Figure A25. Define interaction property for chip-tool contact in cutting.

Tangential behavior is of friction coefficient 0.6 with shear stress limit of 143 MPa.

Figure A26 shows the definition of interaction-2, which is used for heat transfer across the cohesive zone.

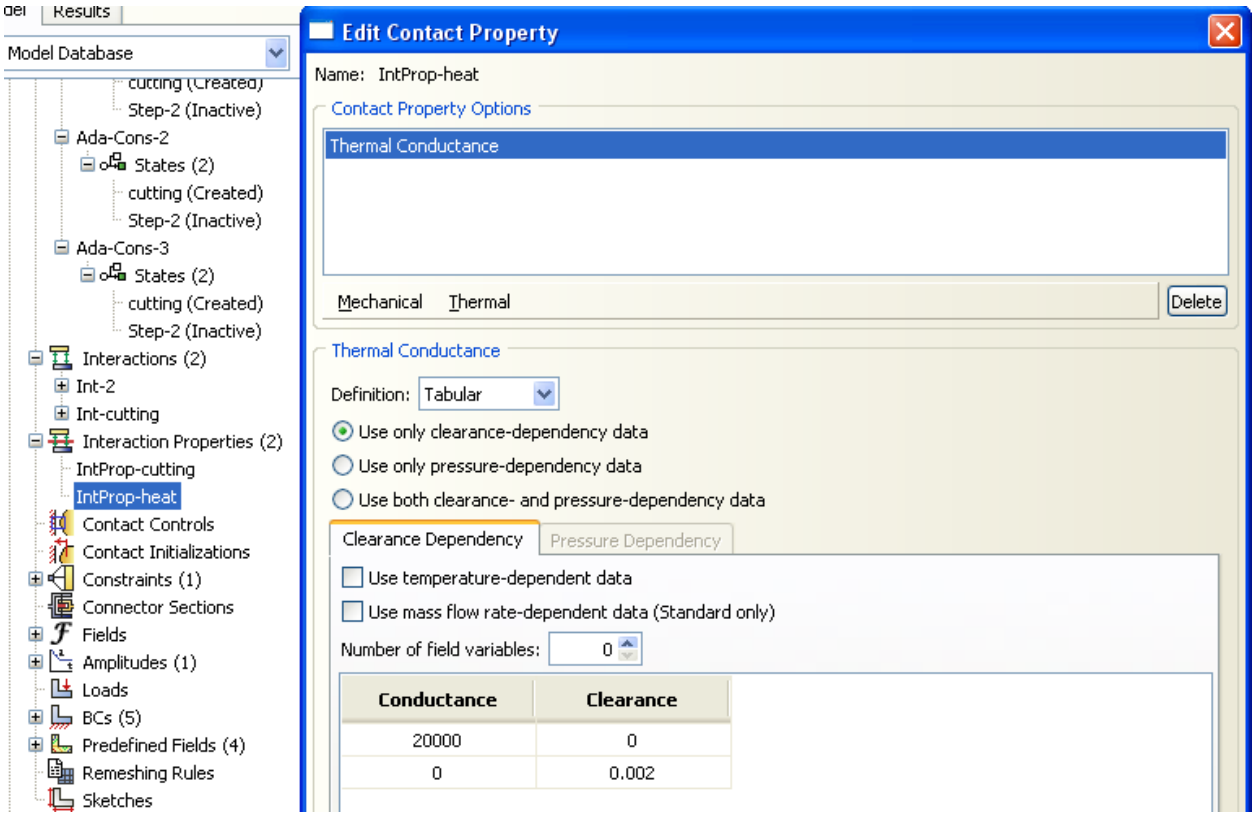

Figure A26. Define interaction property for tool heat transfer.

11. Create two interactions for cutting simulation. One is the interaction between coating internal surface and substrate outer surface, which uses penalty contact method, the other is that between workpiece and tool for chip contact and heat transfer description.

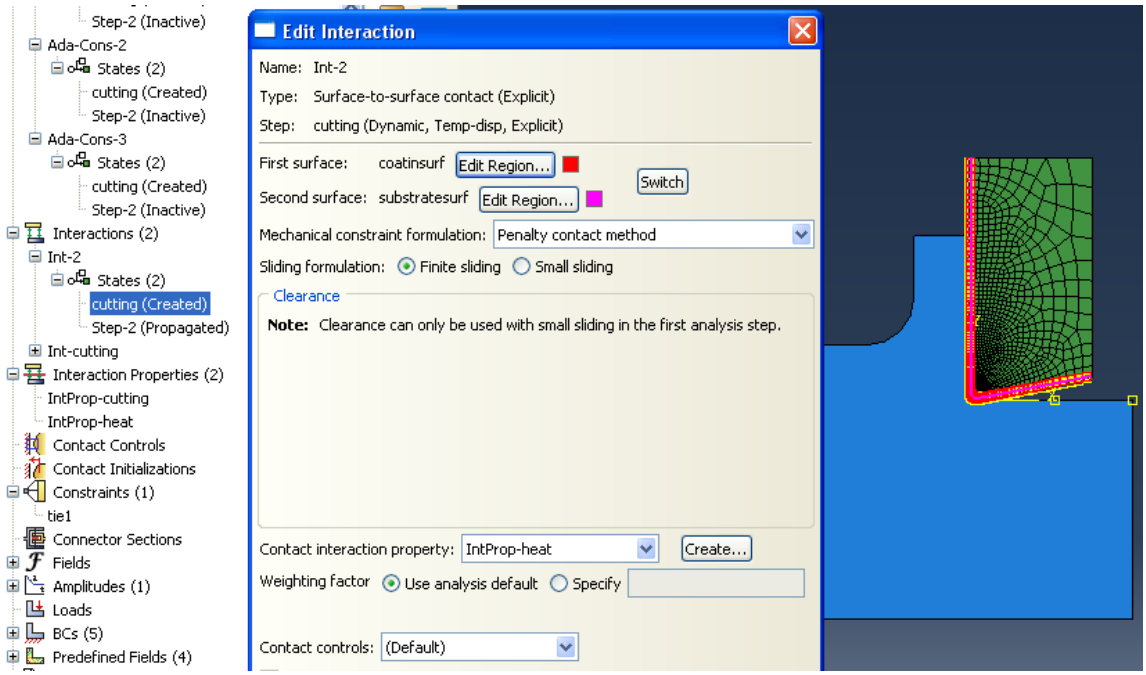

Figure A27. Define surface penalty contact interaction between coating surface and substrate surface to specify the heat transfer interaction property.

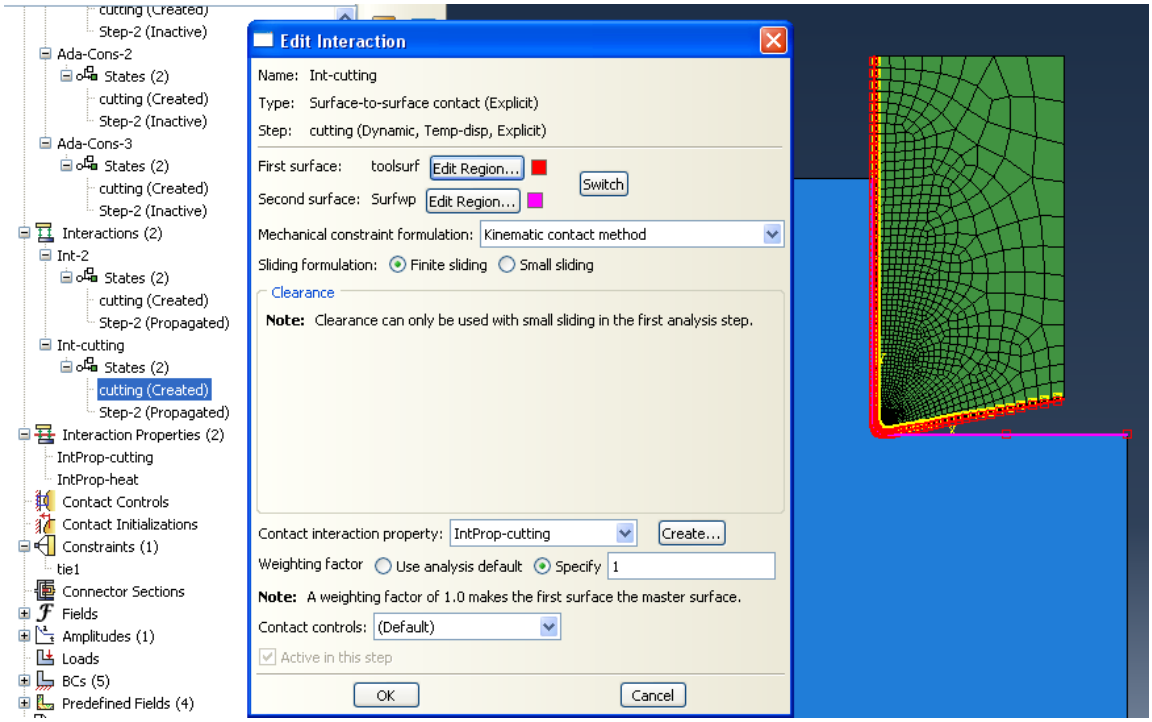

Figure A28. Define surface kinematic contact interaction between tool surface and chip (workpiece) surface as highlighted.

12. Define a temporary tie constraint (shown in figure 29) for later modification in input file.

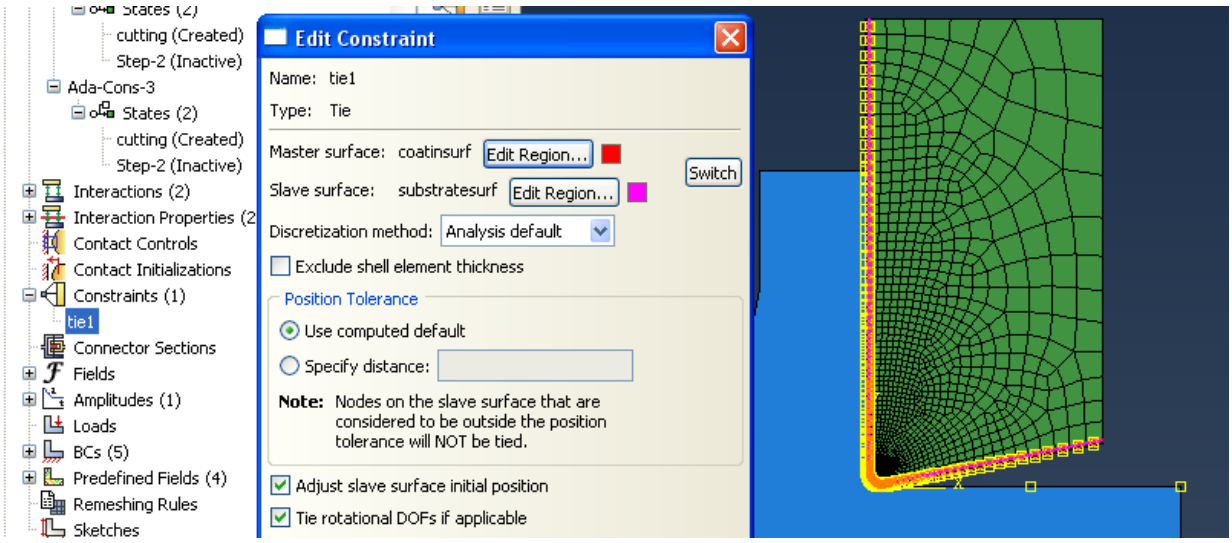

Figure A29. Tie constraint definition for coating and substrate used for later modification in input file.

13. Define displacement load amplitude for workpiece withdrawal process (shown in figure A30).

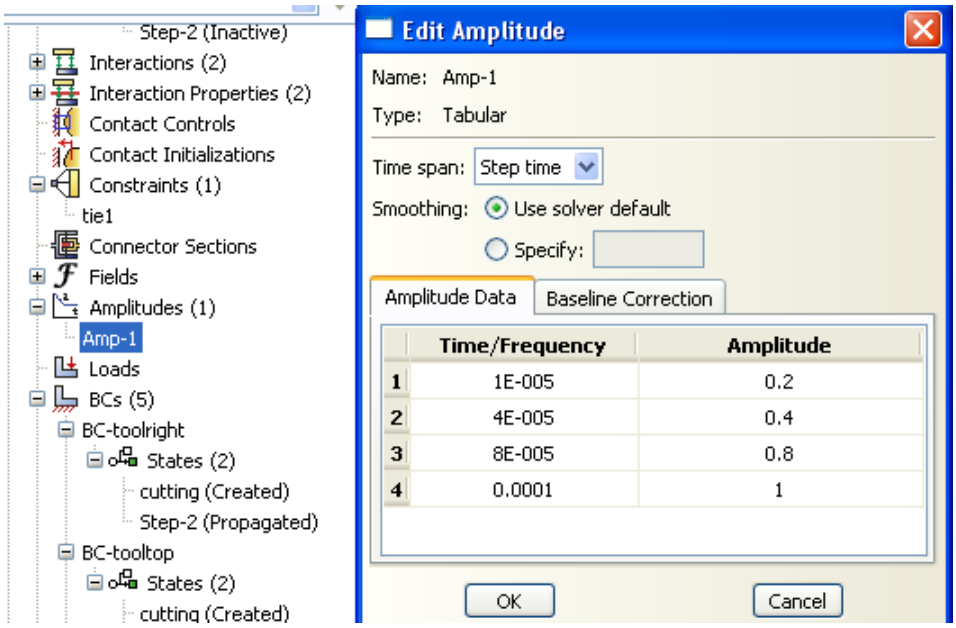

Figure A30. Definition of a displacement load amplitude.

14. Define boundary conditions for workpiece and tool. Figure A31 shows the tool is constrained in y direction for top edge and x direction for right edge.

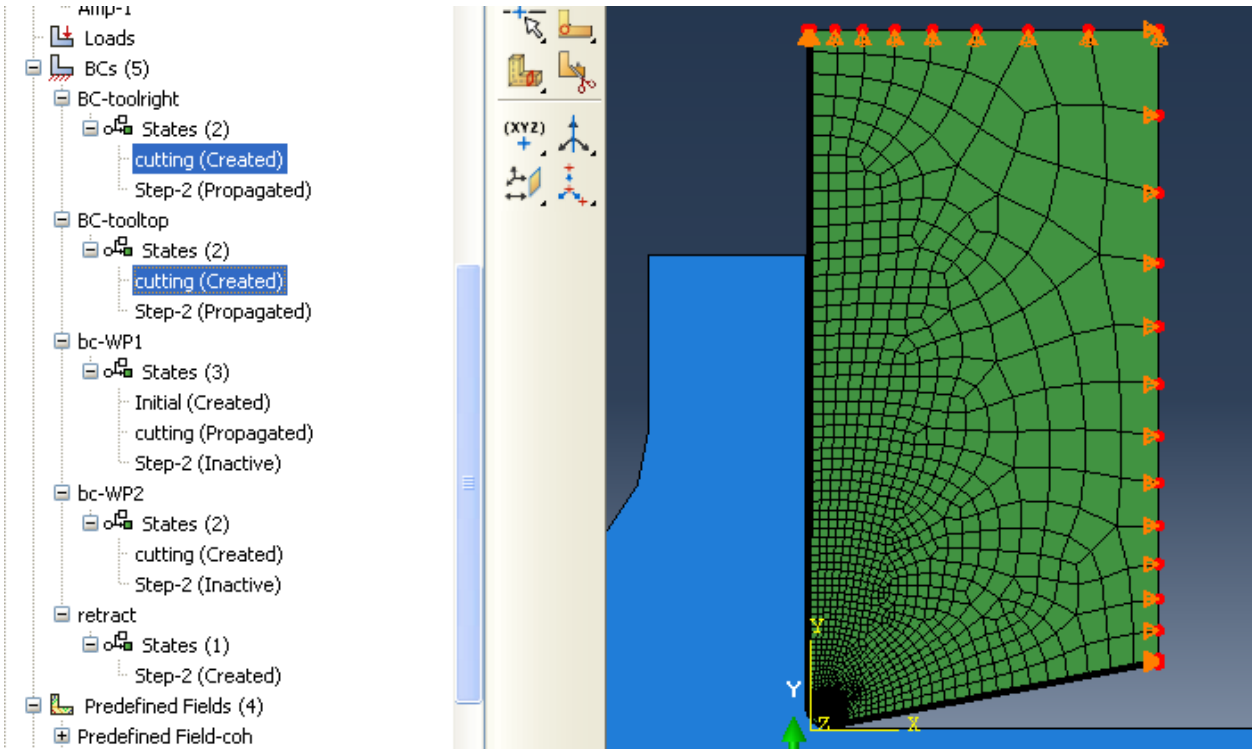

Figure A31. Boundary conditions for tool as highlighted.

Figure A32 shows boundary conitions for workpiece. Workpiece bottom is constrained in y direction and a material flows in from workpiece left at a speed of 5.0 m/s. This needs further keywords modification which will be addressed in the sequel.

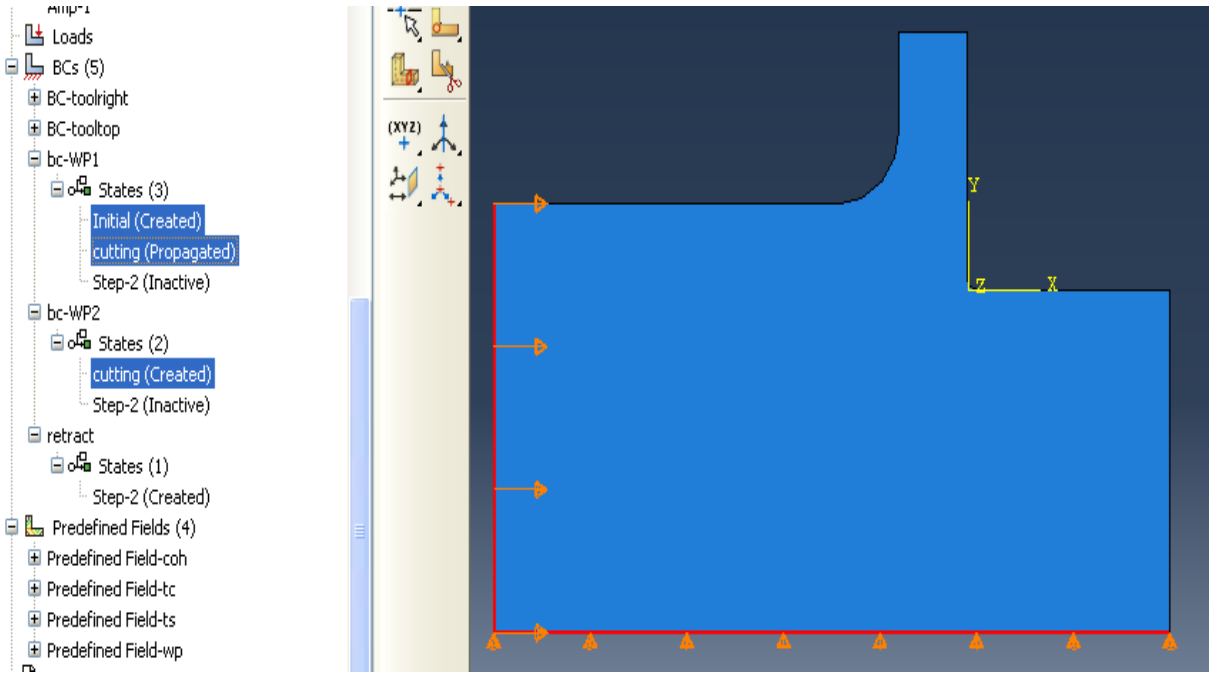

Figure A32. Boundary conditions for workpiece as highlighted.

Figure A33 shows how to make workpiece withdrawal process. In the definition, workpiece will take a displacement load after cutting process. The displacement cites an amplitude loading history which is defined before in Step 13. Note that the boundary conditions of workpiece will be deactivated in workpiece withdrawal simulation.

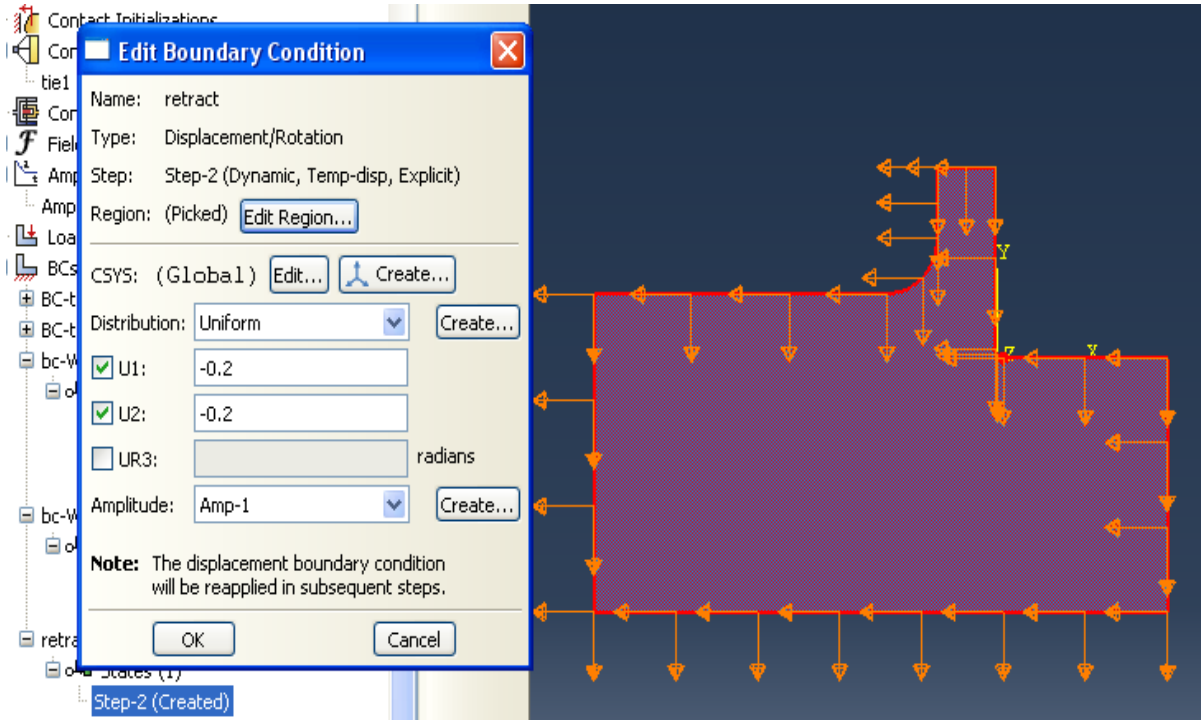

Figure A33. definition of workpiece withdrawal as highlighted.

15. Define ALE adaptive mesh.

Go to main menu, then “other” to define ALE adaptive mesh controls and domain. Figure A34 is the definition of ALE adaptive mesh domain. The workpiece geometry is defined as ALE adaptive mesh domain. FigureA 35 shows the ALE adaptive mesh controls, which will be employed in ALE adaptive mesh domain definition.

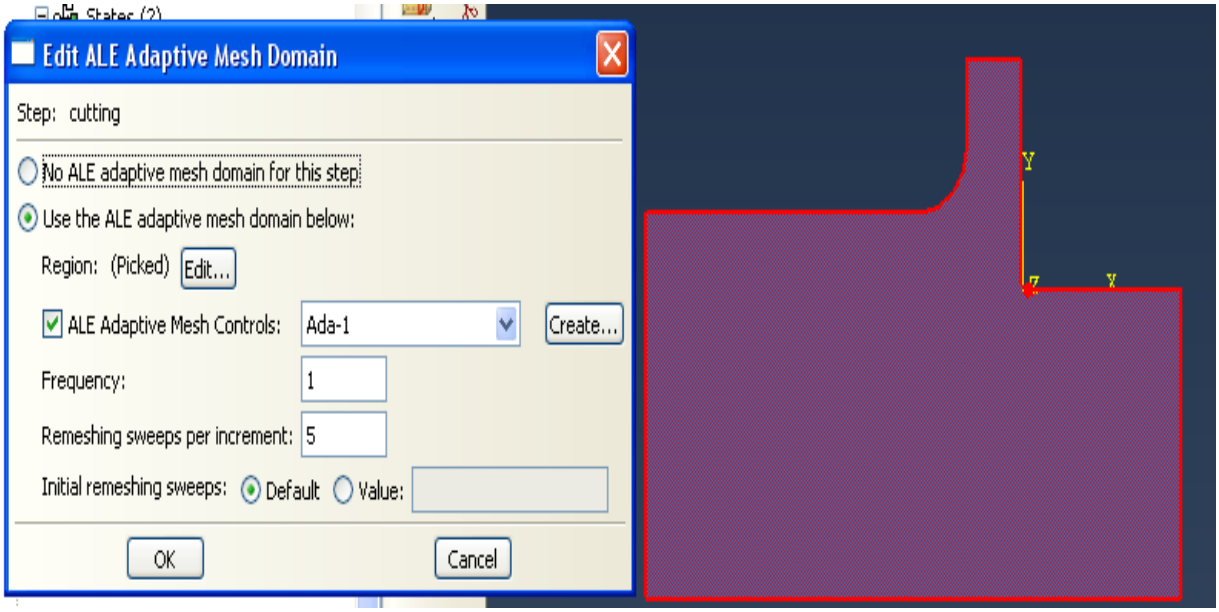

Figure A34. Definition of ALE adaptive mesh domain as highlighted.

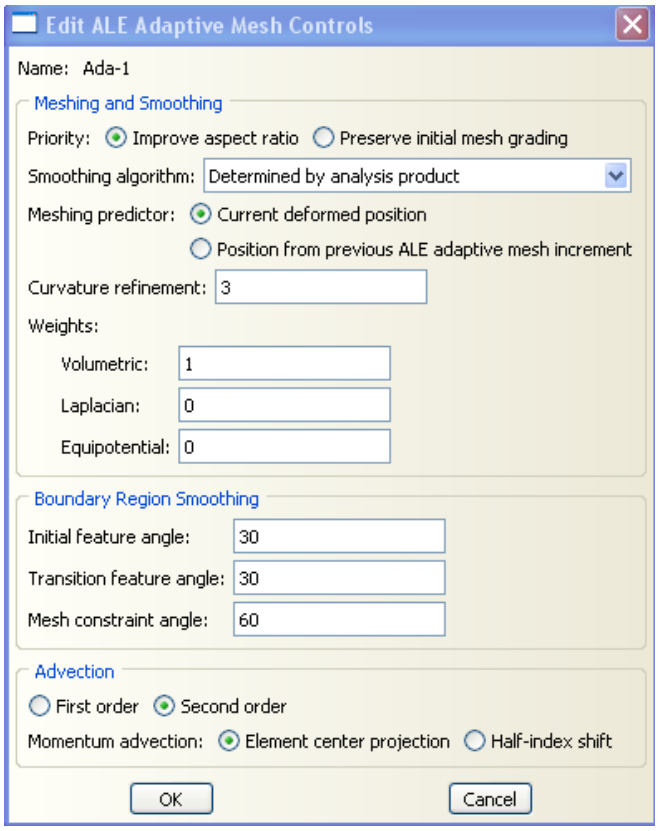

Figure A35. Definition ALE adaptive mesh controls.

16. Mesh workpiece. Element type is CPE4RT. Free meshing is chosen for workpiece. The element seeds are defined as follows.

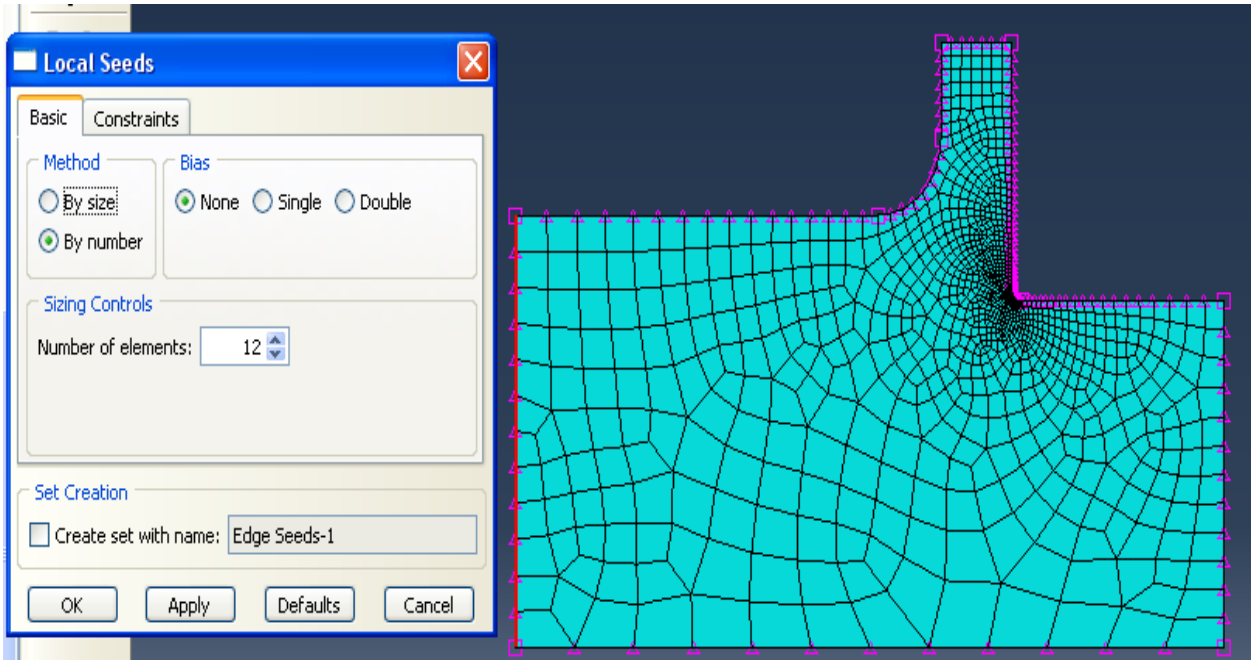

Figure A36. Element seeds of workpiece left edge as highlighted.

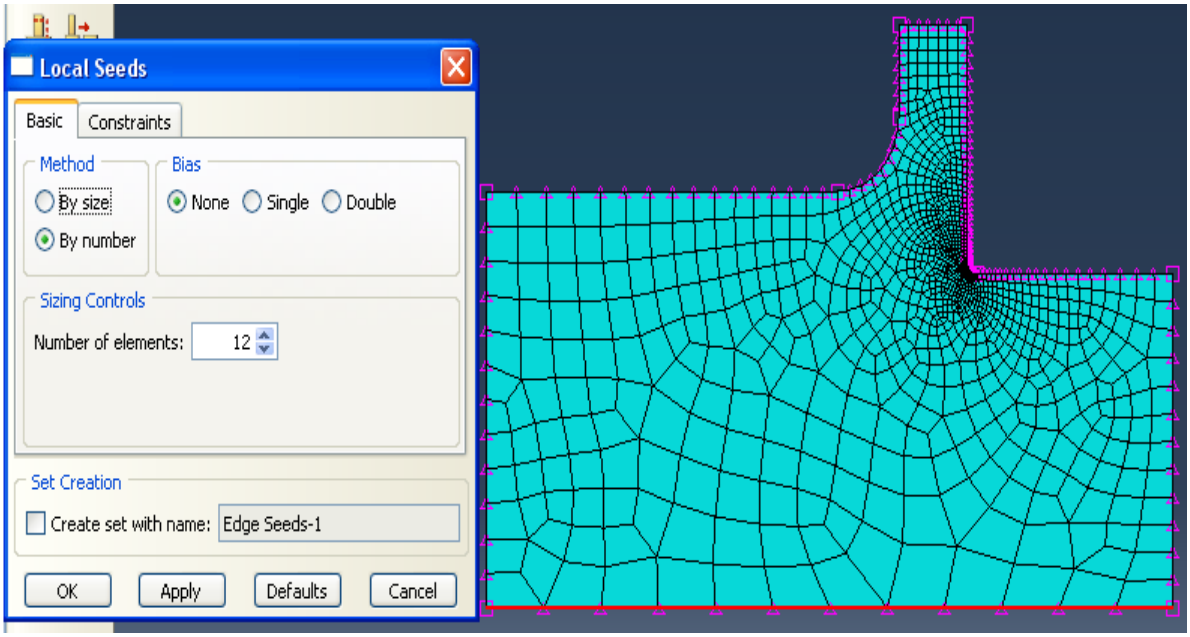

Figure A37. Element seeds of workpiece bottom edge as highlighted.

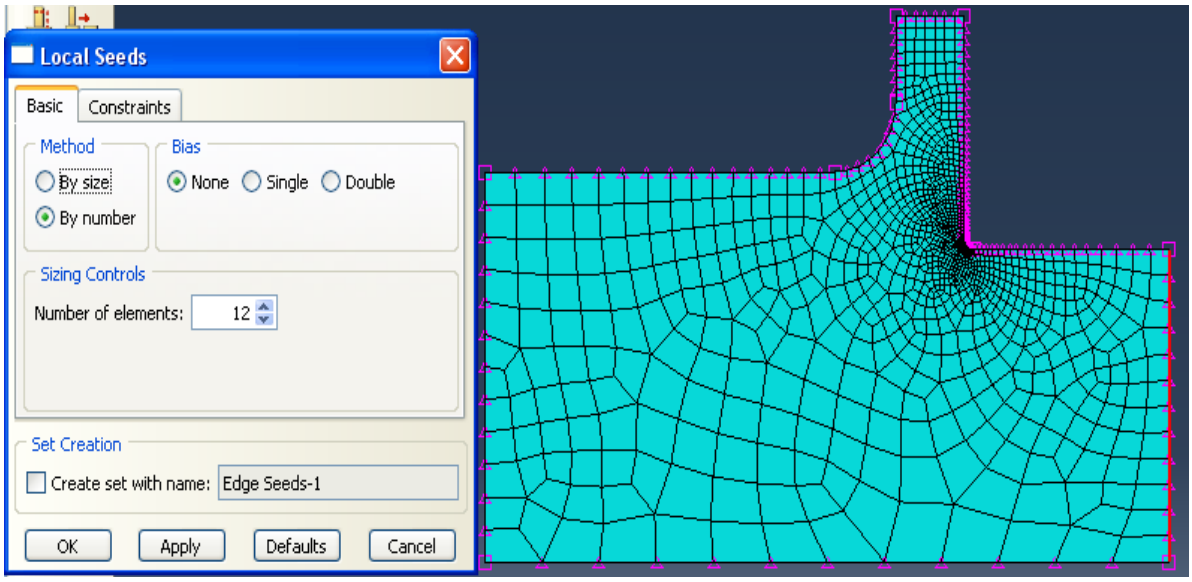

Figure A38. Element seeds of workpiece right edge as highlighted.

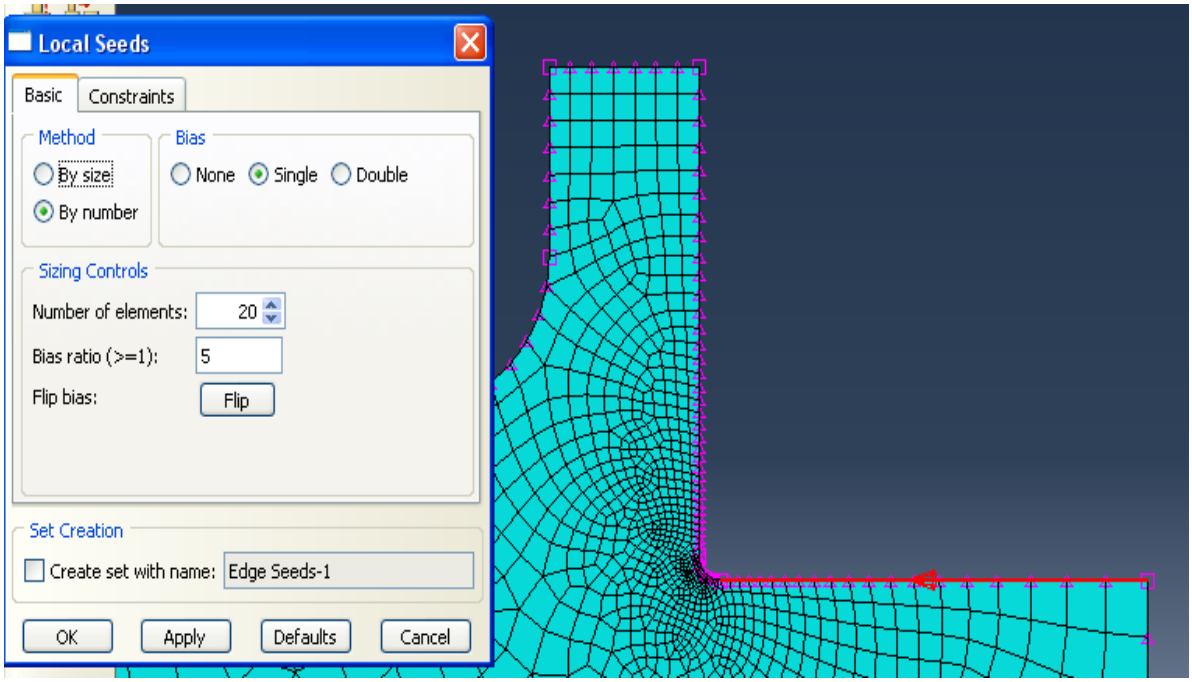

Figure A39. Element seeds of workpiece right-top edge as highlighted.

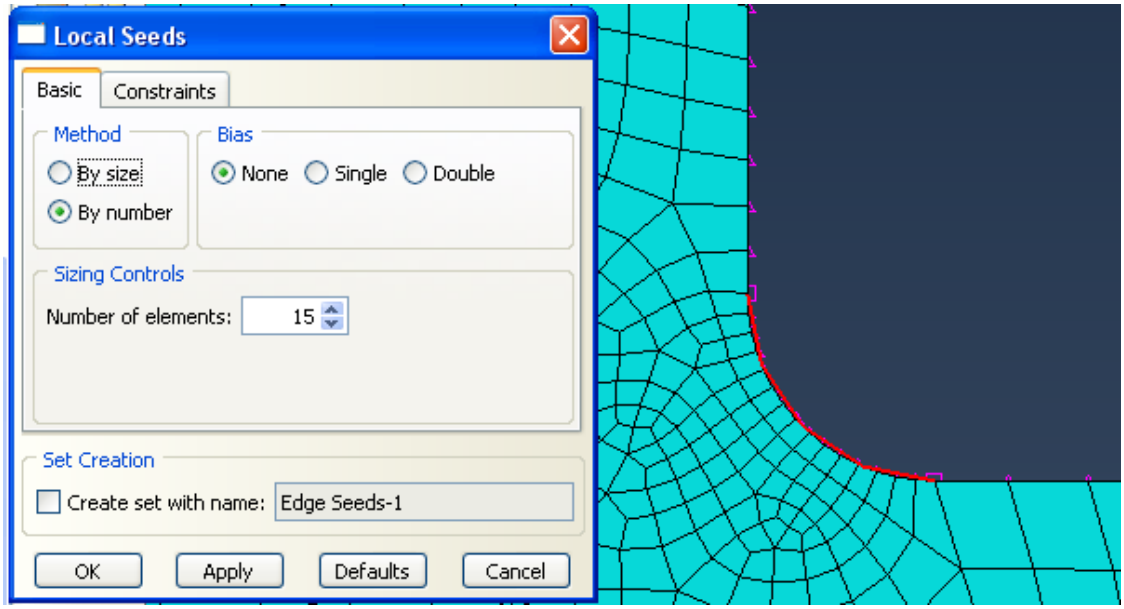

Figure A40. Element seeds of workpiece arc edge as highlighted.

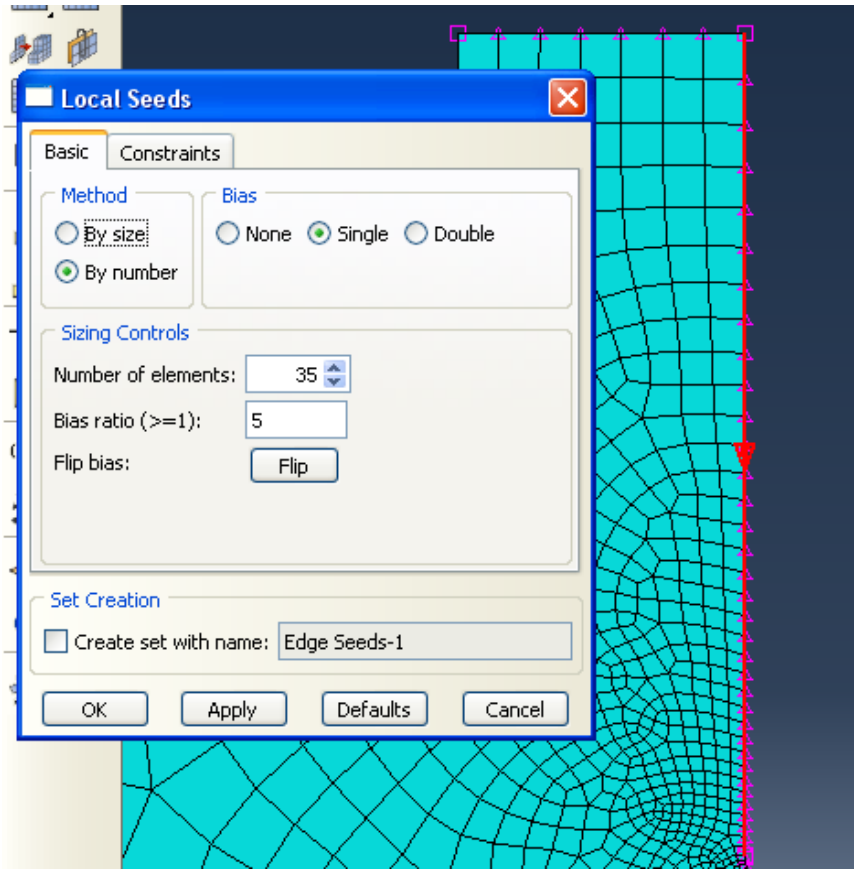

Figure A41. Element seeds of chip right edge as highlighted.

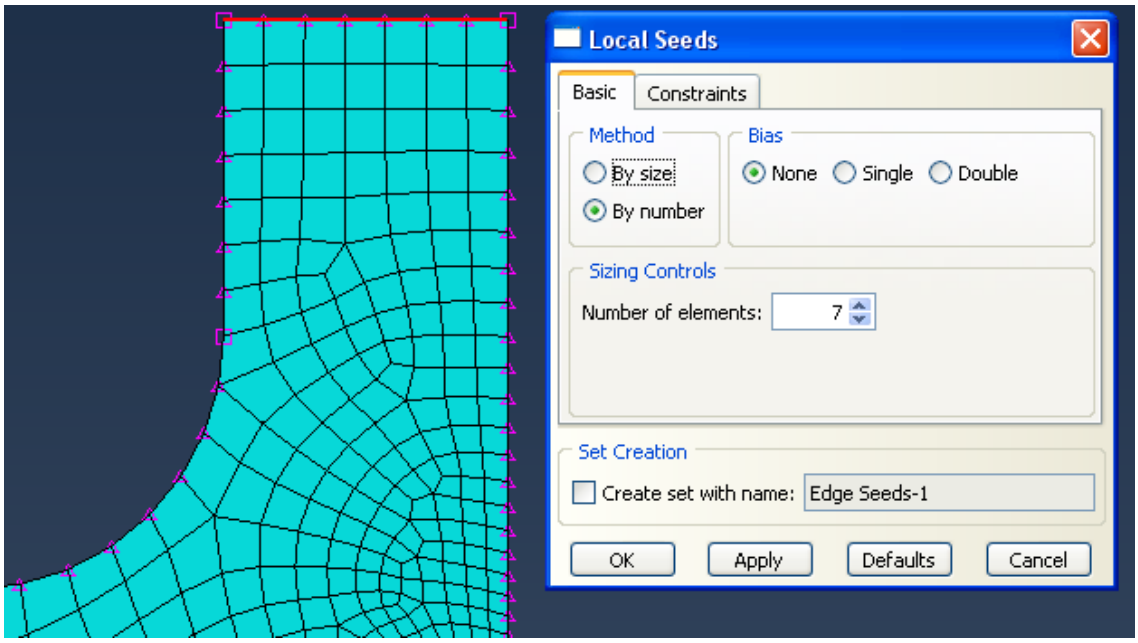

Figure A42. Element seeds of chip top edge as highlighted.

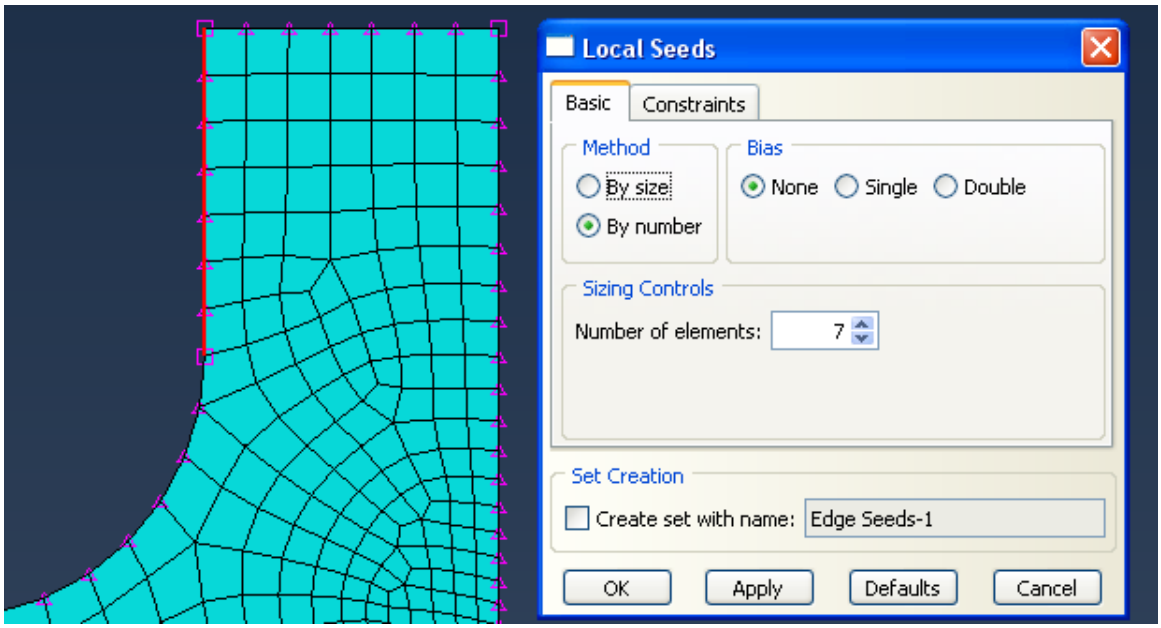

Figure A43. Element seeds of chip right edge as highlighted.

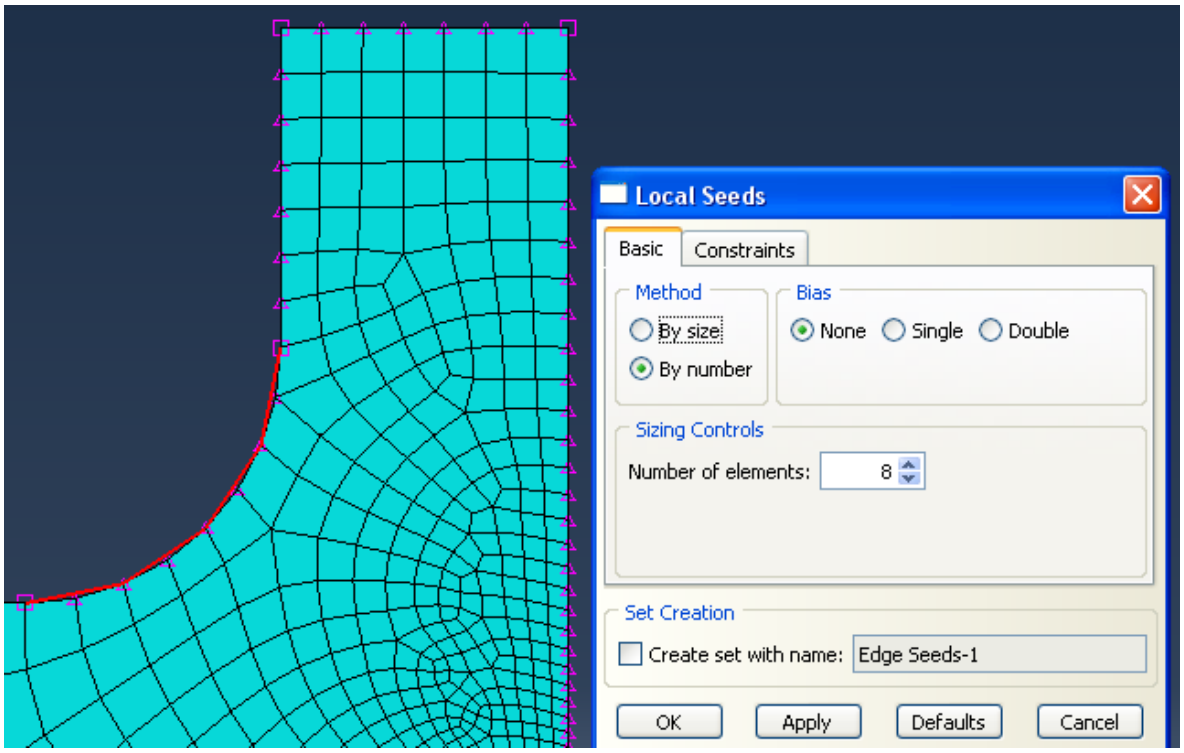

Figure A44. Element seeds of chip left arc edge as highlighted.

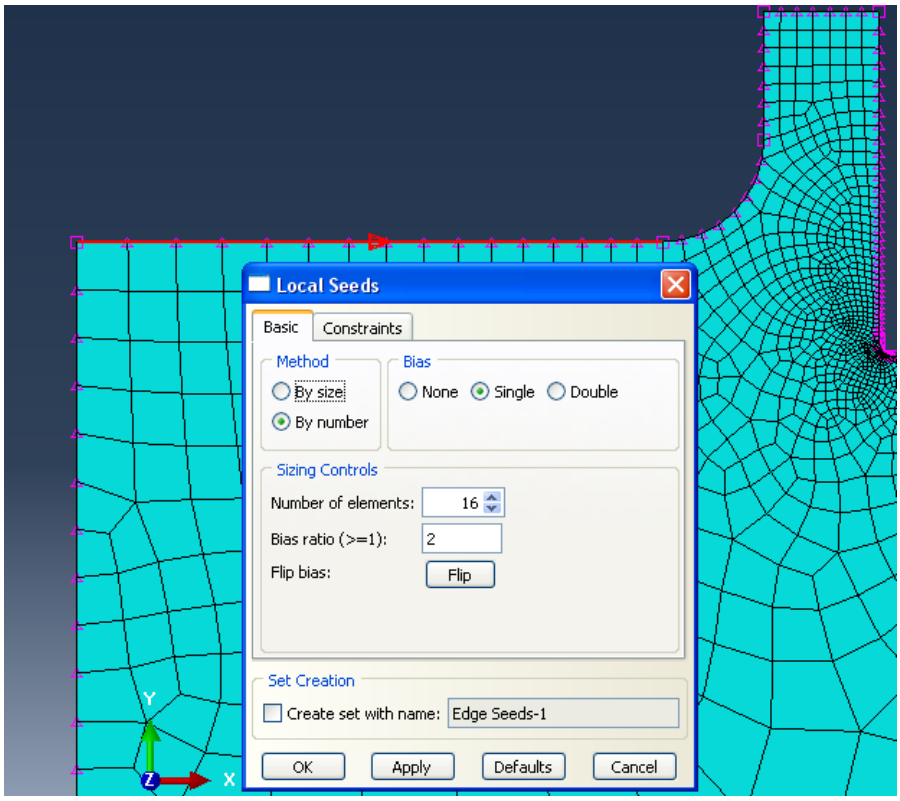

Figure A45. Element seeds of workpiece left-top edge as highlighted.

17. Modify keywords for material flow definition.

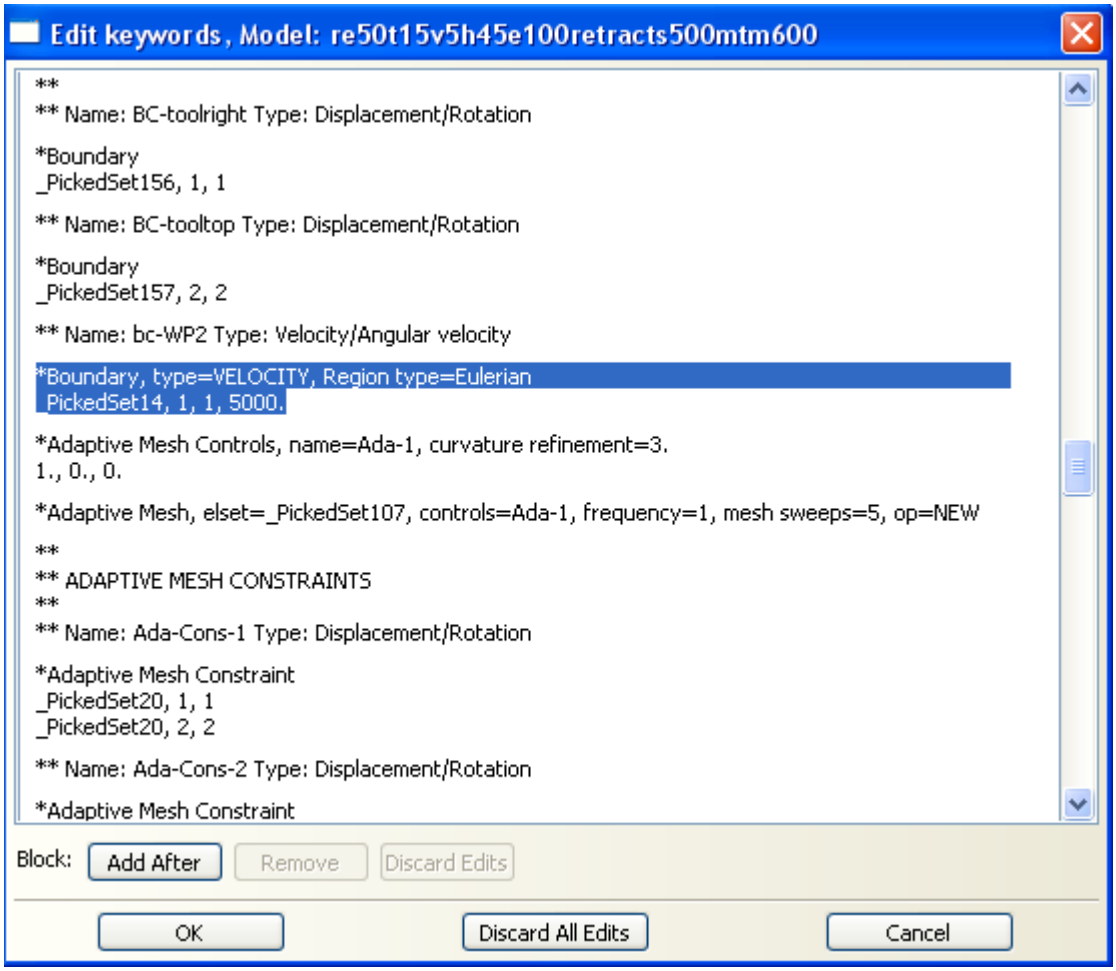

Figure A46. Modification of material flow definition as highlighted.

18. Define imported job state for tool parts and initial temperature field for workpiece.

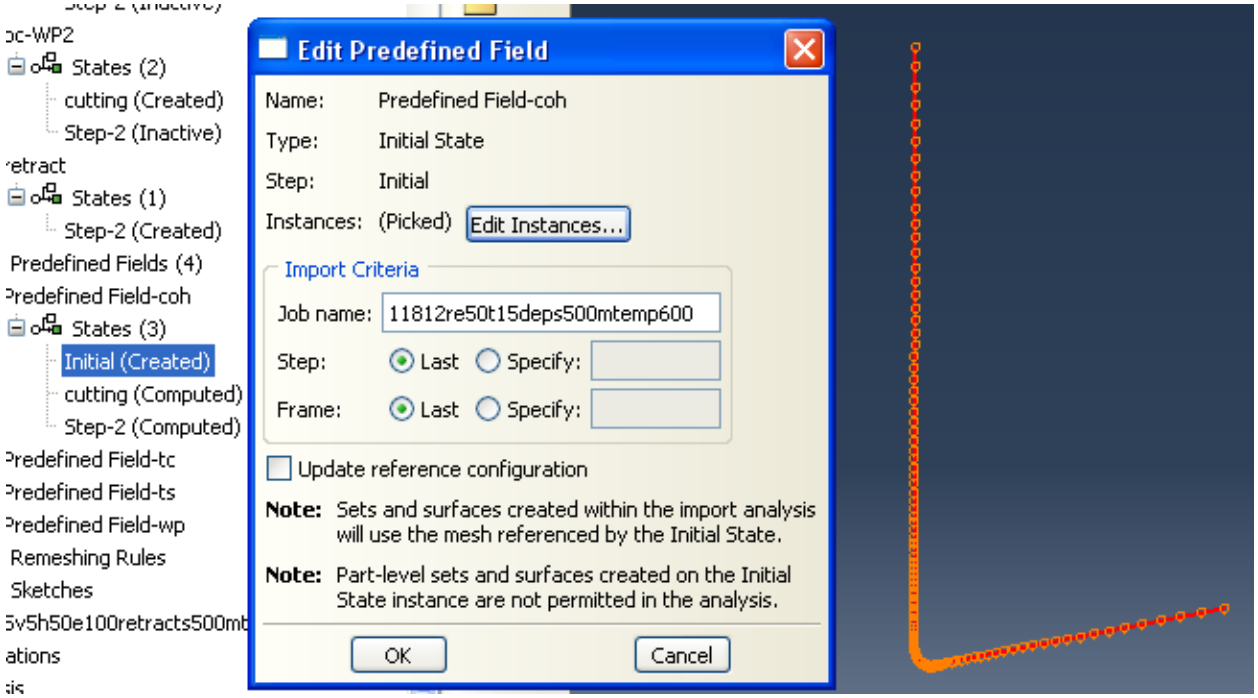

Figure A47. Definition of cohesive zone initial state before cutting.

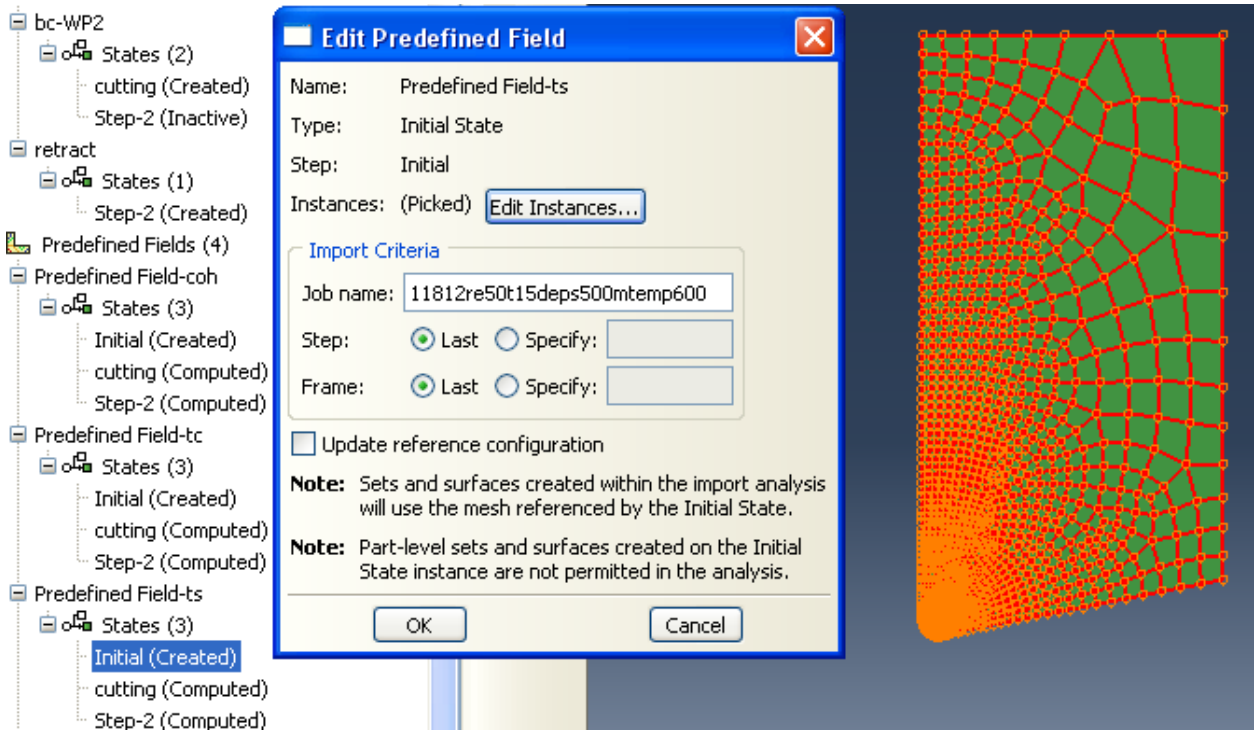

Figure A48. Definition of substrate initial state before cutting.

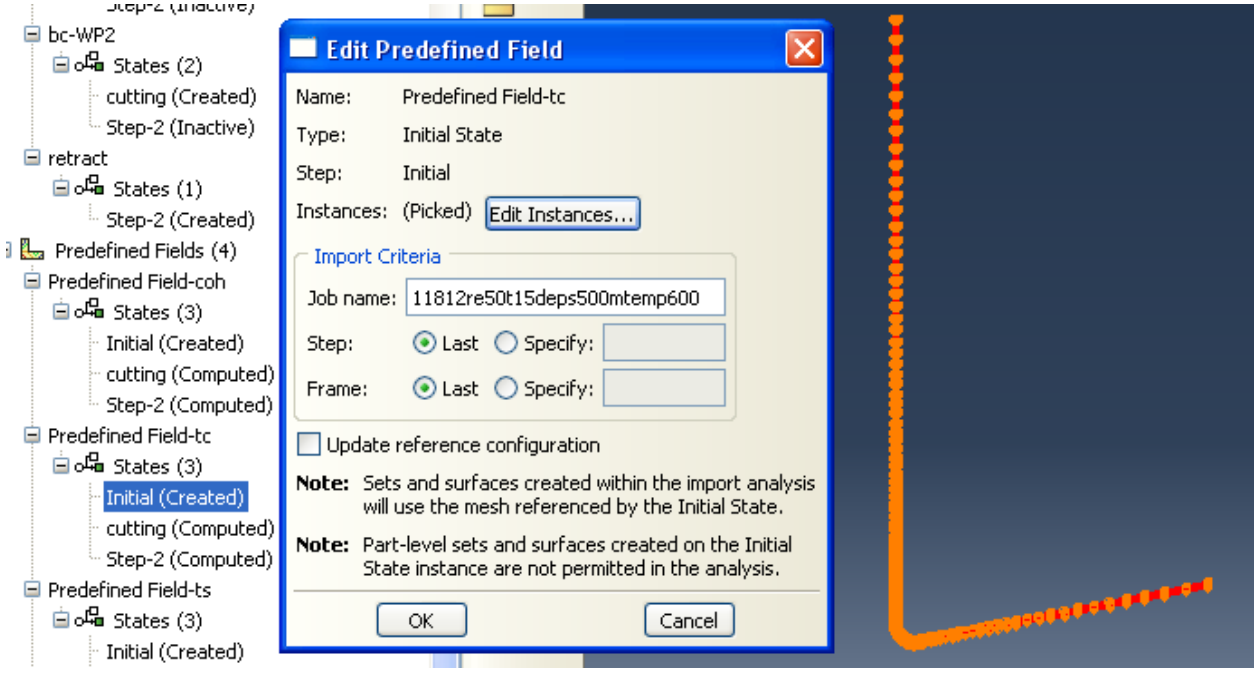

Figure A49. Definition of coating initial state before cutting.

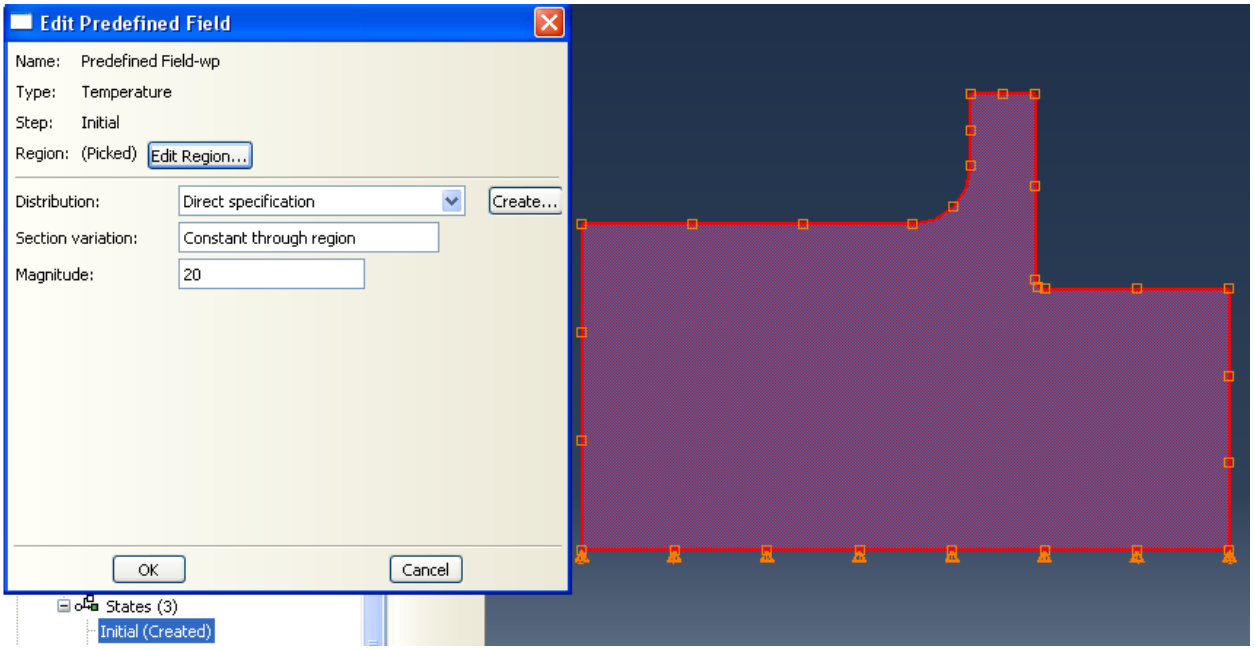

Figure A50. Definition of workpiece initial temperature field before cutting.

19. Create job input file.

20. Modify the input file as highlighted.

```
*Elset, elset=cohesive, instance=INTERLAY-1, generate
   1,  120,    1
*Surface, type=element, name=cohesivein
cohesive, S1
*Surface, type=element, name=cohesiveout
cohesive, S3
```

Figure A51. Definition of cohesive surfaces in input file.

```
** Constraint: tie1
*Tie, name=tie1, adjust=yes
cohesiveout, coatinsurf
** Constraint: tie2
*Tie, name=tie2, adjust=yes
cohesivein, substratesurf
```

Figure A52. Definition of tie constraints in input file.

21. Run the input file using command: C:\abaqusjobs\abq6101 job=… int

APPENDIX B

A TYPICAL INPUT FILE FOR DEPOSITION RESIDUAL

STRESS SIMULATION INCLUDING COHESIVE ZONE

```
*Heading
** Job name: 11012czm0re50t15depsig500m
Model name: czm0re50t15 100j
** Generated by: Abaqus/CAE 6.10-1
*Preprint, echo=NO, model=NO, history=NO,
contact=NO
**
** PARTS
**
*Part, name=COAT
*Node
      1,           0., 0.0915198326
      2,           0.,           2.
      3, -0.0149999997,           2.
      4, -0.0149999997, 0.0915198326
      5, 0.0898383558, 0.0174628068
      6, 0.0595404506, 0.0115734907
      7,           0., 0.0606548488
      8, 0.0624025837, -0.00315091666
      9, -0.0149999997, 0.0606548488
     10, 0.0927004889, 0.00273839966
     11,           1.,  0.194380313
     12,           1.,   0.17909956
     13,           0.,  0.104273289
     14,           0.,  0.117379434
     15,           0.,   0.13084802
     16,           0.,  0.144689053
     17,           0.,  0.158912867
     18,           0.,  0.173530012
     19,           0.,  0.188551381
     20,           0.,  0.203988165
     21,           0.,  0.219851822
     22,           0.,  0.236154184
     23,           0.,  0.252907366
     24,           0.,  0.270123839
     25,           0.,  0.287816435
     26,           0.,  0.305998296
     27,           0.,  0.324682951
     28,           0.,  0.343884319
     29,           0.,  0.363616705
     30,           0.,  0.383894742
     31,           0.,  0.404733539
     32,           0.,  0.426148653
     33,           0.,  0.448155969
     34,           0.,  0.470771849
     35,           0.,   0.49401319
     36,           0.,  0.517897189
     37,           0.,  0.542441726
     38,           0.,   0.56766504
     39,           0.,  0.593585849
     40,           0.,  0.620223463
     41,           0.,   0.64759773
     42,           0.,  0.675729036
     43,           0.,  0.704638243
     44,           0.,  0.734346926
     45,           0.,    0.7648772
     46,           0.,  0.796251714
     47,           0.,  0.828493893
     48,           0.,  0.861627638
     49,           0.,  0.895677745
     50,           0.,  0.930669427
     51,           0.,   0.96662879
     52,           0.,    1.0035826
     53,           0.,   1.04155827
     54,           0.,   1.08058417
     55,           0.,   1.12068927
     56,           0.,    1.1619035
     57,           0.,   1.20425749
     58,           0.,   1.24778259
     59,           0.,   1.29251146
     60,           0.,   1.33847725
     61,           0.,   1.38571417
     62,           0.,   1.43425739
     63,           0.,   1.48414302
     64,           0.,   1.53540814
     65,           0.,   1.58809102
     66,           0.,   1.64223075
     67,           0.,   1.69786763
     68,           0.,   1.75504327
     69,           0.,   1.81379986
     70,           0.,   1.87418139
     71,           0.,   1.93623269
     72, -0.00499999989,           2.
     73, -0.00999999978,           2.
     74, -0.0149999997,   1.93623269
     75, -0.0149999997,   1.87418139
     76, -0.0149999997,   1.81379986
     77, -0.0149999997,   1.75504327
     78, -0.0149999997,   1.69786763
     79, -0.0149999997,   1.64223075
     80, -0.0149999997,   1.58809102
     81, -0.0149999997,   1.53540814
     82, -0.0149999997,   1.48414302
     83, -0.0149999997,   1.43425739
     84, -0.0149999997,   1.38571417
     85, -0.0149999997,   1.33847725
     86, -0.0149999997,   1.29251146
     87, -0.0149999997,   1.24778259
     88, -0.0149999997,   1.20425749
     89, -0.0149999997,    1.1619035
     90, -0.0149999997,   1.12068927
     91, -0.0149999997,   1.08058417
     92, -0.0149999997,   1.04155827
     93, -0.0149999997,    1.0035826
     94, -0.0149999997,   0.96662879
     95, -0.0149999997,  0.930669427
     96, -0.0149999997,  0.895677745
     97, -0.0149999997,  0.861627638
     98, -0.0149999997,  0.828493893
     99, -0.0149999997,  0.796251714
    100, -0.0149999997,    0.7648772
    101, -0.0149999997,  0.734346926
    102, -0.0149999997,  0.704638243
    103, -0.0149999997,  0.675729036
    104, -0.0149999997,   0.64759773
    105, -0.0149999997,  0.620223463
    106, -0.0149999997,  0.593585849
    107, -0.0149999997,   0.56766504
    108, -0.0149999997,  0.542441726
    109, -0.0149999997,  0.517897189
    110, -0.0149999997,   0.49401319
    111, -0.0149999997,  0.470771849
    112, -0.0149999997,  0.448155969
    113, -0.0149999997,  0.426148653
    114, -0.0149999997,  0.404733539
    115, -0.0149999997,  0.383894742
    116, -0.0149999997,  0.363616705
    117, -0.0149999997,  0.343884319
    118, -0.0149999997,  0.324682951
    119, -0.0149999997,  0.305998296
    120, -0.0149999997,  0.287816435
    121, -0.0149999997,  0.270123839
    122, -0.0149999997,  0.252907366
    123, -0.0149999997,  0.236154184
    124, -0.0149999997,  0.219851822
    125, -0.0149999997,  0.203988165
```

126, -0.0149999997, 0.188551381
127, -0.0149999997, 0.173530012
128, -0.0149999997, 0.158912867
129, -0.0149999997, 0.144689053
130, -0.0149999997, 0.13084802
131, -0.0149999997, 0.117379434
132, -0.0149999997, 0.104273289
133, -0.00999999978, 0.0915198326
134, -0.00499999989, 0.0915198326
135, 0.0868085623, 0.0168738756
136, 0.0837787762, 0.0162849445
137, 0.0807489827, 0.0156960133
138, 0.0777191967, 0.0151070813
139, 0.0746894032, 0.0145181492
140, 0.0716596097, 0.0139292181
141, 0.0686298236, 0.013340286
142, 0.0656000301, 0.0127513539
143, 0.0625702441, 0.0121624228
144, 0.0537199304, 0.0107934205
145, 0.0478480905, 0.0107011786
146, 0.0420059413, 0.0112980371
147, 0.0362740643, 0.0125757623
148, 0.0307315364, 0.014516728
149, 0.0254548118, 0.0170941595
150, 0.0205166843, 0.0202725027
151, 0.015985271, 0.0240079109
152, 0.011923085, 0.0282488558
153, 0.00838616118, 0.0329368338
154, 0.00542329205, 0.0380071774
155, 0.00307534891, 0.0433899388
156, 0.00137472153, 0.0490108691
157, 0.000344869739, 0.0547924228
158, 0., 0.0637413487
159, 0., 0.0668278486
160, 0., 0.0699143484
161, 0., 0.0730008408
162, 0., 0.0760873407
163, 0., 0.0791738406
164, 0., 0.0822603405
165, 0., 0.0853468403
166, 0., 0.0884333327
167, 0.0654323772, -0.00256198505
168, 0.0684621632, -0.00197305344
169, 0.0714919567, -0.00138412183
170, 0.0745217502, -0.000795190106
171, 0.0775515363, -0.000206258483
172, 0.0805813298, 0.00038267317
173, 0.0836111158, 0.000971604779
174, 0.0866409093, 0.00156053645
175, 0.0896707028, 0.00214946805
176, -0.0145516694, 0.0530336946
177, -0.0132128624, 0.0455176756
178, -0.0110020461, 0.0382104665
179, -0.00794972014, 0.0312128756
180, -0.00409799069, 0.0246214289
181, 0.000500010035, 0.018527057
182, 0.0057808524, 0.0130138276
183, 0.0116716884, 0.00815779716
184, 0.0180912558, 0.00402595242
185, 0.0249509979, 0.000675291347
186, 0.0321562849, -0.00184796448
187, 0.0396077223, -0.00350900693
188, 0.0472025201, -0.0042849225
189, 0.0548359081, -0.00416500773
190, -0.0149999997, 0.0884333327
191, -0.0149999997, 0.0853468403
192, -0.0149999997, 0.0822603405
193, -0.0149999997, 0.0791738406
194, -0.0149999997, 0.0760873407
195, -0.0149999997, 0.0730008408
196, -0.0149999997, 0.0699143484
197, -0.0149999997, 0.0668278486
198, -0.0149999997, 0.0637413487
199, 0.0917464495, 0.00764653552
200, 0.0907924026, 0.0125546716
201, 0.927385151, 0.180265412
202, 0.859480202, 0.167066023
203, 0.795979619, 0.154722765
204, 0.736597717, 0.143180087
205, 0.681067348, 0.132386088
206, 0.629138768, 0.122292183
207, 0.580578268, 0.112852991
208, 0.535167515, 0.104026027
209, 0.492702097, 0.0957715809
210, 0.452991009, 0.0880525336
211, 0.415855646, 0.0808341503
212, 0.381128907, 0.0740839541
213, 0.348654568, 0.0677715838
214, 0.318286538, 0.0618686341
215, 0.289888203, 0.0563485585
216, 0.263331801, 0.0511865169
217, 0.238497883, 0.0463592932
218, 0.215274706, 0.0418451652
219, 0.193557799, 0.0376238264
220, 0.173249483, 0.033676289
221, 0.15425837, 0.029984789
222, 0.136499047, 0.0265327264
223, 0.119891599, 0.0233045649
224, 0.104361326, 0.0202857871
225, 0.107177787, 0.00555250095
226, 0.122659221, 0.0085617872
227, 0.139214441, 0.0117797963
228, 0.15691793, 0.0152210053
229, 0.175849319, 0.0189008936
230, 0.196093783, 0.0228360184
231, 0.217742383, 0.0270440821
232, 0.240892529, 0.0315440148
233, 0.265648365, 0.0363560617
234, 0.292121232, 0.0415018685
235, 0.320430279, 0.0470045842
236, 0.350702792, 0.0528889708
237, 0.383075029, 0.0591814928
238, 0.417692572, 0.0659104586
239, 0.454711169, 0.0731061473
240, 0.494297355, 0.0808009207
241, 0.53662926, 0.089029409
242, 0.581897199, 0.0978286117
243, 0.630304992, 0.107238129
244, 0.682070255, 0.117300279
245, 0.737425983, 0.128060341
246, 0.796621144, 0.13956672
247, 0.859922051, 0.151871175
248, 0.927613497, 0.165029049
249, 1., 0.184193149
250, 1., 0.189286724
251, -0.00499999989, 0.104273289
252, -0.00499999989, 0.117379434
253, -0.00499999989, 0.13084802
254, -0.00499999989, 0.144689053
255, -0.00499999989, 0.158912867
256, -0.00499999989, 0.173530012
257, -0.00499999989, 0.188551381
258, -0.00499999989, 0.203988165
259, -0.00499999989, 0.219851822
260, -0.00499999989, 0.236154184
261, -0.00499999989, 0.252907366
262, -0.00499999989, 0.270123839
263, -0.00499999989, 0.287816435
264, -0.00499999989, 0.305998296
265, -0.00499999989, 0.324682951
266, -0.00499999989, 0.343884319
267, -0.00499999989, 0.363616705

268, -0.00499999989, 0.383894742
269, -0.00499999989, 0.404733539
270, -0.00499999989, 0.426148653
271, -0.00499999989, 0.448155969
272, -0.00499999989, 0.470771849
273, -0.00499999989, 0.49401319
274, -0.00499999989, 0.517897189
275, -0.00499999989, 0.542441726
276, -0.00499999989, 0.56766504
277, -0.00499999989, 0.593585849
278, -0.00499999989, 0.620223463
279, -0.00499999989, 0.64759773
280, -0.00499999989, 0.675729036
281, -0.00499999989, 0.704638243
282, -0.00499999989, 0.734346926
283, -0.00499999989, 0.7648772
284, -0.00499999989, 0.796251714
285, -0.00499999989, 0.828493893
286, -0.00499999989, 0.861627638
287, -0.00499999989, 0.895677745
288, -0.00499999989, 0.930669427
289, -0.00499999989, 0.96662879
290, -0.00499999989, 1.0035826
291, -0.00499999989, 1.04155827
292, -0.00499999989, 1.08058417
293, -0.00499999989, 1.12068927
294, -0.00499999989, 1.1619035
295, -0.00499999989, 1.20425749
296, -0.00499999989, 1.24778259
297, -0.00499999989, 1.29251146
298, -0.00499999989, 1.33847725
299, -0.00499999989, 1.38571417
300, -0.00499999989, 1.43425739
301, -0.00499999989, 1.48414302
302, -0.00499999989, 1.53540814
303, -0.00499999989, 1.58809102
304, -0.00499999989, 1.64223075
305, -0.00499999989, 1.69786763
306, -0.00499999989, 1.75504327
307, -0.00499999989, 1.81379986
308, -0.00499999989, 1.87418139
309, -0.00499999989, 1.93623269
310, -0.00999999978, 0.104273289
311, -0.00999999978, 0.117379434
312, -0.00999999978, 0.13084802
313, -0.00999999978, 0.144689053
314, -0.00999999978, 0.158912867
315, -0.00999999978, 0.173530012
316, -0.00999999978, 0.188551381
317, -0.00999999978, 0.203988165
318, -0.00999999978, 0.219851822
319, -0.00999999978, 0.236154184
320, -0.00999999978, 0.252907366
321, -0.00999999978, 0.270123839
322, -0.00999999978, 0.287816435
323, -0.00999999978, 0.305998296
324, -0.00999999978, 0.324682951
325, -0.00999999978, 0.343884319
326, -0.00999999978, 0.363616705
327, -0.00999999978, 0.383894742
328, -0.00999999978, 0.404733539
329, -0.00999999978, 0.426148653
330, -0.00999999978, 0.448155969
331, -0.00999999978, 0.470771849
332, -0.00999999978, 0.49401319
333, -0.00999999978, 0.517897189
334, -0.00999999978, 0.542441726
335, -0.00999999978, 0.56766504
336, -0.00999999978, 0.593585849
337, -0.00999999978, 0.620223463
338, -0.00999999978, 0.64759773
339, -0.00999999978, 0.675729036
340, -0.00999999978, 0.704638243
341, -0.00999999978, 0.734346926
342, -0.00999999978, 0.7648772
343, -0.00999999978, 0.796251714
344, -0.00999999978, 0.828493893
345, -0.00999999978, 0.861627638
346, -0.00999999978, 0.895677745
347, -0.00999999978, 0.930669427
348, -0.00999999978, 0.96662879
349, -0.00999999978, 1.0035826
350, -0.00999999978, 1.04155827
351, -0.00999999978, 1.08058417
352, -0.00999999978, 1.12068927
353, -0.00999999978, 1.1619035
354, -0.00999999978, 1.20425749
355, -0.00999999978, 1.24778259
356, -0.00999999978, 1.29251146
357, -0.00999999978, 1.33847725
358, -0.00999999978, 1.38571417
359, -0.00999999978, 1.43425739
360, -0.00999999978, 1.48414302
361, -0.00999999978, 1.53540814
362, -0.00999999978, 1.58809102
363, -0.00999999978, 1.64223075
364, -0.00999999978, 1.69786763
365, -0.00999999978, 1.75504327
366, -0.00999999978, 1.81379986
367, -0.00999999978, 1.87418139
368, -0.00999999978, 1.93623269
369, 0.0877626091, 0.0119657395
370, 0.0847328231, 0.0113768084
371, 0.0817030296, 0.0107878763
372, 0.0786732361, 0.0101989452
373, 0.07564345, 0.0096100131
374, 0.0726136565, 0.00902108196
375, 0.069583863, 0.00843214989
376, 0.066554077, 0.00784321874
377, 0.0635242835, 0.00725428667
378, 0.0604944937, 0.00666535506
379, 0.0540919229, 0.00580727821
380, 0.0476329029, 0.00570581155
381, 0.041206535, 0.00636235578
382, 0.0349014737, 0.00776785333
383, 0.0288046896, 0.00990291592
384, 0.0230002943, 0.0127380909
385, 0.0175683517, 0.0162342675
386, 0.0125837978, 0.0203432161
387, 0.00811539311, 0.0250082556
388, 0.00422477722, 0.0301650316
389, 0.000965621031, 0.0357424095
390, -0.00161711627, 0.0416634493
391, -0.0034878063, 0.04784647
392, -0.00462064333, 0.0542061813
393, -0.00499999989, 0.0606548488
394, -0.00499999989, 0.0637413487
395, -0.00499999989, 0.0668278486
396, -0.00499999989, 0.0699143484
397, -0.00499999989, 0.0730008408
398, -0.00499999989, 0.0760873407
399, -0.00499999989, 0.0791738406
400, -0.00499999989, 0.0822603405
401, -0.00499999989, 0.0853468403
402, -0.00499999989, 0.0884333327
403, 0.088716656, 0.00705760391
404, 0.0856868625, 0.00646867231
405, 0.0826570764, 0.0058797407
406, 0.0796272829, 0.00529080909
407, 0.0765974894, 0.00470187748
408, 0.0735677034, 0.00411294587
409, 0.0705379099, 0.00352401403

```
410, 0.0675081238, 0.00293508242
411, 0.0644783303, 0.00234615081
412, 0.0614485405, 0.0017572192
413, 0.0544639155, 0.000821135065
414, 0.0474177115, 0.000710444467
415, 0.0404071286, 0.00142667431
416, 0.0335288793, 0.00295994431
417, 0.0268778447, 0.00528910337
418, 0.0205457751, 0.00838202145
419, 0.0146200201, 0.0121960323
420, 0.00918232556, 0.0166785214
421, 0.00430770172, 0.0217676554
422,  6.3393396e-05, 0.0273932312
423, -0.00349204987, 0.0334776416
424, -0.00630958145, 0.0399369597
425, -0.00835033413, 0.0466820747
426, -0.00958615635, 0.0536199398
427, -0.00999999978, 0.0606548488
428, -0.00999999978, 0.0637413487
429, -0.00999999978, 0.0668278486
430, -0.00999999978, 0.0699143484
431, -0.00999999978, 0.0730008408
432, -0.00999999978, 0.0760873407
433, -0.00999999978, 0.0791738406
434, -0.00999999978, 0.0822603405
435, -0.00999999978, 0.0853468403
436, -0.00999999978, 0.0884333327
437,  0.927461267,  0.175186634
438,  0.859627485,  0.162001073
439,  0.796193421,   0.14967075
440,  0.736873806,  0.138140172
441,   0.68140167,  0.127357483
442,  0.629527509,  0.117274165
443,  0.581017911,  0.107844859
444,  0.535654724, 0.0990271494
445,   0.49323383, 0.0907813609
446,  0.453564405, 0.0830704048
447,  0.416467935, 0.0758595839
448,  0.381777614, 0.0691164657
449,   0.34933731, 0.0628107116
450,  0.319001108, 0.0569139495
451,  0.290632546, 0.0513996594
452,  0.264103979, 0.0462430306
453,  0.239296094, 0.0414208658
454,  0.216097265,  0.036911469
455,  0.194403127, 0.0326945558
456,   0.17411609, 0.0287511572
457,  0.155144885, 0.0250635277
458,  0.137404174, 0.0216150824
459,  0.120814137, 0.0183903053
460,  0.105300143, 0.0153746912
461,  0.927537382,  0.170107841
462,  0.859774768,  0.156936124
463,  0.796407282,  0.144618735
464,  0.737149894,  0.133100256
465,  0.681735992,  0.122328885
466,  0.629916251,  0.112256147
467,  0.581457555,  0.102836736
468,  0.536141992, 0.0940282792
469,  0.493765593, 0.0857911408
470,  0.454137772, 0.0780882761
471,  0.417080253,  0.070885025
472,  0.382426322, 0.0641489774
473,  0.350020051, 0.0578498393
474,  0.319715679, 0.0519592687
475,  0.291376889, 0.0464507639
476,  0.264876187, 0.0412995443
477,  0.240094319, 0.0364824384
478,  0.216919824, 0.0319777764
479,  0.195248455, 0.0277652871
480,  0.174982712, 0.0238260254
481,  0.156031415, 0.0201422665
482,  0.138309315, 0.0166974403
483,  0.121736683, 0.0134760467
484,  0.106238969, 0.0104635963
*Element, type=CPE4RT
  1,   1,  13, 251, 134
  2,  13,  14, 252, 251
  3,  14,  15, 253, 252
  4,  15,  16, 254, 253
  5,  16,  17, 255, 254
  6,  17,  18, 256, 255
  7,  18,  19, 257, 256
  8,  19,  20, 258, 257
  9,  20,  21, 259, 258
 10,  21,  22, 260, 259
 11,  22,  23, 261, 260
 12,  23,  24, 262, 261
 13,  24,  25, 263, 262
 14,  25,  26, 264, 263
 15,  26,  27, 265, 264
 16,  27,  28, 266, 265
 17,  28,  29, 267, 266
 18,  29,  30, 268, 267
 19,  30,  31, 269, 268
 20,  31,  32, 270, 269
 21,  32,  33, 271, 270
 22,  33,  34, 272, 271
 23,  34,  35, 273, 272
 24,  35,  36, 274, 273
 25,  36,  37, 275, 274
 26,  37,  38, 276, 275
 27,  38,  39, 277, 276
 28,  39,  40, 278, 277
 29,  40,  41, 279, 278
 30,  41,  42, 280, 279
 31,  42,  43, 281, 280
 32,  43,  44, 282, 281
 33,  44,  45, 283, 282
 34,  45,  46, 284, 283
 35,  46,  47, 285, 284
 36,  47,  48, 286, 285
 37,  48,  49, 287, 286
 38,  49,  50, 288, 287
 39,  50,  51, 289, 288
 40,  51,  52, 290, 289
 41,  52,  53, 291, 290
 42,  53,  54, 292, 291
 43,  54,  55, 293, 292
 44,  55,  56, 294, 293
 45,  56,  57, 295, 294
 46,  57,  58, 296, 295
 47,  58,  59, 297, 296
 48,  59,  60, 298, 297
 49,  60,  61, 299, 298
 50,  61,  62, 300, 299
 51,  62,  63, 301, 300
 52,  63,  64, 302, 301
 53,  64,  65, 303, 302
 54,  65,  66, 304, 303
 55,  66,  67, 305, 304
 56,  67,  68, 306, 305
 57,  68,  69, 307, 306
 58,  69,  70, 308, 307
 59,  70,  71, 309, 308
 60,  71,   2,  72, 309
 61, 134, 251, 310, 133
 62, 251, 252, 311, 310
 63, 252, 253, 312, 311
 64, 253, 254, 313, 312
 65, 254, 255, 314, 313
 66, 255, 256, 315, 314
```

67, 256, 257, 316, 315
68, 257, 258, 317, 316
69, 258, 259, 318, 317
70, 259, 260, 319, 318
71, 260, 261, 320, 319
72, 261, 262, 321, 320
73, 262, 263, 322, 321
74, 263, 264, 323, 322
75, 264, 265, 324, 323
76, 265, 266, 325, 324
77, 266, 267, 326, 325
78, 267, 268, 327, 326
79, 268, 269, 328, 327
80, 269, 270, 329, 328
81, 270, 271, 330, 329
82, 271, 272, 331, 330
83, 272, 273, 332, 331
84, 273, 274, 333, 332
85, 274, 275, 334, 333
86, 275, 276, 335, 334
87, 276, 277, 336, 335
88, 277, 278, 337, 336
89, 278, 279, 338, 337
90, 279, 280, 339, 338
91, 280, 281, 340, 339
92, 281, 282, 341, 340
93, 282, 283, 342, 341
94, 283, 284, 343, 342
95, 284, 285, 344, 343
96, 285, 286, 345, 344
97, 286, 287, 346, 345
98, 287, 288, 347, 346
99, 288, 289, 348, 347
100, 289, 290, 349, 348
101, 290, 291, 350, 349
102, 291, 292, 351, 350
103, 292, 293, 352, 351
104, 293, 294, 353, 352
105, 294, 295, 354, 353
106, 295, 296, 355, 354
107, 296, 297, 356, 355
108, 297, 298, 357, 356
109, 298, 299, 358, 357
110, 299, 300, 359, 358
111, 300, 301, 360, 359
112, 301, 302, 361, 360
113, 302, 303, 362, 361
114, 303, 304, 363, 362
115, 304, 305, 364, 363
116, 305, 306, 365, 364
117, 306, 307, 366, 365
118, 307, 308, 367, 366
119, 308, 309, 368, 367
120, 309, 72, 73, 368
121, 133, 310, 132, 4
122, 310, 311, 131, 132
123, 311, 312, 130, 131
124, 312, 313, 129, 130
125, 313, 314, 128, 129
126, 314, 315, 127, 128
127, 315, 316, 126, 127
128, 316, 317, 125, 126
129, 317, 318, 124, 125
130, 318, 319, 123, 124
131, 319, 320, 122, 123
132, 320, 321, 121, 122
133, 321, 322, 120, 121
134, 322, 323, 119, 120
135, 323, 324, 118, 119
136, 324, 325, 117, 118
137, 325, 326, 116, 117
138, 326, 327, 115, 116
139, 327, 328, 114, 115
140, 328, 329, 113, 114
141, 329, 330, 112, 113
142, 330, 331, 111, 112
143, 331, 332, 110, 111
144, 332, 333, 109, 110
145, 333, 334, 108, 109
146, 334, 335, 107, 108
147, 335, 336, 106, 107
148, 336, 337, 105, 106
149, 337, 338, 104, 105
150, 338, 339, 103, 104
151, 339, 340, 102, 103
152, 340, 341, 101, 102
153, 341, 342, 100, 101
154, 342, 343, 99, 100
155, 343, 344, 98, 99
156, 344, 345, 97, 98
157, 345, 346, 96, 97
158, 346, 347, 95, 96
159, 347, 348, 94, 95
160, 348, 349, 93, 94
161, 349, 350, 92, 93
162, 350, 351, 91, 92
163, 351, 352, 90, 91
164, 352, 353, 89, 90
165, 353, 354, 88, 89
166, 354, 355, 87, 88
167, 355, 356, 86, 87
168, 356, 357, 85, 86
169, 357, 358, 84, 85
170, 358, 359, 83, 84
171, 359, 360, 82, 83
172, 360, 361, 81, 82
173, 361, 362, 80, 81
174, 362, 363, 79, 80
175, 363, 364, 78, 79
176, 364, 365, 77, 78
177, 365, 366, 76, 77
178, 366, 367, 75, 76
179, 367, 368, 74, 75
180, 368, 73, 3, 74
181, 5, 135, 369, 200
182, 135, 136, 370, 369
183, 136, 137, 371, 370
184, 137, 138, 372, 371
185, 138, 139, 373, 372
186, 139, 140, 374, 373
187, 140, 141, 375, 374
188, 141, 142, 376, 375
189, 142, 143, 377, 376
190, 143, 6, 378, 377
191, 6, 144, 379, 378
192, 144, 145, 380, 379
193, 145, 146, 381, 380
194, 146, 147, 382, 381
195, 147, 148, 383, 382
196, 148, 149, 384, 383
197, 149, 150, 385, 384
198, 150, 151, 386, 385
199, 151, 152, 387, 386
200, 152, 153, 388, 387
201, 153, 154, 389, 388
202, 154, 155, 390, 389
203, 155, 156, 391, 390
204, 156, 157, 392, 391
205, 157, 7, 393, 392
206, 7, 158, 394, 393
207, 158, 159, 395, 394
208, 159, 160, 396, 395

209, 160, 161, 397, 396
210, 161, 162, 398, 397
211, 162, 163, 399, 398
212, 163, 164, 400, 399
213, 164, 165, 401, 400
214, 165, 166, 402, 401
215, 166, 1, 134, 402
216, 200, 369, 403, 199
217, 369, 370, 404, 403
218, 370, 371, 405, 404
219, 371, 372, 406, 405
220, 372, 373, 407, 406
221, 373, 374, 408, 407
222, 374, 375, 409, 408
223, 375, 376, 410, 409
224, 376, 377, 411, 410
225, 377, 378, 412, 411
226, 378, 379, 413, 412
227, 379, 380, 414, 413
228, 380, 381, 415, 414
229, 381, 382, 416, 415
230, 382, 383, 417, 416
231, 383, 384, 418, 417
232, 384, 385, 419, 418
233, 385, 386, 420, 419
234, 386, 387, 421, 420
235, 387, 388, 422, 421
236, 388, 389, 423, 422
237, 389, 390, 424, 423
238, 390, 391, 425, 424
239, 391, 392, 426, 425
240, 392, 393, 427, 426
241, 393, 394, 428, 427
242, 394, 395, 429, 428
243, 395, 396, 430, 429
244, 396, 397, 431, 430
245, 397, 398, 432, 431
246, 398, 399, 433, 432
247, 399, 400, 434, 433
248, 400, 401, 435, 434
249, 401, 402, 436, 435
250, 402, 134, 133, 436
251, 199, 403, 175, 10
252, 403, 404, 174, 175
253, 404, 405, 173, 174
254, 405, 406, 172, 173
255, 406, 407, 171, 172
256, 407, 408, 170, 171
257, 408, 409, 169, 170
258, 409, 410, 168, 169
259, 410, 411, 167, 168
260, 411, 412, 8, 167
261, 412, 413, 189, 8
262, 413, 414, 188, 189
263, 414, 415, 187, 188
264, 415, 416, 186, 187
265, 416, 417, 185, 186
266, 417, 418, 184, 185
267, 418, 419, 183, 184
268, 419, 420, 182, 183
269, 420, 421, 181, 182
270, 421, 422, 180, 181
271, 422, 423, 179, 180
272, 423, 424, 178, 179
273, 424, 425, 177, 178
274, 425, 426, 176, 177
275, 426, 427, 9, 176
276, 427, 428, 198, 9
277, 428, 429, 197, 198
278, 429, 430, 196, 197
279, 430, 431, 195, 196
280, 431, 432, 194, 195
281, 432, 433, 193, 194
282, 433, 434, 192, 193
283, 434, 435, 191, 192
284, 435, 436, 190, 191
285, 436, 133, 4, 190
286, 11, 201, 437, 250
287, 201, 202, 438, 437
288, 202, 203, 439, 438
289, 203, 204, 440, 439
290, 204, 205, 441, 440
291, 205, 206, 442, 441
292, 206, 207, 443, 442
293, 207, 208, 444, 443
294, 208, 209, 445, 444
295, 209, 210, 446, 445
296, 210, 211, 447, 446
297, 211, 212, 448, 447
298, 212, 213, 449, 448
299, 213, 214, 450, 449
300, 214, 215, 451, 450
301, 215, 216, 452, 451
302, 216, 217, 453, 452
303, 217, 218, 454, 453
304, 218, 219, 455, 454
305, 219, 220, 456, 455
306, 220, 221, 457, 456
307, 221, 222, 458, 457
308, 222, 223, 459, 458
309, 223, 224, 460, 459
310, 224, 5, 200, 460
311, 250, 437, 461, 249
312, 437, 438, 462, 461
313, 438, 439, 463, 462
314, 439, 440, 464, 463
315, 440, 441, 465, 464
316, 441, 442, 466, 465
317, 442, 443, 467, 466
318, 443, 444, 468, 467
319, 444, 445, 469, 468
320, 445, 446, 470, 469
321, 446, 447, 471, 470
322, 447, 448, 472, 471
323, 448, 449, 473, 472
324, 449, 450, 474, 473
325, 450, 451, 475, 474
326, 451, 452, 476, 475
327, 452, 453, 477, 476
328, 453, 454, 478, 477
329, 454, 455, 479, 478
330, 455, 456, 480, 479
331, 456, 457, 481, 480
332, 457, 458, 482, 481
333, 458, 459, 483, 482
334, 459, 460, 484, 483
335, 460, 200, 199, 484
336, 249, 461, 248, 12
337, 461, 462, 247, 248
338, 462, 463, 246, 247
339, 463, 464, 245, 246
340, 464, 465, 244, 245
341, 465, 466, 243, 244
342, 466, 467, 242, 243
343, 467, 468, 241, 242
344, 468, 469, 240, 241
345, 469, 470, 239, 240
346, 470, 471, 238, 239
347, 471, 472, 237, 238
348, 472, 473, 236, 237
349, 473, 474, 235, 236
350, 474, 475, 234, 235

```
351, 475, 476, 233, 234
352, 476, 477, 232, 233
353, 477, 478, 231, 232
354, 478, 479, 230, 231
355, 479, 480, 229, 230
356, 480, 481, 228, 229
357, 481, 482, 227, 228
358, 482, 483, 226, 227
359, 483, 484, 225, 226
360, 484, 199,  10, 225
*Nset, nset=_PICKEDSET22, internal, generate
   1,  484,    1
*Elset, elset=_PICKEDSET22, internal,
generate
   1,  360,    1
** Section: coat
*Solid Section, elset=_PICKEDSET22,
material=COAT
,
*End Part
**
*Part, name=INTERLAY
*Node
      1,           0., 0.0915198326
      2,           0.,          2.
      5, 0.0898383558, 0.0174628068
      6, 0.0595404506, 0.0115734907
      7,           0., 0.0606548488
     11,           1.,  0.194380313
     13,           0.,  0.104273289
     14,           0.,  0.117379434
     15,           0.,   0.13084802
     16,           0.,  0.144689053
     17,           0.,  0.158912867
     18,           0.,  0.173530012
     19,           0.,  0.188551381
     20,           0.,  0.203988165
     21,           0.,  0.219851822
     22,           0.,  0.236154184
     23,           0.,  0.252907366
     24,           0.,  0.270123839
     25,           0.,  0.287816435
     26,           0.,  0.305998296
     27,           0.,  0.324682951
     28,           0.,  0.343884319
     29,           0.,  0.363616705
     30,           0.,  0.383894742
     31,           0.,  0.404733539
     32,           0.,  0.426148653
     33,           0.,  0.448155969
     34,           0.,  0.470771849
     35,           0.,   0.49401319
     36,           0.,  0.517897189
     37,           0.,  0.542441726
     38,           0.,   0.56766504
     39,           0.,  0.593585849
     40,           0.,  0.620223463
     41,           0.,   0.64759773
     42,           0.,  0.675729036
     43,           0.,  0.704638243
     44,           0.,  0.734346926
     45,           0.,   0.7648772
     46,           0.,  0.796251714
     47,           0.,  0.828493893
     48,           0.,  0.861627638
     49,           0.,  0.895677745
     50,           0.,  0.930669427
     51,           0.,   0.96662879
     52,           0.,    1.0035826
     53,           0.,   1.04155827
     54,           0.,   1.08058417
     55,           0.,   1.12068927
     56,           0.,    1.1619035
     57,           0.,   1.20425749
     58,           0.,   1.24778259
     59,           0.,   1.29251146
     60,           0.,   1.33847725
     61,           0.,   1.38571417
     62,           0.,   1.43425739
     63,           0.,   1.48414302
     64,           0.,   1.53540814
     65,           0.,   1.58809102
     66,           0.,   1.64223075
     67,           0.,   1.69786763
     68,           0.,   1.75504327
     69,           0.,   1.81379986
     70,           0.,   1.87418139
     71,           0.,   1.93623269
    135, 0.0868085623, 0.0168738756
    136, 0.0837787762, 0.0162849445
    137, 0.0807489827, 0.0156960133
    138, 0.0777191967, 0.0151070813
    139, 0.0746894032, 0.0145181492
    140, 0.0716596097, 0.0139292181
    141, 0.0686298236,  0.013340286
    142, 0.0656000301, 0.0127513539
    143, 0.0625702441, 0.0121624228
    144, 0.0537199304, 0.0107934205
    145, 0.0478480905, 0.0107011786
    146, 0.0420059413, 0.0112980371
    147, 0.0362740643, 0.0125757623
    148, 0.0307315364,  0.014516728
    149, 0.0254548118, 0.0170941595
    150, 0.0205166843, 0.0202725027
    151,  0.015985271, 0.0240079109
    152,  0.011923085, 0.0282488558
    153, 0.00838616118, 0.0329368338
    154, 0.00542329205, 0.0380071774
    155, 0.00307534891, 0.0433899388
    156, 0.00137472153, 0.0490108691
    157, 0.000344869739, 0.0547924228
    158,           0., 0.0637413487
    159,           0., 0.0668278486
    160,           0., 0.0699143484
    161,           0., 0.0730008408
    162,           0., 0.0760873407
    163,           0., 0.0791738406
    164,           0., 0.0822603405
    165,           0., 0.0853468403
    166,           0., 0.0884333327
    201,  0.927385151,  0.180265412
    202,  0.859480202,  0.167066023
    203,  0.795979619,  0.154722765
    204,  0.736597717,  0.143180087
    205,  0.681067348,  0.132386088
    206,  0.629138768,  0.122292183
    207,  0.580578268,  0.112852991
    208,  0.535167515,  0.104026027
    209,  0.492702097, 0.0957715809
    210,  0.452991009, 0.0880525336
    211,  0.415855646, 0.0808341503
    212,  0.381128907, 0.0740839541
    213,  0.348654568, 0.0677715838
    214,  0.318286538, 0.0618686341
    215,  0.289888203, 0.0563485585
    216,  0.263331801, 0.0511865169
    217,  0.238497883, 0.0463592932
    218,  0.215274706, 0.0418451652
    219,  0.193557799, 0.0376238264
    220,  0.173249483,  0.033676289
    221,   0.15425837,  0.029984789
    222,  0.136499047, 0.0265327264
```

```
 223,  0.119891599, 0.0233045649
 224,  0.104361326, 0.0202857871
1001,           0., 0.0915198326
1002,           0.,          2.
1005, 0.0898383558, 0.0174628068
1006, 0.0595404506, 0.0115734907
1007,           0., 0.0606548488
1011,           1.,  0.194380313
1013,           0.,  0.104273289
1014,           0.,  0.117379434
1015,           0.,   0.13084802
1016,           0.,  0.144689053
1017,           0.,  0.158912867
1018,           0.,  0.173530012
1019,           0.,  0.188551381
1020,           0.,  0.203988165
1021,           0.,  0.219851822
1022,           0.,  0.236154184
1023,           0.,  0.252907366
1024,           0.,  0.270123839
1025,           0.,  0.287816435
1026,           0.,  0.305998296
1027,           0.,  0.324682951
1028,           0.,  0.343884319
1029,           0.,  0.363616705
1030,           0.,  0.383894742
1031,           0.,  0.404733539
1032,           0.,  0.426148653
1033,           0.,  0.448155969
1034,           0.,  0.470771849
1035,           0.,   0.49401319
1036,           0.,  0.517897189
1037,           0.,  0.542441726
1038,           0.,   0.56766504
1039,           0.,  0.593585849
1040,           0.,  0.620223463
1041,           0.,   0.64759773
1042,           0.,  0.675729036
1043,           0.,  0.704638243
1044,           0.,  0.734346926
1045,           0.,    0.7648772
1046,           0.,  0.796251714
1047,           0.,  0.828493893
1048,           0.,  0.861627638
1049,           0.,  0.895677745
1050,           0.,  0.930669427
1051,           0.,   0.96662879
1052,           0.,    1.0035826
1053,           0.,   1.04155827
1054,           0.,   1.08058417
1055,           0.,   1.12068927
1056,           0.,    1.1619035
1057,           0.,   1.20425749
1058,           0.,   1.24778259
1059,           0.,   1.29251146
1060,           0.,   1.33847725
1061,           0.,   1.38571417
1062,           0.,   1.43425739
1063,           0.,   1.48414302
1064,           0.,   1.53540814
1065,           0.,   1.58809102
1066,           0.,   1.64223075
1067,           0.,   1.69786763
1068,           0.,   1.75504327
1069,           0.,   1.81379986
1070,           0.,   1.87418139
1071,           0.,   1.93623269
1135, 0.0868085623, 0.0168738756
1136, 0.0837787762, 0.0162849445
1137, 0.0807489827, 0.0156960133
1138, 0.0777191967, 0.0151070813
1139, 0.0746894032, 0.0145181492
1140, 0.0716596097, 0.0139292181
1141, 0.0686298236,  0.013340286
1142, 0.0656000301, 0.0127513539
1143, 0.0625702441, 0.0121624228
1144, 0.0537199304, 0.0107934205
1145, 0.0478480905, 0.0107011786
1146, 0.0420059413, 0.0112980371
1147, 0.0362740643, 0.0125757623
1148, 0.0307315364,  0.014516728
1149, 0.0254548118, 0.0170941595
1150, 0.0205166843, 0.0202725027
1151,  0.015985271, 0.0240079109
1152,  0.011923085, 0.0282488558
1153, 0.00838616118, 0.0329368338
1154, 0.00542329205, 0.0380071774
1155, 0.00307534891, 0.0433899388
1156, 0.00137472153, 0.0490108691
1157, 0.000344869739, 0.0547924228
1158,           0., 0.0637413487
1159,           0., 0.0668278486
1160,           0., 0.0699143484
1161,           0., 0.0730008408
1162,           0., 0.0760873407
1163,           0., 0.0791738406
1164,           0., 0.0822603405
1165,           0., 0.0853468403
1166,           0., 0.0884333327
1201,  0.927385151,  0.180265412
1202,  0.859480202,  0.167066023
1203,  0.795979619,  0.154722765
1204,  0.736597717,  0.143180087
1205,  0.681067348,  0.132386088
1206,  0.629138768,  0.122292183
1207,  0.580578268,  0.112852991
1208,  0.535167515,  0.104026027
1209,  0.492702097, 0.0957715809
1210,  0.452991009, 0.0880525336
1211,  0.415855646, 0.0808341503
1212,  0.381128907, 0.0740839541
1213,  0.348654568, 0.0677715838
1214,  0.318286538, 0.0618686341
1215,  0.289888203, 0.0563485585
1216,  0.263331801, 0.0511865169
1217,  0.238497883, 0.0463592932
1218,  0.215274706, 0.0418451652
1219,  0.193557799, 0.0376238264
1220,  0.173249483,  0.033676289
1221,   0.15425837,  0.029984789
1222,  0.136499047, 0.0265327264
1223,  0.119891599, 0.0233045649
1224,  0.104361326, 0.0202857871
*Element, type=COH2D4
  1,   71,    2, 1002, 1071
  2,   70,   71, 1071, 1070
  3,   69,   70, 1070, 1069
  4,   68,   69, 1069, 1068
  5,   67,   68, 1068, 1067
  6,   66,   67, 1067, 1066
  7,   65,   66, 1066, 1065
  8,   64,   65, 1065, 1064
  9,   63,   64, 1064, 1063
 10,   62,   63, 1063, 1062
 11,   61,   62, 1062, 1061
 12,   60,   61, 1061, 1060
 13,   59,   60, 1060, 1059
 14,   58,   59, 1059, 1058
 15,   57,   58, 1058, 1057
 16,   56,   57, 1057, 1056
 17,   55,   56, 1056, 1055
 18,   54,   55, 1055, 1054
```

```
19,   53,   54, 1054, 1053
20,   52,   53, 1053, 1052
21,   51,   52, 1052, 1051
22,   50,   51, 1051, 1050
23,   49,   50, 1050, 1049
24,   48,   49, 1049, 1048
25,   47,   48, 1048, 1047
26,   46,   47, 1047, 1046
27,   45,   46, 1046, 1045
28,   44,   45, 1045, 1044
29,   43,   44, 1044, 1043
30,   42,   43, 1043, 1042
31,   41,   42, 1042, 1041
32,   40,   41, 1041, 1040
33,   39,   40, 1040, 1039
34,   38,   39, 1039, 1038
35,   37,   38, 1038, 1037
36,   36,   37, 1037, 1036
37,   35,   36, 1036, 1035
38,   34,   35, 1035, 1034
39,   33,   34, 1034, 1033
40,   32,   33, 1033, 1032
41,   31,   32, 1032, 1031
42,   30,   31, 1031, 1030
43,   29,   30, 1030, 1029
44,   28,   29, 1029, 1028
45,   27,   28, 1028, 1027
46,   26,   27, 1027, 1026
47,   25,   26, 1026, 1025
48,   24,   25, 1025, 1024
49,   23,   24, 1024, 1023
50,   22,   23, 1023, 1022
51,   21,   22, 1022, 1021
52,   20,   21, 1021, 1020
53,   19,   20, 1020, 1019
54,   18,   19, 1019, 1018
55,   17,   18, 1018, 1017
56,   16,   17, 1017, 1016
57,   15,   16, 1016, 1015
58,   14,   15, 1015, 1014
59,   13,   14, 1014, 1013
60,    1,   13, 1013, 1001
61,  166,    1, 1001, 1166
62,  165,  166, 1166, 1165
63,  164,  165, 1165, 1164
64,  163,  164, 1164, 1163
65,  162,  163, 1163, 1162
66,  161,  162, 1162, 1161
67,  160,  161, 1161, 1160
68,  159,  160, 1160, 1159
69,  158,  159, 1159, 1158
70,    7,  158, 1158, 1007
71,  157,    7, 1007, 1157
72,  156,  157, 1157, 1156
73,  155,  156, 1156, 1155
74,  154,  155, 1155, 1154
75,  153,  154, 1154, 1153
76,  152,  153, 1153, 1152
77,  151,  152, 1152, 1151
78,  150,  151, 1151, 1150
79,  149,  150, 1150, 1149
80,  148,  149, 1149, 1148
81,  147,  148, 1148, 1147
82,  146,  147, 1147, 1146
83,  145,  146, 1146, 1145
84,  144,  145, 1145, 1144
85,    6,  144, 1144, 1006
86,  143,    6, 1006, 1143
87,  142,  143, 1143, 1142
88,  141,  142, 1142, 1141
89,  140,  141, 1141, 1140
90,  139,  140, 1140, 1139
91,  138,  139, 1139, 1138
92,  137,  138, 1138, 1137
93,  136,  137, 1137, 1136
94,  135,  136, 1136, 1135
95,    5,  135, 1135, 1005
96,  224,    5, 1005, 1224
97,  223,  224, 1224, 1223
98,  222,  223, 1223, 1222
99,  221,  222, 1222, 1221
100, 220,  221, 1221, 1220
101, 219,  220, 1220, 1219
102, 218,  219, 1219, 1218
103, 217,  218, 1218, 1217
104, 216,  217, 1217, 1216
105, 215,  216, 1216, 1215
106, 214,  215, 1215, 1214
107, 213,  214, 1214, 1213
108, 212,  213, 1213, 1212
109, 211,  212, 1212, 1211
110, 210,  211, 1211, 1210
111, 209,  210, 1210, 1209
112, 208,  209, 1209, 1208
113, 207,  208, 1208, 1207
114, 206,  207, 1207, 1206
115, 205,  206, 1206, 1205
116, 204,  205, 1205, 1204
117, 203,  204, 1204, 1203
118, 202,  203, 1203, 1202
119, 201,  202, 1202, 1201
120,  11,  201, 1201, 1011
*Nset, nset=_PICKEDSET2, internal
    1,    2,    5,    6,    7,   11,   13,
14,   15,   16,   17,   18,   19,   20,
21,   22
   23,   24,   25,   26,   27,   28,   29,
30,   31,   32,   33,   34,   35,   36,
37,   38
   39,   40,   41,   42,   43,   44,   45,
46,   47,   48,   49,   50,   51,   52,
53,   54
   55,   56,   57,   58,   59,   60,   61,
62,   63,   64,   65,   66,   67,   68,
69,   70
   71,  135,  136,  137,  138,  139,  140,
141,  142,  143,  144,  145,  146,  147,
148,  149
  150,  151,  152,  153,  154,  155,  156,
157,  158,  159,  160,  161,  162,  163,
164,  165
  166,  201,  202,  203,  204,  205,  206,
207,  208,  209,  210,  211,  212,  213,
214,  215
  216,  217,  218,  219,  220,  221,  222,
223,  224, 1001, 1002, 1005, 1006, 1007,
1011, 1013
 1014, 1015, 1016, 1017, 1018, 1019, 1020,
1021, 1022, 1023, 1024, 1025, 1026, 1027,
1028, 1029
 1030, 1031, 1032, 1033, 1034, 1035, 1036,
1037, 1038, 1039, 1040, 1041, 1042, 1043,
1044, 1045
 1046, 1047, 1048, 1049, 1050, 1051, 1052,
1053, 1054, 1055, 1056, 1057, 1058, 1059,
1060, 1061
 1062, 1063, 1064, 1065, 1066, 1067, 1068,
1069, 1070, 1071, 1135, 1136, 1137, 1138,
1139, 1140
 1141, 1142, 1143, 1144, 1145, 1146, 1147,
1148, 1149, 1150, 1151, 1152, 1153, 1154,
1155, 1156
```

```
 1157, 1158, 1159, 1160, 1161, 1162, 1163,
1164, 1165, 1166, 1201, 1202, 1203, 1204,
1205, 1206
 1207, 1208, 1209, 1210, 1211, 1212, 1213,
1214, 1215, 1216, 1217, 1218, 1219, 1220,
1221, 1222
 1223, 1224
*Elset, elset=_PICKEDSET2, internal,
generate
   1,  120,    1
*Elset, elset=_PickedSet4, internal,
generate
   1,  120,    1
** Section: cohesive
*Cohesive Section, elset=_PickedSet4,
material=COHESIVE, response=TRACTION
SEPARATION
,
*End Part
**
*Part, name=SUB
*Node
      1,           0., 0.0915198326
      2, 0.0754431263, 0.0915198326
      3, 0.0898383558, 0.0174628068
      4,           1.,  0.194380313
      5,           1.,           2.
      6,           0.,           2.
      7,           0., 0.0606548488
      8, 0.0595404506, 0.0115734907
      9, 0.00301772519, 0.0915198326
     10, 0.00603545038, 0.0915198326
     11, 0.00905317534, 0.0915198326
     12, 0.0120709008, 0.0915198326
     13, 0.0150886262, 0.0915198326
     14, 0.0181063507, 0.0915198326
     15, 0.0211240761, 0.0915198326
     16, 0.0241418015, 0.0915198326
     17, 0.0271595269, 0.0915198326
     18, 0.0301772524, 0.0915198326
     19, 0.0331949778, 0.0915198326
     20, 0.0362127014, 0.0915198326
     21, 0.0392304286, 0.0915198326
     22, 0.0422481522, 0.0915198326
     23, 0.0452658758, 0.0915198326
     24,  0.048283603, 0.0915198326
     25, 0.0513013266, 0.0915198326
     26, 0.0543190539, 0.0915198326
     27, 0.0573367774, 0.0915198326
     28, 0.0603545047, 0.0915198326
     29, 0.0633722246, 0.0915198326
     30, 0.0663899556, 0.0915198326
     31, 0.0694076791, 0.0915198326
     32, 0.0724254027, 0.0915198326
     33, 0.0760429278, 0.0884341225
     34, 0.0766427293, 0.0853484124
     35, 0.0772425309, 0.0822627023
     36, 0.0778423324, 0.0791769922
     37,  0.078442134, 0.0760912895
     38, 0.0790419355, 0.0730055794
     39,  0.079641737, 0.0699198693
     40, 0.0802415386, 0.0668341592
     41, 0.0808413401, 0.0637484491
     42, 0.0814411417,  0.060662739
     43, 0.0820409432, 0.0575770289
     44, 0.0826407447, 0.0544913188
     45, 0.0832405463, 0.0514056124
     46, 0.0838403478, 0.0483199023
     47, 0.0844401494, 0.0452341922
     48, 0.0850399509, 0.0421484821
     49,  0.085639745, 0.0390627719
     50, 0.0862395465, 0.0359770656
     51, 0.0868393481, 0.0328913555
     52, 0.0874391496, 0.0298056453
     53, 0.0880389512, 0.0267199352
     54, 0.0886387527,  0.023634227
     55, 0.0892385542, 0.0205485169
     56,  0.104361326, 0.0202857871
     57,  0.119891599, 0.0233045649
     58,  0.136499047, 0.0265327264
     59,   0.15425837,  0.029984789
     60,  0.173249483,  0.033676289
     61,  0.193557799, 0.0376238264
     62,  0.215274706, 0.0418451652
     63,  0.238497883, 0.0463592932
     64,  0.263331801, 0.0511865169
     65,  0.289888203, 0.0563485585
     66,  0.318286538, 0.0618686341
     67,  0.348654568, 0.0677715838
     68,  0.381128907, 0.0740839541
     69,  0.415855646, 0.0808341503
     70,  0.452991009, 0.0880525336
     71,  0.492702097, 0.0957715809
     72,  0.535167515,  0.104026027
     73,  0.580578268,  0.112852991
     74,  0.629138768,  0.122292183
     75,  0.681067348,  0.132386088
     76,  0.736597717,  0.143180087
     77,  0.795979619,  0.154722765
     78,  0.859480202,  0.167066023
     79,  0.927385151,  0.180265412
     80,           1.,  0.276297897
     81,           1.,  0.366819412
     82,           1.,  0.466848522
     83,           1.,  0.577383876
     84,           1.,  0.699528873
     85,           1.,  0.834502995
     86,           1.,  0.983653605
     87,           1.,   1.14846981
     88,           1.,    1.3305968
     89,           1.,   1.53185296
     90,           1.,   1.75424719
     91,  0.796878636,           2.
     92,  0.623260379,           2.
     93,  0.474859923,           2.
     94,  0.348014444,           2.
     95,  0.239593074,           2.
     96,  0.146919757,           2.
     97, 0.0677071214,           2.
     98,           0.,   1.93623269
     99,           0.,   1.87418139
    100,           0.,   1.81379986
    101,           0.,   1.75504327
    102,           0.,   1.69786763
    103,           0.,   1.64223075
    104,           0.,   1.58809102
    105,           0.,   1.53540814
    106,           0.,   1.48414302
    107,           0.,   1.43425739
    108,           0.,   1.38571417
    109,           0.,   1.33847725
    110,           0.,   1.29251146
    111,           0.,   1.24778259
    112,           0.,   1.20425749
    113,           0.,    1.1619035
    114,           0.,   1.12068927
    115,           0.,   1.08058417
    116,           0.,   1.04155827
    117,           0.,    1.0035826
    118,           0.,   0.96662879
    119,           0.,  0.930669427
    120,           0.,  0.895677745
```

```
121,            0.,  0.861627638
122,            0.,  0.828493893
123,            0.,  0.796251714
124,            0.,    0.7648772
125,            0.,  0.734346926
126,            0.,  0.704638243
127,            0.,  0.675729036
128,            0.,   0.64759773
129,            0.,  0.620223463
130,            0.,  0.593585849
131,            0.,   0.56766504
132,            0.,  0.542441726
133,            0.,  0.517897189
134,            0.,   0.49401319
135,            0.,  0.470771849
136,            0.,  0.448155969
137,            0.,  0.426148653
138,            0.,  0.404733539
139,            0.,  0.383894742
140,            0.,  0.363616705
141,            0.,  0.343884319
142,            0.,  0.324682951
143,            0.,  0.305998296
144,            0.,  0.287816435
145,            0.,  0.270123839
146,            0.,  0.252907366
147,            0.,  0.236154184
148,            0.,  0.219851822
149,            0.,  0.203988165
150,            0.,  0.188551381
151,            0.,  0.173530012
152,            0.,  0.158912867
153,            0.,  0.144689053
154,            0.,   0.13084802
155,            0.,  0.117379434
156,            0.,  0.104273289
157,            0., 0.0884333327
158,            0., 0.0853468403
159,            0., 0.0822603405
160,            0., 0.0791738406
161,            0., 0.0760873407
162,            0., 0.0730008408
163,            0., 0.0699143484
164,            0., 0.0668278486
165,            0., 0.0637413487
166, 0.000344869739, 0.0547924228
167, 0.00137472153, 0.0490108691
168, 0.00307534891, 0.0433899388
169, 0.00542329205, 0.0380071774
170, 0.00838616118, 0.0329368338
171,  0.011923085, 0.0282488558
172,  0.015985271, 0.0240079109
173, 0.0205166843, 0.0202725027
174, 0.0254548118, 0.0170941595
175, 0.0307315364,  0.014516728
176, 0.0362740643, 0.0125757623
177, 0.0420059413, 0.0112980371
178, 0.0478480905, 0.0107011786
179, 0.0537199304, 0.0107934205
180, 0.0625702441, 0.0121624228
181, 0.0656000301, 0.0127513539
182, 0.0686298236,  0.013340286
183, 0.0716596097, 0.0139292181
184, 0.0746894032, 0.0145181492
185, 0.0777191967, 0.0151070813
186, 0.0807489827, 0.0156960133
187, 0.0837787762, 0.0162849445
188, 0.0868085623, 0.0168738756
189,  0.268075109,   1.03800631
190,  0.740786314,  0.546891332
191,  0.763528049,  0.321781725
192,  0.502114713,  0.264198393
193,  0.259578437,  0.268797189
194,  0.538158953,  0.506522536
195,  0.259330243,  0.515170097
196,  0.753887415,   1.12491238
197,  0.532808602,   1.04746449
198,  0.289557487,  0.776985288
199,  0.498335481,  0.779753804
200,  0.786760986,  0.854349136
201,  0.704917669,   1.26172876
202,  0.480125695,   1.22950196
203,  0.277329296,   1.21595252
204,  0.536315262,   1.52755558
205,  0.319081455,   1.51693213
206,  0.536469698,   1.83913422
207,   0.27804184,   1.74736989
208, 0.00501891226,  0.099185802
209,  0.878158391,  0.576815546
210,  0.886215746,  0.992092788
211, 0.0502873994,   1.64084125
212,  0.379649699,  0.105219483
213,  0.672059059,  0.188139692
214,   0.33980006,   1.90696168
215,  0.839057565,   1.78302193
216, 0.0468750037,   1.34232271
217,  0.035972517,   1.00591969
218, 0.0274981577,  0.706344724
219, 0.0189382955,  0.384997636
220, 0.0734192282, 0.0962303877
221, 0.0970056579, 0.0245713871
222, 0.0798145235, 0.0912826434
223,  0.174168274, 0.0503860638
224,  0.194043875, 0.0553842448
225,  0.215321198, 0.0610400029
226,  0.238192558,  0.067203939
227,  0.262738168, 0.0738079399
228,  0.288990736, 0.0808974057
229,  0.317237258, 0.0885329023
230,  0.347479582, 0.0966594294
231,  0.414122164,    0.1143445
232,  0.450790435,  0.123836458
233,  0.489682883,  0.133692071
234,  0.530923665,  0.144191891
235,  0.574768841,  0.156094745
236,  0.621758521,  0.170439661
237,  0.726893127,  0.210307971
238,  0.854139805,  0.252543986
239,  0.925398886,  0.266477764
240,  0.921195567,    0.3570337
241,  0.911559165,  0.455363363
242,  0.890559971,  0.714413047
243,  0.892238796,  0.847991168
244,  0.870167315,   1.15327704
245,  0.152088076,   1.93018055
246,  0.240978792,   1.92234087
247,  0.444103152,   1.88024557
248, 0.0121585298,  0.189742699
249, 0.0129812891,  0.205070123
250, 0.0137823168,  0.220886141
251, 0.0145317819,  0.237178266
252, 0.0152183147,  0.253944069
253, 0.0158380903,  0.271174937
254,  0.016408354,  0.288862079
255, 0.0169512443,  0.307060748
256, 0.0174699742,  0.325748175
257, 0.0179923214,  0.345003128
258, 0.0184992347,  0.364782512
259, 0.0194582734,  0.405850351
260, 0.0200026426,  0.427326441
261, 0.0205567833,  0.449389309
262, 0.0211389475,  0.472055972
```

263, 0.021752676, 0.495372266
264, 0.0223800987, 0.519338012
265, 0.0230129734, 0.543930411
266, 0.0236612167, 0.569144011
267, 0.0243846849, 0.595084965
268, 0.0251820907, 0.621834397
269, 0.0259878803, 0.649325132
270, 0.0267952085, 0.677544653
271, 0.0283747353, 0.736078262
272, 0.0293021128, 0.766699076
273, 0.0302100535, 0.798145533
274, 0.0310937464, 0.830391347
275, 0.0319935121, 0.86357981
276, 0.0328925624, 0.897619367
277, 0.0338855386, 0.932732224
278, 0.0349751897, 0.968909204
279, 0.0371244326, 1.0440383
280, 0.0383648835, 1.08322918
281, 0.0397662148, 1.12367737
282, 0.0412141681, 1.16518271
283, 0.0427044593, 1.20777118
284, 0.0442655347, 1.25171709
285, 0.0456835702, 1.29667246
286, 0.0480845682, 1.38942182
287, 0.0488703512, 1.4377811
288, 0.0491724014, 1.48712993
289, 0.0492384806, 1.53742182
290, 0.0491725095, 1.58868158
291, 0.0547853373, 1.69553006
292, 0.0612429865, 1.75163221
293, 0.0676563606, 1.81012249
294, 0.772033632, 0.62800467
295, 0.0979893357, 1.63775957
296, 0.0970245153, 1.39296424
297, 0.0823856592, 0.077280499
298, 0.0818542913, 0.080433473
299, 0.707255065, 1.78650975
300, 0.0773385689, 1.08515739
301, 0.0624912642, 0.831531405
302, 0.5647282, 0.197083801
303, 0.0489456765, 0.59594208
304, 0.00974659901, 0.0944601521
305, 0.0104395086, 0.10377942
306, 0.0123725375, 0.0951631293
307, 0.0154378284, 0.0955158249
308, 0.0184839163, 0.0955585837
309, 0.021613529, 0.0955236852
310, 0.0247676838, 0.0955825076
311, 0.0278543588, 0.095611982
312, 0.0308099352, 0.0955234021
313, 0.0336628295, 0.0953175873
314, 0.0365908965, 0.0951870456
315, 0.0395669155, 0.095504418
316, 0.0425379053, 0.0954696983
317, 0.0456442796, 0.0953491107
318, 0.048698131, 0.095229581
319, 0.0516941771, 0.0950519443
320, 0.0545456037, 0.0947900563
321, 0.0573735274, 0.0945982561
322, 0.0602283031, 0.0949750245
323, 0.0632072389, 0.0954777673
324, 0.0663931146, 0.0959079564
325, 0.0697207451, 0.0961932838
326, 0.0113618337, 0.174935728
327, 0.0825657845, 0.0740686432
328, 0.137141377, 0.0418949202
329, 0.0828485712, 0.0710037425
330, 0.0837596878, 0.0681926459
331, 0.0848620161, 0.0654233992
332, 0.0860609263, 0.0624878556
333, 0.0871833265, 0.0595212765
334, 0.0878065825, 0.0562132969
335, 0.120986149, 0.0364004262
336, 0.0882797465, 0.0527203232
337, 0.088772133, 0.0493629277
338, 0.0891501233, 0.0461883396
339, 0.0893376619, 0.0429815724
340, 0.089430362, 0.0398276076
341, 0.108150035, 0.0323496088
342, 0.0896081701, 0.0367546715
343, 0.0902953446, 0.0338178389
344, 0.0908121243, 0.0308743939
345, 0.0908152089, 0.0281340983
346, 0.0812486112, 0.0838047415
347, 0.0806157887, 0.0873662978
348, 0.155317277, 0.0461416431
349, 0.787704825, 0.235009775
350, 0.848970652, 1.57047558
351, 0.0727749541, 1.93390846
352, 0.14786914, 1.86299109
353, 0.00920661911, 0.110411182
354, 0.00904319342, 0.121003784
355, 0.0093383994, 0.13340117
356, 0.00992497336, 0.146695361
357, 0.0106226252, 0.160632715
358, 0.0329559222, 0.289389551
359, 0.0475933552, 0.57002914
360, 0.0660340115, 0.89882046
361, 0.0864192247, 1.2106849
362, 0.0996191651, 1.54016817
363, 0.122383863, 1.74152541
364, 0.834795058, 0.425961524
365, 0.777875125, 0.985913455
366, 0.107812412, 1.68831825
367, 0.286090016, 0.104627252
368, 0.399609506, 1.77558053
369, 0.0749612227, 1.04589021
370, 0.0570986532, 0.737089217
371, 0.0390861481, 0.406485289
372, 0.078183651, 0.0960121453
373, 0.193299025, 0.0729418322
374, 0.213880926, 0.079918921
375, 0.236235723, 0.0875868127
376, 0.260361612, 0.0958296582
377, 0.313968271, 0.114148572
378, 0.343821019, 0.124357164
379, 0.375676692, 0.135293826
380, 0.409724772, 0.146938145
381, 0.445860773, 0.159046516
382, 0.483819753, 0.171203539
383, 0.523432016, 0.183466092
384, 0.654421866, 0.237167537
385, 0.608510733, 0.214238986
386, 0.844646394, 0.339961857
387, 0.80505079, 0.504165113
388, 0.786374509, 0.734004021
389, 0.826093495, 1.35592771
390, 0.228844017, 1.8474344
391, 0.0261556879, 0.205611646
392, 0.0277139898, 0.221353084
393, 0.0291920211, 0.237632334
394, 0.0305576324, 0.254425555
395, 0.0318159536, 0.271699667
396, 0.0350703746, 0.326309383
397, 0.0340666845, 0.307625026
398, 0.0381264649, 0.385660052
399, 0.0361169726, 0.345586926
400, 0.0371567272, 0.365395099
401, 0.0401532166, 0.427994967
402, 0.0412623584, 0.450086921
403, 0.0424113572, 0.472776979
404, 0.0436375029, 0.496135682

405, 0.0449338034, 0.520147741
406, 0.0462996662, 0.544801116
407, 0.0505367517, 0.622742891
408, 0.0521864593, 0.650290132
409, 0.0554554984, 0.707433462
410, 0.0538873449, 0.678571165
411, 0.0589471199, 0.76774627
412, 0.0608233958, 0.799301207
413, 0.0643495098, 0.864843667
414, 0.0679705366, 0.933978975
415, 0.0701326281, 0.970225692
416, 0.0725989938, 1.00761437
417, 0.0803537294, 1.12600052
418, 0.0835789368, 1.16795254
419, 0.0948989391, 1.34602153
420, 0.0896758586, 1.25510883
421, 0.0925329775, 1.30027115
422, 0.098429203, 1.441571
423, 0.0990462378, 1.49062479
424, 0.0993336141, 1.58997178
425, 0.67238754, 0.969859362
426, 0.644372821, 1.08687782
427, 0.369074434, 0.163784355
428, 0.685428977, 0.8529073
429, 0.712548256, 1.61054277
430, 0.484057516, 1.71761072
431, 0.0116885006, 0.0990689695
432, 0.0220181905, 0.0993988141
433, 0.0872096643, 0.0783283859
434, 0.0931032673, 0.0576567799
435, 0.0937112048, 0.03983628
436, 0.034492936, 0.099367857
437, 0.052348081, 0.0987677872
438, 0.0594539493, 0.0985661894
439, 0.630483747, 0.276898682
440, 0.314198643, 1.81973743
441, 0.02301866, 0.175898269
442, 0.0858165845, 0.0816958323
443, 0.0834965631, 0.0986905843
444, 0.70391649, 0.269955873
445, 0.0245828927, 0.190491542
446, 0.0638436154, 0.472800791
447, 0.0890804306, 0.767909884
448, 0.140935227, 1.30370605
449, 0.681680799, 0.64878118
450, 0.606589019, 1.19641149
451, 0.182700813, 1.72201896
452, 0.149707764, 1.49478257
453, 0.0845708773, 0.0890414119
454, 0.513431191, 0.222620562
455, 0.0188461188, 0.0997652188
456, 0.0285608117, 0.100039348
457, 0.0395208672, 0.10046073
458, 0.0461497419, 0.0991303995
459, 0.0186695568, 0.124105625
460, 0.0551959872, 0.0982841253
461, 0.0573179498, 0.0972611234
462, 0.0193081405, 0.135740593
463, 0.0624882542, 0.0996387303
464, 0.0660063997, 0.100565627
465, 0.0696098655, 0.101146579
466, 0.0734452307, 0.101188235
467, 0.0862834901, 0.0744361952
468, 0.0855059326, 0.0718080699
469, 0.0870355889, 0.0701049641
470, 0.135992348, 0.0580313951
471, 0.0932776406, 0.0537667535
472, 0.118704364, 0.0474763475
473, 0.100006737, 0.0314917564
474, 0.0850865841, 0.0852189288
475, 0.0840968788, 0.0934840739
476, 0.174314082, 0.0669875145
477, 0.155858308, 0.0619111508
478, 0.0161131714, 0.105346709
479, 0.0492255576, 0.0990093425
480, 0.020331556, 0.148424923
481, 0.0215988029, 0.161967114
482, 0.0738375783, 0.596068144
483, 0.144212708, 1.35000312
484, 0.155686423, 1.59797013
485, 0.157915235, 1.67247152
486, 0.117614232, 1.08660674
487, 0.0943861902, 0.831921458
488, 0.0604950972, 0.428031385
489, 0.211025447, 0.0983573794
490, 0.232752278, 0.107267968
491, 0.281436145, 0.127294064
492, 0.256256372, 0.116894752
493, 0.308687657, 0.138457954
494, 0.337896347, 0.150538579
495, 0.402460277, 0.178174749
496, 0.437995106, 0.193588242
497, 0.475244969, 0.208804816
498, 0.551801264, 0.235898763
499, 0.591382682, 0.253128022
500, 0.762586236, 0.465180486
501, 0.685326993, 0.744711816
502, 0.0417622961, 0.221187353
503, 0.0439367592, 0.237447798
504, 0.0459631495, 0.254266441
505, 0.0478550047, 0.271535635
506, 0.0496258959, 0.289276034
507, 0.0528677776, 0.326237619
508, 0.0559346229, 0.365316182
509, 0.0513102934, 0.307502121
510, 0.0589751974, 0.406536043
511, 0.0544376895, 0.345500171
512, 0.0574941672, 0.385637373
513, 0.0621744432, 0.45012483
514, 0.0717591122, 0.570106506
515, 0.0656880513, 0.496145755
516, 0.0676526427, 0.520137072
517, 0.0697277561, 0.544797778
518, 0.0761998594, 0.622803926
519, 0.0786962509, 0.650323987
520, 0.0837580413, 0.707551956
521, 0.086491555, 0.737310529
522, 0.0812829658, 0.678618073
523, 0.0918729901, 0.799545944
524, 0.097110182, 0.86527586
525, 0.0997735709, 0.899390101
526, 0.102573819, 0.934453368
527, 0.105747841, 0.970630169
528, 0.10948278, 1.00812423
529, 0.113716587, 1.04695892
530, 0.122385912, 1.12773907
531, 0.127271399, 1.16982937
532, 0.132237136, 1.21338773
533, 0.146756485, 1.39732575
534, 0.137073249, 1.25847769
535, 0.148756281, 1.44635534
536, 0.150096267, 1.54366064
537, 0.136958718, 1.63572049
538, 0.0831480473, 0.449309915
539, 0.667309582, 0.31077987
540, 0.387373835, 1.5106318
541, 0.534285665, 1.41468894
542, 0.615420401, 1.76339805
543, 0.347855031, 1.69598246
544, 0.0900823846, 0.0731902942
545, 0.0330235921, 0.105184481
546, 0.0466342382, 0.102950014

547, 0.142103001, 0.0754004717
548, 0.196837768, 1.40197957
549, 0.159382373, 1.08705223
550, 0.126878485, 0.831385195
551, 0.0989431813, 0.595110357
552, 0.025125809, 0.104015931
553, 0.0186554547, 0.113543764
554, 0.0363863297, 0.103655875
555, 0.0650552437, 0.105568863
556, 0.0902795941, 0.0648659617
557, 0.0947634205, 0.0468655042
558, 0.107243434, 0.0411076695
559, 0.0942275524, 0.0349220596
560, 0.207894057, 1.78054476
561, 0.578984439, 0.946656466
562, 0.0371342748, 0.190598473
563, 0.359856635, 0.190097108
564, 0.697621644, 0.357885391
565, 0.0809778497, 0.427247822
566, 0.194533959, 1.3549279
567, 0.621876478, 1.35977077
568, 0.602046609, 0.648997068
569, 0.537974238, 0.273146957
570, 0.0348491184, 0.176382318
571, 0.0960431173, 0.569108248
572, 0.123429276, 0.798777401
573, 0.191183627, 1.30820954
574, 0.671043515, 0.56594038
575, 0.514346898, 1.15184891
576, 0.195398316, 1.58278906
577, 0.0887882859, 0.0863536447
578, 0.0309386887, 0.149686202
579, 0.0279743951, 0.126348034
580, 0.0777770653, 0.102239341
581, 0.0731845349, 0.105440699
582, 0.0917950496, 0.0700048506
583, 0.0973800793, 0.0545901321
584, 0.156932965, 0.0778539702
585, 0.191421956, 0.0903556719
586, 0.0884975791, 0.0947827697
587, 0.0223060176, 0.102687709
588, 0.0327536538, 0.162823901
589, 0.238687798, 1.69058514
590, 0.0789130777, 0.405741572
591, 0.206856266, 0.116097197
592, 0.250575274, 0.136822313
593, 0.227869034, 0.125979915
594, 0.301463574, 0.161201209
595, 0.27514261, 0.148457423
596, 0.329726905, 0.174861848
597, 0.392010063, 0.207069814
598, 0.463548839, 0.247137859
599, 0.426524282, 0.226429865
600, 0.572949886, 0.288328737
601, 0.716915429, 0.481112361
602, 0.581422091, 0.743074715
603, 0.0394528657, 0.205603138
604, 0.0557650067, 0.220263183
605, 0.0586351342, 0.236495316
606, 0.061355304, 0.253343165
607, 0.0639372319, 0.270595968
608, 0.0663828403, 0.288294733
609, 0.0686778277, 0.306516856
610, 0.0708236024, 0.325286716
611, 0.0728776082, 0.344586939
612, 0.0748867467, 0.364412338
613, 0.0769107863, 0.384770989
614, 0.0878607109, 0.495230943
615, 0.0932178348, 0.543757498
616, 0.0854719952, 0.471949071
617, 0.0904946253, 0.519130111
618, 0.102141872, 0.621718884
619, 0.108923651, 0.677456915
620, 0.112536125, 0.706432402
621, 0.11621853, 0.736266196
622, 0.105532929, 0.649172485
623, 0.119924314, 0.767034233
624, 0.130583853, 0.864880025
625, 0.134238973, 0.899106503
626, 0.137988046, 0.934089541
627, 0.142084703, 0.970067143
628, 0.147033304, 1.00749564
629, 0.153086364, 1.04665065
630, 0.166684046, 1.12855673
631, 0.173166007, 1.17080331
632, 0.179682791, 1.21526897
633, 0.186074391, 1.26147091
634, 0.20018205, 1.45183933
635, 0.199691668, 1.54656553
636, 0.233648241, 1.60860872
637, 0.198833987, 1.64412844
638, 0.554131389, 1.28205276
639, 0.419315279, 1.61119556
640, 0.628869712, 0.339314342
641, 0.435482323, 1.06169057
642, 0.397530407, 1.41325736
643, 0.0958313197, 0.071348533
644, 0.0290218238, 0.105214059
645, 0.0993432105, 0.0379428566
646, 0.103049032, 0.0472571477
647, 0.0531257838, 0.102605253
648, 0.0611388385, 0.103836633
649, 0.13209112, 0.07731691
650, 0.0918003097, 0.0819185898
651, 0.0696231127, 0.107601032
652, 0.124152273, 0.592818558
653, 0.202212095, 1.08540237
654, 0.160065219, 0.829696834
655, 0.0496831462, 0.190012187
656, 0.348218292, 0.21404098
657, 0.592876494, 0.847433209
658, 0.534612536, 0.630512893
659, 0.0526701324, 0.204802543
660, 0.101395205, 0.425525874
661, 0.11333698, 0.517045498
662, 0.179527104, 0.9685781
663, 0.304910928, 1.45550394
664, 0.319503427, 1.58466542
665, 0.107056886, 0.470143974
666, 0.0294095557, 0.137458652
667, 0.132438466, 0.6466223
668, 0.0230532233, 0.108662762
669, 0.0422278829, 0.104899727
670, 0.112514541, 0.055591166
671, 0.0957591757, 0.0670103878
672, 0.0466768108, 0.176140562
673, 0.292493254, 0.182227999
674, 0.658463717, 0.493987381
675, 0.0987851545, 0.404024333
676, 0.247574136, 1.36163557
677, 0.603958547, 0.570899606
678, 0.52883786, 0.305719405
679, 0.0414401218, 0.150310457
680, 0.0765421465, 0.10744974
681, 0.120393433, 0.566861093
682, 0.15555124, 0.796832323
683, 0.243651524, 1.31283212
684, 0.428107589, 1.12894094
685, 0.0271931235, 0.117644124
686, 0.0887677446, 0.10035973
687, 0.0438476689, 0.163016573
688, 0.0932032838, 0.0621518232

689, 0.188062459, 0.107087702
690, 0.171275735, 0.0991602316
691, 0.0924420655, 0.0866271704
692, 0.144112244, 0.08924485
693, 0.221654132, 0.143695861
694, 0.201429203, 0.13288556
695, 0.26722157, 0.168201044
696, 0.243664116, 0.155355215
697, 0.319537163, 0.197297335
698, 0.411130756, 0.255076915
699, 0.378524572, 0.232740819
700, 0.447397321, 0.283172816
701, 0.709774196, 0.417875081
702, 0.069553718, 0.218415126
703, 0.0731327683, 0.234645844
704, 0.0766557381, 0.251518846
705, 0.0801111758, 0.268645853
706, 0.0833510607, 0.286251694
707, 0.0862930417, 0.304508924
708, 0.0889671594, 0.323396951
709, 0.0914600417, 0.342789263
710, 0.0962842479, 0.383048087
711, 0.0938726589, 0.362647116
712, 0.116808586, 0.54151541
713, 0.104177468, 0.447517544
714, 0.110144056, 0.49327001
715, 0.136958882, 0.674808681
716, 0.141615137, 0.703863382
717, 0.146336034, 0.733847022
718, 0.128243819, 0.619235933
719, 0.151061818, 0.764837503
720, 0.164912745, 0.863433063
721, 0.16978699, 0.897794545
722, 0.174837857, 0.932831585
723, 0.192364275, 1.04442668
724, 0.185369089, 1.00571775
725, 0.214643955, 1.12770545
726, 0.221488461, 1.17053437
727, 0.228541285, 1.21617055
728, 0.236248478, 1.26329625
729, 0.334367871, 0.236199543
730, 0.356657177, 1.10560739
731, 0.352461815, 1.43890548
732, 0.0628037304, 0.110255897
733, 0.475210607, 1.42327011
734, 0.310747087, 1.37595582
735, 0.242399454, 1.07854116
736, 0.0584035851, 0.174990356
737, 0.0984324217, 0.057971593
738, 0.504650533, 0.91861254
739, 0.512781024, 0.848031282
740, 0.118330956, 0.0726378337
741, 0.0561708212, 0.108518854
742, 0.0395719223, 0.108799227
743, 0.0811561868, 0.110212386
744, 0.0394192412, 0.138291329
745, 0.100940019, 0.072801441
746, 0.0970459282, 0.0829126537
747, 0.118522555, 0.40143016
748, 0.0621536933, 0.188617125
749, 0.362535059, 0.255654663
750, 0.493360162, 0.317478389
751, 0.651579916, 0.431310952
752, 0.555505991, 0.323513418
753, 0.510843337, 0.687463164
754, 0.194854453, 0.14868629
755, 0.140413702, 0.538056791
756, 0.128666475, 0.467291355
757, 0.474595964, 0.977137208
758, 0.0331005231, 0.118534394
759, 0.281892836, 0.201634556
760, 0.542525947, 0.56804198
761, 0.132496402, 0.490268707
762, 0.144781336, 0.563311577
763, 0.22427617, 1.00329602
764, 0.12506178, 0.444808394
765, 0.0377514884, 0.126487866
766, 0.159521148, 0.642459154
767, 0.0462981798, 0.107281223
768, 0.109189093, 0.0662192106
769, 0.0515878126, 0.150213271
770, 0.0546347536, 0.162359089
771, 0.596323729, 0.500193357
772, 0.392241567, 0.278232127
773, 0.0740494728, 0.112121247
774, 0.187951803, 0.79349184
775, 0.342288136, 1.30871356
776, 0.0352507681, 0.112857826
777, 0.167277411, 0.114017636
778, 0.0928422138, 0.099913083
779, 0.134805605, 0.0884382129
780, 0.153939143, 0.106401116
781, 0.0832173452, 0.215429604
782, 0.183262289, 0.122978851
783, 0.257914662, 0.186494216
784, 0.235476777, 0.172753006
785, 0.21449171, 0.16021654
786, 0.307433069, 0.218107626
787, 0.0656218603, 0.203162566
788, 0.0872360542, 0.231859207
789, 0.0917850062, 0.248632312
790, 0.0965788066, 0.265422195
791, 0.10077621, 0.28298521
792, 0.104288474, 0.301477998
793, 0.107367501, 0.320677459
794, 0.112856656, 0.360179812
795, 0.115615033, 0.380480856
796, 0.110187635, 0.340252429
797, 0.136457354, 0.513727307
798, 0.121668026, 0.422853857
799, 0.165038913, 0.670636117
800, 0.170785531, 0.699834824
801, 0.182383493, 0.761287034
802, 0.17668961, 0.730032086
803, 0.149476886, 0.589133084
804, 0.154425398, 0.61531651
805, 0.193774432, 0.82660228
806, 0.199963555, 0.860637486
807, 0.206499755, 0.895098269
808, 0.213145539, 0.930342257
809, 0.230773792, 1.04027212
810, 0.219245926, 0.96652621
811, 0.272691905, 1.12165749
812, 0.270834565, 1.17036307
813, 0.484698683, 0.510891795
814, 0.434333056, 0.797719836
815, 0.16144444, 0.127541333
816, 0.066759102, 0.113528982
817, 0.496710628, 1.33931148
818, 0.269024581, 1.06705737
819, 0.583141029, 0.429876655
820, 0.10416197, 0.0614149384
821, 0.0646734238, 0.160610199
822, 0.206275567, 0.175890595
823, 0.113124244, 0.0797879621
824, 0.180799931, 0.609976053
825, 0.227411255, 0.821972072
826, 0.100171722, 0.228709757
827, 0.155170932, 0.486075729
828, 0.0591609329, 0.113987111
829, 0.0493290015, 0.138740167
830, 0.060918048, 0.149544314

831, 0.0787547603, 0.115655981
832, 0.330201596, 1.2135607
833, 0.0956147015, 0.0910560414
834, 0.0989187062, 0.0773036554
835, 0.343705297, 0.277956814
836, 0.392315, 0.326045513
837, 0.21403268, 0.756406426
838, 0.293285608, 0.237371042
839, 0.397723377, 1.1948241
840, 0.363009781, 1.3588531
841, 0.090108417, 0.107700832
842, 0.444386244, 0.850491524
843, 0.138016388, 0.398115247
844, 0.150335029, 0.463281095
845, 0.0698531196, 0.172686681
846, 0.423572689, 0.308883548
847, 0.465818465, 0.725077093
848, 0.169095501, 0.558556378
849, 0.16434744, 0.533287942
850, 0.365950018, 1.05658591
851, 0.444839865, 0.902322054
852, 0.0465396196, 0.122531094
853, 0.269710183, 0.219464555
854, 0.461753935, 0.652473688
855, 0.160051614, 0.509198666
856, 0.145757765, 0.441136003
857, 0.0456849188, 0.113510266
858, 0.192944273, 0.665182769
859, 0.0530835651, 0.106203027
860, 0.106808849, 0.0751757696
861, 0.525853634, 0.449069023
862, 0.314373314, 1.17588174
863, 0.134687841, 0.0979737639
864, 0.149023771, 0.118165515
865, 0.0779584125, 0.200769886
866, 0.177042007, 0.137785405
867, 0.247337967, 0.203473672
868, 0.226239994, 0.189046577
869, 0.318010926, 0.257359326
870, 0.0748238787, 0.186456591
871, 0.106316052, 0.244283512
872, 0.113752291, 0.260307729
873, 0.119026557, 0.278442442
874, 0.122737974, 0.297673225
875, 0.126000479, 0.317458689
876, 0.134855777, 0.37728411
877, 0.129069835, 0.337285221
878, 0.13197802, 0.357128352
879, 0.141630352, 0.419441342
880, 0.199826851, 0.694478154
881, 0.220860019, 0.788790643
882, 0.207104519, 0.724881053
883, 0.174876228, 0.584207058
884, 0.186717689, 0.636809945
885, 0.235311925, 0.856105208
886, 0.244536802, 0.890243888
887, 0.261061013, 0.964074492
888, 0.266562283, 1.00240433
889, 0.416386068, 0.748319089
890, 0.0863719508, 0.11419297
891, 0.215834841, 0.204574451
892, 0.391299963, 1.26011813
893, 0.312002599, 1.04625487
894, 0.169571996, 0.151515871
895, 0.284142286, 0.88150239
896, 0.0880632773, 0.198164374
897, 0.406209618, 0.359720021
898, 0.200187743, 0.577982008
899, 0.17189014, 0.457912236
900, 0.0515811518, 0.111808762
901, 0.499233574, 0.396751314
902, 0.385728866, 0.855390608
903, 0.336608797, 1.14705777
904, 0.0683958307, 0.149382755
905, 0.118838817, 0.236952916
906, 0.0632977039, 0.118851282
907, 0.302199751, 1.08584428
908, 0.12222594, 0.0902607143
909, 0.101097569, 0.0892375037
910, 0.380593032, 0.807953835
911, 0.192878544, 0.552924216
912, 0.0601925366, 0.137595162
913, 0.0768687651, 0.121414132
914, 0.299035192, 0.276497275
915, 0.359511137, 0.336970598
916, 0.260977477, 0.816029727
917, 0.277292401, 0.254357964
918, 0.0978745893, 0.104294039
919, 0.0504629612, 0.120203316
920, 0.0542816892, 0.127501175
921, 0.178254783, 0.480395585
922, 0.456382692, 0.353126198
923, 0.430756807, 0.682133436
924, 0.208354011, 0.603018761
925, 0.188481301, 0.527713239
926, 0.362511188, 1.00603366
927, 0.256090283, 0.235705927
928, 0.428791016, 0.630234361
929, 0.184913784, 0.503361344
930, 0.166156366, 0.436459333
931, 0.22873491, 0.68786031
932, 0.476631224, 0.462371558
933, 0.133407265, 0.104870528
934, 0.105776764, 0.0924419761
935, 0.153779283, 0.139462784
936, 0.0980749056, 0.210041761
937, 0.187474623, 0.163468018
938, 0.235581875, 0.219338715
939, 0.322388738, 0.304541677
940, 0.0898774788, 0.184042111
941, 0.132737115, 0.251461804
942, 0.138403445, 0.273357362
943, 0.141399622, 0.293782353
944, 0.144635156, 0.314192504
945, 0.157096297, 0.394401073
946, 0.148200706, 0.334113836
947, 0.151394024, 0.353816718
948, 0.154049695, 0.37372008
949, 0.161105484, 0.415420741
950, 0.237786025, 0.718267202
951, 0.246621117, 0.750277877
952, 0.213771746, 0.630189478
953, 0.220608994, 0.658901989
954, 0.269926101, 0.849372089
955, 0.29669705, 0.919073284
956, 0.306171626, 0.961210251
957, 0.312686294, 1.00460088
958, 0.204335347, 0.219574958
959, 0.370090395, 0.762556136
960, 0.0715705082, 0.142735586
961, 0.17940563, 0.177484542
962, 0.0548997596, 0.117412694
963, 0.353299916, 0.957180977
964, 0.329619437, 0.860391498
965, 0.0831205621, 0.118187785
966, 0.065628022, 0.129886881
967, 0.327833682, 0.339721501
968, 0.393196076, 0.703962326
969, 0.212177813, 0.523548484
970, 0.241315335, 0.250521302
971, 0.140048251, 0.232632294
972, 0.1797546, 0.410872161

973,	0.296233684,	0.810985863
974,	0.0713764578,	0.117425717
975,	0.44297725,	0.388446122
976,	0.200368002,	0.472599417
977,	0.461636186,	0.419214278
978,	0.088542901,	0.161275029
979,	0.110386983,	0.226957574
980,	0.0592771955,	0.123665258
981,	0.224308625,	0.569118023
982,	0.186256751,	0.430488288
983,	0.276811481,	0.290499419
984,	0.367975056,	0.367100298
985,	0.193531886,	0.450785309
986,	0.0947524682,	0.115018465
987,	0.214360327,	0.547159314
988,	0.161810368,	0.164408013
989,	0.4344531,	0.55615294
990,	0.400779098,	0.644130707
991,	0.214169607,	0.495822072
992,	0.290649444,	0.316088289
993,	0.269369274,	0.709714472
994,	0.435587823,	0.512024462
995,	0.127545625,	0.10614448
996,	0.142431542,	0.12730664
997,	0.110630043,	0.0978837609
998,	0.105000645,	0.194600806
999,	0.113658801,	0.215935856
1000,	0.197282836,	0.190722287
1001,	0.0987183675,	0.172535673
1002,	0.161621347,	0.268840253
1003,	0.159512386,	0.291356921
1004,	0.162913039,	0.311026454
1005,	0.167855322,	0.330634922
1006,	0.171969026,	0.350558877
1007,	0.173230827,	0.370362997
1008,	0.17544958,	0.390816569
1009,	0.280814201,	0.742734134
1010,	0.239795178,	0.624655485
1011,	0.247177124,	0.651948214
1012,	0.257975638,	0.679529965
1013,	0.343085021,	0.909269869
1014,	0.334639788,	0.811951339
1015,	0.121049173,	0.115730792
1016,	0.420683563,	0.43078354
1017,	0.0738638937,	0.125838384
1018,	0.102503829,	0.116000295
1019,	0.21781072,	0.442524046
1020,	0.091144897,	0.120664254
1021,	0.170842633,	0.191193059
1022,	0.232936531,	0.473647952
1023,	0.0761841014,	0.133987516
1024,	0.205726549,	0.422137797
1025,	0.328326225,	0.771252692
1026,	0.222661138,	0.234435186
1027,	0.114464305,	0.0917199254
1028,	0.120559365,	0.0962882489
1029,	0.154590771,	0.177947715
1030,	0.177412286,	0.250283122
1031,	0.196862459,	0.348248094
1032,	0.180732131,	0.306335986
1033,	0.287018836,	0.667798877
1034,	0.068466112,	0.123318307
1035,	0.411119699,	0.394024938
1036,	0.354447484,	0.720664203
1037,	0.230301782,	0.542343616
1038,	0.174127489,	0.292164356
1039,	0.126007438,	0.224663526
1040,	0.241286963,	0.504869878
1041,	0.430347651,	0.470030695
1042,	0.080154486,	0.151019305
1043,	0.379651517,	0.597800553
1044,	0.196899265,	0.405678868
1045,	0.334179014,	0.371147245
1046,	0.234216839,	0.525676966
1047,	0.125492483,	0.191593349
1048,	0.36902824,	0.663939536
1049,	0.243241519,	0.55391407
1050,	0.29805097,	0.344257325
1051,	0.302356511,	0.698360741
1052,	0.14301239,	0.15071407
1053,	0.131408632,	0.212165877
1054,	0.187165409,	0.205208525
1055,	0.105639696,	0.162192598
1056,	0.111697204,	0.182489201
1057,	0.182518616,	0.279958934
1058,	0.241840065,	0.280758679
1059,	0.255178422,	0.300723493
1060,	0.187689647,	0.325753033
1061,	0.264224768,	0.323876172
1062,	0.191679314,	0.369145334
1063,	0.192438439,	0.387970924
1064,	0.240678817,	0.593738973
1065,	0.27086556,	0.605202675
1066,	0.272499561,	0.642302036
1067,	0.123152234,	0.135308519
1068,	0.374403089,	0.400469005
1069,	0.1752868,	0.219666243
1070,	0.262384117,	0.567771077
1071,	0.0862766951,	0.143277884
1072,	0.345685244,	0.628154397
1073,	0.11174313,	0.122981548
1074,	0.146907195,	0.190662935
1075,	0.389810443,	0.551698625
1076,	0.215716079,	0.336173266
1077,	0.138356209,	0.167143643
1078,	0.236201361,	0.307896048
1079,	0.205613628,	0.372378945
1080,	0.317207217,	0.733389139
1081,	0.243208706,	0.4515962
1082,	0.256301194,	0.485234678
1083,	0.231205598,	0.425925642
1084,	0.211495966,	0.278297216
1085,	0.159899637,	0.234191537
1086,	0.208823338,	0.249276638
1087,	0.19857727,	0.296317488
1088,	0.336078912,	0.683108509
1089,	0.226178735,	0.264326036
1090,	0.393442512,	0.511454403
1091,	0.0988429189,	0.127039716
1092,	0.387017369,	0.474475414
1093,	0.28805843,	0.581643701
1094,	0.254736334,	0.533870578
1095,	0.303277373,	0.373842865
1096,	0.191529766,	0.234609783
1097,	0.0955658555,	0.15278782
1098,	0.132256851,	0.180039376
1099,	0.194991812,	0.264482141
1100,	0.241404951,	0.32755658
1101,	0.219800383,	0.313130468
1102,	0.268944472,	0.348864585
1103,	0.216712102,	0.363348305
1104,	0.224940777,	0.407102108
1105,	0.295064121,	0.624895513
1106,	0.084255144,	0.126295701
1107,	0.341387838,	0.483180165
1108,	0.118224531,	0.171274215
1109,	0.126355007,	0.148061603
1110,	0.226036027,	0.291068673
1111,	0.350790441,	0.539286673
1112,	0.305042118,	0.553323746
1113,	0.15090932,	0.214488402
1114,	0.238284022,	0.351457566

1115,	0.317349344,	0.601442993
1116,	0.110182904,	0.134822041
1117,	0.316669136,	0.650930762
1118,	0.283813298,	0.506048858
1119,	0.250257432,	0.428911865
1120,	0.269212544,	0.460860848
1121,	0.250335366,	0.404521465
1122,	0.380817294,	0.437322497
1123,	0.33919245,	0.404317528
1124,	0.102250323,	0.143972337
1125,	0.273908973,	0.376009494
1126,	0.225304633,	0.383275062
1127,	0.319569379,	0.520740092
1128,	0.342117041,	0.441051036
1129,	0.111369066,	0.152976453
1130,	0.276957214,	0.404501587
1131,	0.362123489,	0.511953533
1132,	0.0928376764,	0.135342941
1133,	0.276163131,	0.43336919
1134,	0.300663322,	0.472258091
1135,	0.306887865,	0.405229539
1136,	0.247166425,	0.378923059
1137,	0.307046324,	0.438493341
1138,	0.00791424606,	0.0962696001
1139,	0.0930662677,	0.0267739147
1140,	0.0720787272,	1.87091303
1141,	0.0947717726,	0.0312132947
1142,	0.0926834047,	0.0371845178
1143,	0.0942915827,	0.0432022437
1144,	0.0942327082,	0.0502557978
1145,	0.0885259733,	0.0676271915
1146,	0.136911303,	1.80020857
1147,	0.678286195,	1.46081364
1148,	0.0155618731,	0.0999698043
1149,	0.0990079567,	0.0425415784
1150,	0.09994331,	0.0519953631
1151,	0.099331744,	0.0621767156
1152,	0.0252489839,	0.0997499526
1153,	0.0316774733,	0.099989213
1154,	0.0367386267,	0.0984830484
1155,	0.0429655463,	0.0994506329
1156,	0.0927350298,	0.0674034655
1157,	0.101195469,	0.0671459958
1158,	0.0901111811,	0.0766172633
1159,	0.0889338404,	0.0833405107
1160,	0.0932575688,	0.0782871321
1161,	0.08858978,	0.0903169811
1162,	0.0830325931,	0.104758054
1163,	0.587622702,	1.65174425
1164,	0.12540254,	0.0656147972
1165,	0.0924181566,	0.090947248
1166,	0.0930383727,	0.095385842
1167,	0.1041568,	0.0568857379
1168,	0.094642736,	0.0748989433
1169,	0.287996233,	1.64511895
1170,	0.124423645,	0.0808114186
1171,	0.769912422,	0.40833962
1172,	0.448427677,	1.47184539
1173,	0.118498899,	0.0855377913
1174,	0.0198622104,	0.10426271
1175,	0.0285552293,	0.111420274
1176,	0.0570919216,	0.1024305
1177,	0.0439759642,	0.102591321
1178,	0.0497084856,	0.102917008
1179,	0.173645318,	0.0834507346
1180,	0.0965434313,	0.0795356184
1181,	0.0967619643,	0.0874416232
1182,	0.0983072817,	0.0953216553
1183,	0.127511695,	0.0891985446
1184,	0.253225297,	1.56246173
1185,	0.257440954,	1.51028836
1186,	0.156678617,	0.0928773209
1187,	0.103012897,	0.08221706
1188,	0.109150358,	0.0865458101
1189,	0.6046924,	0.308584213
1190,	0.646624565,	0.380888432
1191,	0.444188446,	1.3774488
1192,	0.0599754751,	0.107623018
1193,	0.127622291,	0.0974895433
1194,	0.252520591,	1.45701873
1195,	0.201929942,	1.50133443
1196,	0.102815837,	0.0965364575
1197,	0.105124086,	0.102358669
1198,	0.109734386,	0.110099621
1199,	0.143109128,	0.100877441
1200,	0.446748465,	1.28848624
1201,	0.582571745,	0.330953956
1202,	0.589414299,	0.358029753
1203,	0.0414240509,	0.118950628
1204,	0.409007877,	1.332178
1205,	0.0501014218,	0.107222557
1206,	0.118168592,	0.105379798
1207,	0.380707234,	1.29997885
1208,	0.605570793,	0.389264047
1209,	0.139247864,	0.110407099
1210,	0.046988029,	0.128921136
1211,	0.287637949,	1.41076398
1212,	0.246253192,	1.40703821
1213,	0.479579002,	0.610851884
1214,	0.486760199,	0.562216699
1215,	0.336729914,	1.25906229
1216,	0.419393808,	1.00143528
1217,	0.540421963,	0.368007392
1218,	0.114277087,	0.116397351
1219,	0.131868079,	0.116890527
1220,	0.115954876,	0.145938665
1221,	0.296690434,	1.31482947
1222,	0.439116269,	0.942424893
1223,	0.121302046,	0.124899767
1224,	0.286388576,	1.26257789
1225,	0.0733727291,	0.157285467
1226,	0.0803180262,	0.168586254
1227,	0.123697273,	0.160299793
1228,	0.430909723,	0.597639382
1229,	0.392394006,	0.90303272
1230,	0.254031181,	0.926260769
1231,	0.129030481,	0.124790356
1232,	0.134783611,	0.134098336
1233,	0.370356798,	0.297785521
1234,	0.118956111,	0.203516409
1235,	0.401282042,	0.951625168
1236,	0.337958962,	0.57276082
1237,	0.351938665,	0.31327334
1238,	0.138941675,	0.201692343
1239,	0.161386862,	0.204263046
1240,	0.254524112,	0.78312695
1241,	0.298024595,	0.839516222
1242,	0.141405806,	0.219698146
1243,	0.151432827,	0.25163582
1244,	0.261031657,	0.623675942
1245,	0.277584374,	0.540972292
1246,	0.217203155,	0.463295341
1247,	0.215166852,	0.300147772
1248,	0.204601273,	0.31851387
1249,	0.208570108,	0.385799289
1250,	0.22531195,	0.325992942
1251,	0.210023075,	0.39948222
1252,	0.0048666345,	0.0548501909
1253,	0.0189802088,	0.0274640117
1254,	0.0322221667,	0.0194837768
1255,	0.0527430065,	0.0152681842
1256,	0.0678943545,	0.0167756993

1257, 0.00300132413, 0.0884724855
1258, 0.00604077661, 0.0884934366
1259, 0.00909686461, 0.0885092691
1260, 0.0121577121, 0.088517189
1261, 0.0151977455, 0.0885176882
1262, 0.0182319451, 0.0885068551
1263, 0.0212628674, 0.0884923711
1264, 0.0242888574, 0.0884796754
1265, 0.0273180529, 0.0884762704
1266, 0.0303306226, 0.0884812996
1267, 0.0333551578, 0.0884911492
1268, 0.0363816991, 0.0885153115
1269, 0.0393946916, 0.0885444954
1270, 0.0424078815, 0.0885718912
1271, 0.0454271659, 0.0886027142
1272, 0.0484437235, 0.0886376053
1273, 0.0612496361, 0.0160276238
1274, 0.0514523461, 0.088672556
1275, 0.0646233857, 0.016404314
1276, 0.0544565469, 0.0887113586
1277, 0.0574547164, 0.0887475312
1278, 0.0742028952, 0.0176543947
1279, 0.00433051167, 0.0596114658
1280, 0.00413134182, 0.0632499307
1281, 0.00389931258, 0.0666082054
1282, 0.00367011875, 0.0698343962
1283, 0.00346212974, 0.0730081648
1284, 0.00328976079, 0.0761425123
1285, 0.00316532655, 0.0792441219
1286, 0.00308437319, 0.0823230818
1287, 0.0575861745, 0.0155937551
1288, 0.0475440361, 0.0155371353
1289, 0.0371766724, 0.0176984649
1290, 0.0274574012, 0.0216533002
1291, 0.0230066441, 0.0242464188
1292, 0.0154822674, 0.0312222317
1293, 0.00998145808, 0.0400390849
1294, 0.00607876386, 0.049828887
1295, 0.0710569993, 0.0172057841
1296, 0.0604476295, 0.0887524486
1297, 0.0634258464, 0.0887139365
1298, 0.0772674233, 0.0181671828
1299, 0.0802945793, 0.0187180098
1300, 0.0694803447, 0.0884643644
1301, 0.083297953, 0.0193035323
1302, 0.0862836987, 0.019914126
1303, 0.072691828, 0.0882191956
1304, 0.0780179426, 0.063068144
1305, 0.0786004663, 0.0599789806
1306, 0.0791857243, 0.0568975247
1307, 0.0797748119, 0.0538268909
1308, 0.0803688839, 0.0507363603
1309, 0.0809679478, 0.0476572514
1310, 0.0815658942, 0.0445654728
1311, 0.0821606815, 0.0414745957
1312, 0.0827604979, 0.038376011
1313, 0.0833667368, 0.0352841504
1314, 0.0839721486, 0.0322029032
1315, 0.0845716298, 0.0291231796
1316, 0.0851594582, 0.0260457639
1317, 0.0125181973, 0.0354313366
1318, 0.033509329, 0.0244323034
1319, 0.00765346596, 0.0665153563
1320, 0.0305437949, 0.0854283571
1321, 0.0775063336, 0.0501504689
1322, 0.0072590881, 0.0698026344
1323, 0.00690436596, 0.0730317459
1324, 0.00661027059, 0.0761861652
1325, 0.00303234044, 0.085401386
1326, 0.0565106533, 0.0196487959
1327, 0.0423044004, 0.01637071
1328, 0.0216315109, 0.0304897092
1329, 0.0634047687, 0.0858379453
1330, 0.0605002306, 0.0859553218
1331, 0.0546272621, 0.0859382153
1332, 0.0516511239, 0.0858573392
1333, 0.0486626439, 0.0857741386
1334, 0.0426373743, 0.085621506
1335, 0.0396307744, 0.0855592266
1336, 0.0335862264, 0.0854575709
1337, 0.0456596315, 0.0856950432
1338, 0.0787030905, 0.0439802669
1339, 0.0804804936, 0.0346440487
1340, 0.00781336613, 0.0448240414
1341, 0.0106699355, 0.0507696606
1342, 0.0757629424, 0.0593363717
1343, 0.0781142041, 0.0470855236
1344, 0.0184098203, 0.0854908377
1345, 0.00805916823, 0.0630599186
1346, 0.021452602, 0.0854619294
1347, 0.0244909041, 0.085435003
1348, 0.02753767, 0.0854246467
1349, 0.0366237015, 0.0855045021
1350, 0.0251432024, 0.028073784
1351, 0.0774329007, 0.0661631227
1352, 0.0768824294, 0.0692434683
1353, 0.076372385, 0.0723083168
1354, 0.0758604333, 0.0753327012
1355, 0.075263761, 0.0782930776
1356, 0.0638786554, 0.0199357402
1357, 0.0575692281, 0.0859891921
1358, 0.0743170157, 0.0812971145
1359, 0.079876937, 0.0377547666
1360, 0.00934486836, 0.0551948659
1361, 0.0153607428, 0.0855100378
1362, 0.0122950478, 0.085510619
1363, 0.00919229537, 0.0854935944
1364, 0.00610418105, 0.0854429156
1365, 0.00639239419, 0.0792901143
1366, 0.0521278791, 0.0197261907
1367, 0.029112963, 0.0261893533
1368, 0.0727391243, 0.0845570043
1369, 0.0663867146, 0.0886137486
1370, 0.0810850263, 0.0315573178
1371, 0.0816750973, 0.0284839775
1372, 0.0857302696, 0.0229749698
1373, 0.0380476713, 0.0227344893
1374, 0.076323472, 0.0562859029
1375, 0.0769185945, 0.0532509163
1376, 0.0603124723, 0.0197856743
1377, 0.0672437176, 0.0201463681
1378, 0.0705046803, 0.0204323065
1379, 0.0792873353, 0.0408852957
1380, 0.0736879334, 0.0207999386
1381, 0.0767872855, 0.0212450568
1382, 0.0798054039, 0.0217705816
1383, 0.0827818811, 0.0223548319
1384, 0.082239911, 0.0254132506
1385, 0.0518749468, 0.0830354169
1386, 0.0734986663, 0.0557708703
1387, 0.0547911711, 0.0831616223
1388, 0.0144788083, 0.0418428034
1389, 0.0247519072, 0.0824029371
1390, 0.0459290408, 0.0827773735
1391, 0.0746255219, 0.0655464232
1392, 0.073333703, 0.0746877789
1393, 0.0112921186, 0.0665452331
1394, 0.0103090247, 0.0730682164
1395, 0.00936355907, 0.0824411884
1396, 0.0189174917, 0.0337789617
1397, 0.0308181122, 0.0823933631
1398, 0.0632769987, 0.0234577544

1399, 0.0559219718, 0.0236877948
1400, 0.077007629, 0.037242718
1401, 0.0762777925, 0.0243265983
1402, 0.0107581262, 0.0698188543
1403, 0.0156059582, 0.0824651346
1404, 0.0474652387, 0.0202823784
1405, 0.0166299045, 0.0375923105
1406, 0.0489105023, 0.082901597
1407, 0.0692428499, 0.0855918452
1408, 0.0741093233, 0.0686573386
1409, 0.0344431736, 0.0294216089
1410, 0.0429225713, 0.0826650262
1411, 0.0225085504, 0.0356145017
1412, 0.0399115868, 0.0825673938
1413, 0.0338640027, 0.0824349076
1414, 0.0217245463, 0.0824284256
1415, 0.0368957371, 0.0824926496
1416, 0.0753462464, 0.0466092192
1417, 0.0666774884, 0.0235014018
1418, 0.0124102831, 0.0462267138
1419, 0.0752235204, 0.0624302849
1420, 0.0747503042, 0.0496955812
1421, 0.0186942779, 0.0824398994
1422, 0.011858942, 0.0631393865
1423, 0.0277994238, 0.0823905393
1424, 0.0264815688, 0.0320569202
1425, 0.0576266423, 0.0832088217
1426, 0.0737185478, 0.0717227906
1427, 0.0604272448, 0.0831125155
1428, 0.0729768649, 0.0773801655
1429, 0.0596832931, 0.0235272013
1430, 0.0719121099, 0.0798476413
1431, 0.0764587373, 0.0404088944
1432, 0.0125535037, 0.0596114621
1433, 0.0099225156, 0.0762155876
1434, 0.0125212288, 0.0824413449
1435, 0.00623649638, 0.0823604688
1436, 0.00962391123, 0.0793184936
1437, 0.0518458113, 0.024107499
1438, 0.0301765539, 0.0309277847
1439, 0.070405297, 0.0819097236
1440, 0.0662493706, 0.0856762677
1441, 0.0775859728, 0.0341165699
1442, 0.0427227058, 0.0213166177
1443, 0.0730321556, 0.0588186458
1444, 0.0741335303, 0.0527583994
1445, 0.0699710548, 0.0236618333
1446, 0.0759295747, 0.0435343534
1447, 0.0781695247, 0.0310022458
1448, 0.0731602684, 0.0239580199
1449, 0.079274632, 0.0248460043
1450, 0.0787247196, 0.0279302672
1451, 0.0601640381, 0.0801617801
1452, 0.0432060286, 0.0261559431
1453, 0.0208890811, 0.039305903
1454, 0.0548832305, 0.0802812725
1455, 0.0711543411, 0.0713018626
1456, 0.0304042399, 0.0357792266
1457, 0.0341288634, 0.0793991908
1458, 0.0431969166, 0.0796698034
1459, 0.0136076361, 0.0731013268
1460, 0.0461825319, 0.079809323
1461, 0.0713127926, 0.0681786016
1462, 0.0699550211, 0.0782211721
1463, 0.0280860253, 0.0793525502
1464, 0.015949022, 0.079371579
1465, 0.0741614252, 0.0369049758
1466, 0.0491422415, 0.0799705908
1467, 0.0725885779, 0.061857596
1468, 0.0662149042, 0.0268618874
1469, 0.0751971602, 0.0305786785
1470, 0.0475646742, 0.0249341577
1471, 0.0371576734, 0.0794609413
1472, 0.071946688, 0.0649922118
1473, 0.0250780098, 0.0793581605
1474, 0.0694827735, 0.0269060135
1475, 0.0721828267, 0.0493183583
1476, 0.0146995187, 0.0666963086
1477, 0.0188590325, 0.0433971137
1478, 0.0401766524, 0.0795482919
1479, 0.0310962535, 0.0793685615
1480, 0.0220733993, 0.0793643594
1481, 0.0727888867, 0.0462819077
1482, 0.0190480351, 0.0793614388
1483, 0.0140887434, 0.0699044392
1484, 0.0135358041, 0.0558493957
1485, 0.0153639913, 0.0634029508
1486, 0.0349739753, 0.0342531912
1487, 0.0575555861, 0.0802921653
1488, 0.0707359463, 0.0744600445
1489, 0.0712795183, 0.0767604858
1490, 0.0628119633, 0.0270069968
1491, 0.0683289021, 0.0800312012
1492, 0.0592889041, 0.0272782631
1493, 0.0149555504, 0.051835008
1494, 0.013173366, 0.0762373284
1495, 0.0128229195, 0.0793321356
1496, 0.0556277707, 0.0277168397
1497, 0.0707533732, 0.0553759187
1498, 0.0662097409, 0.082271412
1499, 0.0632072017, 0.0828028098
1500, 0.0746617094, 0.0337443314
1501, 0.0520388968, 0.0801368132
1502, 0.0714595243, 0.0523002222
1503, 0.0726475269, 0.0271216724
1504, 0.0732644051, 0.0432150438
1505, 0.0737097934, 0.0401068106
1506, 0.0757102072, 0.0274893977
1507, 0.0658169091, 0.0754568055
1508, 0.0387837701, 0.0277071223
1509, 0.0404162668, 0.0764967278
1510, 0.0373820215, 0.0764011517
1511, 0.0230428912, 0.04482219
1512, 0.0648425072, 0.0790248513
1513, 0.0177380946, 0.0669417977
1514, 0.0716971979, 0.0335322767
1515, 0.0573864505, 0.0773122385
1516, 0.0658364892, 0.0302661266
1517, 0.0590895452, 0.031040391
1518, 0.0478180572, 0.029420428
1519, 0.0162497982, 0.0601834916
1520, 0.0393728241, 0.0324546471
1521, 0.0688952208, 0.0712066814
1522, 0.0688889921, 0.0517177656
1523, 0.0704130083, 0.0585006513
1524, 0.0548666827, 0.0772868991
1525, 0.0252400078, 0.0404037796
1526, 0.0682289526, 0.067843616
1527, 0.0434184857, 0.0766334906
1528, 0.0355281569, 0.0388986878
1529, 0.0521544367, 0.0771516412
1530, 0.070665881, 0.0431025773
1531, 0.0493212454, 0.0769655481
1532, 0.0343641378, 0.0763326213
1533, 0.0694824755, 0.0643339455
1534, 0.0224777199, 0.0762662962
1535, 0.0681123808, 0.0550322346
1536, 0.0172445793, 0.070012711
1537, 0.0174410418, 0.0568297766
1538, 0.0254495163, 0.0762630403
1539, 0.0625016093, 0.0305767544
1540, 0.0163510721, 0.0762513131

1541, 0.0194607116, 0.076256074
1542, 0.0313697308, 0.0762910694
1543, 0.0284098722, 0.0762669593
1544, 0.051796481, 0.0284023229
1545, 0.0668288842, 0.0777746141
1546, 0.0699313208, 0.0489683561
1547, 0.0207617618, 0.049060598
1548, 0.0702855587, 0.0613708682
1549, 0.0463812053, 0.0767867416
1550, 0.0626072809, 0.079725109
1551, 0.0712926835, 0.036777541
1552, 0.0690380186, 0.0302031431
1553, 0.0704084113, 0.0461039245
1554, 0.0709626526, 0.0399986431
1555, 0.0721356049, 0.0303469878
1556, 0.0494522639, 0.0739397258
1557, 0.061474856, 0.0737622157
1558, 0.0316683687, 0.0730900913
1559, 0.0663097128, 0.0505187809
1560, 0.0465582684, 0.073758699
1561, 0.0522021316, 0.0741208121
1562, 0.0199184604, 0.0731349736
1563, 0.051948946, 0.0325852893
1564, 0.0229365528, 0.0731013864
1565, 0.0167808551, 0.0731204599
1566, 0.0619990937, 0.076672554
1567, 0.0406140238, 0.073475115
1568, 0.0196339507, 0.061270427
1569, 0.0183314607, 0.0639716163
1570, 0.0265598297, 0.0463295467
1571, 0.0548056364, 0.0742219239
1572, 0.0442239158, 0.0351870246
1573, 0.0346218385, 0.0731894076
1574, 0.0636329949, 0.0726953074
1575, 0.0676094368, 0.0586663559
1576, 0.0656701997, 0.0700715631
1577, 0.03759747, 0.0733386576
1578, 0.0399998389, 0.0368928164
1579, 0.0623580143, 0.0341361165
1580, 0.0658526048, 0.0656366944
1581, 0.0684834719, 0.0610586442
1582, 0.0203655027, 0.0700062066
1583, 0.0226271674, 0.0545675829
1584, 0.0655586198, 0.0337166339
1585, 0.0258516017, 0.073058255
1586, 0.0287546068, 0.0730353966
1587, 0.055566106, 0.0317027904
1588, 0.0682023615, 0.0485680662
1589, 0.0680166781, 0.0462302268
1590, 0.0241804458, 0.0505124368
1591, 0.0673134401, 0.0630895048
1592, 0.0435856432, 0.0736173019
1593, 0.0686585829, 0.0335451327
1594, 0.0680631995, 0.0432806686
1595, 0.0681915507, 0.0401214398
1596, 0.0683831573, 0.0368642658
1597, 0.0557037368, 0.0356100686
1598, 0.0204794388, 0.064732939
1599, 0.0300516617, 0.0412807912
1600, 0.0547282957, 0.0711557865
1601, 0.0591670908, 0.0721301511
1602, 0.0378817208, 0.0702890381
1603, 0.0270589404, 0.0518754348
1604, 0.0655608699, 0.0612232871
1605, 0.0495095402, 0.0709585547
1606, 0.0656368509, 0.046973791
1607, 0.0653828084, 0.0405056439
1608, 0.0653464049, 0.0546900071
1609, 0.0623326153, 0.0657297447
1610, 0.0408300161, 0.0409674719
1611, 0.0466393158, 0.0707820728
1612, 0.0486462116, 0.0378570668
1613, 0.0291089602, 0.0695197731
1614, 0.0597525276, 0.0771198869
1615, 0.0593637079, 0.0743127242
1616, 0.0294538159, 0.0558851436
1617, 0.0437338874, 0.0706636384
1618, 0.0448141284, 0.039287053
1619, 0.0349742882, 0.0699710548
1620, 0.0605860054, 0.0712592974
1621, 0.0408270843, 0.0705572292
1622, 0.0521647073, 0.0711285248
1623, 0.063918151, 0.059212409
1624, 0.0205694251, 0.0670384467
1625, 0.0233221687, 0.0698164031
1626, 0.0320295319, 0.0696569532
1627, 0.0590667799, 0.034781687
1628, 0.0631430596, 0.0476986058
1629, 0.0654414743, 0.0437709503
1630, 0.0314408503, 0.0510503575
1631, 0.0638936311, 0.063500382
1632, 0.0654081628, 0.0371649526
1633, 0.0592152514, 0.0384516977
1634, 0.033909291, 0.057464093
1635, 0.0467022173, 0.0678232536
1636, 0.0263112597, 0.065619126
1637, 0.057143297, 0.0742691532
1638, 0.0526684038, 0.0405119509
1639, 0.0609351359, 0.0677444562
1640, 0.0455615632, 0.0432287306
1641, 0.062497478, 0.0411355607
1642, 0.0598923229, 0.0635310709
1643, 0.0383468829, 0.0672921762
1644, 0.0495073609, 0.0680931881
1645, 0.0520871431, 0.0682318583
1646, 0.0609377548, 0.0516714118
1647, 0.0623538084, 0.0376950502
1648, 0.0543857589, 0.0682557151
1649, 0.0366775841, 0.0428556576
1650, 0.0491890796, 0.0417496935
1651, 0.0599148422, 0.0453991592
1652, 0.0438358337, 0.0676893443
1653, 0.0356005095, 0.0666502193
1654, 0.0410992429, 0.0677654892
1655, 0.035975948, 0.0522951595
1656, 0.0579118207, 0.0602898821
1657, 0.0326138176, 0.065964222
1658, 0.0302248877, 0.0603694692
1659, 0.0626766682, 0.0567896888
1660, 0.0627492815, 0.0444599129
1661, 0.0581694543, 0.0670218542
1662, 0.0572707988, 0.0709959492
1663, 0.0543197989, 0.065424934
1664, 0.0380522609, 0.0466963649
1665, 0.0495781749, 0.0653548241
1666, 0.0564083196, 0.0430429652
1667, 0.0367357992, 0.0632532984
1668, 0.0591419302, 0.0557780638
1669, 0.0436352938, 0.0642828196
1670, 0.0468986072, 0.064840503
1671, 0.0520804264, 0.065361701
1672, 0.0498793684, 0.0454962701
1673, 0.0418150127, 0.0448369645
1674, 0.0575627685, 0.0497759059
1675, 0.0412988141, 0.0654495806
1676, 0.0393107235, 0.0643402264
1677, 0.0372691602, 0.0556935556
1678, 0.0352854878, 0.0596390702
1679, 0.0582711101, 0.05282069
1680, 0.0594952926, 0.0419818386
1681, 0.056404639, 0.0680036321
1682, 0.0538273118, 0.058589898

```
1683, 0.0551256202, 0.0620950386
1684, 0.0569339097, 0.0464676991
1685, 0.0449641272, 0.0617828257
1686, 0.0531935096, 0.0441682152
1687, 0.0478219464, 0.0614997298
1688, 0.0464414544, 0.0469300337
1689, 0.0429017618, 0.0485503413
1690, 0.0384734385, 0.0594381019
1691, 0.0498223603, 0.0631159246
1692, 0.0555051938, 0.0541175418
1693, 0.0546287782, 0.0509913266
1694, 0.0452875756, 0.0552353635
1695, 0.0516146533, 0.0522936769
1696, 0.0538602769, 0.0476418473
1697, 0.0419907458, 0.0570208319
1698,  0.050914064, 0.0597495027
1699, 0.0393749177, 0.0503426939
1700, 0.0466033779,  0.058220055
1701, 0.0496766753, 0.0567926541
1702, 0.0506914072, 0.0489505082
1703, 0.0526545607, 0.0553967245
1704, 0.0406586193, 0.0538239479
1705, 0.0485101566, 0.0536655001
1706, 0.00852369796,   0.05936189
1707, 0.0167624094,  0.047609929
1708, 0.0235299952, 0.0326711908
1709, 0.0687009916,  0.083272934
1710, 0.0436394103, 0.0307983737
1711,  0.026287131, 0.0360773057
1712, 0.0189104881, 0.0531178825
1713, 0.0686957836, 0.0762805268
1714, 0.0639875755,  0.076040566
1715, 0.0676121637, 0.0743711516
1716, 0.0691028535, 0.0734359249
1717,  0.048158966, 0.0337269045
1718, 0.0522381552, 0.0366057456
1719, 0.0325722098, 0.0451911166
1720, 0.0668852925, 0.0721634999
1721, 0.0212418288, 0.0583032593
1722, 0.0653701425, 0.0733466074
1723, 0.0559889786, 0.0393756889
1724, 0.0345096588, 0.0487590283
1725,    0.0262038, 0.0695645213
1726, 0.0623102933, 0.0699523017
1727, 0.0641142949, 0.0679102838
1728, 0.0292722732, 0.0484138094
1729,  0.023311777, 0.0664191544
1730, 0.0327352211, 0.0542452708
1731, 0.0222797859, 0.0632546991
1732, 0.0292105675, 0.0528635643
1733, 0.0253648236, 0.0606592856
1734, 0.0260922201, 0.0558169372
1735, 0.0294830389, 0.0653760806
1736, 0.0592516586, 0.0692510232
1737,  0.059618365,   0.06623099
1738, 0.0619425513, 0.0612159893
1739, 0.0603980385, 0.0486109182
1740, 0.0474239774, 0.0503814071
1741, 0.0440599136, 0.0519882701
1742, 0.0657057688, 0.0576449633
1743,  0.033721853, 0.0623010769
1744, 0.0559603162, 0.0658921376
1745, 0.0573491752, 0.0645620599
1746, 0.0635571927, 0.0508061349
1747, 0.0411366113, 0.0617974587
1748, 0.0519970618, 0.0624709092
1749, 0.0603274852, 0.0585573651
1750, 0.0436111391, 0.0596621558
1751, 0.0635512546, 0.0534170941
1752, 0.0615675338, 0.0544512682
1753, 0.0565422215, 0.0571846031
```

```
*Element, type=CPE4RT
   1,  208,  156,    1,    9
   2,  513,  488,  565,  538
   3,  729,  656,  699,  749
   4,  384,  444,  539,  439
   5,  241,  240,   81,   82
   6,  294,  209,  242,  388
   7,   83,   84,  242,  209
   8,   85,   86,  210,  243
   9,  244,  210,   86,   87
  10,  567,  638,  450,  201
  11,  543,  639,  430,  368
  12,  292,  293,  100,  101
  13,  289,  290,  104,  105
  14,  295,  211,  290,  424
  15,  296,  286,  216,  419
  16,  907,  811,  735,  818
  17,  425,  365,  196,  426
  18,  201,  196,  244,  389
  19,   36,   37,  297,  298
  20,  212,   68,   69,  231
  21,  379,  380,  495,  427
  22,  237,   76,   77,  349
  23,  240,  239,   80,   81
  24,   88,  389,  244,   87
  25,   89,  350,  389,   88
  26,  541,  567, 1147,  204
  27,   93,  247,  206,   92
  28,   96,  245,  246,   95
  29, 1147,  389,  350,  429
  30,  206,  542,  299,   92
  31,  247,   93,   94,  214
  32,    5,   91,  215,   90
  33,  429,  350,  215,  299
  34,  108,  109,  216,  286
  35,  300,  280,  279,  369
  36, 1216,  641,  850,  926
  37,  388,  501,  449,  294
  38,  425,  428,  200,  365
  39,  116,  117,  217,  279
  40,  301,  274,  273,  412
  41,  854,  753,  847,  923
  42,  640,  539,  564, 1190
  43,  501,  388,  200,  428
  44,  269,  270,  127,  128
  45,  598,  700,  698,  599
  46,  814,  889,  847,  199
  47,  235,  236,  385,  302
  48,  303,  267,  266,  359
  49,  257,  258,  140,  141
  50,  684,  575,  202,  839
  51,  842,  739,  738,  851
  52,  733, 1172,  642, 1191
  53,  205,  663,  731,  540
  54,  207,  543,  368,  440
  55,  304,   11,   12,  306
  56,  431, 1138,  304,  306
  57,  305,  208, 1138,  431
  58,   13,  307,  306,   12
  59,   14,  308,  307,   13
  60,   15,  309,  308,   14
  61,  313,   19,   20,  314
  62,  310, 1152,  432,  309
  63,   16,  310,  309,   15
  64,   17,  311,  310,   16
  65,   18,  312,  311,   17
  66,  317,   23,   24,  318
  67,   19,  313,  312,   18
  68,   21,  315,  314,   20
  69,   22,  316,  315,   21
  70,   26,  320,  319,   25
```

71,	28,	322,	321,	27
72,	30,	324,	323,	29
73,	32,	220,	325,	31
74,	220,	32,	2,	372
75,	150,	151,	326,	248
76,	37,	38,	327,	297
77,	348,	59,	60,	223
78,	467,	327,	329,	468
79,	39,	40,	330,	329
80,	40,	41,	331,	330
81,	332,	331,	41,	42
82,	58,	328,	335,	57
83,	334,	333,	43,	44
84,	334,	336,	471,	434
85,	337,	336,	45,	46
86,	338,	337,	46,	47
87,	339,	338,	47,	48
88,	57,	335,	341,	56
89,	435,	1142,	559,	645
90,	343,	342,	50,	51
91,	345,	1139,	1141,	344
92,	53,	54,	1139,	345
93,	3,	56,	221,	55
94,	298,	346,	35,	36
95,	33,	34,	347,	222
96,	223,	60,	61,	224
97,	433,	467,	544,	1158
98,	225,	62,	63,	226
99,	62,	225,	224,	61
100,	64,	227,	226,	63
101,	65,	228,	227,	64
102,	67,	230,	229,	66
103,	70,	232,	231,	69
104,	71,	233,	232,	70
105,	72,	234,	233,	71
106,	73,	235,	234,	72
107,	75,	213,	236,	74
108,	76,	237,	213,	75
109,	78,	238,	349,	77
110,	238,	78,	79,	239
111,	4,	80,	239,	79
112,	238,	239,	240,	386
113,	209,	241,	82,	83
114,	243,	242,	84,	85
115,	90,	215,	350,	89
116,	6,	98,	351,	97
117,	1140,	352,	245,	351
118,	91,	92,	299,	215
119,	156,	208,	305,	353
120,	155,	156,	353,	354
121,	456,	1153,	545,	644
122,	154,	155,	354,	355
123,	546,	767,	669,	1177
124,	323,	463,	438,	322
125,	356,	357,	152,	153
126,	248,	249,	149,	150
127,	148,	149,	249,	250
128,	250,	251,	147,	148
129,	251,	252,	146,	147
130,	252,	253,	145,	146
131,	253,	254,	144,	145
132,	358,	254,	253,	395
133,	142,	143,	255,	256
134,	256,	257,	141,	142
135,	219,	259,	138,	139
136,	137,	138,	259,	260
137,	135,	136,	261,	262
138,	134,	135,	262,	263
139,	133,	134,	263,	264
140,	132,	133,	264,	265
141,	131,	132,	265,	266
142,	130,	131,	266,	267
143,	264,	405,	406,	265
144,	268,	269,	128,	129
145,	218,	271,	125,	126
146,	124,	125,	271,	272
147,	123,	124,	272,	273
148,	122,	123,	273,	274
149,	121,	122,	274,	275
150,	120,	121,	275,	276
151,	413,	275,	274,	301
152,	276,	277,	119,	120
153,	115,	116,	279,	280
154,	114,	115,	280,	281
155,	113,	114,	281,	282
156,	112,	113,	282,	283
157,	361,	283,	282,	418
158,	283,	284,	111,	112
159,	286,	287,	107,	108
160,	287,	288,	106,	107
161,	288,	289,	105,	106
162,	362,	289,	288,	423
163,	211,	291,	102,	103
164,	291,	292,	101,	102
165,	363,	292,	291,	366
166,	351,	245,	96,	97
167,	208,	9,	10,	1138
168,	11,	304,	1138,	10
169,	240,	241,	364,	386
170,	196,	365,	210,	244
171,	243,	210,	365,	200
172,	211,	295,	366,	291
173,	228,	229,	377,	367
174,	385,	384,	439,	499
175,	247,	214,	440,	368
176,	214,	94,	95,	246
177,	284,	285,	110,	111
178,	419,	216,	285,	421
179,	277,	278,	118,	119
180,	278,	415,	416,	217
181,	370,	271,	218,	409
182,	371,	259,	219,	398
183,	222,	372,	2,	33
184,	441,	326,	357,	481
185,	54,	55,	221,	1139
186,	671,	1157,	745,	643
187,	373,	476,	223,	224
188,	453,	347,	346,	474
189,	225,	226,	375,	374
190,	228,	65,	66,	229
191,	226,	227,	376,	375
192,	367,	376,	227,	228
193,	229,	230,	378,	377
194,	230,	67,	68,	212
195,	379,	378,	230,	212
196,	381,	380,	231,	232
197,	382,	381,	232,	233
198,	235,	73,	74,	236
199,	383,	382,	233,	234
200,	444,	384,	213,	237
201,	384,	385,	236,	213
202,	191,	444,	237,	349
203,	387,	209,	294,	190
204,	387,	364,	241,	209
205,	243,	200,	388,	242
206,	352,	390,	246,	245
207,	440,	390,	560,	207
208,	445,	248,	326,	441
209,	249,	391,	392,	250
210,	250,	392,	393,	251
211,	251,	393,	394,	252
212,	255,	397,	396,	256

213, 143, 144, 254, 255
214, 254, 358, 397, 255
215, 257, 399, 400, 258
216, 256, 396, 399, 257
217, 258, 219, 139, 140
218, 259, 371, 401, 260
219, 136, 137, 260, 261
220, 402, 261, 260, 401
221, 403, 262, 261, 402
222, 446, 403, 402, 513
223, 408, 269, 268, 407
224, 267, 268, 129, 130
225, 267, 303, 407, 268
226, 269, 408, 410, 270
227, 270, 218, 126, 127
228, 447, 411, 370, 521
229, 271, 370, 411, 272
230, 275, 413, 360, 276
231, 276, 360, 414, 277
232, 117, 118, 278, 217
233, 418, 282, 281, 417
234, 280, 300, 417, 281
235, 283, 361, 420, 284
236, 448, 421, 420, 534
237, 285, 216, 109, 110
238, 286, 296, 422, 287
239, 424, 290, 289, 362
240, 103, 104, 290, 211
241, 1146, 352, 1140, 293
242, 560, 1146, 363, 451
243, 99, 100, 293, 1140
244, 450, 426, 196, 201
245, 426, 450, 575, 197
246, 295, 537, 485, 366
247, 533, 483, 566, 548
248, 452, 423, 422, 535
249, 38, 39, 329, 327
250, 34, 35, 346, 347
251, 369, 279, 217, 416
252, 530, 486, 549, 630
253, 272, 411, 412, 273
254, 524, 487, 550, 624
255, 383, 302, 498, 454
256, 234, 235, 302, 383
257, 359, 266, 265, 406
258, 518, 482, 551, 618
259, 308, 455, 1148, 307
260, 1148, 478, 305, 431
261, 313, 436, 1153, 312
262, 316, 22, 23, 317
263, 436, 313, 314, 1154
264, 318, 24, 25, 319
265, 478, 553, 353, 305
266, 1177, 1155, 458, 546
267, 320, 26, 27, 321
268, 437, 479, 318, 319
269, 668, 552, 644, 1175
270, 546, 458, 479, 1178
271, 321, 322, 438, 461
272, 322, 28, 29, 323
273, 459, 553, 685, 579
274, 323, 324, 464, 463
275, 325, 465, 464, 324
276, 1176, 648, 1192, 741
277, 324, 30, 31, 325
278, 466, 220, 372, 580
279, 555, 464, 465, 651
280, 355, 356, 153, 154
281, 329, 330, 469, 468
282, 328, 58, 59, 348
283, 42, 43, 333, 332
284, 469, 330, 331, 1145
285, 44, 45, 336, 334
286, 556, 332, 333, 688
287, 328, 470, 472, 335
288, 336, 337, 1144, 471
289, 582, 544, 469, 1145
290, 48, 49, 340, 339
291, 338, 339, 1143, 557
292, 49, 50, 342, 340
293, 558, 646, 1149, 645
294, 646, 557, 1143, 1149
295, 1141, 559, 343, 344
296, 51, 52, 344, 343
297, 343, 559, 1142, 342
298, 52, 53, 345, 344
299, 473, 221, 56, 341
300, 645, 473, 341, 558
301, 442, 298, 297, 433
302, 474, 346, 298, 442
303, 223, 476, 477, 348
304, 98, 99, 1140, 351
305, 555, 648, 463, 464
306, 355, 462, 480, 356
307, 357, 326, 151, 152
308, 252, 394, 395, 253
309, 263, 404, 405, 264
310, 514, 359, 406, 517
311, 415, 278, 277, 414
312, 421, 448, 483, 419
313, 287, 422, 423, 288
314, 424, 362, 536, 484
315, 207, 560, 451, 589
316, 364, 387, 500, 1171
317, 191, 349, 238, 386
318, 425, 561, 657, 428
319, 537, 295, 424, 484
320, 374, 373, 224, 225
321, 543, 1169, 664, 639
322, 206, 247, 368, 430
323, 416, 528, 529, 369
324, 409, 218, 270, 410
325, 412, 523, 487, 301
326, 398, 219, 258, 400
327, 510, 371, 398, 512
328, 866, 782, 694, 754
329, 562, 445, 441, 570
330, 374, 375, 490, 489
331, 375, 376, 492, 490
332, 491, 492, 376, 367
333, 377, 378, 494, 493
334, 212, 231, 380, 379
335, 380, 381, 496, 495
336, 597, 495, 496, 599
337, 381, 382, 497, 496
338, 382, 383, 454, 497
339, 564, 539, 444, 191
340, 499, 498, 302, 385
341, 500, 387, 190, 601
342, 214, 246, 390, 440
343, 502, 392, 391, 603
344, 391, 249, 248, 445
345, 392, 502, 503, 393
346, 393, 503, 504, 394
347, 394, 504, 505, 395
348, 358, 506, 509, 397
349, 399, 511, 508, 400
350, 395, 505, 506, 358
351, 488, 510, 590, 565
352, 507, 396, 397, 509
353, 511, 399, 396, 507
354, 488, 401, 371, 510

355, 405, 516, 517, 406
356, 403, 446, 515, 404
357, 262, 403, 404, 263
358, 359, 514, 482, 303
359, 303, 482, 518, 407
360, 408, 519, 522, 410
361, 520, 409, 410, 522
362, 519, 408, 407, 518
363, 411, 447, 523, 412
364, 301, 487, 524, 413
365, 525, 360, 413, 524
366, 526, 414, 360, 525
367, 527, 415, 414, 526
368, 528, 416, 415, 527
369, 300, 486, 530, 417
370, 418, 531, 532, 361
371, 284, 420, 421, 285
372, 419, 483, 533, 296
373, 423, 452, 536, 362
374, 561, 425, 426, 197
375, 493, 491, 367, 377
376, 378, 379, 427, 494
377, 567, 201, 389, 1147
378, 501, 602, 568, 449
379, 430, 1163, 542, 206
380, 542, 1163, 429, 299
381, 309, 432, 455, 308
382, 456, 311, 312, 1153
383, 297, 327, 467, 433
384, 434, 688, 333, 334
385, 435, 1143, 339, 340
386, 315, 316, 1155, 457
387, 320, 460, 437, 319
388, 325, 220, 466, 465
389, 462, 355, 354, 459
390, 539, 640, 1189, 439
391, 569, 498, 499, 600
392, 356, 480, 481, 357
393, 222, 347, 453, 475
394, 782, 689, 591, 694
395, 443, 372, 222, 475
396, 1171, 191, 386, 364
397, 588, 481, 480, 578
398, 401, 488, 513, 402
399, 514, 517, 615, 571
400, 409, 520, 521, 370
401, 621, 623, 447, 521
402, 361, 532, 534, 420
403, 573, 566, 483, 448
404, 574, 449, 568, 677
405, 190, 294, 449, 574
406, 202, 575, 450, 638
407, 451, 363, 366, 485
408, 296, 533, 535, 422
409, 634, 1195, 452, 535
410, 547, 470, 477, 584
411, 1159, 442, 433, 650
412, 552, 1152, 456, 644
413, 436, 1154, 457, 554
414, 317, 458, 1155, 316
415, 479, 458, 317, 318
416, 1176, 460, 461, 438
417, 459, 354, 353, 553
418, 461, 460, 320, 321
419, 647, 437, 460, 1176
420, 816, 651, 773, 974
421, 465, 466, 581, 651
422, 372, 443, 1162, 580
423, 463, 648, 1176, 438
424, 443, 475, 586, 686
425, 445, 562, 603, 391
426, 1145, 556, 1156, 582
427, 331, 332, 556, 1145
428, 1150, 1144, 557, 646
429, 328, 348, 477, 470
430, 584, 477, 476, 1179
431, 338, 557, 1144, 337
432, 341, 335, 472, 558
433, 470, 547, 649, 1164
434, 1139, 221, 473, 1141
435, 474, 577, 1161, 453
436, 585, 373, 374, 489
437, 432, 587, 1174, 455
438, 437, 647, 1178, 479
439, 732, 555, 651, 816
440, 618, 551, 652, 718
441, 535, 533, 548, 634
442, 637, 485, 537, 484
443, 589, 451, 485, 637
444, 549, 629, 723, 653
445, 486, 300, 369, 529
446, 550, 572, 682, 654
447, 400, 508, 512, 398
448, 612, 613, 512, 508
449, 603, 562, 655, 659
450, 593, 490, 492, 592
451, 592, 492, 491, 595
452, 596, 494, 427, 563
453, 493, 594, 595, 491
454, 494, 596, 594, 493
455, 599, 496, 497, 598
456, 656, 563, 597, 699
457, 454, 192, 598, 497
458, 495, 597, 563, 427
459, 192, 454, 498, 569
460, 600, 499, 439, 1189
461, 601, 190, 574, 674
462, 657, 602, 501, 428
463, 658, 568, 602, 753
464, 502, 603, 659, 604
465, 604, 605, 503, 502
466, 504, 503, 605, 606
467, 538, 565, 660, 713
468, 506, 505, 607, 608
469, 509, 506, 608, 609
470, 507, 509, 609, 610
471, 616, 614, 515, 446
472, 571, 551, 482, 514
473, 404, 515, 516, 405
474, 538, 616, 446, 513
475, 665, 714, 614, 616
476, 622, 619, 522, 519
477, 619, 620, 520, 522
478, 521, 520, 620, 621
479, 519, 518, 618, 622
480, 572, 550, 487, 523
481, 525, 524, 624, 625
482, 526, 525, 625, 626
483, 626, 627, 527, 526
484, 627, 628, 528, 527
485, 628, 627, 662, 724
486, 417, 530, 531, 418
487, 531, 530, 630, 631
488, 631, 632, 532, 531
489, 448, 534, 633, 573
490, 484, 576, 636, 637
491, 664, 1169, 636, 1184
492, 713, 665, 616, 538
493, 1211, 663, 1194, 1212
494, 639, 204, 1163, 430
495, 1204, 1200, 817, 1191
496, 638, 567, 541, 817

497, 543, 207, 589, 1169
498, 650, 433, 1158, 1160
499, 579, 666, 462, 459
500, 476, 373, 585, 1179
501, 1161, 586, 475, 453
502, 734, 731, 663, 1211
503, 628, 629, 529, 528
504, 809, 189, 818, 735
505, 626, 625, 721, 722
506, 622, 618, 718, 667
507, 1152, 552, 587, 432
508, 553, 478, 1174, 668
509, 436, 554, 545, 1153
510, 457, 1155, 1177, 669
511, 672, 687, 770, 736
512, 670, 646, 558, 472
513, 688, 671, 1156, 556
514, 820, 1167, 670, 768
515, 1142, 435, 340, 342
516, 390, 352, 1146, 560
517, 561, 197, 757, 738
518, 561, 738, 739, 657
519, 570, 441, 481, 588
520, 570, 588, 687, 672
521, 697, 596, 563, 656
522, 564, 191, 1171, 701
523, 611, 612, 508, 511
524, 590, 613, 710, 675
525, 676, 1212, 548, 566
526, 674, 574, 677, 771
527, 678, 569, 600, 752
528, 666, 579, 765, 744
529, 466, 580, 680, 581
530, 614, 617, 516, 515
531, 661, 712, 615, 617
532, 632, 633, 534, 532
533, 683, 676, 566, 573
534, 751, 674, 771, 819
535, 575, 684, 641, 197
536, 576, 484, 536, 635
537, 1164, 740, 768, 670
538, 578, 480, 462, 666
539, 685, 553, 668, 1175
540, 742, 669, 767, 857
541, 580, 1162, 743, 680
542, 578, 666, 744, 679
543, 468, 469, 544, 467
544, 583, 737, 434, 471
545, 690, 1179, 585, 689
546, 650, 1160, 1180, 746
547, 489, 591, 689, 585
548, 691, 650, 746, 1181
549, 1186, 584, 1179, 690
550, 668, 1174, 587, 552
551, 511, 507, 610, 611
552, 660, 675, 747, 798
553, 591, 489, 490, 593
554, 736, 748, 655, 672
555, 696, 592, 595, 695
556, 693, 593, 592, 696
557, 594, 673, 695, 595
558, 596, 697, 673, 594
559, 749, 699, 698, 772
560, 750, 192, 569, 678
561, 701, 601, 674, 751
562, 1201, 752, 600, 1189
563, 701, 751, 1190, 564
564, 753, 602, 199, 847
565, 841, 890, 743, 1162
566, 1057, 1002, 1030, 1099
567, 702, 703, 605, 604
568, 505, 504, 606, 607
569, 606, 605, 703, 704
570, 607, 606, 704, 705
571, 608, 607, 705, 706
572, 609, 608, 706, 707
573, 610, 609, 707, 708
574, 611, 610, 708, 709
575, 709, 711, 612, 611
576, 675, 660, 565, 590
577, 613, 590, 510, 512
578, 761, 797, 661, 714
579, 617, 615, 517, 516
580, 714, 665, 756, 761
581, 667, 715, 619, 622
582, 620, 619, 715, 716
583, 716, 717, 621, 620
584, 523, 447, 623, 572
585, 623, 621, 717, 719
586, 654, 720, 624, 550
587, 625, 624, 720, 721
588, 629, 549, 486, 529
589, 653, 725, 630, 549
590, 725, 726, 631, 630
591, 726, 727, 632, 631
592, 728, 727, 203, 1224
593, 1194, 1185, 1195, 634
594, 635, 536, 452, 1195
595, 576, 635, 1184, 636
596, 1169, 589, 637, 636
597, 733, 541, 204, 1172
598, 540, 639, 664, 205
599, 639, 540, 1172, 204
600, 1215, 892, 1207, 775
601, 833, 1182, 1166, 1165
602, 582, 643, 1168, 544
603, 1143, 435, 645, 1149
604, 1150, 583, 471, 1144
605, 647, 859, 1205, 1178
606, 669, 742, 554, 457
607, 1203, 776, 742, 857
608, 555, 732, 1192, 648
609, 823, 740, 1170, 1173
610, 577, 1159, 650, 691
611, 1158, 544, 1168, 1160
612, 672, 655, 562, 570
613, 551, 571, 681, 652
614, 762, 848, 883, 803
615, 907, 893, 850, 730
616, 801, 837, 881, 774
617, 786, 697, 656, 729
618, 699, 597, 599, 698
619, 199, 602, 657, 739
620, 658, 760, 677, 568
621, 754, 937, 894, 866
622, 827, 761, 756, 844
623, 755, 762, 681, 712
624, 808, 810, 662, 722
625, 663, 205, 1185, 1194
626, 634, 548, 1212, 1194
627, 764, 756, 665, 713
628, 734, 1221, 775, 840
629, 715, 667, 766, 799
630, 767, 546, 1178, 1205
631, 1164, 670, 472, 470
632, 745, 1157, 768, 860
633, 1156, 671, 643, 582
634, 434, 737, 1151, 688
635, 679, 744, 829, 769
636, 830, 821, 770, 769
637, 771, 194, 861, 819
638, 794, 795, 710, 711

639, 1221, 734, 676, 683
640, 194, 771, 677, 760
641, 588, 578, 679, 687
642, 680, 743, 831, 773
643, 581, 680, 773, 651
644, 686, 841, 1162, 443
645, 712, 681, 571, 615
646, 682, 719, 801, 774
647, 727, 728, 633, 632
648, 1215, 775, 1221, 1224
649, 727, 726, 812, 203
650, 758, 776, 1203, 765
651, 1161, 577, 691, 1165
652, 689, 782, 777, 690
653, 583, 1150, 1167, 737
654, 694, 591, 593, 693
655, 547, 692, 779, 649
656, 692, 547, 584, 1186
657, 690, 777, 780, 1186
658, 821, 845, 736, 770
659, 659, 655, 748, 787
660, 673, 759, 783, 695
661, 695, 783, 784, 696
662, 697, 786, 759, 673
663, 700, 598, 192, 750
664, 729, 749, 835, 869
665, 1233, 835, 749, 772
666, 500, 601, 701, 1171
667, 604, 659, 787, 702
668, 781, 788, 703, 702
669, 704, 703, 788, 789
670, 705, 704, 789, 790
671, 706, 705, 790, 791
672, 707, 706, 791, 792
673, 708, 707, 792, 793
674, 793, 796, 709, 708
675, 711, 710, 613, 612
676, 711, 709, 796, 794
677, 714, 661, 617, 614
678, 799, 800, 716, 715
679, 800, 880, 882, 802
680, 800, 802, 717, 716
681, 652, 681, 762, 803
682, 667, 718, 804, 766
683, 719, 682, 572, 623
684, 774, 805, 654, 682
685, 720, 654, 805, 806
686, 721, 720, 806, 807
687, 627, 626, 722, 662
688, 807, 808, 722, 721
689, 724, 723, 629, 628
690, 189, 809, 763, 888
691, 724, 662, 810, 763
692, 735, 811, 725, 653
693, 811, 812, 726, 725
694, 728, 683, 573, 633
695, 772, 698, 700, 846
696, 759, 786, 838, 853
697, 641, 684, 730, 850
698, 540, 731, 642, 1172
699, 1176, 741, 859, 647
700, 1210, 829, 744, 765
701, 731, 734, 840, 642
702, 763, 809, 723, 724
703, 841, 686, 778, 918
704, 886, 885, 954, 895
705, 1025, 1014, 973, 198
706, 860, 768, 740, 823
707, 685, 1175, 776, 758
708, 554, 742, 776, 545
709, 1052, 1232, 996, 935
710, 765, 579, 685, 758
711, 1157, 1151, 820, 768
712, 863, 779, 692, 1199
713, 843, 747, 795, 876
714, 764, 856, 844, 756
715, 865, 870, 940, 896
716, 846, 700, 750, 922
717, 1233, 836, 915, 1237
718, 1202, 1217, 752, 1201
719, 897, 836, 846, 922
720, 1190, 1208, 1202, 640
721, 754, 694, 693, 785
722, 785, 693, 696, 784
723, 911, 848, 849, 925
724, 755, 849, 848, 762
725, 753, 854, 1213, 658
726, 761, 827, 855, 797
727, 766, 884, 858, 799
728, 798, 764, 713, 660
729, 899, 844, 856, 930
730, 859, 741, 900, 1205
731, 884, 766, 804, 824
732, 803, 804, 718, 652
733, 852, 1203, 857, 919
734, 643, 745, 834, 1168
735, 687, 679, 769, 770
736, 819, 861, 901, 1217
737, 1035, 1068, 984, 897
738, 995, 1219, 1015, 1206
739, 916, 954, 885, 825
740, 903, 862, 812, 811
741, 1200, 1204, 1207, 892
742, 638, 817, 1200, 202
743, 830, 912, 960, 904
744, 686, 586, 1166, 778
745, 1183, 908, 1173, 1170
746, 779, 1183, 1170, 649
747, 1186, 780, 1199, 692
748, 777, 815, 864, 780
749, 702, 787, 865, 781
750, 853, 867, 783, 759
751, 867, 868, 784, 783
752, 822, 1000, 961, 937
753, 845, 870, 748, 736
754, 826, 871, 789, 788
755, 872, 790, 789, 871
756, 873, 791, 790, 872
757, 874, 792, 791, 873
758, 877, 796, 793, 875
759, 675, 710, 795, 747
760, 876, 795, 794, 878
761, 875, 793, 792, 874
762, 797, 755, 712, 661
763, 747, 843, 879, 798
764, 799, 858, 880, 800
765, 881, 837, 951, 1240
766, 802, 801, 719, 717
767, 824, 804, 803, 883
768, 805, 825, 885, 806
769, 807, 806, 885, 886
770, 810, 887, 888, 763
771, 809, 735, 653, 723
772, 839, 832, 862, 903
773, 839, 903, 730, 684
774, 975, 977, 1016, 1035
775, 194, 760, 1214, 813
776, 993, 950, 931, 1012
777, 814, 199, 739, 842
778, 870, 865, 787, 748
779, 815, 777, 782, 866
780, 962, 828, 906, 980

781, 642, 840, 1204, 1191
782, 957, 956, 963, 926
783, 678, 752, 1217, 750
784, 819, 1217, 1202, 1208
785, 1167, 820, 1151, 737
786, 754, 785, 822, 937
787, 785, 784, 868, 822
788, 765, 1203, 852, 1210
789, 1187, 860, 823, 1188
790, 952, 884, 824, 924
791, 825, 805, 774, 881
792, 826, 788, 781, 936
793, 848, 911, 898, 883
794, 828, 741, 1192, 732
795, 913, 1017, 1034, 974
796, 769, 829, 912, 830
797, 890, 965, 831, 743
798, 773, 831, 913, 974
799, 892, 1215, 832, 839
800, 203, 812, 862, 832
801, 1187, 909, 1181, 746
802, 746, 1180, 834, 1187
803, 838, 869, 914, 917
804, 985, 982, 1024, 1019
805, 801, 802, 882, 837
806, 853, 838, 917, 927
807, 869, 838, 786, 729
808, 839, 202, 1200, 892
809, 863, 1199, 1209, 933
810, 1028, 1206, 997, 1027
811, 851, 738, 757, 1222
812, 919, 857, 900, 962
813, 912, 966, 1023, 960
814, 985, 1019, 1246, 976
815, 844, 899, 921, 827
816, 856, 764, 798, 879
817, 1018, 1091, 1020, 986
818, 1041, 1016, 977, 932
819, 847, 889, 968, 923
820, 849, 755, 797, 855
821, 921, 976, 991, 929
822, 197, 641, 1216, 757
823, 907, 730, 903, 811
824, 926, 850, 893, 957
825, 1230, 808, 807, 886
826, 1228, 1213, 854, 928
827, 827, 921, 929, 855
828, 843, 945, 949, 879
829, 857, 767, 1205, 900
830, 880, 858, 953, 931
831, 900, 741, 828, 962
832, 194, 813, 932, 861
833, 935, 815, 866, 894
834, 998, 936, 896, 940
835, 193, 970, 927, 917
836, 1096, 1086, 1099, 1030
837, 869, 835, 939, 914
838, 871, 905, 941, 872
839, 942, 873, 872, 941
840, 943, 874, 873, 942
841, 878, 794, 796, 877
842, 1006, 947, 946, 1005
843, 944, 875, 874, 943
844, 946, 877, 875, 944
845, 877, 946, 947, 878
846, 931, 950, 882, 880
847, 837, 882, 950, 951
848, 924, 824, 883, 898
849, 953, 858, 884, 952
850, 1241, 973, 1014, 964
851, 886, 895, 955, 1230
852, 1230, 887, 810, 808
853, 955, 1013, 963, 956
854, 955, 956, 887, 1230
855, 910, 814, 842, 902
856, 1080, 1036, 959, 1025
857, 822, 868, 891, 1000
858, 868, 867, 938, 891
859, 818, 189, 893, 907
860, 956, 957, 888, 887
861, 1054, 1000, 891, 958
862, 954, 916, 973, 1241
863, 851, 1222, 1235, 1229
864, 936, 781, 865, 896
865, 1226, 940, 870, 845
866, 772, 846, 836, 1233
867, 975, 922, 901, 977
868, 1049, 1070, 1064, 981
869, 976, 1246, 1022, 991
870, 930, 856, 879, 949
871, 902, 842, 851, 1229
872, 821, 830, 904, 1225
873, 871, 826, 979, 905
874, 826, 936, 999, 979
875, 919, 962, 980, 920
876, 1182, 918, 778, 1166
877, 833, 1181, 909, 1182
878, 889, 814, 910, 959
879, 925, 849, 855, 929
880, 911, 987, 981, 898
881, 919, 920, 1210, 852
882, 966, 1034, 1017, 1023
883, 949, 972, 982, 930
884, 917, 914, 983, 193
885, 836, 897, 984, 915
886, 982, 972, 1044, 1024
887, 916, 825, 881, 1240
888, 841, 986, 1020, 890
889, 920, 912, 829, 1210
890, 925, 969, 987, 911
891, 961, 988, 894, 937
892, 901, 922, 750, 1217
893, 923, 990, 928, 854
894, 990, 1043, 1228, 928
895, 1216, 1235, 1222, 757
896, 1235, 1216, 926, 963
897, 867, 853, 927, 938
898, 970, 1026, 938, 927
899, 1214, 1213, 1228, 989
900, 976, 921, 899, 985
901, 945, 843, 876, 948
902, 992, 939, 967, 1050
903, 952, 1010, 1011, 953
904, 989, 994, 813, 1214
905, 863, 933, 995, 1193
906, 935, 996, 864, 815
907, 934, 1188, 1027, 997
908, 1193, 1028, 908, 1183
909, 998, 940, 1001, 1056
910, 961, 1021, 1029, 988
911, 1069, 1054, 958, 1096
912, 1237, 939, 835, 1233
913, 1226, 978, 1001, 940
914, 1002, 942, 941, 1243
915, 1030, 1002, 1243, 1085
916, 1003, 943, 942, 1002
917, 878, 947, 948, 876
918, 1007, 1006, 1031, 1062
919, 1004, 944, 943, 1003
920, 1005, 946, 944, 1004
921, 1005, 1060, 1031, 1006
922, 947, 1006, 1007, 948

923, 950, 993, 1009, 951
924, 198, 1240, 951, 1009
925, 924, 898, 981, 1064
926, 993, 1012, 1033, 1051
927, 964, 1013, 955, 895
928, 957, 893, 189, 888
929, 891, 938, 1026, 958
930, 966, 912, 920, 980
931, 999, 936, 998, 1234
932, 974, 1034, 906, 816
933, 902, 964, 1014, 910
934, 1013, 964, 902, 1229
935, 913, 831, 965, 1106
936, 986, 841, 918, 1018
937, 980, 906, 1034, 966
938, 967, 939, 1237, 915
939, 975, 1035, 897, 922
940, 889, 959, 1036, 968
941, 1040, 1046, 969, 991
942, 969, 925, 929, 991
943, 1003, 1002, 1057, 1038
944, 971, 941, 905, 1039
945, 1039, 905, 979, 999
946, 972, 949, 945, 1008
947, 948, 1007, 1008, 945
948, 973, 916, 1240, 198
949, 959, 910, 1014, 1025
950, 977, 901, 861, 932
951, 1040, 991, 1022, 1082
952, 930, 982, 985, 899
953, 994, 1041, 932, 813
954, 1042, 1225, 904, 960
955, 1173, 1027, 1188, 823
956, 1173, 908, 1028, 1027
957, 990, 1048, 1072, 1043
958, 992, 983, 914, 939
959, 915, 984, 1045, 967
960, 1218, 1198, 1206, 1015
961, 1046, 1040, 195, 1094
962, 935, 894, 988, 1052
963, 1047, 1098, 1074, 1238
964, 1043, 1075, 989, 1228
965, 1048, 968, 1036, 1088
966, 1010, 952, 924, 1064
967, 1049, 981, 987, 1037
968, 953, 1011, 1012, 931
969, 1092, 1090, 1131, 1107
970, 1193, 995, 1206, 1028
971, 1209, 864, 996, 1219
972, 1196, 1197, 918, 1182
973, 1055, 1108, 1056, 1001
974, 1077, 1098, 1108, 1227
975, 1038, 1032, 1004, 1003
976, 1032, 1087, 1248, 1060
977, 1059, 1058, 193, 983
978, 1005, 1004, 1032, 1060
979, 1062, 1031, 1103, 1079
980, 1062, 1063, 1008, 1007
981, 1051, 1080, 1009, 993
982, 1010, 1064, 1065, 1244
983, 1244, 1066, 1011, 1010
984, 933, 1209, 1219, 995
985, 1055, 1129, 1227, 1108
986, 1035, 1016, 1122, 1068
987, 965, 890, 1020, 1106
988, 1042, 1071, 1097, 978
989, 1104, 1024, 1044, 1251
990, 1119, 1081, 1019, 1083
991, 960, 1023, 1071, 1042
992, 999, 1234, 1053, 1039
993, 1021, 961, 1000, 1054
994, 1022, 1081, 1120, 1082
995, 1071, 1023, 1106, 1132
996, 1251, 1044, 1063, 1249
997, 198, 1009, 1080, 1025
998, 1247, 1087, 1084, 1110
999, 1197, 1196, 934, 997
1000, 1188, 934, 909, 1187
1001, 1085, 971, 1242, 1113
1002, 1026, 970, 1089, 1086
1003, 1061, 1059, 983, 992
1004, 1110, 1084, 1089, 1058
1005, 923, 968, 1048, 990
1006, 1036, 1080, 1051, 1088
1007, 1245, 1118, 1127, 1112
1008, 1058, 1089, 970, 193
1009, 1075, 1090, 994, 989
1010, 1123, 1068, 1122, 1128
1011, 1132, 1106, 1020, 1091
1012, 1111, 1236, 1112, 1127
1013, 1128, 1122, 1092, 1107
1014, 1045, 984, 1068, 1123
1015, 1037, 987, 969, 1046
1016, 1047, 1234, 998, 1056
1017, 1070, 1093, 1065, 1064
1018, 1037, 1046, 1094, 1049
1019, 967, 1045, 1095, 1050
1020, 1088, 1051, 1033, 1117
1021, 1098, 1077, 1029, 1074
1022, 1124, 1116, 1220, 1129
1023, 1021, 1239, 1074, 1029
1024, 1086, 1096, 958, 1026
1025, 1055, 1001, 978, 1097
1026, 1056, 1108, 1098, 1047
1027, 1057, 1099, 1084, 1087
1028, 1100, 1061, 1102, 1114
1029, 1038, 1057, 1087, 1032
1030, 1061, 992, 1050, 1102
1031, 1076, 1114, 1103, 1031
1032, 972, 1008, 1063, 1044
1033, 1079, 1249, 1063, 1062
1034, 1105, 1065, 1093, 1115
1035, 1066, 1244, 1065, 1105
1036, 1012, 1011, 1066, 1033
1037, 1117, 1033, 1066, 1105
1038, 1067, 1116, 1073, 1223
1039, 1067, 1223, 1231, 1232
1040, 1090, 1092, 1041, 994
1041, 1118, 1082, 1120, 1134
1042, 1021, 1054, 1069, 1239
1043, 1093, 1112, 1236, 1115
1044, 1048, 1088, 1117, 1072
1045, 1018, 1198, 1218, 1073
1046, 1015, 1223, 1073, 1218
1047, 1239, 1113, 1238, 1074
1048, 1076, 1031, 1060, 1248
1049, 1100, 1078, 1059, 1061
1050, 1077, 1052, 988, 1029
1051, 1058, 1059, 1078, 1110
1052, 1106, 1023, 1017, 913
1053, 1081, 1022, 1246, 1019
1054, 1082, 1118, 195, 1040
1055, 1119, 1083, 1104, 1121
1056, 1126, 1136, 1121, 1104
1057, 1099, 1086, 1089, 1084
1058, 1085, 1243, 941, 971
1059, 1242, 971, 1039, 1053
1060, 1096, 1030, 1085, 1069
1061, 1250, 1101, 1078, 1100
1062, 1127, 1107, 1131, 1111
1063, 1073, 1116, 1091, 1018
1064, 1092, 1122, 1016, 1041

1065, 1112, 1093, 1070, 1245
1066, 1070, 1049, 1094, 1245
1067, 1071, 1132, 1124, 1097
1068, 1250, 1100, 1114, 1076
1069, 1050, 1095, 1125, 1102
1070, 1126, 1103, 1114, 1136
1071, 1024, 1104, 1083, 1019
1072, 1117, 1105, 1115, 1072
1073, 1111, 1131, 1090, 1075
1074, 1133, 1120, 1081, 1119
1075, 1129, 1055, 1097, 1124
1076, 1109, 1067, 1232, 1052
1077, 1052, 1077, 1227, 1109
1078, 1247, 1110, 1078, 1101
1079, 1111, 1075, 1043, 1236
1080, 1069, 1085, 1113, 1239
1081, 1053, 1238, 1113, 1242
1082, 1072, 1115, 1236, 1043
1083, 1129, 1220, 1109, 1227
1084, 1133, 1130, 1135, 1137
1085, 1125, 1095, 1135, 1130
1086, 1127, 1118, 1134, 1107
1087, 1126, 1104, 1251, 1249
1088, 1130, 1121, 1136, 1125
1089, 1045, 1123, 1135, 1095
1090, 1091, 1116, 1124, 1132
1091, 1079, 1103, 1126, 1249
1092, 1136, 1114, 1102, 1125
1093, 1133, 1137, 1134, 1120
1094, 1130, 1133, 1119, 1121
1095, 1137, 1135, 1123, 1128
1096, 1134, 1137, 1128, 1107
1097, 1146, 293, 292, 363
1098, 1147, 429, 1163, 204
1099, 431, 306, 307, 1148
1100, 478, 1148, 455, 1174
1101, 473, 645, 559, 1141
1102, 1167, 1150, 646, 670
1103, 671, 688, 1151, 1157
1104, 1152, 310, 311, 456
1105, 1154, 314, 315, 457
1106, 1159, 577, 474, 442
1107, 740, 1164, 649, 1170
1108, 586, 1161, 1165, 1166
1109, 1165, 691, 1181, 833
1110, 1168, 834, 1180, 1160
1111, 863, 1193, 1183, 779
1112, 834, 745, 860, 1187
1113, 205, 664, 1184, 1185
1114, 1185, 1184, 635, 1195
1115, 1201, 1189, 640, 1202
1116, 1191, 817, 541, 733
1117, 1196, 1182, 909, 934
1118, 1197, 1198, 1018, 918
1119, 997, 1206, 1198, 1197
1120, 1209, 1199, 780, 864
1121, 1175, 644, 545, 776
1122, 1207, 1204, 840, 775
1123, 1208, 1190, 751, 819
1124, 676, 734, 1211, 1212
1125, 760, 658, 1213, 1214
1126, 1224, 203, 832, 1215
1127, 1223, 1015, 1219, 1231
1128, 732, 816, 906, 828
1129, 1220, 1116, 1067, 1109
1130, 1224, 1221, 683, 728
1131, 1231, 1219, 996, 1232
1132, 845, 821, 1225, 1226
1133, 1235, 963, 1013, 1229
1134, 1225, 1042, 978, 1226
1135, 1234, 1047, 1238, 1053
1136, 895, 954, 1241, 964
1137, 1245, 1094, 195, 1118
1138, 1248, 1087, 1247, 1101
1139, 1250, 1076, 1248, 1101
1140, 7, 166, 1252, 1279
1141, 1292, 1317, 170, 171
1142, 1253, 1292, 171, 172
1143, 172, 173, 1291, 1253
1144, 175, 176, 1289, 1254
1145, 1331, 1332, 1385, 1387
1146, 1273, 1287, 8, 180
1147, 182, 183, 1295, 1256
1148, 30, 29, 1297, 1369
1149, 9, 1, 157, 1257
1150, 1285, 1286, 159, 160
1151, 11, 10, 1258, 1259
1152, 12, 11, 1259, 1260
1153, 13, 12, 1260, 1261
1154, 1282, 1281, 1319, 1322
1155, 1261, 1262, 14, 13
1156, 1262, 1263, 15, 14
1157, 1263, 1264, 16, 15
1158, 18, 17, 1265, 1266
1159, 19, 18, 1266, 1267
1160, 1348, 1265, 1264, 1347
1161, 20, 19, 1267, 1268
1162, 21, 20, 1268, 1269
1163, 22, 21, 1269, 1270
1164, 23, 22, 1270, 1271
1165, 1256, 1275, 181, 182
1166, 1271, 1272, 24, 23
1167, 1375, 1374, 1386, 1444
1168, 1272, 1274, 25, 24
1169, 1274, 1276, 26, 25
1170, 1278, 1295, 183, 184
1171, 165, 7, 1279, 1280
1172, 1280, 1281, 164, 165
1173, 1283, 1282, 1322, 1323
1174, 1284, 1283, 1323, 1324
1175, 1284, 1285, 160, 161
1176, 157, 158, 1325, 1257
1177, 1273, 1275, 1356, 1376
1178, 178, 179, 1255, 1288
1179, 1288, 1327, 177, 178
1180, 174, 175, 1254, 1290
1181, 1253, 1291, 1350, 1328
1182, 166, 167, 1294, 1252
1183, 28, 27, 1277, 1296
1184, 29, 28, 1296, 1297
1185, 185, 186, 1299, 1298
1186, 1298, 1278, 184, 185
1187, 32, 31, 1300, 1303
1188, 1301, 1299, 186, 187
1189, 55, 1302, 188, 3
1190, 2, 32, 1303, 33
1191, 1329, 1297, 1296, 1330
1192, 1330, 1296, 1277, 1357
1193, 1333, 1272, 1271, 1337
1194, 1269, 1335, 1334, 1270
1195, 1411, 1708, 1424, 1711
1196, 1340, 1293, 1388, 1418
1197, 1274, 1332, 1331, 1276
1198, 1304, 1305, 42, 41
1199, 1326, 1366, 1255, 1287
1200, 1305, 1306, 43, 42
1201, 1378, 1295, 1278, 1380
1202, 1307, 1308, 45, 44
1203, 1308, 1309, 46, 45
1204, 1309, 1343, 1338, 1310
1205, 49, 48, 1311, 1312
1206, 50, 49, 1312, 1313

1207, 1339, 1313, 1312, 1359
1208, 1314, 1315, 52, 51
1209, 1302, 1301, 187, 188
1210, 1293, 1340, 168, 169
1211, 1264, 1265, 17, 16
1212, 1347, 1346, 1414, 1389
1213, 1275, 1273, 180, 181
1214, 1337, 1334, 1410, 1390
1215, 1308, 1321, 1343, 1309
1216, 1257, 1258, 10, 9
1217, 161, 162, 1283, 1284
1218, 162, 163, 1282, 1283
1219, 1261, 1361, 1344, 1262
1220, 1281, 1280, 1345, 1319
1221, 1361, 1261, 1260, 1362
1222, 1346, 1263, 1262, 1344
1223, 1263, 1346, 1347, 1264
1224, 1336, 1267, 1266, 1320
1225, 41, 40, 1351, 1304
1226, 40, 39, 1352, 1351
1227, 1272, 1333, 1332, 1274
1228, 1391, 1351, 1352, 1408
1229, 1354, 1353, 38, 37
1230, 179, 8, 1287, 1255
1231, 1451, 1427, 1425, 1487
1232, 27, 26, 1276, 1277
1233, 1275, 1256, 1377, 1356
1234, 1358, 1355, 36, 35
1235, 1252, 1294, 1341, 1360
1236, 1280, 1279, 1706, 1345
1237, 163, 164, 1281, 1282
1238, 1393, 1319, 1345, 1422
1239, 1402, 1322, 1319, 1393
1240, 1435, 1395, 1363, 1364
1241, 1257, 1325, 1364, 1258
1242, 1324, 1365, 1285, 1284
1243, 1258, 1364, 1363, 1259
1244, 158, 159, 1286, 1325
1245, 1306, 1307, 44, 43
1246, 1327, 1289, 176, 177
1247, 1318, 1367, 1290, 1254
1248, 173, 174, 1290, 1291
1249, 1328, 1396, 1292, 1253
1250, 1317, 1293, 169, 170
1251, 1320, 1348, 1423, 1397
1252, 1340, 1294, 167, 168
1253, 1309, 1310, 47, 46
1254, 1303, 1368, 34, 33
1255, 1440, 1407, 1300, 1369
1256, 51, 50, 1313, 1314
1257, 1313, 1339, 1370, 1314
1258, 1407, 1368, 1303, 1300
1259, 31, 30, 1369, 1300
1260, 55, 54, 1372, 1302
1261, 1315, 1316, 53, 52
1262, 1452, 1442, 1404, 1470
1263, 1342, 1305, 1304, 1419
1264, 1305, 1342, 1374, 1306
1265, 1417, 1377, 1378, 1445
1266, 1376, 1429, 1399, 1326
1267, 1295, 1378, 1377, 1256
1268, 48, 47, 1310, 1311
1269, 1298, 1381, 1380, 1278
1270, 1339, 1359, 1400, 1441
1271, 1382, 1449, 1401, 1381
1272, 1302, 1372, 1383, 1301
1273, 1315, 1371, 1384, 1316
1274, 1301, 1383, 1382, 1299
1275, 54, 53, 1316, 1372
1276, 1254, 1289, 1373, 1318
1277, 1432, 1706, 1360, 1484
1278, 1322, 1402, 1394, 1323
1279, 1320, 1266, 1265, 1348
1280, 1321, 1308, 1307, 1375
1281, 1375, 1307, 1306, 1374
1282, 1421, 1414, 1346, 1344
1283, 1259, 1363, 1362, 1260
1284, 1366, 1404, 1288, 1255
1285, 1396, 1411, 1453, 1405
1286, 1501, 1385, 1406, 1466
1287, 1368, 1358, 35, 34
1288, 1357, 1277, 1276, 1331
1289, 1353, 1352, 39, 38
1290, 1408, 1352, 1353, 1426
1291, 1337, 1271, 1270, 1334
1292, 1462, 1491, 1545, 1713
1293, 1442, 1452, 1508, 1373
1294, 1334, 1335, 1412, 1410
1295, 1478, 1471, 1510, 1509
1296, 1335, 1269, 1268, 1349
1297, 1479, 1397, 1423, 1463
1298, 1349, 1268, 1267, 1336
1299, 1336, 1320, 1397, 1413
1300, 1403, 1421, 1344, 1361
1301, 1471, 1457, 1532, 1510
1302, 1310, 1338, 1379, 1311
1303, 1343, 1321, 1420, 1416
1304, 1445, 1378, 1380, 1448
1305, 1359, 1312, 1311, 1379
1306, 1453, 1525, 1511, 1477
1307, 1419, 1304, 1351, 1391
1308, 1321, 1375, 1444, 1420
1309, 1279, 1252, 1360, 1706
1310, 1434, 1403, 1361, 1362
1311, 1394, 1402, 1483, 1459
1312, 1348, 1347, 1389, 1423
1313, 1367, 1350, 1291, 1290
1314, 1478, 1412, 1415, 1471
1315, 1357, 1331, 1387, 1425
1316, 37, 36, 1355, 1354
1317, 1455, 1461, 1408, 1426
1318, 1330, 1357, 1425, 1427
1319, 1491, 1498, 1512, 1545
1320, 1356, 1398, 1429, 1376
1321, 1358, 1430, 1428, 1355
1322, 1338, 1343, 1416, 1446
1323, 1513, 1476, 1485, 1569
1324, 1323, 1394, 1433, 1324
1325, 1464, 1495, 1494, 1540
1326, 1286, 1435, 1364, 1325
1327, 1365, 1435, 1286, 1285
1328, 1324, 1433, 1436, 1365
1329, 1400, 1431, 1505, 1465
1330, 1326, 1399, 1437, 1366
1331, 1410, 1458, 1460, 1390
1332, 1439, 1430, 1358, 1368
1333, 1297, 1329, 1440, 1369
1334, 1370, 1371, 1315, 1314
1335, 1299, 1382, 1381, 1298
1336, 1404, 1442, 1327, 1288
1337, 1342, 1419, 1467, 1443
1338, 1376, 1326, 1287, 1273
1339, 1503, 1474, 1445, 1448
1340, 1379, 1338, 1446, 1431
1341, 1469, 1500, 1514, 1555
1342, 1383, 1384, 1449, 1382
1343, 1383, 1372, 1316, 1384
1344, 1450, 1449, 1384, 1371
1345, 1332, 1333, 1406, 1385
1346, 1333, 1337, 1390, 1406
1347, 1374, 1342, 1443, 1386
1348, 1396, 1405, 1317, 1292

1349, 1424, 1350, 1367, 1438
1350, 1529, 1531, 1556, 1561
1351, 1438, 1409, 1486, 1456
1352, 1386, 1497, 1502, 1444
1353, 1461, 1472, 1391, 1408
1354, 1354, 1392, 1426, 1353
1355, 1392, 1354, 1355, 1428
1356, 1487, 1454, 1524, 1515
1357, 1422, 1345, 1706, 1432
1358, 1484, 1360, 1341, 1493
1359, 1395, 1434, 1362, 1363
1360, 1435, 1365, 1436, 1395
1361, 1708, 1411, 1396, 1328
1362, 1480, 1414, 1421, 1482
1363, 1356, 1377, 1417, 1398
1364, 1552, 1516, 1468, 1474
1365, 1475, 1420, 1444, 1502
1366, 1359, 1379, 1431, 1400
1367, 1441, 1447, 1370, 1339
1368, 1381, 1401, 1448, 1380
1369, 1485, 1422, 1432, 1519
1370, 1481, 1475, 1546, 1553
1371, 1405, 1388, 1293, 1317
1372, 1550, 1499, 1427, 1451
1373, 1318, 1409, 1438, 1367
1374, 1409, 1318, 1373, 1508
1375, 1335, 1349, 1415, 1412
1376, 1413, 1457, 1471, 1415
1377, 1349, 1336, 1413, 1415
1378, 1463, 1423, 1389, 1473
1379, 1482, 1421, 1403, 1464
1380, 1418, 1341, 1294, 1340
1381, 1452, 1470, 1518, 1710
1382, 1481, 1416, 1420, 1475
1383, 1414, 1480, 1473, 1389
1384, 1493, 1341, 1418, 1707
1385, 1519, 1432, 1484, 1537
1386, 1409, 1508, 1520, 1486
1387, 1487, 1425, 1387, 1454
1388, 1462, 1489, 1428, 1430
1389, 1713, 1488, 1489, 1462
1390, 1329, 1330, 1427, 1499
1391, 1445, 1474, 1468, 1417
1392, 1491, 1462, 1430, 1439
1393, 1431, 1446, 1504, 1505
1394, 1547, 1707, 1477, 1511
1395, 1567, 1592, 1527, 1509
1396, 1394, 1459, 1494, 1433
1397, 1395, 1436, 1495, 1434
1398, 1433, 1494, 1495, 1436
1399, 1523, 1443, 1467, 1548
1400, 1439, 1368, 1407, 1709
1401, 1491, 1439, 1709, 1498
1402, 1400, 1465, 1500, 1441
1403, 1442, 1373, 1289, 1327
1404, 1566, 1714, 1512, 1550
1405, 1497, 1386, 1443, 1523
1406, 1450, 1506, 1401, 1449
1407, 1416, 1481, 1504, 1446
1408, 1371, 1370, 1447, 1450
1409, 1506, 1503, 1448, 1401
1410, 1447, 1469, 1506, 1450
1411, 1454, 1387, 1385, 1501
1412, 1426, 1392, 1488, 1455
1413, 1470, 1404, 1366, 1437
1414, 1405, 1453, 1477, 1388
1415, 1711, 1525, 1453, 1411
1416, 1455, 1488, 1716, 1521
1417, 1456, 1711, 1424, 1438
1418, 1457, 1413, 1397, 1479
1419, 1542, 1543, 1586, 1558
1420, 1509, 1527, 1458, 1478
1421, 1458, 1410, 1412, 1478
1422, 1483, 1402, 1393, 1476
1423, 1476, 1393, 1422, 1485
1424, 1535, 1497, 1523, 1575
1425, 1390, 1460, 1466, 1406
1426, 1472, 1467, 1419, 1391
1427, 1464, 1403, 1434, 1495
1428, 1429, 1398, 1490, 1492
1429, 1554, 1551, 1465, 1505
1430, 1549, 1527, 1592, 1560
1431, 1468, 1490, 1398, 1417
1432, 1469, 1447, 1441, 1500
1433, 1399, 1429, 1492, 1496
1434, 1457, 1479, 1542, 1532
1435, 1533, 1472, 1461, 1526
1436, 1541, 1540, 1565, 1562
1437, 1518, 1544, 1563, 1717
1438, 1476, 1513, 1536, 1483
1439, 1562, 1564, 1534, 1541
1440, 1496, 1544, 1437, 1399
1441, 1489, 1488, 1392, 1428
1442, 1512, 1498, 1499, 1550
1443, 1475, 1502, 1522, 1546
1444, 1540, 1494, 1459, 1565
1445, 1544, 1518, 1470, 1437
1446, 1548, 1467, 1472, 1533
1447, 1460, 1458, 1527, 1549
1448, 1499, 1498, 1440, 1329
1449, 1500, 1465, 1551, 1514
1450, 1587, 1517, 1627, 1597
1451, 1552, 1555, 1514, 1593
1452, 1504, 1530, 1554, 1505
1453, 1503, 1555, 1552, 1474
1454, 1451, 1487, 1515, 1614
1455, 1716, 1715, 1720, 1521
1456, 1568, 1519, 1537, 1721
1457, 1569, 1485, 1519, 1568
1458, 1712, 1493, 1707, 1547
1459, 1456, 1599, 1525, 1711
1460, 1714, 1566, 1557, 1574
1461, 1463, 1473, 1538, 1543
1462, 1534, 1538, 1473, 1480
1463, 1454, 1501, 1529, 1524
1464, 1524, 1529, 1561, 1571
1465, 1539, 1517, 1492, 1490
1466, 1490, 1468, 1516, 1539
1467, 1496, 1492, 1517, 1587
1468, 1537, 1484, 1493, 1712
1469, 1598, 1569, 1568, 1731
1470, 1508, 1452, 1710, 1520
1471, 1455, 1521, 1526, 1461
1472, 1714, 1574, 1722, 1507
1473, 1502, 1497, 1535, 1522
1474, 1501, 1466, 1531, 1529
1475, 1576, 1526, 1521, 1720
1476, 1528, 1599, 1456, 1486
1477, 1571, 1561, 1622, 1600
1478, 1510, 1532, 1573, 1577
1479, 1572, 1578, 1520, 1710
1480, 1539, 1516, 1584, 1579
1481, 1481, 1553, 1530, 1504
1482, 1466, 1460, 1549, 1531
1483, 1615, 1557, 1566, 1614
1484, 1480, 1482, 1541, 1534
1485, 1523, 1548, 1581, 1575
1486, 1483, 1536, 1565, 1459
1487, 1582, 1536, 1513, 1624
1488, 1619, 1573, 1558, 1626
1489, 1543, 1542, 1479, 1463
1490, 1482, 1464, 1540, 1541

1491, 1538, 1534, 1564, 1585
1492, 1627, 1579, 1647, 1633
1493, 1713, 1545, 1507, 1715
1494, 1522, 1559, 1588, 1546
1495, 1732, 1616, 1734, 1603
1496, 1591, 1580, 1631, 1604
1497, 1509, 1510, 1577, 1567
1498, 1611, 1560, 1592, 1617
1499, 1614, 1566, 1550, 1451
1500, 1593, 1584, 1516, 1552
1501, 1555, 1503, 1506, 1469
1502, 1606, 1589, 1588, 1559
1503, 1530, 1594, 1595, 1554
1504, 1607, 1595, 1594, 1629
1505, 1535, 1575, 1742, 1608
1506, 1531, 1549, 1560, 1556
1507, 1714, 1507, 1545, 1512
1508, 1574, 1557, 1620, 1726
1509, 1558, 1573, 1532, 1542
1510, 1612, 1618, 1572, 1717
1511, 1522, 1535, 1608, 1559
1512, 1652, 1617, 1621, 1654
1513, 1591, 1581, 1548, 1533
1514, 1564, 1562, 1582, 1625
1515, 1597, 1718, 1563, 1587
1516, 1544, 1496, 1587, 1563
1517, 1729, 1636, 1725, 1625
1518, 1543, 1538, 1585, 1586
1519, 1536, 1582, 1562, 1565
1520, 1583, 1590, 1603, 1734
1521, 1621, 1567, 1577, 1602
1522, 1712, 1583, 1721, 1537
1523, 1547, 1590, 1583, 1712
1524, 1624, 1729, 1625, 1582
1525, 1570, 1511, 1525, 1599
1526, 1515, 1637, 1615, 1614
1527, 1515, 1524, 1571, 1637
1528, 1723, 1638, 1718, 1597
1529, 1586, 1613, 1626, 1558
1530, 1722, 1720, 1715, 1507
1531, 1580, 1591, 1533, 1526
1532, 1526, 1576, 1727, 1580
1533, 1620, 1601, 1662, 1736
1534, 1650, 1640, 1618, 1612
1535, 1578, 1528, 1486, 1520
1536, 1553, 1589, 1594, 1530
1537, 1517, 1539, 1579, 1627
1538, 1726, 1620, 1736, 1639
1539, 1575, 1604, 1623, 1742
1540, 1624, 1513, 1569, 1598
1541, 1590, 1547, 1511, 1570
1542, 1554, 1595, 1596, 1551
1543, 1546, 1588, 1589, 1553
1544, 1589, 1606, 1629, 1594
1545, 1570, 1599, 1719, 1728
1546, 1609, 1631, 1580, 1727
1547, 1661, 1737, 1639, 1736
1548, 1749, 1659, 1623, 1738
1549, 1593, 1514, 1551, 1596
1550, 1632, 1596, 1595, 1607
1551, 1584, 1593, 1596, 1632
1552, 1733, 1734, 1616, 1658
1553, 1528, 1578, 1610, 1649
1554, 1622, 1561, 1556, 1605
1555, 1605, 1556, 1560, 1611
1556, 1601, 1620, 1557, 1615
1557, 1601, 1615, 1637, 1662
1558, 1602, 1577, 1573, 1619
1559, 1619, 1653, 1643, 1602
1560, 1590, 1570, 1728, 1603
1561, 1664, 1724, 1719, 1649
1562, 1611, 1635, 1644, 1605
1563, 1581, 1591, 1604, 1575
1564, 1617, 1592, 1567, 1621
1565, 1628, 1606, 1559, 1746
1566, 1608, 1751, 1746, 1559
1567, 1607, 1641, 1647, 1632
1568, 1645, 1644, 1665, 1671
1569, 1612, 1718, 1638, 1650
1570, 1680, 1666, 1723, 1633
1571, 1586, 1585, 1725, 1613
1572, 1585, 1564, 1625, 1725
1573, 1568, 1721, 1733, 1731
1574, 1602, 1643, 1654, 1621
1575, 1618, 1610, 1578, 1572
1576, 1653, 1657, 1743, 1667
1577, 1653, 1619, 1626, 1657
1578, 1630, 1724, 1655, 1730
1579, 1631, 1609, 1642, 1738
1580, 1634, 1658, 1616, 1730
1581, 1633, 1647, 1641, 1680
1582, 1738, 1623, 1604, 1631
1583, 1606, 1628, 1660, 1629
1584, 1579, 1584, 1632, 1647
1585, 1651, 1660, 1628, 1739
1586, 1597, 1627, 1633, 1723
1587, 1730, 1655, 1677, 1634
1588, 1656, 1642, 1745, 1683
1589, 1635, 1611, 1617, 1652
1590, 1613, 1725, 1636, 1735
1591, 1735, 1658, 1743, 1657
1592, 1637, 1571, 1600, 1662
1593, 1736, 1662, 1681, 1661
1594, 1659, 1608, 1742, 1623
1595, 1726, 1639, 1609, 1727
1596, 1622, 1645, 1648, 1600
1597, 1689, 1688, 1740, 1741
1598, 1610, 1618, 1640, 1673
1599, 1641, 1607, 1629, 1660
1600, 1656, 1749, 1738, 1642
1601, 1605, 1644, 1645, 1622
1602, 1656, 1683, 1682, 1753
1603, 1650, 1638, 1686, 1672
1604, 1746, 1646, 1739, 1628
1605, 1648, 1681, 1662, 1600
1606, 1599, 1528, 1649, 1719
1607, 1659, 1752, 1751, 1608
1608, 1660, 1651, 1680, 1641
1609, 1739, 1674, 1684, 1651
1610, 1654, 1643, 1676, 1675
1611, 1626, 1613, 1735, 1657
1612, 1667, 1676, 1643, 1653
1613, 1675, 1669, 1652, 1654
1614, 1730, 1616, 1732, 1630
1615, 1702, 1696, 1693, 1695
1616, 1636, 1729, 1731, 1733
1617, 1634, 1678, 1743, 1658
1618, 1752, 1668, 1679, 1646
1619, 1737, 1661, 1745, 1642
1620, 1671, 1663, 1648, 1645
1621, 1744, 1745, 1661, 1681
1622, 1644, 1635, 1670, 1665
1623, 1649, 1610, 1673, 1664
1624, 1747, 1676, 1667, 1690
1625, 1635, 1652, 1669, 1670
1626, 1666, 1686, 1638, 1723
1627, 1659, 1749, 1668, 1752
1628, 1694, 1697, 1704, 1741
1629, 1748, 1698, 1682, 1683
1630, 1648, 1663, 1744, 1681
1631, 1640, 1650, 1672, 1688
1632, 1679, 1692, 1693, 1674

```
1633, 1646, 1679, 1674, 1739
1634, 1688, 1689, 1673, 1640
1635, 1677, 1690, 1678, 1634
1636, 1678, 1690, 1667, 1743
1637, 1689, 1699, 1664, 1673
1638, 1750, 1747, 1690, 1697
1639, 1663, 1671, 1748, 1683
1640, 1685, 1687, 1670, 1669
1641, 1668, 1753, 1692, 1679
1642, 1696, 1684, 1674, 1693
1643, 1651, 1684, 1666, 1680
1644, 1753, 1682, 1703, 1692
1645, 1695, 1705, 1740, 1702
1646, 1670, 1687, 1691, 1665
1647, 1698, 1701, 1703, 1682
1648, 1747, 1669, 1675, 1676
1649, 1686, 1666, 1684, 1696
1650, 1703, 1701, 1705, 1695
1651, 1750, 1685, 1669, 1747
1652, 1699, 1689, 1741, 1704
1653, 1704, 1677, 1655, 1699
1654, 1698, 1748, 1691, 1687
1655, 1700, 1694, 1705, 1701
1656, 1696, 1702, 1672, 1686
1657, 1750, 1700, 1687, 1685
1658, 1695, 1693, 1692, 1703
1659, 1700, 1750, 1697, 1694
1660, 1697, 1690, 1677, 1704
1661, 1701, 1698, 1687, 1700
1662, 1699, 1655, 1724, 1664
1663, 1688, 1672, 1702, 1740
1664, 1740, 1705, 1694, 1741
1665, 1707, 1418, 1388, 1477
1666, 1708, 1328, 1350, 1424
1667, 1709, 1407, 1440, 1498
1668, 1710, 1518, 1717, 1572
1669, 1488, 1713, 1715, 1716
1670, 1717, 1563, 1718, 1612
1671, 1630, 1728, 1719, 1724
1672, 1576, 1720, 1722, 1574
1673, 1576, 1574, 1726, 1727
1674, 1603, 1728, 1630, 1732
1675, 1729, 1624, 1598, 1731
1676, 1734, 1733, 1721, 1583
1677, 1735, 1636, 1733, 1658
1678, 1737, 1642, 1609, 1639
1679, 1745, 1744, 1663, 1683
1680, 1748, 1671, 1665, 1691
1681, 1749, 1656, 1753, 1668
1682, 1646, 1746, 1751, 1752
*Nset, nset=_PICKEDSET18, internal, generate
    1,  1753,     1
*Elset, elset=_PICKEDSET18, internal,
generate
    1,  1682,     1
** Section: substrate
*Solid Section, elset=_PICKEDSET18,
material=SUBSTRATE
,
*End Part
**
**
** ASSEMBLY
**
*Assembly, name=Assembly
**
*Instance, name=COAT-1, part=COAT
*End Instance
**
*Instance, name=SUB-1, part=SUB
*End Instance
**
*Instance, name=INTERLAY-1, part=INTERLAY
*End Instance
**
*Elset, elset=_SURF-COATIN_S1, internal,
instance=COAT-1
   1,   2,   3,   4,   5,   6,   7,   8,
9,  10,  11,  12,  13,  14,  15,  16
  17,  18,  19,  20,  21,  22,  23,  24,
25,  26,  27,  28,  29,  30,  31,  32
  33,  34,  35,  36,  37,  38,  39,  40,
41,  42,  43,  44,  45,  46,  47,  48
  49,  50,  51,  52,  53,  54,  55,  56,
57,  58,  59,  60, 181, 182, 183, 184
 185, 186, 187, 188, 189, 190, 191, 192,
193, 194, 195, 196, 197, 198, 199, 200
 201, 202, 203, 204, 205, 206, 207, 208,
209, 210, 211, 212, 213, 214, 215, 286
 287, 288, 289, 290, 291, 292, 293, 294,
295, 296, 297, 298, 299, 300, 301, 302
 303, 304, 305, 306, 307, 308, 309, 310
*Elset, elset=_SURF-SUBOUT_S2, internal,
instance=SUB-1
    1,   20,   22,   77,   96,   98,  110,
190,  194,  198,  282, 1149
*Elset, elset=_SURF-SUBOUT_S4, internal,
instance=SUB-1
  82,  88,  99, 100, 101, 102, 103, 104,
105, 106, 107, 108, 109, 111
*Elset, elset=_SURF-SUBOUT_S1, internal,
instance=SUB-1
   34,   39,   75,   93,  116,  120,  122,
127,  133,  136,  137,  138,  139,  140,
141,  142
  146,  147,  148,  149,  150,  153,  154,
155,  156,  213,  219,  232,  240,  243,
304, 1140
 1143, 1144, 1147, 1171, 1176, 1178, 1180,
1182, 1185, 1217, 1218, 1230, 1237, 1244,
1248
*Elset, elset=_SURF-SUBOUT_S3, internal,
instance=SUB-1
   12,   13,   44,   49,  125,  126,  128,
129,  130,  131,  134,  135,  144,  145,
152,  158
  159,  160,  161,  163,  164,  177,  179,
217,  224,  227,  237,  280,  307, 1141,
1142, 1146
 1150, 1165, 1170, 1172, 1175, 1179, 1186,
1188, 1189, 1209, 1210, 1213, 1246, 1250,
1252
*Nset, nset=_PickedSet35, internal,
instance=COAT-1, generate
   1,  484,    1
*Nset, nset=_PickedSet35, internal,
instance=SUB-1, generate
    1,  1753,     1
*Nset, nset=_PickedSet38, internal,
instance=COAT-1, generate
   1,  484,    1
*Nset, nset=_PickedSet38, internal,
instance=SUB-1, generate
    1,  1753,     1
*Elset, elset=cohesive, instance=INTERLAY-1,
generate
   1,  120,    1
*Surface, type=element, name=cohesivein
cohesive, S1
*Surface, type=element, name=cohesiveout
cohesive, S3
```

```
*Nset, nset=_PickedSet42, internal,
instance=COAT-1
  11,  12, 249, 250
*Nset, nset=_PickedSet42, internal,
instance=SUB-1
  4,  5, 80, 81, 82, 83, 84, 85, 86, 87, 88,
89, 90
*Nset, nset=_PickedSet42, internal,
instance=INTERLAY-1
   11, 1011
*Nset, nset=_PickedSet43, internal,
instance=COAT-1
  2,  3, 72, 73
*Nset, nset=_PickedSet43, internal,
instance=SUB-1
  5,  6, 91, 92, 93, 94, 95, 96, 97
*Nset, nset=_PickedSet43, internal,
instance=INTERLAY-1
    2, 1002
*Elset, elset=_SURF-COATIN_S1_1, internal,
instance=COAT-1
   1,   2,   3,   4,   5,   6,   7,   8,
9,  10,  11,  12,  13,  14,  15,  16
  17,  18,  19,  20,  21,  22,  23,  24,
25,  26,  27,  28,  29,  30,  31,  32
  33,  34,  35,  36,  37,  38,  39,  40,
41,  42,  43,  44,  45,  46,  47,  48
  49,  50,  51,  52,  53,  54,  55,  56,
57,  58,  59,  60, 181, 182, 183, 184
 185, 186, 187, 188, 189, 190, 191, 192,
193, 194, 195, 196, 197, 198, 199, 200
 201, 202, 203, 204, 205, 206, 207, 208,
209, 210, 211, 212, 213, 214, 215, 286
 287, 288, 289, 290, 291, 292, 293, 294,
295, 296, 297, 298, 299, 300, 301, 302
 303, 304, 305, 306, 307, 308, 309, 310
*Surface, type=ELEMENT, name=SURF-COATIN
_SURF-COATIN_S1_1, S1
*Elset, elset=_SURF-SUBOUT_S2_1, internal,
instance=SUB-1
    1,   20,   22,   77,   96,   98,  110,
190,  194,  198,  282, 1149
*Elset, elset=_SURF-SUBOUT_S4_1, internal,
instance=SUB-1
  82,  88,  99, 100, 101, 102, 103, 104,
105, 106, 107, 108, 109, 111
*Elset, elset=_SURF-SUBOUT_S1_1, internal,
instance=SUB-1
   34,   39,   75,   93,  116,  120,  122,
127,  133,  136,  137,  138,  139,  140,
141,  142
  146,  147,  148,  149,  150,  153,  154,
155,  156,  213,  219,  232,  240,  243,
304, 1140
 1143, 1144, 1147, 1171, 1176, 1178, 1180,
1182, 1185, 1217, 1218, 1230, 1237, 1244,
1248
*Elset, elset=_SURF-SUBOUT_S3_1, internal,
instance=SUB-1
   12,   13,   44,   49,  125,  126,  128,
129,  130,  131,  134,  135,  144,  145,
152,  158
  159,  160,  161,  163,  164,  177,  179,
217,  224,  227,  237,  280,  307, 1141,
1142, 1146
 1150, 1165, 1170, 1172, 1175, 1179, 1186,
1188, 1189, 1209, 1210, 1213, 1246, 1250,
1252
*Surface, type=ELEMENT, name=SURF-SUBOUT
_SURF-SUBOUT_S2_1, S2
_SURF-SUBOUT_S4_1, S4
_SURF-SUBOUT_S1_1, S1
_SURF-SUBOUT_S3_1, S3
** Constraint: TIE1
*Tie, name=TIE1, adjust=yes
cohesiveout, SURF-COATIN
** Constraint: TIE2
*Tie, name=TIE2, adjust=yes
SURF-SUBOUT, cohesivein
** Constraint: TIE3
*Tie, name=TIE3, adjust=yes
SURF-COATIN, SURF-SUBOUT
*End Assembly
**
** MATERIALS
**
*Material, name=COAT
*Conductivity
900.,
*Density
 3.5e-09,
*Elastic
 1.2e+06, 0.07
*Expansion
 2.5e-06,
*Specific Heat
 5.09e+08,
** COMMENTS FROM *DAMAGE INITIATION
** ================================
**
** Change cohesive zone prop with 0.10
energy
*Material, name=COHESIVE
*Damage Initiation, criterion=MAXS
500.,100000.,     0.
*Damage Evolution, type=ENERGY
 0.1,
*Density
 7.9e-09,
*Elastic, type=TRACTION
 5e+06, 5e+06,    0.
*Material, name=SUBSTRATE
*Conductivity
 84.02,
*Density
 1.58e-08,
*Elastic
620000., 0.24
*Expansion
 5.5e-06,
*Plastic
   5760.,   0.
 5863.27, 0.01
 6943.71, 0.02
 7665.81, 0.03
 8223.34, 0.04
 8683.38, 0.05
  9078.4, 0.06
 9426.36, 0.07
 9738.55, 0.08
 10022.5, 0.09
*Specific Heat
 2e+08,
**
** INTERACTION PROPERTIES
**
*Surface Interaction, name=CSUB
**
** BOUNDARY CONDITIONS
**
** Name: Disp-BC Type: Displacement/Rotation
*Boundary
```

```
_PickedSet42, 1, 1
** Name: Disp-BC2 Type:
Displacement/Rotation
*Boundary
_PickedSet43, 2, 2
**
** PREDEFINED FIELDS
**
** Name: Field-1   Type: Temperature
*Initial Conditions, type=TEMPERATURE
_PickedSet38, 600.
** ----------------------------------------
----------------------
**
** STEP: depositionstep
**
*Step, name=depositionstep
*Dynamic Temperature-displacement, Explicit,
element by element
, 0.001
*Bulk Viscosity
0.06, 1.2
**
** BOUNDARY CONDITIONS
**
** Name: Temp-BC-1 Type: Temperature
*Boundary
_PickedSet35, 11, 11, 20.
**
** INTERACTIONS
**
** Interaction: Int-1
*Contact Pair, interaction=CSUB, mechanical
constraint=PENALTY, cpset=Int-1
SURF-COATIN, SURF-SUBOUT
**
** OUTPUT REQUESTS
**
*Restart, write, number interval=1, time
marks=NO
**
** FIELD OUTPUT: F-Output-1
**
*Output, field, number interval=100
*Node Output
NT, RF, RT, U
*Element Output, directions=YES
DAMAGEC, DAMAGEFC, DAMAGEFT, DAMAGEMC,
DAMAGEMT, DAMAGESHR, DAMAGET, DMICRT, E, LE,
MISESMAX, PE, PEEQ, S, SDEG, STATUS
*Contact Output
CSTRESS,
**
** HISTORY OUTPUT: H-Output-1
**
*Output, history, variable=PRESELECT,
frequency=1
*End Step
```

APPENDIX C

CUTTING SIMULATION AND WORKPIECE WITHDRAWAL

SIMULATION INCLUDING COHESIVE ZONE AND

DEPOSITION RESIDUAL STRESS

```
*Heading
** Job name: re50t15v5h45e100s500tm600 Model
name: re50t15v5h45e100retracts500mtm600
** Generated by: Abaqus/CAE 6.10-1
*Preprint, echo=NO, model=NO, history=NO,
contact=NO
**
** PARTS
**
*Part, name=WP
*Node
      1,  0.421485752, -0.573579609
      2,  0.402500004,  -0.56629163
      3,  0.391506523, -0.558304429
      4,  0.378708363, -0.542500019
      5,  0.373181313,   -0.5300861
      6,  0.435000002, -0.574999988
      7,  0.370000005,  -0.50999999
      8,  0.370000005,   0.13047953
      9,  0.370000005,  0.774999976
     10, -0.0799999982,  0.774999976
     11, -0.0799999982,  0.275000006
     12,  -0.40196386, -0.117314115
     13, -0.257771909, -0.0575878434
     14, -0.197157294, -0.0078427121
     15, -0.147412151, 0.0527719073
     16, -0.0876858905,  0.196963876
     17, -0.479999989,       -0.125
     18,  -2.03723645,       -0.125
     19,  -1.28249323,       -0.125
     20,  -2.77999997,       -0.125
     21,  -2.77999997,       -1.625
     22,  -2.77999997,       -0.875
     23,  -2.77999997,       -2.375
     24,  0.970000029,       -2.375
     25,  0.219999999,       -2.375
     26, -0.529999971,       -2.375
     27,  -1.27999997,       -2.375
     28,  -2.02999997,       -2.375
     29,   1.72000003,       -2.375
     30,   1.72000003,  -1.17499995
     31,   1.72000003,  -1.77499998
     32,   1.72000003, -0.574999988
     33,   1.09272826, -0.574999988
     34,  -2.20576119, -0.319220603
     35,   0.20840162,  -0.28882426
     36, -0.322988957, -0.338156313
     37, -0.794494033, -0.382509112
     38,  -1.28426182, -0.277434498
     39,  -1.71325302, -0.301485866
     40,  -2.15037298, -0.925972641
     41,  -1.77768159, -0.907275558
     42,   -1.1520257, -0.974444866
     43, -0.801568925,  -1.05430448
     44, -0.373209834, -0.886909425
     45,  0.192131385,  -0.81155616
     46,   0.71651566, -0.844932795
     47,   1.16883564, -0.800727844
     48,  0.222138137,  0.226247236
     49,  -2.23884392,  -1.54614902
     50,  -1.78220248,  -1.45743454
     51,  -1.20654345,  -1.40759695
     52, -0.723003924,  -1.52867424
     53, -0.247071952,  -1.48916304
     54,    0.2902987,   -1.5074079
     55,  0.712060153,  -1.37280738
     56,   1.18801665,  -1.40777826
     57,  -2.21892524,  -1.93037724
     58,  -1.82209134,  -1.92087221
     59,  -1.28134859,  -1.88187933
     60, -0.739479661,   -1.9353435
     61, -0.319753915,  -1.90621912
     62,  0.746367514,  -1.92520118
     63,   1.15974867,  -1.72594583
     64,  0.428205639,  -0.57464391
     65,  0.414913893,  -0.57181865
     66,  0.408562124, -0.569380462
     67,  0.396793962, -0.562586129
     68,  0.386695594,   -0.5534935
     69,  0.382413894, -0.548206031
     70,  0.375619531, -0.536437869
     71,  0.371420413, -0.523514271
     72,  0.370356083, -0.516794324
     73,  0.370000005,  0.701585948
     74,  0.370000005,  0.631566107
     75,  0.370000005,  0.564783573
     76,  0.370000005,   0.50108856
     77,  0.370000005,  0.440338403
     78,  0.370000005,  0.382396966
     79,  0.370000005,  0.327134341
     80,  0.370000005,  0.274426728
     81,  0.370000005,  0.224155948
     82,  0.370000005,  0.176209375
     83,  0.370000005, 0.0868639424
     84,  0.370000005, 0.0452648625
     85,  0.370000005, 0.00558904745
     86,  0.370000005, -0.0322524123
     87,  0.370000005, -0.0683443323
     88,  0.370000005, -0.102767594
     89,  0.370000005, -0.135599345
     90,  0.370000005, -0.166913167
     91,  0.370000005, -0.196779251
     92,  0.370000005, -0.225264519
     93,  0.370000005, -0.252432793
     94,  0.370000005, -0.278345019
     95,  0.370000005, -0.303059191
     96,  0.370000005, -0.326630771
     97,  0.370000005,  -0.34911254
     98,  0.370000005, -0.370554894
     99,  0.370000005, -0.391005903
    100,  0.370000005, -0.410511404
    101,  0.370000005, -0.429115057
    102,  0.370000005, -0.446858644
    103,  0.370000005, -0.463781834
    104,  0.370000005, -0.479922652
    105,  0.370000005, -0.495317191
    106, -0.0157142859,  0.774999976
    107, 0.0485714301,  0.774999976
    108,  0.112857141,  0.774999976
    109,  0.177142859,  0.774999976
    110,  0.241428569,  0.774999976
    111,  0.305714279,  0.774999976
    112, -0.0799999982,  0.346428573
    113, -0.0799999982,   0.41785714
    114, -0.0799999982,  0.489285707
    115, -0.0799999982,  0.560714304
    116, -0.0799999982,  0.632142842
    117, -0.0799999982,  0.703571439
    118, -0.326926619, -0.0945518166
    119, -0.110448189,  0.121926628
    120,  -2.58124685,       -0.125
    121,    -2.391469,       -0.125
    122,  -2.21026111,       -0.125
```

```
123,  -1.87202513,       -0.125
124,  -1.71427453,       -0.125
125,  -1.56364775,       -0.125
126,  -1.41982305,       -0.125
127,  -1.15136492,       -0.125
128,  -1.02615821,       -0.125
129, -0.906605721,       -0.125
130, -0.792451918,       -0.125
131, -0.683453202,       -0.125
132, -0.579376638,       -0.125
133,  -2.77999997,       -2.1875
134,  -2.77999997,            -2.
135,  -2.77999997,       -1.8125
136,  -2.77999997,       -1.4375
137,  -2.77999997,         -1.25
138,  -2.77999997,       -1.0625
139,  -2.77999997,       -0.6875
140,  -2.77999997,          -0.5
141,  -2.77999997,       -0.3125
142,   1.34500003,         -2.375
143,  0.595000029,         -2.375
144, -0.155000001,         -2.375
145, -0.904999971,         -2.375
146,  -1.65499997,         -2.375
147,  -2.40499997,         -2.375
148,   1.72000003, -0.725000024
149,   1.72000003,       -0.875
150,   1.72000003,  -1.02499998
151,   1.72000003,  -1.32500005
152,   1.72000003,  -1.47500002
153,   1.72000003,        -1.625
154,   1.72000003,  -1.92499995
155,   1.72000003,  -2.07500005
156,   1.72000003,   -2.2249999
157,  0.460572302, -0.574999988
158,  0.488405138, -0.574999988
159,  0.518698394, -0.574999988
160,  0.551669478, -0.574999988
161,   0.58755517, -0.574999988
162,  0.626613081, -0.574999988
163,  0.669123709, -0.574999988
164,  0.715392172, -0.574999988
165,  0.765750647, -0.574999988
166,  0.820560813, -0.574999988
167,  0.880216062, -0.574999988
168,  0.945144713, -0.574999988
169,   1.01581299, -0.574999988
170,   1.17644262, -0.574999988
171,   1.26755726, -0.574999988
172,    1.3667264, -0.574999988
173,   1.47466183, -0.574999988
174,   1.59213853, -0.574999988
175,   0.41810599, -0.587313771
176,  0.397725344, -0.573079109
177,  0.385787547, -0.564102173
178,  0.352360547, -0.495889515
179,  0.322561413,  0.179168552
180, -0.00115137873,  0.233623937
181, -0.0177297201,  0.136882812
182, -0.0949978828, -0.00951661263
183,  0.299350023,   -2.0415616
184, -0.235932469, -0.112365544
185, -0.479031503, -0.228225246
186, -0.578470409, -0.251004308
187,   -1.2984457,  -2.13700104
188,  -2.03302264, -0.315169662
189,  -2.57922626, -0.317685664
190,  -2.55900741, -0.912011147
191,  -2.59804821,  -1.60519171
192,   1.10199547, -0.647283733
193,   1.07156038,  -2.16310668
194,   1.57336926,  -1.18937087
195,   1.52516067,  -1.78048563
196,  0.427684426,  -0.59420836
197,  0.410706162,  -0.58209306
198,  0.404084474, -0.577499866
199,  0.391534984, -0.568703115
200,  0.380528957,   -0.5590505
201,  0.375625789, -0.553353608
202,   0.3668859, -0.540272832
203,  0.361949235, -0.525740623
204,  0.359331727, -0.518065512
205,  0.306166589,  0.634109855
206,  0.306627691,  0.567372859
207,  0.307993233,  0.503708422
208,  0.310217232,  0.443177998
209,  0.313156515,  0.385457546
210,  0.316103667,  0.330192775
211,  0.318496495,  0.277240962
212,  0.320429653,  0.226533622
213,  0.326015383,  0.134333283
214,  0.329995722, 0.0914868712
215,  0.333181739, 0.0507148542
216,  0.334514439, 0.0121415881
217,  0.335434079, -0.024351256
218,  0.336410135, -0.0599374771
219,  0.337470889, -0.0941767097
220,  0.338575572, -0.126974463
221,  0.339788765, -0.158403605
222,  0.341180474, -0.188592225
223,  0.342651814, -0.217462391
224,   0.34386459,  -0.24466522
225,  0.344684303, -0.270454407
226,  0.345509291, -0.295407295
227,  0.346448004,  -0.31954053
228,  0.347431839, -0.342590213
229,  0.348326683,  -0.36452648
230,  0.348993331, -0.385431111
231,  0.349290401, -0.405364275
232,   0.34908095, -0.424372911
233,  0.348253459, -0.442549407
234,  0.346628696, -0.460234672
235,  0.343877763, -0.478759706
236, 0.0478595942,  0.704355717
237,  0.112289332,  0.704464436
238,  0.176885471,  0.704515576
239,  0.241615459,  0.704366446
240,  0.306120425,  0.703548312
241, -0.0154023133,   0.29194051
242, -0.0214826446,  0.358290821
243, -0.0211971346,  0.424562931
244, -0.019259112,   0.49265191
245, -0.0177976098,  0.562529385
246, -0.0168897454,  0.633245766
247, -0.309254199, -0.157369852
248, -0.0539440177, 0.0756622478
249,  -1.86931884, -0.308916152
250,  -1.56348538, -0.293642461
251,  -1.42028975, -0.285509825
252,  -1.15445387, -0.270285666
253,  -1.02975035,  -0.26382339
254, -0.910201073, -0.258752406
255, -0.682720363, -0.254798859
256,  -2.50777531,  -2.00604081
257,  -2.57324004,   -1.7925539
258,   -2.6193769,  -1.42209029
259,  -2.65386415,  -1.26693499
260,   -2.5508616,  -1.14391434
261,  -2.56782889, -0.707921982
262,  -2.57461047, -0.511395872
263,   1.40291178,  -2.22609377
264,  0.672445595,  -2.13645148
```

265, -0.053887669, -2.02854466
266, -1.66668928, -2.09646964
267, -2.27717257, -2.12358332
268, 1.58157182, -0.859029412
269, 1.54119313, -1.02348042
270, 1.57847178, -1.3384521
271, 1.56891406, -1.48420644
272, 1.549999, -1.63118792
273, 1.4999938, -1.92756593
274, 1.46891892, -2.07627726
275, 0.469380856, -0.605444014
276, 0.497210085, -0.606160998
277, 0.527894676, -0.607818305
278, 0.561431944, -0.610208988
279, 0.597935498, -0.613079488
280, 0.637634397, -0.616334915
281, 0.68078655, -0.619880378
282, 0.727637827, -0.623599887
283, 0.77855134, -0.627485156
284, 0.833705485, -0.631324768
285, 0.893241584, -0.634985864
286, 0.957271814, -0.638556719
287, 1.02657533, -0.642403781
288, 1.1844666, -0.654533148
289, 1.27363932, -0.665172994
290, 1.37074912, -0.679680705
291, 1.47823536, -0.696940541
292, 1.59547925, -0.713444829
293, 0.363623202, -0.533165872
294, 0.0350949802, 0.36976102
295, 0.0603588894, 0.263229907
296, 0.297196716, 0.0530110598
297, -0.14653866, -0.13132678
298, 1.03132272, -0.710992396
299, 0.418822795, -0.607602
300, -2.37926197, -0.517444193
301, -1.85496497, -0.497416347
302, -2.19334245, -0.517199218
303, -2.39836788, -1.74864459
304, 1.2811718, -1.9165864
305, 1.38575709, -1.61721146
306, -0.450170636, -0.330936641
307, -1.55147433, -0.465066433
308, 0.289937049, 0.0912204012
309, 0.371053278, -0.547082603
310, 0.242234811, 0.567601025
311, 0.0407156534, 0.428917408
312, 0.248879492, 0.441928774
313, -0.795125127, -0.255880147
314, -2.37449932, -1.89406002
315, -2.36714768, -0.718291402
316, 1.4126569, -0.937470853
317, 1.44676828, -1.34822166
318, 1.3553586, -0.783013523
319, 0.379680455, -0.570684016
320, 0.0337226838, 0.182340592
321, 0.513667464, -1.83092308
322, -0.213288501, -0.173893183
323, -0.362503052, -0.273036897
324, -0.559401214, -0.407384515
325, -0.993293226, -1.92228329
326, -2.01808548, -0.510206103
327, -2.38781452, -0.320104063
328, -2.35276175, -0.923604548
329, 1.10307705, -0.718521178
330, 1.44289529, -1.22186482
331, 1.3329109, -1.76579189
332, 0.444491088, -0.605760872
333, 0.411087453, -0.597766697
334, 0.392834038, -0.579346359
335, 0.404779285, -0.590297043
336, 0.386224926, -0.57499665
337, 0.374015152, -0.565247178
338, 0.368794888, -0.558910191
339, 0.349084765, -0.521958768
340, 0.344533533, -0.512851536
341, 0.0462981835, 0.563551068
342, 0.0433543995, 0.312587798
343, 0.255710155, 0.384082913
344, 0.262665838, 0.329228729
345, 0.267779082, 0.277054369
346, 0.270115972, 0.226029456
347, 0.271262467, 0.17810601
348, 0.279710978, 0.133054614
349, 0.296975344, 0.0178176276
350, 0.0356610268, 0.0955015942
351, 0.298657864, -0.0176353715
352, 0.301508039, -0.0531582832
353, 0.30343017, -0.0871265233
354, 0.305447578, -0.119961679
355, 0.308052897, -0.151706025
356, 0.311312348, -0.182392538
357, 0.314471871, -0.211495891
358, 0.316322476, -0.238164723
359, 0.317970484, -0.263671398
360, 0.319995999, -0.289072096
361, 0.322128922, -0.313936204
362, 0.324264139, -0.337520689
363, 0.326226234, -0.359804511
364, 0.327855587, -0.380956382
365, 0.328875124, -0.401003689
366, 0.328930587, -0.419961631
367, 0.32781142, -0.437840462
368, 0.325261056, -0.454567283
369, 0.320736527, -0.469657898
370, 0.176631793, 0.634810805
371, 0.244430959, 0.502958
372, 0.111728005, 0.634250045
373, 0.0471487269, 0.633803189
374, -0.284682781, -0.221650153
375, -0.0211029369, -0.0218614973
376, -1.70056188, -0.482097059
377, -1.40882993, -0.448661834
378, -1.2750293, -0.432935774
379, -1.02434075, -0.402998894
380, -0.906787217, -0.391216695
381, -2.42348623, -1.57229733
382, -2.28488588, -1.34730363
383, -2.33119416, -1.13360548
384, -0.0451679714, -1.76734209
385, -1.55755782, -1.80922604
386, -2.00329208, -2.15377593
387, 1.40473533, -1.1097002
388, 1.42534447, -1.4797107
389, 0.477193654, -0.637978196
390, 0.50380218, -0.639002383
391, 0.53405422, -0.642200291
392, 0.567528903, -0.647035599
393, 0.60414809, -0.652979553
394, 0.644059241, -0.659731686
395, 0.687485218, -0.667072535
396, 0.734654367, -0.674800992
397, 0.78589344, -0.682768106
398, 0.841420889, -0.690702498
399, 0.901098073, -0.698182166
400, 0.964391589, -0.704888761
401, 1.18129909, -0.731051564
402, 1.26437926, -0.752576649
403, 1.4600631, -0.820875227
404, 0.17693463, 0.566173196
405, 0.137196824, -1.56610143
406, -1.12970603, -0.566964269

407, -0.748994172, -1.72951293
408, -0.959879041, -2.15531349
409, -1.38444412, -0.614824355
410, -1.24957502, -1.63348532
411, -1.82652318, -0.69403708
412, -2.01217246, -1.941993
413, -2.12733793, -1.12919962
414, 0.645243943, -1.67072189
415, 0.334152818, -0.51862818
416, 0.267204463, 0.0532380044
417, -0.126389414, -0.196442157
418, -0.466723979, -0.492298782
419, -0.681131423, -0.384250313
420, -1.99113429, -0.712445199
421, 0.481243551, -0.668991983
422, 0.36372596, -0.552122593
423, 0.351796627, -0.536231041
424, 0.112783059, 0.288829237
425, 0.00235161628, 0.04276691
426, 0.241584688, 0.634979129
427, 0.198237643, 0.376792312
428, 0.111533098, 0.494261593
429, -0.0826705396, -0.0999086574
430, -0.425967455, -2.08118534
431, 1.29696608, -1.45720613
432, 0.0964807272, 0.333976746
433, 0.252634019, 0.026441453
434, 0.266223192, -0.0485342219
435, 1.03225493, -0.783847809
436, -2.173805, -0.720306039
437, -1.5268358, -0.638221204
438, -2.21340728, -1.73594904
439, 0.954888821, -1.77319896
440, 0.802617133, -1.74662542
441, -0.396408707, -0.405078024
442, 0.209348753, 0.173199907
443, 0.25149709, 0.0828656107
444, 0.0803700984, 0.373207927
445, 1.32974553, -1.2480619
446, 1.23726666, -1.58048785
447, 1.23879886, -0.832393885
448, 0.0861092731, 0.21747376
449, 1.09877598, -0.789479911
450, 1.3318094, -1.34820426
451, 0.428224385, -0.622173905
452, 0.406367838, -0.616638362
453, 0.397675008, -0.596275687
454, 0.372817069, -0.579542756
455, 0.388371736, -0.585200071
456, 0.3667759, -0.571882904
457, 0.358319163, -0.544859827
458, 0.361717492, -0.564581335
459, 0.33837378, -0.502088487
460, 0.302039206, -0.464473784
461, 0.210803792, 0.323246956
462, 0.21972762, 0.274464041
463, 0.259528786, -0.0135440482
464, 0.267407, -0.0810448602
465, 0.270295918, -0.114609733
466, 0.274169236, -0.147307947
467, 0.280787051, -0.178947926
468, 0.286304176, -0.207520783
469, 0.286681563, -0.232349113
470, 0.28971085, -0.258166313
471, 0.293794453, -0.284389436
472, 0.29744944, -0.310084403
473, 0.300595105, -0.334054232
474, 0.30367896, -0.356605381
475, 0.30654195, -0.377895921
476, 0.308570772, -0.397775352
477, 0.309270144, -0.416322798
478, 0.308396429, -0.433613509
479, 0.305863738, -0.449641645
480, 0.328590274, -0.49146381
481, 0.178697705, 0.49900803
482, 0.184531912, 0.435406148
483, 0.111382641, 0.564357162
484, -0.253557533, -0.283264667
485, -1.67479503, -0.667202413
486, -1.25353515, -0.5929721
487, -1.00838971, -0.54220891
488, -0.788085401, -0.506343126
489, -0.276082367, -1.69727063
490, -1.78488338, -1.73149335
491, 0.455303729, -0.639921725
492, 0.507149637, -0.67213577
493, 0.536650836, -0.677607656
494, 0.569526613, -0.685226142
495, 0.605700672, -0.694529891
496, 0.645330906, -0.705119491
497, 0.688617289, -0.716615856
498, 0.735730708, -0.72867924
499, 0.787024438, -0.741087317
500, 0.842920184, -0.753694773
501, 0.903322697, -0.7658934
502, 0.966949046, -0.77645582
503, 0.521352887, -1.56196177
504, -0.568562329, -1.92507219
505, -0.529446959, -1.79016459
506, -0.990417719, -1.6886369
507, -2.03396034, -1.52196217
508, 0.748208225, -1.53191531
509, 0.220192239, 0.0633222088
510, 0.0835876465, 0.0624930859
511, 0.339159638, -0.529715121
512, 0.174804062, 0.266693443
513, 0.898757637, -0.837865651
514, 0.885843277, -1.58925581
515, -0.188094795, -0.23596774
516, -0.629262924, -0.571324229
517, 0.435760587, -0.6455459
518, 0.356832296, -0.557467461
519, 0.232181951, 0.12292774
520, 0.236283153, -0.0478820913
521, 0.318178892, -0.502393246
522, 0.112287194, 0.420549065
523, 0.226559758, -0.0732894689
524, -2.09502983, -1.32989728
525, -0.0472361483, -1.554708
526, -1.51204848, -1.55147803
527, 1.32389629, -1.03423119
528, 0.480394781, -0.698884845
529, 0.780989408, -0.802434504
530, 0.378107339, -1.67483342
531, -0.980938137, -0.674947143
532, -1.49070239, -0.804433167
533, -1.34913945, -0.785262167
534, -1.95265794, -0.924142897
535, 0.327088684, -0.510110617
536, -0.387273163, -0.540821791
537, 0.344837517, -0.544424057
538, 0.161057889, 0.310188025
539, -0.0233169477, -0.089974001
540, 0.143945038, 0.360321969
541, -0.0684930459, -0.167853832
542, 1.02716327, -1.65225482
543, 0.191195577, 0.0390390307
544, -0.276072025, -0.396849245
545, 0.161569729, 0.206171289
546, 1.22417998, -1.26055026
547, 1.24986756, -0.965761185
548, 0.0764621496, 0.138776362

549, 1.15199971, -0.855790555
550, 0.411378086, -0.63200736
551, 0.39234066, -0.621584713
552, 0.37446183, -0.589505672
553, 0.38926211, -0.599604845
554, 0.351468921, -0.550628722
555, 0.362193197, -0.585816383
556, 0.353929609, -0.569871426
557, 0.214848444, -0.0167043973
558, 0.234868452, -0.111243747
559, 0.236059919, -0.146922871
560, 0.251773655, -0.181240544
561, 0.2627168, -0.205514938
562, 0.250387341, -0.224535748
563, 0.260609359, -0.255649865
564, 0.268703938, -0.282280564
565, 0.273310781, -0.30810371
566, 0.275927097, -0.331996888
567, 0.280493885, -0.355277598
568, 0.285020471, -0.376679808
569, 0.288306653, -0.396069169
570, 0.285031319, -0.460919023
571, 0.289992213, -0.413927883
572, 0.289952666, -0.43055281
573, 0.288069487, -0.446209073
574, 0.312672824, -0.483758479
575, -0.216425046, -0.342025071
576, -1.09659219, -0.718066335
577, -0.867917717, -0.655985773
578, 0.459133357, -0.668277979
579, 0.506057203, -0.705061197
580, 0.534813702, -0.713544071
581, 0.56669873, -0.724485278
582, 0.601821661, -0.737581909
583, 0.640585303, -0.752492309
584, 0.68327719, -0.768680573
585, 0.729999781, -0.785585523
586, 0.837008655, -0.82007277
587, 1.03230655, -0.864538968
588, 0.272495329, -0.428924561
589, 0.633354247, -1.45505297
590, -0.224089354, -0.452432424
591, -0.494817108, -1.60844553
592, 0.191141218, 0.0995589569
593, 0.175144136, -0.0708733723
594, -0.701104581, -0.489117682
595, 0.458079427, -0.694864511
596, -0.0211981982, -1.39002061
597, -0.95171231, -0.785374105
598, -0.962989926, -1.46415401
599, -1.44688082, -1.32412672
600, -1.93572819, -1.30221748
601, 0.429451823, -1.43319988
602, 0.474936396, -0.727805853
603, -0.335693747, -0.461392581
604, 0.121284813, 0.174844623
605, 1.21565866, -1.13886285
606, 0.349801213, -0.562673748
607, 0.267905414, -0.396322608
608, 0.767107785, -0.866832554
609, -1.91887772, -1.13761723
610, 0.815558195, -1.40168476
611, 0.32584101, -0.531253576
612, 0.13243553, 0.245916113
613, 0.822672069, -0.888459146
614, 1.11339676, -1.32034445
615, -0.103018798, -0.254307508
616, 0.159622371, 0.137361839
617, 0.316344053, -0.519351721
618, 0.20299153, -0.0846186876
619, 0.110525474, -1.43375576
620, -0.843715727, -0.815866768
621, -1.32574356, -0.962998092
622, -0.51591146, -0.621755481
623, 0.335526496, -0.540622652
624, 0.0387773775, -0.0342231207
625, -0.0507449359, -0.224214122
626, -0.0145062609, -0.151044384
627, 0.155985147, 0.0691665858
628, 0.169462621, 0.00829406735
629, 0.118069395, 0.102080986
630, 1.03334498, -0.957359254
631, 1.15287352, -1.03844321
632, 0.415361375, -0.652341127
633, 0.394112468, -0.637285352
634, 0.379497379, -0.598458469
635, 0.37771529, -0.622766018
636, 0.345331341, -0.556415677
637, 0.370952278, -0.600080192
638, 0.339965761, -0.551468611
639, 0.348398119, -0.582784772
640, 0.190817356, -0.0446934551
641, 0.202644736, -0.107529655
642, 0.212515667, -0.16657798
643, 0.228847906, -0.192718327
644, 0.216757938, -0.233761355
645, 0.2367796, -0.260746598
646, 0.247974932, -0.283510417
647, 0.2507568, -0.306581795
648, 0.247678369, -0.331197768
649, 0.257111222, -0.35694325
650, 0.263244033, -0.377877951
651, 0.268769979, -0.458518922
652, 0.304319382, -0.497648478
653, 0.270897299, -0.413228601
654, 0.2714158, -0.444108546
655, 0.295929193, -0.479081541
656, -0.158461511, -0.294240981
657, 0.439152539, -0.669399261
658, 0.500293314, -0.737032056
659, 0.527853608, -0.749152303
660, 0.558068931, -0.7643466
661, 0.591305971, -0.781963766
662, 0.670342505, -0.823127747
663, 0.955772698, -0.938064158
664, -1.69039857, -1.17695177
665, -0.927265227, -1.22719491
666, 0.556037426, -1.35176253
667, -0.00108162058, -0.203270674
668, 0.127543345, 0.0342189521
669, 0.452021271, -0.72105515
670, 1.02450931, -1.08240044
671, -0.420919895, -0.646123767
672, 0.46634832, -0.755108893
673, 1.07304466, -1.20502687
674, 0.345197469, -0.574533641
675, 0.251972258, -0.415064663
676, -0.634482622, -0.716106296
677, -0.460945398, -1.41027546
678, -0.2033647, -1.28950286
679, -0.679959536, -1.32258308
680, 0.366196781, -1.30124652
681, -0.316626847, -0.573621571
682, -0.274873465, -0.510092199
683, -0.123809263, -0.346309304
684, 0.694285035, -0.907945216
685, 0.973515093, -1.42073405
686, 0.314582586, -0.531351268
687, 0.745103478, -0.935212672
688, -0.0757009462, -0.304300666
689, 0.299372464, -0.510870278
690, 0.168470293, -0.099858515

691, 0.209876224, -1.34228611
692, 0.0334334597, -0.0887642279
693, 0.129390225, -0.0940924287
694, 0.105449155, -0.00407165196
695, 0.150292605, -0.0237646047
696, 0.418604225, -0.673893511
697, 0.395241201, -0.657659292
698, 0.362364143, -0.620279193
699, 0.376799583, -0.638226509
700, 0.342168629, -0.567286968
701, 0.367246687, -0.608326197
702, 0.332699269, -0.548948944
703, 0.338591456, -0.561517417
704, 0.352046996, -0.592319667
705, 0.135923177, -0.0580154322
706, 0.167834699, -0.127483472
707, 0.187496737, -0.177061871
708, 0.178024411, -0.208213598
709, 0.184082597, -0.246298119
710, 0.223489627, -0.315512091
711, 0.226444989, -0.344019562
712, 0.23516652, -0.363049388
713, 0.246491536, -0.399174243
714, 0.253456444, -0.456929922
715, 0.256197929, -0.429007918
716, 0.256130844, -0.443062693
717, 0.280104071, -0.475105971
718, 0.287792563, -0.494492531
719, -0.173693851, -0.397047579
720, 0.438996792, -0.691878617
721, 0.490520865, -0.766683102
722, 0.515175223, -0.783007801
723, 0.542258561, -0.804043412
724, 0.607845366, -0.851347923
725, 0.648531675, -0.879434943
726, 0.862587571, -0.981915832
727, 0.929152846, -1.02290475
728, 0.130953833, -0.129565015
729, -0.543819904, -0.796948075
730, 0.442677975, -0.747510254
731, -0.0450508893, -0.345410168
732, 0.272452265, -0.489545494
733, -0.070450455, -1.18911374
734, -0.607191026, -1.1007905
735, 0.49252966, -1.24730182
736, 0.543261349, -0.873955846
737, 0.200762346, -0.317393512
738, -0.72463882, -0.760039985
739, -0.0295422655, -0.271967232
740, 0.0903724879, -0.0461800359
741, 0.324522913, -0.540460885
742, 0.358994991, -0.635650277
743, 0.219457567, -0.272806525
744, 0.301101089, -0.522537708
745, 0.477845967, -0.791841567
746, 0.141541481, -0.161611214
747, 0.949796915, -1.2674073
748, -0.335628003, -0.655018151
749, 0.337858647, -0.586627007
750, 0.218096882, -1.18612707
751, -0.262739301, -0.597748399
752, 0.686106563, -1.26602972
753, 0.660926044, -0.974052668
754, 0.0486884341, -0.189428017
755, 0.0383194052, -0.141714334
756, 0.423899263, -0.68979764
757, 0.396077037, -0.685281396
758, 0.375405639, -0.657166302
759, 0.341653347, -0.631085515
760, 0.336333185, -0.556737244
761, 0.334936887, -0.577905118
762, 0.3454763, -0.613071859
763, 0.0843264014, -0.0908402428
764, 0.16111806, -0.186947465
765, 0.159937039, -0.215290204
766, 0.203485385, -0.304942608
767, 0.212485448, -0.369579941
768, 0.216399729, -0.387295425
769, 0.223440647, -0.405032903
770, 0.243673995, -0.431594729
771, 0.242241308, -0.441949904
772, 0.239513755, -0.454177618
773, 0.264516294, -0.472156346
774, 0.279198617, -0.512398958
775, -0.167056009, -0.509219825
776, 0.432013661, -0.714575469
777, 0.457166404, -0.780331969
778, 0.495926231, -0.812396824
779, 0.616438448, -0.935323238
780, 0.578190267, -0.90038836
781, 0.865132987, -1.09098577
782, 0.918032229, -1.16145909
783, -0.416056871, -1.22259951
784, -0.236123696, -1.11636043
785, 0.163656652, -0.361583591
786, -0.217496291, -0.565307558
787, 0.672427237, -1.09499049
788, -0.421845198, -0.771551371
789, 0.101633668, -0.182193726
790, 0.476441681, -0.873507023
791, -0.0852569416, -0.389682323
792, -0.36157915, -1.07484913
793, 0.304120839, -0.531569242
794, 0.057928782, -0.23273401
795, 0.100889564, -1.16253984
796, 0.340334892, -0.5979352
797, 0.184717461, -0.394187719
798, 0.599112391, -1.17965508
799, 0.761860371, -1.1395309
800, -0.473121345, -0.969302416
801, -0.00559572317, -0.311951339
802, 0.382525444, -0.711925089
803, 0.43428579, -0.774837554
804, -0.328024834, -0.744172692
805, 0.218954936, -0.458215833
806, 0.33599478, -1.17098832
807, 0.611653626, -1.04051387
808, 0.401347131, -0.727450967
809, 0.3717843, -0.678895712
810, 0.355564386, -0.653428793
811, 0.286641359, -0.52900964
812, 0.32830286, -0.565867186
813, 0.328067631, -0.588527322
814, 0.139028072, -0.203468889
815, 0.132992998, -0.229521602
816, 0.179488525, -0.276687026
817, 0.18017453, -0.301616549
818, 0.166065693, -0.329207867
819, 0.200033337, -0.412941366
820, 0.231050432, -0.422894359
821, 0.228440776, -0.439820677
822, 0.261314631, -0.48371169
823, 0.314110219, -0.552027464
824, 0.26101163, -0.502602696
825, -0.125532463, -0.445586413
826, 0.421047926, -0.740492463
827, 0.469312727, -0.832137346
828, 0.570052087, -0.986239374
829, 0.547151685, -0.941642404
830, 0.832021058, -1.19780684
831, -0.133408234, -1.08077335
832, 0.5407511, -1.09812474

833, 0.497166425, -0.93471849
834, -0.263527393, -0.718526363
835, 0.214875028, -1.06620097
836, 0.0877874419, -0.136104465
837, 0.122613557, -1.06292689
838, 0.326399267, -0.61273241
839, 0.0330627449, -0.287454098
840, 0.146490067, -0.283117235
841, 0.0701108947, -0.270947635
842, 0.248228803, -0.471577495
843, 0.23204577, -0.467200726
844, 0.449188501, -0.803858817
845, -0.0130466791, -0.377875268
846, -0.0749536157, -0.478569716
847, 0.324865997, -0.555167735
848, 0.145810679, -0.384166241
849, -0.28435564, -0.824431121
850, 0.446708977, -1.14227235
851, 0.368732542, -0.734735727
852, 0.40646404, -0.776105106
853, 0.363163888, -0.700593352
854, 0.320878029, -0.579481006
855, 0.350503296, -0.672262013
856, 0.261882097, -0.526638091
857, 0.325690091, -0.598953485
858, 0.144771188, -0.342095286
859, 0.019883493, -0.345111042
860, 0.168816715, -0.416142493
861, 0.184273437, -0.422818005
862, 0.206840128, -0.429631889
863, 0.20282644, -0.470945001
864, 0.243647829, -0.490510225
865, 0.296559066, -0.542938352
866, -0.100755163, -0.564368784
867, 0.423198909, -0.88063848
868, 0.319290668, -1.03954136
869, 0.0852709115, -0.303502977
870, -0.170981854, -0.651341975
871, 0.229061484, -0.509276748
872, -0.301911622, -0.970639586
873, 0.193899319, -0.97518456
874, 0.122235678, -0.358086735
875, 0.417062074, -0.810395539
876, -0.0453951508, -0.4212192
877, 0.365768164, -0.774399281
878, 0.336770564, -0.648258507
879, 0.114476979, -0.399532795
880, 0.506511688, -1.0189085
881, 0.051827617, -1.04837918
882, 0.309601218, -0.569984853
883, 0.256982476, -0.549192011
884, -0.236877874, -1.019683
885, 0.375887364, -0.801756144
886, 0.351926297, -0.720647931
887, 0.309065431, -0.612443805
888, 0.31184724, -0.624262214
889, 0.343193591, -0.691176355
890, 0.221175864, -0.482674986
891, 0.0530121922, -0.320864856
892, 0.0194184594, -0.403124481
893, 0.158386901, -0.44080922
894, 0.189952746, -0.455585003
895, -0.0297454428, -0.546828628
896, 0.301586151, -0.557936192
897, -0.211109027, -0.756386578
898, 0.124559179, -0.431492805
899, 0.102414064, -0.332013309
900, 0.424502283, -1.04121614
901, 0.345365018, -0.785426438
902, 0.330465317, -0.665521443
903, 0.287160009, -0.567286789
904, 0.115981989, -0.291375011
905, 0.0743565634, -0.349397063
906, 0.0911111906, -0.409141243
907, 0.380498677, -0.896162868
908, 0.425971717, -0.954301655
909, -0.132920861, -0.821543992
910, 0.352623761, -0.75368154
911, 0.308291048, -0.594985604
912, 0.11500255, -0.977124214
913, 0.218181133, -0.53267312
914, 0.0710986853, -0.39398247
915, 0.0249205064, -0.968549132
916, 0.333475828, -0.818302155
917, 0.319072664, -0.642434359
918, 0.33431235, -0.709495246
919, -0.00471862126, -0.442580134
920, -0.0237837695, -0.49131313
921, 0.191205889, -0.523694456
922, -0.094188109, -0.706857502
923, 0.183047071, -0.488918543
924, -0.05128536, -0.630508661
925, 0.115618251, -0.904249668
926, 0.0867368579, -0.432869077
927, 0.353661925, -0.864056766
928, 0.361969084, -0.949241996
929, 0.280607969, -0.592025638
930, 0.0500851944, -0.883237004
931, 0.243848741, -0.570164084
932, 0.313405216, -0.78382045
933, 0.334464371, -0.769679189
934, 0.323108703, -0.683084071
935, 0.29155001, -0.601915419
936, 0.0518978089, -0.422081858
937, 0.23209165, -0.886345267
938, 0.202623233, -0.556132197
939, 0.339184046, -0.738412619
940, 0.140775844, -0.542761207
941, 0.29226616, -0.649454474
942, 0.0248976685, -0.497082949
943, -0.0241106469, -0.827522755
944, 0.157379389, -0.470559061
945, 0.244320333, -0.593668997
946, 0.0363387242, -0.457081705
947, 0.312874824, -0.903115332
948, 0.0210136622, -0.541855633
949, 0.145860985, -0.498541594
950, 0.143857166, -0.802943528
951, -0.0191455036, -0.731523931
952, 0.222480208, -0.566016555
953, 0.265653878, -0.608792722
954, 0.313710421, -0.741035402
955, 0.311664671, -0.763754785
956, 0.287759095, -0.6194489
957, 0.295276284, -0.694433451
958, 0.308643848, -0.717398167
959, 0.173674062, -0.567584455
960, 0.302921504, -0.675768435
961, 0.0344148427, -0.798120201
962, 0.116716124, -0.469415009
963, 0.230510518, -0.619946837
964, 0.0679585934, -0.500929236
965, 0.16895014, -0.822830439
966, 0.253462195, -0.629324675
967, 0.279370993, -0.843785286
968, 0.00817349833, -0.658883333
969, 0.0341161937, -0.594087362
970, 0.10535349, -0.57284075
971, 0.110070705, -0.512195408
972, 0.213877276, -0.588580489
973, 0.289340734, -0.735693514
974, 0.289679468, -0.7147035

975, 0.273796558, -0.639420688
976, 0.282684386, -0.668442488
977, 0.107822433, -0.763757765
978, 0.221522987, -0.64366436
979, 0.169037774, -0.855048835
980, 0.0783965886, -0.553088665
981, 0.0801858306, -0.614704728
982, 0.0456601083, -0.741989613
983, 0.279959619, -0.781129479
984, 0.242689341, -0.651745558
985, 0.201788604, -0.614572823
986, 0.208665892, -0.843912423
987, 0.274101526, -0.689736426
988, 0.164707512, -0.748347998
989, 0.117977098, -0.707001925
990, 0.195226923, -0.641828239
991, 0.126245424, -0.588498175
992, 0.237715945, -0.816818774
993, 0.0709005892, -0.675319016
994, 0.242286995, -0.711259484
995, 0.216196328, -0.663840055
996, 0.166521132, -0.607717514
997, 0.251621872, -0.684267402
998, 0.213279292, -0.801058531
999, 0.211378455, -0.774992764
1000, 0.163882986, -0.710325778
1001, 0.16323252, -0.643100977
1002, 0.207457349, -0.703925371
1003, 0.244550824, -0.779164732
1004, 0.241069034, -0.74345541
1005, 0.356544822, -0.509044111
1006, -0.016312819, 0.704105437
1007, -2.55870771, -2.18242693
1008, -0.38979581, -0.196862549
1009, -0.167854548, -0.0629226118
1010, -0.655495763, -2.14353871
1011, -1.14766598, -0.417807609
1012, 0.189954191, -1.76672804
1013, 0.353912294, -0.527970195
1014, 0.398959875, -0.584370196
1015, 0.401658595, -0.605198085
1016, 0.0448142253, 0.494257838
1017, -2.4624362, -1.37692642
1018, -2.0101912, -1.72861743
1019, 1.27547288, -2.03973818
1020, -0.893806338, -0.52376312
1021, 0.0563843735, 0.0172362011
1022, 1.03324974, -1.91731763
1023, 0.390484571, -0.609391332
1024, 0.381832093, -0.58164835
1025, 0.325410783, -0.523419201
1026, 0.3117145, -0.511110127
1027, 1.31722474, -0.879011095
1028, 1.31628895, -1.1688025
1029, -1.62967122, -0.855644047
1030, -1.2166996, -0.764534175
1031, -0.75777036, -0.625431955
1032, 0.393666923, -0.589882851
1033, 0.312536091, -0.542094946
1034, 0.357975155, -0.577780366
1035, 0.380164981, -0.5874511
1036, 0.384289891, -0.591080546
1037, 0.378750563, -0.610274076
1038, 1.1911155, -0.902024508
1039, 1.09778225, -0.864426494
1040, 0.96487838, -0.854466379
1041, 0.186103463, 0.232635781
1042, -0.659904242, -0.893981457
1043, 0.628572106, -0.801844478
1044, -1.03165364, -0.859175444
1045, 1.11628032, -0.945607603
1046, 0.0505121127, -1.27315974
1047, -1.45105314, -0.938175619
1048, -1.53843629, -1.03361762
1049, -1.36931992, -1.14038038
1050, -1.16833258, -1.19885039
1051, 0.366265446, -0.593981624
1052, 0.323900491, -0.54889369
1053, 0.413292855, -0.704397798
1054, 0.388927281, -0.59357816
1055, 0.386146367, -0.75389266
1056, 0.572658002, -0.827379942
1057, 0.0145707559, -0.248482496
1058, 0.885588229, -0.912251115
1059, 0.271438003, -0.53934741
1060, 0.247224972, -0.516539037
1061, 0.279626876, -0.553371489
1062, 0.800289452, -0.958297729
1063, 1.10455585, -1.51677477
1064, 1.24802423, -1.33721232
1065, -0.225020751, -0.896623731
1066, 0.0983152986, -0.226370737
1067, 0.00548461033, -1.10763562
1068, -0.0530759804, -1.02610266
1069, -0.761751533, -0.921865404
1070, 0.17288056, -0.153485745
1071, 0.220174938, 0.0151483156
1072, 0.357478619, -0.601856828
1073, 0.315244347, -0.700903654
1074, -0.172911525, -0.981577337
1075, -1.00077796, -1.04523301
1076, -0.922437727, -0.951168716
1077, 0.104833096, -0.261535138
1078, 0.137097597, -0.257168621
1079, 0.319072008, -0.560924113
1080, 0.262981087, -0.563645959
1081, 0.269329756, -0.579072177
1082, 0.247497544, -0.538224995
1083, -0.0998241007, -0.935773849
1084, 0.516674757, -0.84235841
1085, 0.71450299, -1.01115501
1086, 0.833231866, -1.03787172
1087, 0.823097527, -1.28564441
1088, -0.258199185, -0.656322002
1089, 0.206165895, -0.501215577
1090, 0.262456179, -0.95124495
1091, 0.238663495, -0.529038191
1092, 0.334795684, -0.570676982
1093, 0.330407023, -0.556546986
1094, 0.324674308, -0.726479828
1095, 0.296362579, -0.580747247
1096, 0.390682191, -0.838055968
1097, 0.324932337, -0.627635002
1098, 0.311082393, -0.658470213
1099, 0.774966836, -1.03587449
1100, 0.464674443, -0.808995843
1101, 0.433763474, -0.797127664
1102, 0.203419387, -0.201932654
1103, 0.24421902, -0.556178689
1104, 0.17689243, -0.906363964
1105, 0.165104017, -0.253185481
1106, 0.160223305, -0.232043415
1107, 0.0457650721, -0.372332245
1108, 0.164270133, -0.512973547
1109, 0.19580406, -0.149392486
1110, 0.177504122, -0.547383964
1111, -0.016543664, -0.589953005
1112, 0.232407257, -0.548592985
1113, 0.128858522, -0.318029881
1114, 0.15486154, -0.307300806
1115, 0.200040415, -0.257551283
1116, 0.324978173, -0.753566802

```
 1117,  0.200588852, -0.131845444
 1118,   0.30224061,  -0.63424778
 1119,  0.268025398, -0.714026392
 1120,  0.303980321, -0.731622159
 1121, -0.0373379923, -0.911788106
 1122,  0.124479815, -0.847104788
 1123, 0.0775915757, -0.824868321
 1124, 0.0957447961, -0.374614894
 1125,   0.18950972, -0.579886377
 1126,  0.240869164, -0.381705195
 1127,  0.185071424, -0.229962319
 1128,  0.229067996,  -0.45045653
 1129,  0.439993948, -0.832350016
 1130,  0.298477024,  -0.75589931
 1131,  0.185436353, -0.321373373
 1132,  0.151275009, -0.576806784
 1133,  0.262395114, -0.660663188
 1134,  0.206993967, -0.352379709
 1135,  0.232846081, -0.286110193
 1136, 0.0569888093, -0.532963514
 1137,  0.077545777, -0.465616584
 1138,  0.123312406,  -0.61711365
 1139,  0.210906461, -0.445004046
 1140,   0.17892541, -0.346171021
 1141,   0.19606714, -0.337095469
 1142,  0.212315038,  -0.32825622
 1143,  0.187858373, -0.371859998
 1144,  0.228938982, -0.300006628
 1145,  0.230164111, -0.675980031
 1146,  0.123384841, -0.652045131
 1147,  0.185035318, -0.438161403
 1148,  0.176582471,  -0.78265661
 1149,  0.267961144,   -0.7426126
 1150,  0.206789792, -0.742590904
 1151,    0.1949462,  -0.67121917
 1152,  0.164414123, -0.675831735
 1153,  0.134374633, -0.677399635
 1154,  0.190908477, -0.357436329
 1155,   0.14741239, -0.409374326
*Element, type=CPE4RT
   1,  196,   64,    1,  175
   2,  175,    1,   65,  197
   3,  198,   66,    2,  176
   4,  200,   68,   69,  201
   5,   68,  200,  177,    3
   6,   71,  203,  293,    5
   7,  105,  104,  235,  178
   8,   82,   81,  212,  179
   9,  243,  242,  294,  311
  10,  404,  310,  426,  370
  11,  241,  180,  295,  342
  12,  180,   16,  181,  320
  13,  296,  215,  214,  308
  14,  182,   15,   14, 1009
  15,  653,  571,  569,  607
  16,  680,  691,   54,  601
  17,  430,  144,  265,   61
  18,  265,  144,   25,  183
  19,  183,   25,  143,  264
  20,  414,  508,  589,  503
  21,  581,  580,  659,  660
  22,  192,  287,  298,  329
  23,  299,  196,  175,  333
  24,  297, 1009,  184,  322
  25,  184,   13,  118,  247
  26,   17,  185, 1008,   12
  27,   17,  132,  186,  185
  28,  128,  127,  252,  253
  29,  486,  378,  377,  409
  30,  325,   60,  407,  506
  31,  408,  187,   27,  145
  32,  504,   60, 1010,  430
  33,   60,  504,  505,  407
  34,  506,  407,   52,  598
  35,   19,  126,  251,   38
  36,  409,  377,  307,  437
  37,  385,   59,  410,  526
  38,  146,  266,  386,   28
  39,  146,   27,  187,  266
  40,  122,   34,  188,   18
  41,  141,  189,  120,   20
  42,  189,  262,  300,  327
  43,  609,  413,  524,  600
  44,  411,  301,  326,  420
  45,  302,  326,  188,   34
  46,  302,   34,  327,  300
  47,  250,  125,  124,   39
  48,  260,  138,  137,  259
  49,  438, 1018,  507,   49
  50,  600,   50,  664,  609
  51,  257,  135,  134,  256
  52,  256, 1007,  147,  267
  53,  267,  386,  412,   57
  54,  507, 1018,  490,   50
  55,  191,  257,  303,  381
  56,  328,  383,  413,   40
  57,  508,  414,  440,  514
  58,  501,  502,  400,  399
  59,  290,  291,  173,  172
  60,  192,   33,  169,  287
  61,  193,   24,  142,  263
  62,  273,  304, 1019,  274
  63,  195,  272,  305,  331
  64,  387,  330,  194,  269
  65,  194,   30,  150,  269
  66,  178, 1005,    7,  105
  67,  441,  603,  544,   36
  68,  306,  185,  186,  324
  69,  324,  186,  255,  419
  70,  677,   53,  678,  783
  71,  407,  505,  591,   52
  72,  253,  252, 1011,  379
  73,  251,  250,  307,  377
  74,  621, 1049, 1050,   42
  75,  665,   43, 1076, 1075
  76,  666,  589,   55,  752
  77, 1067,  733, 1046,  795
  78,  348,  213,  179,  347
  79,  490,  385,  526,   50
  80,  414,  321,   62,  440
  81,  489,  384,  525,   53
  82,  587, 1040,  663,  630
  83, 1022,   62,  264,  193
  84,  272,  153,  152,  271
  85,  176,    2,   67,  199
  86,    3,  177,  199,   67
  87,  309,    4,   70,  202
  88,  204,   72,    7, 1005
  89,   73,    9,  111,  240
  90,   74,  205,  206,   75
  91,  310,  206,  205,  426
  92,  206,  207,   76,   75
  93,   77,   76,  207,  208
  94,  208,  209,   78,   77
  95,  209,  210,   79,   78
  96,  210,  211,   80,   79
  97,  211,  212,   81,   80
  98,  179,  213,    8,   82
  99,   83,    8,  213,  214
 100,  214,  215,   84,   83
 101,  215,  216,   85,   84
 102,   87,   86,  217,  218
```

103,	88,	87,	218,	219
104,	89,	88,	219,	220
105,	90,	89,	220,	221
106,	91,	90,	221,	222
107,	92,	91,	222,	223
108,	93,	92,	223,	224
109,	94,	93,	224,	225
110,	95,	94,	225,	226
111,	96,	95,	226,	227
112,	97,	96,	227,	228
113,	98,	97,	228,	229
114,	229,	230,	99,	98
115,	230,	231,	100,	99
116,	101,	100,	231,	232
117,	103,	102,	233,	234
118,	10,	117,	1006,	106
119,	106,	1006,	236,	107
120,	244,	245,	115,	114
121,	108,	237,	238,	109
122,	73,	240,	205,	74
123,	180,	241,	11,	16
124,	241,	242,	112,	11
125,	310,	371,	207,	206
126,	113,	112,	242,	243
127,	114,	113,	243,	244
128,	117,	116,	246,	1006
129,	12,	1008,	247,	118
130,	15,	182,	248,	119
131,	120,	189,	327,	121
132,	34,	122,	121,	327
133,	18,	188,	249,	123
134,	39,	124,	123,	249
135,	125,	250,	251,	126
136,	127,	19,	38,	252
137,	130,	129,	254,	313
138,	255,	186,	132,	131
139,	256,	134,	133,	1007
140,	314,	256,	267,	57
141,	21,	191,	258,	136
142,	258,	259,	137,	136
143,	22,	190,	261,	139
144,	315,	300,	262,	261
145,	189,	141,	140,	262
146,	29,	156,	263,	142
147,	264,	143,	24,	193
148,	408,	145,	26,	1010
149,	267,	147,	28,	386
150,	148,	32,	174,	292
151,	316,	269,	268,	403
152,	30,	194,	270,	151
153,	151,	270,	271,	152
154,	271,	270,	317,	388
155,	31,	195,	273,	154
156,	331,	304,	273,	195
157,	263,	156,	155,	274
158,	6,	64,	196,	332
159,	157,	275,	276,	158
160,	159,	158,	276,	277
161,	278,	160,	159,	277
162,	279,	161,	160,	278
163,	280,	162,	161,	279
164,	163,	281,	282,	164
165,	282,	283,	165,	164
166,	165,	283,	284,	166
167,	166,	284,	285,	167
168,	167,	285,	286,	168
169,	168,	286,	287,	169
170,	33,	192,	288,	170
171,	170,	288,	289,	171
172,	171,	289,	290,	172
173,	402,	318,	290,	289
174,	173,	291,	292,	174
175,	197,	65,	66,	198
176,	332,	196,	299,	451
177,	201,	69,	4,	309
178,	199,	177,	319,	336
179,	339,	340,	415,	511
180,	295,	180,	320,	448
181,	181,	16,	119,	248
182,	510,	629,	548,	350
183,	14,	13,	184,	1009
184,	519,	442,	616,	592
185,	321,	183,	264,	62
186,	322,	374,	484,	515
187,	247,	1008,	323,	374
188,	255,	313,	37,	419
189,	187,	408,	325,	59
190,	266,	187,	59,	385
191,	139,	261,	262,	140
192,	315,	261,	190,	328
193,	190,	22,	138,	260
194,	191,	21,	135,	257
195,	1019,	193,	263,	274
196,	330,	317,	270,	194
197,	269,	150,	149,	268
198,	195,	31,	153,	272
199,	275,	332,	491,	389
200,	335,	197,	198,	1014
201,	176,	334,	1014,	198
202,	176,	199,	336,	334
203,	202,	70,	5,	293
204,	200,	201,	338,	337
205,	201,	309,	422,	338
206,	203,	204,	339,	1013
207,	203,	71,	72,	204
208,	1013,	339,	511,	423
209,	204,	1005,	340,	339
210,	109,	238,	239,	110
211,	1016,	341,	245,	244
212,	342,	295,	424,	432
213,	208,	312,	343,	209
214,	209,	343,	344,	210
215,	210,	344,	345,	211
216,	211,	345,	346,	212
217,	212,	346,	347,	179
218,	215,	296,	349,	216
219,	375,	425,	248,	182
220,	86,	85,	216,	217
221,	216,	349,	351,	217
222,	352,	218,	217,	351
223,	353,	219,	218,	352
224,	354,	220,	219,	353
225,	355,	221,	220,	354
226,	222,	356,	357,	223
227,	223,	357,	358,	224
228,	224,	358,	359,	225
229,	360,	226,	225,	359
230,	361,	227,	226,	360
231,	362,	228,	227,	361
232,	228,	362,	363,	229
233,	229,	363,	364,	230
234,	102,	101,	232,	233
235,	230,	364,	365,	231
236,	366,	232,	231,	365
237,	104,	103,	234,	235
238,	232,	366,	367,	233
239,	107,	236,	237,	108
240,	240,	239,	426,	205
241,	240,	111,	110,	239
242,	512,	462,	461,	538
243,	207,	371,	312,	208
244,	483,	428,	481,	404

```
245,  246,  373,  236, 1006
246,  341,  373,  246,  245
247,  116,  115,  245,  246
248,  322,  184,  247,  374
249,  429,  182, 1009,  297
250,  376,  307,  250,   39
251,  377,  378,   38,  251
252,  378, 1011,  252,   38
253,  253,  379,  380,  254
254,  129,  128,  253,  254
255,   37,  313,  254,  380
256,  313,  255,  131,  130
257,  314,  303,  257,  256
258, 1007,  133,   23,  147
259,  258,  191,  381, 1017
260, 1017,  382,  383,  260
261,  524,  382,   49,  507
262,  154,  273,  274,  155
263, 1012,  384,  265,  183
264,  386,  266,   58,  412
265,  387,  269,  316,  527
266,  268,  149,  148,  292
267,  317,  450,  431,  388
268,  272,  271,  388,  305
269,  439, 1022,   63,  542
270,  276,  275,  389,  390
271,  157,    6,  332,  275
272,  277,  276,  390,  391
273,  278,  277,  391,  392
274,  279,  278,  392,  393
275,  280,  279,  393,  394
276,  280,  281,  163,  162
277,  394,  395,  281,  280
278,  395,  396,  282,  281
279,  396,  397,  283,  282
280,  397,  398,  284,  283
281,  398,  399,  285,  284
282,  399,  400,  286,  285
283,  329,  401,  288,  192
284,  401,  402,  289,  288
285,  447, 1027,  318,  402
286,  318,  403,  291,  290
287, 1013,  423,  293,  203
288,  242,  241,  342,  294
289,  427,  343,  312,  482
290,  308,  214,  213,  348
291,  433,  349,  296,  416
292,  463,  351,  349,  433
293,  529,  586,  500,  499
294,  329,  298,  435,  449
295,  333,  175,  197,  335
296,  452,  299,  333, 1015
297,  302,  436,  420,  326
298,   39,  249,  301,  376
299,   57,  412, 1018,  438
300,  381,  303,  438,   49
301, 1022,  439,  440,   62
302,  193, 1019,  304, 1022
303,   63,  446, 1063,  542
304,   63,  331,  305,  446
305,  323,  306,  441,   36
306,  418,  441,  306,  324
307,  437,  307,  376,  485
308,  346,   48,  442,  347
309,  592,  616,  629,  627
310,  337,  319,  177,  200
311,  372,  370,  238,  237
312,  244,  243,  311, 1016
313,  311,  294,  444,  522
314,  303,  314,   57,  438
315,  420,  436,   40,  534
316,  403,  268,  292,  291
317,  330,  387, 1028,  445
318,  350,  181,  248,  425
319,  424,  295,  448,  612
320,   54,  530,  503,  601
321, 1012,  183,  321,  530
322,  374,  323,   36,  484
323,  185,  306,  323, 1008
324,  516,  324,  419,  594
325, 1031,  516,  594,  488
326,  325,  506,  410,   59
327,  301,  249,  188,  326
328,  190,  260,  383,  328
329,  328,   40,  436,  315
330,  450,  317,  330,  445
331,  304,  331,   63, 1022
332, 1015,  333,  335,  453
333,  451,  299,  452,  550
334,  451,  517,  491,  332
335,  319,  337,  456,  454
336, 1023, 1015,  453,  553
337, 1024,  455,  334,  336
338,  309,  202,  457,  422
339,  338,  422,  518,  458
340,  459,  178,  235,  480
341,  233,  367,  368,  234
342,  479,  368,  367,  478
343,  372,  237,  236,  373
344,  343,  427,  461,  344
345,  462,  345,  344,  461
346,   48,  346,  345,  462
347,  443,  519,  592,  509
348,  181,  350,  548,  320
349,  463,  433, 1071,  557
350,  434,  352,  351,  463
351,  464,  353,  352,  434
352,  465,  354,  353,  464
353,  466,  355,  354,  465
354,  221,  355,  356,  222
355,  356,  467,  468,  357
356,  357,  468,  469,  358
357,  358,  469,  470,  359
358,  359,  470,  471,  360
359,  472,  361,  360,  471
360,  473,  362,  361,  472
361,  474,  363,  362,  473
362,  363,  474,  475,  364
363,  476,  365,  364,  475
364,  477,  366,  365,  476
365,  234,  368,  369,  235
366,  570,  460,  479,  573
367,  459,  480,  521,  535
368,  480,  235,  369,  574
369,  239,  238,  370,  426
370,  370,  372,  483,  404
371,  404,  481,  371,  310
372,  481,  428,  522,  482
373,  483,  372,  373,  341
374,  539,  429,  541,  626
375,  541,  625,  667,  626
376,  301,  411,  485,  376
377,  379, 1011,  406,  487
378,  488,  594,  419,   37
379,  381,   49,  382, 1017
380,  383,  382,  524,  413
381, 1017,  260,  259,  258
382,  405,  525,  384, 1012
383,   61,  265,  384,  489
384,   58,  266,  385,  490
385,  447, 1038,  547, 1027
386, 1027,  547,  527,  316
```

387, 421, 578, 595, 528
388, 421, 492, 390, 389
389, 391, 390, 492, 493
390, 392, 391, 493, 494
391, 393, 392, 494, 495
392, 495, 496, 394, 393
393, 496, 497, 395, 394
394, 497, 498, 396, 395
395, 498, 499, 397, 396
396, 499, 500, 398, 397
397, 399, 398, 500, 501
398, 287, 286, 400, 298
399, 585, 529, 499, 498
400, 402, 401, 47, 447
401, 341, 1016, 428, 483
402, 405, 1012, 530, 54
403, 619, 596, 525, 405
404, 531, 576, 1044, 597
405, 531, 487, 406, 576
406, 61, 505, 504, 430
407, 60, 325, 408, 1010
408, 409, 437, 532, 533
409, 486, 409, 533, 1030
410, 51, 599, 526, 410
411, 412, 58, 490, 1018
412, 507, 50, 600, 524
413, 458, 456, 337, 338
414, 296, 308, 443, 416
415, 443, 308, 348, 519
416, 627, 668, 628, 543
417, 417, 297, 322, 515
418, 441, 418, 536, 603
419, 488, 37, 380, 1020
420, 436, 302, 300, 315
421, 609, 534, 40, 413
422, 528, 595, 669, 602
423, 293, 423, 457, 202
424, 537, 423, 511, 623
425, 538, 461, 427, 540
426, 763, 693, 705, 740
427, 482, 312, 371, 481
428, 432, 444, 294, 342
429, 375, 182, 429, 539
430, 297, 417, 541, 429
431, 26, 144, 430, 1010
432, 439, 542, 514, 440
433, 512, 538, 424, 612
434, 433, 509, 543, 1071
435, 1045, 1038, 549, 1039
436, 401, 329, 449, 47
437, 437, 485, 1029, 532
438, 446, 305, 388, 431
439, 548, 604, 448, 320
440, 416, 443, 509, 433
441, 348, 347, 442, 519
442, 631, 547, 1038, 1045
443, 450, 445, 546, 1064
444, 47, 549, 1038, 447
445, 612, 545, 1041, 512
446, 1039, 587, 630, 1045
447, 56, 431, 450, 1064
448, 335, 1014, 1032, 453
449, 551, 452, 1015, 1023
450, 319, 454, 1024, 336
451, 550, 452, 551, 633
452, 517, 451, 550, 632
453, 1032, 455, 1036, 1054
454, 422, 457, 554, 518
455, 457, 423, 537, 554
456, 458, 518, 606, 556
457, 178, 459, 340, 1005
458, 460, 369, 368, 479
459, 545, 604, 616, 442
460, 510, 350, 425, 1021
461, 434, 520, 523, 464
462, 558, 465, 464, 523
463, 559, 466, 465, 558
464, 355, 466, 467, 356
465, 467, 560, 561, 468
466, 468, 561, 562, 469
467, 469, 562, 563, 470
468, 470, 563, 564, 471
469, 471, 564, 565, 472
470, 566, 473, 472, 565
471, 567, 474, 473, 566
472, 474, 567, 568, 475
473, 477, 571, 572, 478
474, 475, 568, 569, 476
475, 366, 477, 478, 367
476, 571, 477, 476, 569
477, 574, 369, 460, 655
478, 482, 522, 540, 427
479, 484, 36, 544, 575
480, 411, 41, 1029, 485
481, 378, 486, 406, 1011
482, 531, 577, 1020, 487
483, 380, 379, 487, 1020
484, 738, 676, 516, 1031
485, 489, 591, 505, 61
486, 389, 491, 578, 421
487, 528, 579, 492, 421
488, 493, 492, 579, 580
489, 494, 493, 580, 581
490, 495, 494, 581, 582
491, 582, 583, 496, 495
492, 583, 584, 497, 496
493, 584, 585, 498, 497
494, 46, 608, 529, 585
495, 502, 501, 513, 1040
496, 298, 400, 502, 435
497, 1040, 587, 435, 502
498, 321, 414, 503, 530
499, 591, 489, 53, 677
500, 51, 410, 506, 598
501, 610, 508, 514, 685
502, 55, 589, 508, 610
503, 624, 375, 539, 692
504, 1025, 415, 535, 617
505, 48, 1041, 545, 442
506, 608, 613, 586, 529
507, 670, 631, 1045, 630
508, 747, 685, 614, 673
509, 417, 515, 656, 615
510, 676, 729, 622, 516
511, 418, 324, 516, 622
512, 657, 517, 632, 696
513, 578, 491, 517, 657
514, 552, 454, 555, 1051
515, 434, 463, 557, 520
516, 574, 652, 521, 480
517, 535, 521, 1026, 617
518, 522, 428, 1016, 311
519, 538, 540, 432, 424
520, 593, 618, 523, 640
521, 619, 405, 54, 691
522, 1028, 387, 527, 605
523, 602, 669, 730, 672
524, 576, 406, 486, 1030
525, 577, 531, 597, 620
526, 609, 664, 41, 534
527, 533, 532, 1047, 621
528, 1030, 42, 1044, 576

529, 534, 41, 411, 420
530, 535, 415, 340, 459
531, 544, 603, 682, 590
532, 623, 511, 611, 741
533, 425, 375, 624, 1021
534, 540, 522, 444, 432
535, 417, 615, 625, 541
536, 446, 431, 56, 1063
537, 614, 685, 1063, 56
538, 509, 592, 627, 543
539, 575, 544, 590, 719
540, 605, 527, 547, 631
541, 549, 47, 449, 1039
542, 726, 727, 663, 1058
543, 673, 605, 631, 670
544, 1035, 1024, 454, 552
545, 555, 454, 456, 1034
546, 456, 458, 556, 1034
547, 632, 550, 633, 697
548, 1036, 634, 553, 1054
549, 1037, 1023, 553, 634
550, 639, 1034, 556, 674
551, 518, 554, 636, 606
552, 635, 551, 1023, 1037
553, 638, 537, 623, 702
554, 674, 556, 606, 700
555, 543, 628, 557, 1071
556, 520, 557, 640, 523
557, 558, 523, 618, 641
558, 466, 559, 560, 467
559, 560, 559, 642, 643
560, 562, 644, 645, 563
561, 563, 645, 646, 564
562, 564, 646, 647, 565
563, 565, 647, 648, 566
564, 566, 648, 649, 567
565, 654, 573, 572, 588
566, 1025, 617, 686, 611
567, 573, 479, 478, 572
568, 651, 570, 573, 654
569, 607, 569, 568, 650
570, 675, 653, 607, 713
571, 655, 460, 570, 717
572, 484, 575, 656, 515
573, 1020, 577, 1031, 488
574, 602, 658, 579, 528
575, 580, 579, 658, 659
576, 582, 581, 660, 661
577, 661, 1043, 583, 582
578, 585, 584, 662, 46
579, 586, 513, 501, 500
580, 513, 586, 613, 1058
581, 588, 572, 571, 653
582, 1134, 1154, 1143, 767
583, 589, 666, 601, 503
584, 751, 786, 682, 681
585, 651, 773, 717, 570
586, 1046, 596, 619, 691
587, 53, 525, 596, 678
588, 42, 1075, 1076, 1044
589, 1076, 620, 597, 1044
590, 734, 679, 677, 783
591, 621, 1047, 1048, 1049
592, 50, 526, 599, 664
593, 601, 666, 735, 680
594, 722, 721, 745, 778
595, 681, 536, 671, 748
596, 681, 682, 603, 536
597, 604, 545, 612, 448
598, 616, 604, 548, 629
599, 605, 546, 445, 1028
600, 1037, 634, 637, 701
601, 650, 568, 567, 649
602, 766, 710, 1144, 35
603, 807, 753, 779, 828
604, 726, 1062, 1099, 1086
605, 1063, 685, 514, 542
606, 611, 511, 415, 1025
607, 1058, 663, 1040, 513
608, 684, 687, 608, 46
609, 614, 56, 1064, 546
610, 683, 688, 615, 656
611, 718, 655, 717, 732
612, 741, 611, 686, 1033
613, 690, 641, 618, 593
614, 738, 620, 1069, 1042
615, 1047, 532, 1029, 1048
616, 748, 671, 788, 804
617, 536, 418, 622, 671
618, 638, 636, 554, 537
619, 694, 1021, 624, 740
620, 692, 539, 626, 755
621, 746, 728, 836, 789
622, 668, 694, 695, 628
623, 695, 694, 740, 705
624, 640, 557, 628, 695
625, 629, 510, 668, 627
626, 1051, 637, 634, 552
627, 704, 1072, 1051, 555
628, 699, 635, 698, 742
629, 555, 1034, 639, 704
630, 698, 635, 1037, 701
631, 633, 551, 635, 699
632, 700, 606, 636, 703
633, 696, 632, 697, 757
634, 703, 636, 638, 760
635, 641, 690, 706, 1117
636, 1117, 706, 1070, 1109
637, 765, 1106, 1127, 708
638, 561, 560, 643, 562
639, 644, 1102, 708, 1127
640, 646, 645, 743, 1135
641, 1135, 743, 35, 1144
642, 1144, 710, 648, 647
643, 1142, 711, 648, 710
644, 712, 649, 648, 711
645, 716, 654, 588, 715
646, 689, 744, 617, 1026
647, 652, 689, 1026, 521
648, 652, 574, 655, 718
649, 653, 675, 715, 588
650, 771, 716, 715, 770
651, 657, 720, 595, 578
652, 672, 721, 658, 602
653, 787, 807, 832, 798
654, 659, 658, 721, 722
655, 584, 583, 1043, 662
656, 778, 745, 1100, 827
657, 687, 1062, 613, 608
658, 1075, 42, 1050, 665
659, 598, 665, 1050, 51
660, 1050, 1049, 599, 51
661, 598, 52, 679, 665
662, 55, 610, 1087, 752
663, 661, 660, 723, 1056
664, 625, 615, 688, 739
665, 706, 728, 746, 1070
666, 510, 1021, 694, 668
667, 720, 657, 696, 756
668, 673, 670, 782, 747
669, 1129, 867, 790, 827
670, 673, 614, 546, 605

671, 700, 1092, 761, 674
672, 713, 607, 650, 1126
673, 825, 791, 683, 719
674, 577, 620, 738, 1031
675, 729, 676, 738, 1042
676, 43, 665, 679, 734
677, 52, 591, 677, 679
678, 783, 678, 784, 792
679, 750, 691, 680, 806
680, 751, 681, 748, 1088
681, 719, 683, 656, 575
682, 46, 662, 725, 684
683, 638, 702, 1093, 760
684, 753, 1085, 687, 684
685, 714, 651, 654, 716
686, 744, 793, 686, 617
687, 693, 690, 593, 705
688, 764, 746, 789, 814
689, 750, 795, 1046, 691
690, 754, 755, 626, 667
691, 705, 593, 640, 695
692, 740, 624, 692, 763
693, 749, 639, 674, 761
694, 758, 699, 742, 810
695, 697, 633, 699, 758
696, 701, 637, 1051, 1072
697, 1052, 741, 1033, 823
698, 704, 639, 749, 796
699, 728, 706, 690, 693
700, 1117, 1109, 642, 559
701, 764, 707, 1070, 746
702, 642, 707, 1102, 643
703, 707, 764, 708, 1102
704, 1102, 644, 562, 643
705, 743, 1115, 816, 35
706, 815, 1106, 765, 814
707, 650, 649, 712, 1126
708, 767, 712, 711, 1134
709, 712, 767, 768, 1126
710, 770, 715, 675, 820
711, 769, 713, 1126, 768
712, 769, 820, 675, 713
713, 773, 651, 714, 842
714, 689, 652, 718, 774
715, 775, 590, 682, 786
716, 720, 756, 1053, 776
717, 669, 595, 720, 776
718, 660, 659, 722, 723
719, 1100, 745, 777, 844
720, 721, 672, 777, 745
721, 662, 1043, 724, 725
722, 1056, 724, 1043, 661
723, 779, 753, 684, 725
724, 736, 780, 724, 1056
725, 726, 1086, 781, 727
726, 630, 663, 727, 670
727, 830, 799, 752, 1087
728, 1057, 667, 625, 739
729, 788, 729, 800, 44
730, 671, 622, 729, 788
731, 731, 688, 683, 791
732, 732, 824, 774, 718
733, 733, 678, 596, 1046
734, 666, 752, 798, 735
735, 710, 766, 737, 1142
736, 787, 799, 1099, 1085
737, 1042, 734, 800, 729
738, 688, 731, 801, 739
739, 763, 692, 755, 836
740, 1092, 700, 703, 812
741, 702, 623, 741, 1052
742, 698, 701, 1072, 762
743, 758, 809, 757, 697
744, 1115, 743, 645, 644
745, 689, 774, 811, 744
746, 672, 730, 803, 777
747, 806, 868, 835, 750
748, 727, 781, 782, 670
749, 804, 834, 1088, 748
750, 698, 762, 759, 742
751, 719, 590, 775, 825
752, 821, 771, 770, 820
753, 806, 680, 735, 850
754, 750, 835, 837, 795
755, 752, 799, 787, 798
756, 789, 754, 794, 1066
757, 810, 742, 759, 878
758, 759, 762, 838, 1097
759, 813, 749, 761, 854
760, 704, 796, 762, 1072
761, 812, 854, 761, 1092
762, 838, 762, 796, 857
763, 728, 693, 763, 836
764, 765, 708, 764, 814
765, 841, 839, 891, 869
766, 801, 839, 1057, 739
767, 709, 1105, 816, 1115
768, 1105, 709, 1127, 1106
769, 1077, 1066, 794, 841
770, 797, 768, 767, 1143
771, 768, 797, 819, 769
772, 820, 769, 819, 862
773, 716, 771, 772, 714
774, 1088, 870, 786, 751
775, 824, 732, 822, 864
776, 732, 717, 773, 822
777, 714, 772, 843, 842
778, 793, 865, 1033, 686
779, 822, 773, 842, 864
780, 1091, 1082, 856, 1060
781, 730, 669, 776, 826
782, 777, 803, 1101, 844
783, 778, 1084, 723, 722
784, 780, 779, 725, 724
785, 880, 828, 829, 833
786, 790, 833, 736, 1084
787, 782, 830, 1087, 747
788, 783, 792, 800, 734
789, 872, 792, 784, 884
790, 784, 678, 733, 831
791, 1131, 818, 1140, 1141
792, 845, 731, 791, 876
793, 834, 804, 849, 897
794, 856, 774, 824, 1060
795, 804, 788, 44, 849
796, 1057, 794, 754, 667
797, 736, 833, 829, 780
798, 791, 825, 846, 876
799, 44, 800, 792, 872
800, 837, 835, 873, 912
801, 802, 757, 809, 853
802, 799, 830, 782, 781
803, 781, 1086, 1099, 799
804, 874, 858, 1113, 899
805, 826, 776, 1053, 808
806, 756, 696, 757, 1053
807, 1129, 875, 1096, 867
808, 1128, 805, 843, 772
809, 880, 833, 908, 900
810, 753, 807, 787, 1085
811, 828, 779, 780, 829
812, 754, 789, 836, 755

813, 802, 851, 1055, 808
814, 877, 1055, 851, 910
815, 758, 810, 855, 809
816, 1079, 812, 1093, 847
817, 811, 774, 856, 1059
818, 793, 744, 811, 865
819, 896, 882, 1079, 823
820, 813, 857, 796, 749
821, 858, 818, 1114, 1113
822, 35, 816, 817, 766
823, 1105, 1078, 840, 816
824, 818, 1131, 817, 1114
825, 845, 859, 801, 731
826, 848, 797, 1143, 785
827, 819, 797, 860, 861
828, 874, 848, 785, 858
829, 805, 1128, 821, 1139
830, 864, 842, 843, 890
831, 865, 811, 1059, 1061
832, 866, 775, 786, 870
833, 827, 1100, 844, 1129
834, 803, 730, 826, 852
835, 778, 827, 790, 1084
836, 832, 807, 828, 880
837, 850, 832, 880, 900
838, 870, 1088, 834, 897
839, 849, 44, 872, 1065
840, 925, 1104, 979, 1122
841, 837, 881, 1067, 795
842, 851, 802, 853, 886
843, 794, 1057, 839, 841
844, 817, 816, 840, 1114
845, 1078, 1077, 904, 840
846, 1066, 815, 814, 789
847, 812, 1079, 882, 854
848, 852, 826, 808, 1055
849, 844, 1101, 875, 1129
850, 850, 735, 798, 832
851, 775, 866, 846, 825
852, 821, 820, 862, 1139
853, 848, 1155, 860, 797
854, 858, 785, 1140, 818
855, 879, 848, 874, 1124
856, 897, 849, 1065, 909
857, 852, 1055, 877, 885
858, 885, 877, 901, 916
859, 853, 809, 855, 889
860, 855, 810, 878, 902
861, 854, 911, 857, 813
862, 838, 887, 888, 1097
863, 805, 863, 890, 843
864, 1061, 903, 896, 865
865, 869, 904, 1077, 841
866, 905, 899, 869, 891
867, 801, 859, 891, 839
868, 898, 879, 906, 926
869, 862, 819, 861, 1147
870, 860, 1155, 898, 893
871, 863, 805, 1139, 894
872, 919, 920, 942, 946
873, 864, 871, 1060, 824
874, 865, 896, 823, 1033
875, 1096, 927, 907, 867
876, 790, 867, 908, 833
877, 806, 850, 900, 868
878, 928, 907, 927, 947
879, 899, 1113, 904, 869
880, 952, 931, 1103, 1112
881, 929, 1095, 903, 1081
882, 884, 784, 831, 1074
883, 912, 925, 930, 915
884, 845, 892, 1107, 859
885, 852, 885, 1096, 875
886, 885, 916, 927, 1096
887, 846, 866, 895, 920
888, 910, 851, 886, 939
889, 901, 877, 910, 933
890, 911, 854, 882, 1095
891, 889, 855, 902, 934
892, 879, 898, 1155, 848
893, 1068, 1067, 881, 915
894, 882, 896, 903, 1095
895, 1059, 883, 1080, 1061
896, 883, 1103, 931, 1080
897, 899, 905, 1124, 874
898, 906, 879, 1124, 914
899, 912, 915, 881, 837
900, 884, 1074, 1065, 872
901, 932, 916, 901, 933
902, 803, 852, 875, 1101
903, 910, 939, 1116, 933
904, 887, 838, 857, 911
905, 1097, 917, 878, 759
906, 917, 1097, 888, 1118
907, 886, 853, 889, 918
908, 923, 863, 894, 944
909, 1107, 905, 891, 859
910, 892, 845, 876, 919
911, 876, 846, 920, 919
912, 1147, 894, 1139, 862
913, 944, 893, 898, 962
914, 921, 913, 871, 1089
915, 923, 1089, 890, 863
916, 922, 870, 897, 909
917, 1089, 871, 864, 890
918, 1079, 847, 1052, 823
919, 866, 870, 922, 924
920, 929, 935, 911, 1095
921, 1098, 960, 934, 902
922, 1112, 1103, 883, 1082
923, 1081, 1080, 931, 945
924, 1106, 815, 1078, 1105
925, 892, 936, 914, 1107
926, 946, 936, 892, 919
927, 873, 1090, 937, 1104
928, 868, 900, 908, 928
929, 908, 867, 907, 928
930, 1074, 831, 1068, 1083
931, 972, 945, 931, 952
932, 1090, 873, 835, 868
933, 886, 918, 1094, 939
934, 887, 911, 935, 956
935, 999, 1148, 45, 998
936, 940, 1110, 921, 1108
937, 1124, 905, 1107, 914
938, 1083, 1068, 915, 1121
939, 967, 916, 932, 983
940, 889, 934, 1073, 918
941, 1118, 941, 1098, 917
942, 878, 917, 1098, 902
943, 946, 942, 964, 1137
944, 948, 942, 920, 895
945, 1089, 923, 1108, 921
946, 949, 944, 962, 971
947, 922, 909, 943, 951
948, 1122, 979, 965, 950
949, 893, 944, 894, 1147
950, 971, 964, 1136, 980
951, 895, 866, 924, 1111
952, 912, 873, 1104, 925
953, 963, 966, 953, 945
954, 936, 926, 906, 914

```
 955,  967,  947,  927,  916
 956, 1090,  868,  928,  947
 957,  929, 1081,  945,  953
 958,  955, 1116,  954, 1130
 959,  955,  932,  933, 1116
 960,  888,  887,  956, 1118
 961,  934,  960,  957, 1073
 962,  929,  953,  956,  935
 963,  937,  986,  979, 1104
 964,  938,  913,  921, 1110
 965,  918, 1073,  958, 1094
 966,  980,  969,  981,  970
 967,  953,  966,  975,  956
 968,  960, 1098,  941,  976
 969, 1083, 1121,  943,  909
 970, 1123,  930,  925, 1122
 971,  962,  898,  926, 1137
 972, 1137,  964,  971,  962
 973,  988, 1000,  989,  977
 974,  936,  946, 1137,  926
 975,  937, 1090,  947,  967
 976, 1108,  949,  971,  940
 977,  970,  940,  971,  980
 978,  957,  974,  958, 1073
 979,  922,  951,  968,  924
 980, 1125,  972,  952,  938
 981, 1130,  973, 1149,  983
 982,  932,  955, 1130,  983
 983,  941, 1118,  956,  975
 984,  974,  973, 1120,  958
 985,  939, 1094,  954, 1116
 986, 1094,  958, 1120,  954
 987,  959, 1125,  938, 1110
 988,  961,  943,  930, 1123
 989, 1003,  999,  998,  992
 990,  996, 1001,  990,  985
 991,  964,  942,  948, 1136
 992,  968,  969, 1111,  924
 993, 1123, 1122,  950,  977
 994,  992,  998,   45,  986
 995,  978,  984,  966,  963
 996,  992,  967,  983, 1003
 997,  969,  980, 1136,  948
 998, 1111,  969,  948,  895
 999, 1132,  940,  970,  991
1000,  944,  949, 1108,  923
1001,  963,  945,  972,  985
1002, 1138, 1146, 1001,  996
1003, 1149,  973,  974, 1119
1004,  975,  966,  984, 1133
1005, 1145, 1002,  994,  997
1006,  976,  941,  975, 1133
1007,  976,  987,  957,  960
1008,  961, 1123,  977,  982
1009,  950,  965,   45, 1148
1010,   45,  965,  979,  986
1011,  981,  969,  968,  993
1012,  981,  993, 1146, 1138
1013,  981, 1138,  991,  970
1014, 1132,  996, 1125,  959
1015,  940, 1132,  959, 1110
1016,  968,  951,  982,  993
1017, 1149, 1119,  994, 1004
1018,  988, 1150, 1002, 1000
1019,  997, 1133,  984, 1145
1020,  978,  963,  985,  990
1021, 1125,  996,  985,  972
1022,  937,  967,  992,  986
1023,  957,  987, 1119,  974
1024, 1133,  997,  987,  976
1025,  995,  978,  990, 1151
1026, 1148,  988,  977,  950
1027,  982,  977,  989,  993
1028,  991, 1138,  996, 1132
1029,  989, 1000, 1152, 1153
1030,  987,  997,  994, 1119
1031,  995, 1151, 1002, 1145
1032,  984,  978,  995, 1145
1033,  999, 1150,  988, 1148
1034, 1000, 1002, 1151, 1152
1035, 1150, 1004,  994, 1002
1036, 1003,  983, 1149, 1004
1037,  999, 1003, 1004, 1150
1038, 1032, 1014,  334,  455
1039, 1027,  316,  403,  318
1040, 1048, 1029,   41,  664
1041,  533,  621,   42, 1030
1042,  455, 1024, 1035, 1036
1043, 1036, 1035,  552,  634
1044, 1039,  449,  435,  587
1045, 1041,   48,  462,  512
1046,  734, 1042, 1069,   43
1047, 1053,  757,  802,  808
1048, 1048,  664,  599, 1049
1049, 1054,  553,  453, 1032
1050, 1093,  702, 1052,  847
1051, 1056,  723, 1084,  736
1052, 1058,  613, 1062,  726
1053, 1059,  856, 1082,  883
1054, 1062,  687, 1085, 1099
1055,  831,  733, 1067, 1068
1056, 1069,  620, 1076,   43
1057,  707,  642, 1109, 1070
1058, 1065, 1074, 1083,  909
1059,  815, 1066, 1077, 1078
1060,  903, 1061, 1080, 1081
1061, 1082, 1091,  913, 1112
1062, 1121,  915,  930,  943
1063,  685,  747, 1087,  610
1064, 1091, 1060,  871,  913
1065, 1093,  812,  703,  760
1066,  938,  952, 1112,  913
1067,  840,  904, 1113, 1114
1068, 1117,  559,  558,  641
1069, 1120,  973, 1130,  954
1070, 1127,  709, 1115,  644
1071, 1128,  772,  771,  821
1072, 1131,  737,  766,  817
1073, 1141, 1140, 1154, 1134
1074,  646, 1135, 1144,  647
1075,  961,  982,  951,  943
1076, 1154, 1140,  785, 1143
1077, 1142, 1141, 1134,  711
1078,  737, 1131, 1141, 1142
1079, 1146,  993,  989, 1153
1080,  893, 1147,  861,  860
1081, 1151,  990, 1001, 1152
1082, 1153, 1152, 1001, 1146
*Nset, nset=_PickedSet2, internal, generate
    1,  1155,     1
*Elset, elset=_PickedSet2, internal,
generate
    1,  1082,     1
** Section: wp
*Solid Section, elset=_PickedSet2,
material=wp
,
*End Part
**
**
** ASSEMBLY
**
```

```
*Assembly, name=Assembly
**
*Instance, name=WP-1, part=WP
   -0.384644,     0.579352,           0.
*End Instance
**
*Instance,
library=11812re50t15deps500mtemp600,
instance=COAT-1
**
** PREDEFINED FIELD
**
** Name: Predefined Field-tc   Type: Initial
State
*Import, state=yes, update=no
*End Instance
**
*Instance,
library=11812re50t15deps500mtemp600,
instance=INTERLAY-1
**
** PREDEFINED FIELD
**
** Name: Predefined Field-coh   Type:
Initial State
*Import, state=yes, update=no
*End Instance
**
*Instance,
library=11812re50t15deps500mtemp600,
instance=SUB-1
**
** PREDEFINED FIELD
**
** Name: Predefined Field-ts   Type: Initial
State
*Import, state=yes, update=no
*End Instance
**
*Nset, nset=_PickedSet13, internal,
instance=WP-1
  23,  24,  25,  26,  27,  28,  29, 142,
143, 144, 145, 146, 147
*Elset, elset=_PickedSet13, internal,
instance=WP-1
  18,  19,  31,  38,  39,  61, 146, 147,
148, 149, 258, 431
*Nset, nset=_PickedSet14, internal,
instance=WP-1
  20,  21,  22,  23, 133, 134, 135, 136,
137, 138, 139, 140, 141
*Elset, elset=_PickedSet14, internal,
instance=WP-1
  41,  48,  51, 139, 141, 142, 143, 145,
191, 193, 194, 258
*Nset, nset=_PickedSet20, internal,
instance=WP-1
  20,  21,  22,  23, 133, 134, 135, 136,
137, 138, 139, 140, 141
*Elset, elset=_PickedSet20, internal,
instance=WP-1
  41,  48,  51, 139, 141, 142, 143, 145,
191, 193, 194, 258
*Nset, nset=_PickedSet21, internal,
instance=WP-1
  29,  30,  31,  32, 148, 149, 150, 151,
152, 153, 154, 155, 156
*Elset, elset=_PickedSet21, internal,
instance=WP-1
  65,  84, 146, 150, 152, 153, 155, 157,
197, 198, 262, 266
*Nset, nset=_PickedSet22, internal,
instance=WP-1
   9,  10, 106, 107, 108, 109, 110, 111
*Elset, elset=_PickedSet22, internal,
instance=WP-1
  89, 118, 119, 121, 210, 239, 241
*Nset, nset=_PickedSet23, internal,
instance=WP-1, generate
    1, 1155,     1
*Elset, elset=_PickedSet23, internal,
instance=WP-1, generate
    1, 1082,     1
*Nset, nset=_PickedSet28, internal,
instance=WP-1, generate
    1, 1155,     1
*Elset, elset=_PickedSet28, internal,
instance=WP-1, generate
    1, 1082,     1
*Nset, nset=_PickedSet91, internal,
instance=WP-1, generate
    1, 1155,     1
*Elset, elset=_PickedSet91, internal,
instance=WP-1, generate
    1, 1082,     1
*Nset, nset=_PickedSet94, internal,
instance=WP-1, generate
    1, 1155,     1
*Elset, elset=_PickedSet94, internal,
instance=WP-1, generate
    1, 1082,     1
*Nset, nset=_PickedSet107, internal,
instance=WP-1, generate
    1, 1155,     1
*Elset, elset=_PickedSet107, internal,
instance=WP-1, generate
    1, 1082,     1
*Nset, nset=_PickedSet133, internal,
instance=WP-1, generate
    1, 1155,     1
*Elset, elset=_PickedSet133, internal,
instance=WP-1, generate
    1, 1082,     1
*Elset, elset=cohesive, instance=INTERLAY-1,
generate
   1,  120,    1
*Surface, type=element, name=cohesivein
cohesive, S1
*Surface, type=element, name=cohesiveout
cohesive, S3
*Nset, nset=_PickedSet156, internal,
instance=COAT-1
  11,  12, 249, 250
*Nset, nset=_PickedSet156, internal,
instance=INTERLAY-1
   11, 1011
*Nset, nset=_PickedSet156, internal,
instance=SUB-1
  4,  5, 80, 81, 82, 83, 84, 85, 86, 87, 88,
89, 90
*Nset, nset=_PickedSet157, internal,
instance=COAT-1
  2,  3, 72, 73
*Nset, nset=_PickedSet157, internal,
instance=INTERLAY-1
    2, 1002
*Nset, nset=_PickedSet157, internal,
instance=SUB-1
  5,  6, 91, 92, 93, 94, 95, 96, 97
*Elset, elset=_lag1_S1, internal,
instance=WP-1
```

```
  27,  28,  35, 118, 126, 127, 128, 136,
137, 183, 247, 254
*Elset, elset=_lag1_S3, internal,
instance=WP-1
  41, 120, 123, 124, 138, 256
*Elset, elset=_lag1_S2, internal,
instance=WP-1
  14,  25,  47, 132, 134, 181
*Elset, elset=_lag1_S4, internal,
instance=WP-1
  26,  40, 129, 130, 131, 133, 135
*Surface, type=ELEMENT, name=lag1, Region
type=Lagrangian
_lag1_S1, S1
_lag1_S3, S3
_lag1_S2, S2
_lag1_S4, S4
*Elset, elset=_lag2_S2, internal,
instance=WP-1
   1,   2,   3,   4,  60,  85,  87,  88,
150, 161, 162, 163, 175, 177, 203, 207
*Elset, elset=_lag2_S4, internal,
instance=WP-1
   5,   6,  86,  90, 122, 159, 164, 166,
167, 168, 169, 170, 171, 172, 174
*Elset, elset=_lag2_S1, internal,
instance=WP-1
   7,   8,  89,  93,  99, 102, 103, 104,
105, 106, 107, 108, 109, 110, 111, 112
 113, 116, 117, 158, 160, 220, 234, 237, 271
*Elset, elset=_lag2_S3, internal,
instance=WP-1
  59,  66,  92,  94,  95,  96,  97,  98,
100, 101, 114, 115, 165, 276
*Surface, type=ELEMENT, name=lag2, Region
type=Lagrangian
_lag2_S2, S2
_lag2_S4, S4
_lag2_S1, S1
_lag2_S3, S3
*Elset, elset=_eu1_S4, internal,
instance=WP-1
  41, 141, 143, 191
*Elset, elset=_eu1_S2, internal,
instance=WP-1
  48,  51, 139, 145, 193, 194, 258
*Elset, elset=_eu1_S3, internal,
instance=WP-1
 142,
*Surface, type=ELEMENT, name=eu1, Region
type=Eulerian
_eu1_S4, S4
_eu1_S2, S2
_eu1_S3, S3
*Elset, elset=_eu2_S2, internal,
instance=WP-1
  89, 241
*Elset, elset=_eu2_S4, internal,
instance=WP-1
 118, 119, 121, 210, 239
*Surface, type=ELEMENT, name=eu2, Region
type=Eulerian
_eu2_S2, S2
_eu2_S4, S4
*Elset, elset=_eu3_S2, internal,
instance=WP-1
  65,  84, 157, 197, 198, 266
*Elset, elset=_eu3_S1, internal,
instance=WP-1
 146, 150
*Elset, elset=_eu3_S4, internal,
instance=WP-1
 152, 153, 155, 262
*Surface, type=ELEMENT, name=eu3, Region
type=Eulerian
_eu3_S2, S2
_eu3_S1, S1
_eu3_S4, S4
*Elset, elset=_Surfwp_S2, internal,
instance=WP-1
   1,   2,   3,   4,  60,  85,  87,  88,
150, 161, 162, 163, 175, 177, 203, 207
*Elset, elset=_Surfwp_S4, internal,
instance=WP-1
   5,   6,  86,  90, 122, 159, 164, 166,
167, 168, 169, 170, 171, 172, 174
*Elset, elset=_Surfwp_S1, internal,
instance=WP-1
   7,   8,  89,  93,  99, 102, 103, 104,
105, 106, 107, 108, 109, 110, 111, 112
 113, 116, 117, 158, 160, 220, 234, 237, 271
*Elset, elset=_Surfwp_S3, internal,
instance=WP-1
  59,  66,  92,  94,  95,  96,  97,  98,
100, 101, 114, 115, 165, 276
*Surface, type=ELEMENT, name=Surfwp
_Surfwp_S2, S2
_Surfwp_S4, S4
_Surfwp_S1, S1
_Surfwp_S3, S3
*Elset, elset=_Surf-bot_S2, internal,
instance=WP-1
  18,  19,  61, 147, 148, 149
*Elset, elset=_Surf-bot_S3, internal,
instance=WP-1
  31, 258
*Elset, elset=_Surf-bot_S4, internal,
instance=WP-1
  38, 146
*Elset, elset=_Surf-bot_S1, internal,
instance=WP-1
  39, 431
*Surface, type=ELEMENT, name=Surf-bot,
Region type=Lagrangian
_Surf-bot_S2, S2
_Surf-bot_S3, S3
_Surf-bot_S4, S4
_Surf-bot_S1, S1
*Elset, elset=_coatinsurf_S1, internal,
instance=COAT-1
   1,   2,   3,   4,   5,   6,   7,   8,
9,  10,  11,  12,  13,  14,  15,  16
  17,  18,  19,  20,  21,  22,  23,  24,
25,  26,  27,  28,  29,  30,  31,  32
  33,  34,  35,  36,  37,  38,  39,  40,
41,  42,  43,  44,  45,  46,  47,  48
  49,  50,  51,  52,  53,  54,  55,  56,
57,  58,  59,  60, 181, 182, 183, 184
 185, 186, 187, 188, 189, 190, 191, 192,
193, 194, 195, 196, 197, 198, 199, 200
 201, 202, 203, 204, 205, 206, 207, 208,
209, 210, 211, 212, 213, 214, 215, 286
 287, 288, 289, 290, 291, 292, 293, 294,
295, 296, 297, 298, 299, 300, 301, 302
 303, 304, 305, 306, 307, 308, 309, 310
*Surface, type=ELEMENT, name=coatinsurf
_coatinsurf_S1, S1
*Elset, elset=_toolsurf_S3, internal,
instance=COAT-1
 121, 122, 123, 124, 125, 126, 127, 128,
129, 130, 131, 132, 133, 134, 135, 136
```

```
 137, 138, 139, 140, 141, 142, 143, 144,
145, 146, 147, 148, 149, 150, 151, 152
 153, 154, 155, 156, 157, 158, 159, 160,
161, 162, 163, 164, 165, 166, 167, 168
 169, 170, 171, 172, 173, 174, 175, 176,
177, 178, 179, 180, 251, 252, 253, 254
 255, 256, 257, 258, 259, 260, 261, 262,
263, 264, 265, 266, 267, 268, 269, 270
 271, 272, 273, 274, 275, 276, 277, 278,
279, 280, 281, 282, 283, 284, 285, 336
 337, 338, 339, 340, 341, 342, 343, 344,
345, 346, 347, 348, 349, 350, 351, 352
 353, 354, 355, 356, 357, 358, 359, 360
*Surface, type=ELEMENT, name=toolsurf
_toolsurf_S3, S3
*Elset, elset=_substratesurf_S1, internal,
instance=SUB-1
   34,   39,   75,   93,  116,  120,  122,
127,  133,  136,  137,  138,  139,  140,
141,  142
  146,  147,  148,  149,  150,  153,  154,
155,  156,  213,  219,  232,  240,  243,
304, 1140
 1143, 1144, 1147, 1171, 1176, 1178, 1180,
1182, 1185, 1217, 1218, 1230, 1237, 1244,
1248
*Elset, elset=_substratesurf_S2, internal,
instance=SUB-1
    1,   20,   22,   77,   96,   98,  110,
190,  194,  198,  282, 1149
*Elset, elset=_substratesurf_S3, internal,
instance=SUB-1
   12,   13,   44,   49,  125,  126,  128,
129,  130,  131,  134,  135,  144,  145,
152,  158
  159,  160,  161,  163,  164,  177,  179,
217,  224,  227,  237,  280,  307, 1141,
1142, 1146
 1150, 1165, 1170, 1172, 1175, 1179, 1186,
1188, 1189, 1209, 1210, 1213, 1246, 1250,
1252
*Elset, elset=_substratesurf_S4, internal,
instance=SUB-1
  82,  88,  99, 100, 101, 102, 103, 104,
105, 106, 107, 108, 109, 111
*Surface, type=ELEMENT, name=substratesurf
_substratesurf_S1, S1
_substratesurf_S2, S2
_substratesurf_S4, S4
_substratesurf_S3, S3
** Constraint: tie1
*Tie, name=tie1, adjust=yes
cohesiveout, coatinsurf
** Constraint: tie2
*Tie, name=tie2, adjust=yes
cohesivein, substratesurf
*End Assembly
*Amplitude, name=Amp-1
       1e-05,          0.2,         4e-05,
0.4,         8e-05,          0.8,
0.0001,           1.
**
** MATERIALS
**
*Material, name=wp
*Conductivity
151.,
*Density
 2.67e-09,
*Elastic
72400., 0.33
*Expansion
 2.14e-05, 20.
 2.32e-05,100.
*Inelastic Heat Fraction
         0.9,
*Plastic, hardening=JOHNSON COOK
 0.001,  477., 0.144,  1.62,  585.,    20.
*Rate Dependent, type=JOHNSON COOK
 0.0067,1.
*Specific Heat
 9.63e+08,
**
** INTERACTION PROPERTIES
**
*Surface Interaction, name=IntProp-cutting
*Friction, taumax=143.
 0.6,
*Gap Conductance
20000.,    0.
    0., 0.001
*Gap Heat Generation
1., 0.195
*Surface Interaction, name=IntProp-heat
*Gap Conductance
20000.,    0.
    0., 0.002
**
** BOUNDARY CONDITIONS
**
** Name: bc-WP1 Type: Displacement/Rotation
*Boundary
_PickedSet13, 2, 2
**
** PREDEFINED FIELDS
**
** Name: Predefined Field-wp   Type:
Temperature
*Initial Conditions, type=TEMPERATURE
_PickedSet28, 20.
** ---------------------------------------
----------------------
**
** STEP: cutting
**
*Step, name=cutting
*Dynamic Temperature-displacement, Explicit,
element by element
, 0.002
*Bulk Viscosity
0.06, 1.2
**
** BOUNDARY CONDITIONS
**
** Name: BC-toolright Type:
Displacement/Rotation
*Boundary
_PickedSet156, 1, 1
** Name: BC-tooltop Type:
Displacement/Rotation
*Boundary
_PickedSet157, 2, 2
** Name: bc-WP2 Type: Velocity/Angular
velocity
*Boundary, type=VELOCITY, Region
type=Eulerian
_PickedSet14, 1, 1, 5000.
*Adaptive Mesh Controls, name=Ada-1,
curvature refinement=3.
1., 0., 0.
```

```
*Adaptive Mesh, elset=_PickedSet107,
controls=Ada-1, frequency=1, mesh sweeps=5,
op=NEW
**
** ADAPTIVE MESH CONSTRAINTS
**
** Name: Ada-Cons-1 Type:
Displacement/Rotation
*Adaptive Mesh Constraint
_PickedSet20, 1, 1
_PickedSet20, 2, 2
** Name: Ada-Cons-2 Type:
Displacement/Rotation
*Adaptive Mesh Constraint
_PickedSet21, 1, 1
** Name: Ada-Cons-3 Type:
Displacement/Rotation
*Adaptive Mesh Constraint
_PickedSet22, 2, 2
**
** INTERACTIONS
**
** Interaction: Int-2
*Contact Pair, interaction=IntProp-heat,
mechanical constraint=PENALTY, cpset=Int-2
coatinsurf, substratesurf
** Interaction: Int-cutting
*Contact Pair, interaction=IntProp-cutting,
mechanical constraint=KINEMATIC, weight=1.,
cpset=Int-cutting
toolsurf, Surfwp
**
** OUTPUT REQUESTS
**
*Restart, write, number interval=1, time
marks=NO
**
** FIELD OUTPUT: F-Output-1
**
*Output, field, number interval=100
*Node Output
A, NT, RF, U, V
*Element Output, directions=YES
DAMAGESHR, DMICRT, EVF, HFL, LE, MISESMAX,
PE, PEEQ, PEEQVAVG, PEVAVG, S, SDEG, STATUS,
SVAVG, TEMP
*Contact Output
CSTRESS,
**
** FIELD OUTPUT: F-Output-2
**
*Node Output
NT, RF, U
*Element Output, directions=YES
DAMAGESHR, DAMAGET, E, HFL, LE, PE, PEEQ, S,
SDEG, STATUS, TEMP
*Contact Output
CFORCE,
**
** HISTORY OUTPUT: H-Output-1
**
*Output, history, variable=PRESELECT
*End Step
** ----------------------------------------
----------------------
**
** STEP: Step-2
**
*Step, name=Step-2
*Dynamic Temperature-displacement, Explicit
, 0.0001
*Bulk Viscosity
0.06, 1.2
**
** BOUNDARY CONDITIONS
**
** Name: BC-toolright Type:
Displacement/Rotation
*Boundary, op=NEW
_PickedSet156, 1, 1
** Name: BC-tooltop Type:
Displacement/Rotation
*Boundary, op=NEW
_PickedSet157, 2, 2
** Name: bc-WP1 Type: Displacement/Rotation
*Boundary, op=NEW
** Name: bc-WP2 Type: Velocity/Angular
velocity
*Boundary, op=NEW
** Name: retract Type: Displacement/Rotation
*Boundary, op=NEW, amplitude=Amp-1
_PickedSet133, 1, 1, -0.2
_PickedSet133, 2, 2, -0.2
*Adaptive Mesh, op=NEW
**
** ADAPTIVE MESH CONSTRAINTS
**
** Name: Ada-Cons-1 Type:
Displacement/Rotation
*Adaptive Mesh Constraint, op=NEW
** Name: Ada-Cons-2 Type:
Displacement/Rotation
*Adaptive Mesh Constraint, op=NEW
** Name: Ada-Cons-3 Type:
Displacement/Rotation
*Adaptive Mesh Constraint, op=NEW
**
** OUTPUT REQUESTS
**
*Restart, write, number interval=1, time
marks=NO
**
** FIELD OUTPUT: F-Output-1
**
*Output, field, number interval=100
*Node Output
A, NT, RF, U, V
*Element Output, directions=YES
DAMAGESHR, DMICRT, EVF, HFL, LE, MISESMAX,
PE, PEEQ, PEEQVAVG, PEVAVG, S, SDEG, STATUS,
SVAVG, TEMP
*Contact Output
CSTRESS,
**
** FIELD OUTPUT: F-Output-2
**
*Node Output
NT, RF, U
*Element Output, directions=YES
DAMAGESHR, DAMAGET, E, HFL, LE, PE, PEEQ, S,
SDEG, STATUS, TEMP
*Contact Output
CFORCE,
**
** HISTORY OUTPUT: H-Output-1
**
*Output, history, variable=PRESELECT
*End Step
```